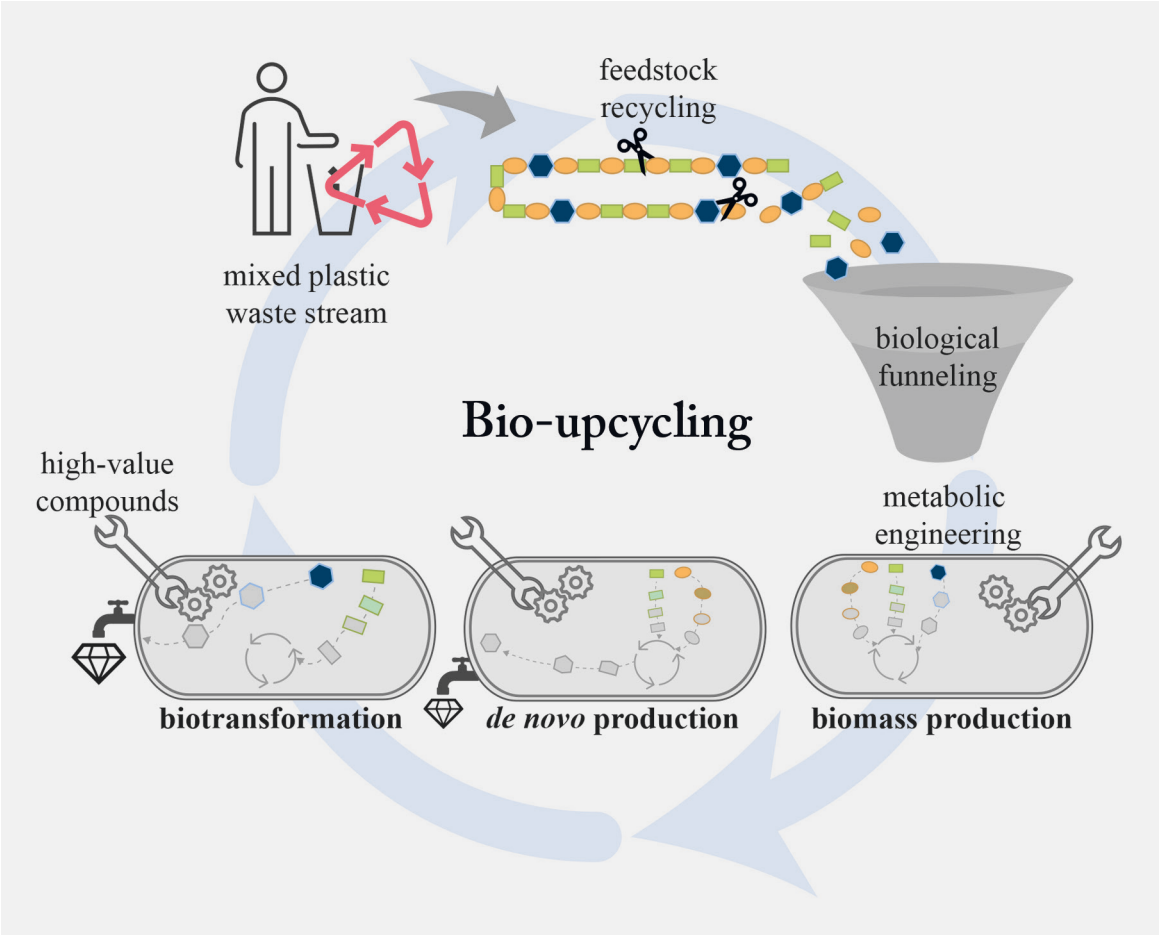

Enabling mixed microbial upcycling of plastic monomers

Yannic Sebastian Ackermann

Schlüsseltechnologien / Key Technologies
Band / Volume 281
ISBN 978-3-95806-749-3

Mitglied der Helmholtz-Gemeinschaft

JÜLICH
Forschungszentrum

Schriften des Forschungszentrums Jülich
Reihe Schlüsseltechnologien / Key Technologies Band / Volume 281

Forschungszentrum Jülich GmbH
Institut für Bio- und Geowissenschaften (IBG)
Biotechnologie (IBG-1)

Enabling mixed microbial upcycling of plastic monomers

Yannic Sebastian Ackermann

Schriften des Forschungszentrums Jülich
Reihe Schlüsseltechnologien / Key Technologies Band / Volume 281

ISSN 1866-1807 ISBN 978-3-95806-749-3

Bibliografische Information der Deutschen Nationalbibliothek.
Die Deutsche Nationalbibliothek verzeichnet diese Publikation in der
Deutschen Nationalbibliografie; detaillierte Bibliografische Daten
sind im Internet über http://dnb.d-nb.de abrufbar.

Herausgeber und Vertrieb:	Forschungszentrum Jülich GmbH Zentralbibliothek, Verlag 52425 Jülich Tel.: +49 2461 61-5368 Fax: +49 2461 61-6103 zb-publikation@fz-juelich.de www.fz-juelich.de/zb
Umschlaggestaltung:	Grafische Medien, Forschungszentrum Jülich GmbH
Druck:	Grafische Medien, Forschungszentrum Jülich GmbH
Copyright:	Forschungszentrum Jülich 2024

Schriften des Forschungszentrums Jülich
Reihe Schlüsseltechnologien / Key Technologies, Band / Volume 281

D 61 (Diss. Düsseldorf, Univ., 2023)

ISSN 1866-1807
ISBN 978-3-95806-749-3

Vollständig frei verfügbar über das Publikationsportal des Forschungszentrums Jülich (JuSER)
unter www.fz-juelich.de/zb/openaccess.

Publications

The results presented in this dissertation have been published in the following original publications or are in the process of being prepared as manuscripts for submission.

Ackermann Y. S., Li W-J., Op de Hipt L., Niehoff P-J., Polen T., Köbbing S., Ballerstedt H., Wynands B., Blank L.M., Wierckx N., (2021). Engineering adipic acid metabolism in *Pseudomonas putida*. *Metabolic Engineering*, 67, 29-40, 10.1016/j.ymben.2021.05.001

Ackermann Y. S., de Witt J., Mezzina P., Schroth C., Polen T., Pablo N., Wynands B., Wierckx N., (2024) Bio-upcycling of even and uneven medium-chain-length diols and dicarboxylates to polyhydroxyalkanoates using engineered *Pseudomonas putida*. *Microbial Cell Factories*, 23, 54, 10.1186/s12934-024-02310-7

Op de Hipt L.,Ackermann Y. S., de Jong H., Polen T., Köbbing S., Ballerstedt H., Wynands B., Wierckx N. Engineering of 1,4-butanediol and adipic acid metabolism in *P. taiwanensis* for upcycling to aromatic compounds. - to be submitted

Other publications not covered in this thesis include:

Eberz J., Doeker M., Ackermann Y. S., Schaffeld D., Wierckx N., Jupke A. Selective Separation of 4,4'-Methylenedianiline, Isophoronediamine and 2,4-Toluenediamine from Enzymatic Hydrolysis Solutions of Polyurethane. *Solvent Extraction and Ion Exchange*, 0.0.1-16.2023, 10.1080/07366299.2023.2193229.

Other publications in the form of posters or oral presentations

Poster presentations
Ackermann Y. S., Li W-J., Op de Hipt L., Niehoff P-J., Polen T., Köbbing S., Ballerstedt H., Wynands B., Blank L.M., Wierckx N., (2021). Enabling adipic acid metabolism in *Pseudomonas putida*. *EFB2021 - virtual conference*, online,

May 2021

Ackermann Y. S., Op de Hipt L., Polen T., Wynands B., Wierckx N., (2022). Enabling the conversion of mcl-dicarboxylic acids from plastic hydrolysates to high-value compounds with *Pseudomonas*. *Biocatalysis for the biological transformation of polymer science*, Cologne/Germany, June 2022

Ackermann Y. S., Op de Hipt L., Polen T., Wynands B., Wierckx N., (2023). Enabling the conversion of mcl-dicarboxylic acids from plastic hydrolysates to high-value compounds with *Pseudomonas*. *2023 Plastics Recycling and Upcycling GRC*, Manchester/NH, United States, July 2023

Oral presentations

Ackermann Y. S., Li W-J., Op de Hipt L., Niehoff P-J., Polen T., Köbbing S., Ballerstedt H., Wynands B., Blank L.M., Wierckx N., (2021). Enabling the conversion of the polyurethane monomer adipic acid to aromatics with Pseudomonas. *EFB2021 - virtual conference*, online Flash-poster, May 2021

Ackermann Y. S., Op de Hipt L., Polen T., Wynands B., Wierckx N., (2022). Enabling the conversion of mcl-dicarboxylic acids from plastic hydrolysates to high-value compounds with Pseudomonas. *Biocatalysis for the biological transformation of polymer science*, Cologne/Germany Flash-Poster, June 2022

In addition, the results were presented orally every six months at Mix-Up project meetings in Strasbourg (France, 2022), Madrid (Spain, 2023) or online.

List of Abbreviations

4-HB	4-hydroxybenzoate
AA	Adipic acid
ALE	Adaptive laboratory evolution
ANT	Anthranilate
ARO	Arogenate
BCD	Bicistronic design element
BDO	1.4-butanediol
BHET	Bis(2-Hydroxyethyl)terephthalat
CDW	Cell dry weight
CHO	Chorismate
CoA	Coenzyme A
CRediT	Contributor Roles Taxonomy
DAHP	3-deoxy-D-arabinoheptulosonate 7-phosphate
DCA	Dicarboxylic acid
DCD	1,2-dihydroxy-3,5-cyclohexadiene-1,4-dicarboxylate
DHQ	3-dehydroquinate
DHS	3-dehydroshikimate
E4P	Erythrose 4-phosphate
ED	Entner-Doudorof
EPSP	5-enolpyruvyl- shikimate 3-phosphate
FID	Flame ionization detector
FRT	Flippase recognition target
GA	Glutaric acid
GC	Gas chromatography

GMO	Genetically modified organism
GRC	Genome reduced chassis
GV	Green value
HAA	Hydroxyalkanoyloxy-alkanoic acid
HDO	1,7-heptanediol
HDPE	High-density polyethylene
HPLC	High performance liquid chromatography
HPP	4-hydroxyphenylpyruvate
IGR	Intergenic region
IUPAC	International Union of Pure and Applied Chemistry
LDPE	Low-density polyethylene
mcl	Medium-chain-length
MHET	Mono(2-Hydroxyethyl)terephthalat
MSM	Mineral salt medium
OD	Optical density
ODO	1,8-octanediol
PA	Polyamide
PAL	Phenylalanine ammonia-lyase
PBAT	Poly(butylene adipate-co-terephthalate)
PBST	Poly(butylene succinate-co-terephthalate)
PBT	Polybutylenterephthalat
PCA	Protocatechuate
PCR	Polymerase chain reaction
PE	Polyethylene
PEP	Phosphoenolpyruvate
PET	Polyethylene terepththalate
PHA	Polyhydroxyalkanoates
PHB	Polyhydroxybutyrate
PLA	Polylactic acids

PP	Polypropylene
PP	Phenylpyruvate
PPP	Pentose phosphate pathway
PRE	Prephenate
PS	Polystyrene
PU	Polyurethanes
PYR	Pyruvate
RND	Resistance-nodulation-division
S3P	Shikimate 3-phosphate
SA	Succinic acid
SEM	Standard error of the mean
SH	Shikimate
scl	Short-chain-length
SNP	Single-nucleotide polymorphism
SNV	Single-nucleotide variant
TA	Terephthalic acid
TAL	Tyrosine ammonia-lyase
TCA cycle	Tricarboxylic acid cycle (citrate cycle)
TDA	2,4-Diaminotoluene
TEA	Techno-economic assessment
Tg	Glass transition temperature
TRP	Tryptophan
TYR	Tyrosine
ucl	Uneven-chain-length

List of Figures

Contents

Summary

The global plastics crisis poses urgent environmental and social challenges due to the excessive production, consumption and disposal of plastic waste. To address this issue, biorecycling within a circular bioeconomy is a potential solution, involving the depolymerization of long-chain polymers by chemical or enzymatic catalysis and subsequent biological transformation of the resulting monomers. The goal of this work was to enable this approach by expanding the substrate range of *Pseudomonas putida* and *P. taiwanensis* to include aliphatic medium-chain length (mcl) dicarboxylic acids (DCAs), aromatic DCAs, and aliphatic diols. The study also aimed to combine plastic monomer degradation with production of biopolymers and aromatic compounds.
To achieve this, in the first chapter *P. putida* was engineered to grow on adipate and other mcl-DCAs by expressing the *dcaAKIJP* operon from *Acinetobacter baylyi* and deleting three β-oxidation regulatory genes, *paaYX* and *psrA*. Cultivation in a nitrogen-limited medium resulted in the production of 25 % PHAs/cell dry weight from adipate as sole carbon source, demonstrating the potential of bioupcycling of DCAs from plastic hydrolysates into new bio-based polymers. However, growth on uneven-chain-length (ucl) DCAs, especially pimelic acid, was limited. Consequently, the second chapter focuses on enabling degradation of ucl-DCAs by laboratory evolution, revealing a bottleneck in the CoA-dependent degradation pathway of glutaryl-CoA, an intermediate in the degradation of uneven DCAs. This step is regulated by GcdR and reverse engineering of two different amino acid exchanges could alter the regulation and thus enable good growth on pimelate as sole carbon source. By combining the metabolic features of an mcl-DCA degrading strain with those of an mcl-diol degrading strain, a microbial platform that enables efficient bio-upcycling of complex plastic hydrolysates to PHAs was successfully constructed. Besides the production of new bio-based plastics, plastic waste could also serve as carbon source for other chemical building blocks, such as aromatic compounds. In the second part of this study (Chapters 2.3 and 2.4), aromatic compounds such as tyrosine and protocatechuic acid were produced by transferring knowledge from *P. putida* to the streamlined chassis strain *P. taiwanensis* GRC3, resulting in specialized strains able to grow on different monomers of poly(butylene adipate-*co*-terephthalate) (PBAT). On the one hand, these strains are able to produce tyrosine from aliphatic monomers such as adipate or 1,4-butanediol. On the other hand, these strains were used for the degradation of realistic PBAT mock hydrolysates. In addition, a biotransformation approach was used to demonstrate the promising potential of biologically funneling a mixture of plastic monomers through a defined mixed culture.

Zusammenfassung

Die globale Kunststoffkrise ist eine dringende ökologische und soziale Herausforderung aufgrund der übermäßigen Produktion, des übermäßigen Verbrauchs und der Entsorgung von Kunststoffabfällen. Eine mögliche Lösung dieses Problems ist das Biorecycling im Rahmen einer zirkulären Bioökonomie, bei der langkettige Polymere durch chemische oder enzymatische Katalyse depolymerisiert und die resultierenden Monomere anschließend biologisch umgesetzt werden. Ziel dieser Arbeit war es, diesen Ansatz durch die Erweiterung des Substratspektrums von *Pseudomonas putida* und *P. taiwanensis* auf aliphatische mittelkettige Dikarbonsäuren (DKS), aromatische DKS und aliphatische Diole zu ermöglichen. Ziel dieser Arbeit war es auch, den Abbau von Kunststoffmonomeren mit der Produktion von Biopolymeren und aromatischen Verbindungen zu kombinieren.
Um dies zu erreichen, wurde im ersten Kapitel das Wachstum von *P. putida* auf Adipat und anderen mittelkettigen DKS ermöglicht indem das *dcaAKIJP*-Operon aus *Acinetobacter baylyi* heterolog exprimiert und die drei β-Oxidationsregulationsgene *paaYX* und *psrA* deletiert wurden. Die Kultivierung in einem stickstofflimitierten Medium ermöglichte die Produktion von 25 % PHAs/Zelltrockengewicht aus Adipinsäure, was das Potenzial des Bio-Upcyclings von DKS aus Kunststoffhydrolysaten zu neuen biobasierten Polymeren zeigt. Das Wachstum auf DKS mit ungerader Kettenlänge, insbesondere Pimelinsäure, war jedoch eingeschränkt. Daher konzentriert sich das zweite Kapitel darauf, den Abbau von ungeraden DKS durch Laborevolution zu ermöglichen, dabei wurde ein Engpass im CoA-abhängigen Abbauweg von Glutaryl-CoA, einem Zwischenprodukt des Abbaus von ungeraden DKS, identifiziert. Dieser Schritt wird durch GcdR reguliert, und konnte durch den Austausch von zwei verschiedenen Aminosäuren so verändert werden, das ein gutes Wachstum auf Pimelinsäure als einziger Kohlenstoffquelle möglich wurde. Durch die Kombination der genetischen Veränderungen des DKS abbauenden Stammes mit denen eines mittelkettigen Diol abbauenden Stammes wurde erfolgreich eine mikrobielle Plattform konstruiert, die ein effizientes Bio-Upcycling von komplexen Kunststoffhydrolysaten in PHA ermöglicht. Neben der Produktion neuer biobasierter Kunststoffe könnten Kunststoffabfälle auch als Kohlenstoffquelle für andere chemische Bausteine wie aromatische Verbindungen dienen. Im zweiten Teil dieser Arbeit (Kapitel 2.3 und 2.4) wurden aromatische Verbindungen wie Tyrosin und Protocatechusäure produziert, indem das Wissen von *P. putida* auf den genomisch reduzierten Stamm *P. taiwanensis* GRC3 übertragen wurde, was zu spezialisierten Stämmen führte, die auf verschiedenen Poly(butylenadipat-*co*-

terephthalat)-Monomeren (PBAT) wachsen können. Einerseits sind diese Stämme in der Lage, Tyrosin aus aliphatischen Monomeren wie Adipat oder 1,4-Butandiol zu produzieren. Andererseits wurden diese Stämme für den Abbau von realistischen PBAT- oder PBAT/Stärke-Mock-Hydrolysaten verwendet. Darüber hinaus wurde ein Biotransformationsansatz verwendet, um das vielversprechende Potenzial der biologischen Umwandlung einer Mischung von Kunststoffmonomeren durch eine definierte Mischkultur zu demonstrieren.

1. Introduction

1.1. Artificial polymers enable social boom

The history of human made polymers is a long story with different chapters of success. In principle, they have accompanied the evolution of humankind for a very long time. Back in the palaeolithic age, *Homo neanderthalensis*, produced a very sticky tar from compounds of birch sap by pyrolysis. This tar was then used for the hafting of weapons and thus made their lives much easier (Koller *et al.* 2001). In 1844, chemist Charles Goodyear patented a vulcanization process that combined natural rubber with sulfur at high temperatures to form a rigid rubber (Goodyear 1844). In parallel with Goodyear, the German pharmacist Johan Eduard Simon by accident discovered the polymerisation of styrene, described as one of the first semi-synthetic plastics (Scheirs *et al.* 2003). The first synthetic polymer was invented in the early 20th century, by Leo Baekeland, who worked with a polycondensation reaction for the production of phenol formaldehyde resins, the so called Bakelite (Thompson *et al.* 2009). Soon after, further synthetic polymers like polyethylene (1933) or nylon (a polyamide, PA) (1935) were invented (Mueller 1962; Spalding *et al.* 2017). Another, nowadays very popular plastic, namely polyethylene terephthalate (PET), was first produced by the two British chemist J. R. Whinfield and J. T. Dickson through a polycondensation reaction of terephthalic acid and ethylene glycol. Their work was successfully patented in 1946 (Whinfield *et al.* 1946). The big industrial breakthrough for synthetic polymers came in the middle of the 20th century. In 1950 total global production volume reached 1.5 Mt and from then increases almost 10 % every year (PlasticsEurope 2006) to a global production of approximately 390.7 Mt of plastic, excluding polymers not used in the manufacturing of plastic parts and products, such as adhesives or coatings (PlasticsEurope 2022).
Basically, so-called plastics are synthetic or semi-synthetic materials that consist mainly of polymers and whose properties could be influenced by various additives. These versatile properties include high flexibility, durability and low weight, in addition to plasticity (Andrady *et al.* 2009). The term plastic comes from the ancient Greek *plastikos* and means mouldable. Almost all plastics used nowadays are based on fossil raw materials, and mass production makes their production costs very low. This leads

to a replacement of various materials that were previously made of steel or other heavy or expensive to manufacture materials (Geyer *et al.* 2017). Moreover, plastics have a high strength-to-weight ratio, resulting in reduced material usage (Andrady *et al.* 2009). Thanks to this, the packaging industry has the largest share in the use of plastics with 44 %, followed by the building and construction industry with 18 % (PlasticsEurope 2022). The tremendous amount of beneficial properties has unfortunately led to a shift in consumer behaviour from reuse to single-use, resulting in an enormous throw-away-society.

There are many ways of classifying the various plastics into specific groups, for example according to their origin or application. Another common way of classifying plastics is by the functional groups within the polymer. Polymers containing ester functionalities within the main chain belong to the group of polyester plastics, such as PET and poly(butylene adipate-*co*-terephthalate) (PBAT) (Figure 1.1.1). On the other hand, polymers resulting from a condensation of a carboxylic acid with an amine and thus having amide bonds in the main chain are called polyamides. A popular example of this group is nylon. In contrast to that, using a polyaddition reaction to react a diol or polyol with a polyisocyanate resulting in urethane bonds between the molecules, are called polyurethanes (PU) (Eling *et al.* 2020). The biggest group of plastic polymers are polyolefines, such as polypropylene (PP) or polyethylene (PE) (Sauter *et al.* 2017). Besides their chemical structures, the chemical process used to synthesise the polymer, such as condensation, polyaddition or cross-linking, can also be used to classify them. In addition, plastics can be classified according to their physical properties, such as hardness, heat resistance or glass transition temperature (T_g). A widely used classification takes into account the thermophysical properties and their importance for manufacturing. Here, a distinction is made between how the polymers react to heating and whether reversible or non-reversible processes are involved. If heating leads to a change in chemical composition and thus to an irreversible change in properties, the plastics are described as thermoset. Common examples are polyepoxides, silicones or PU. To make a thermoset polymer, a single or multiple monomers are necessary that have three or more reactive groups and can form a three-dimensional cross-linked structure. This results in a complex structure that breaks down when heated and cannot be converted back to its previous structure (Pavlacky *et al.* 2013). If the polymer can be heated and formed more than once in a reversible process, it is referred to as thermoplastic. Widely used thermoplastics are polyester, PP, polystyrene (PS) or PA (Bîrcă *et al.* 2019).

Crystallinity is another factor that influences physical and mechanical properties of certain polymers. Normally, most parts of the polymers are randomly oriented or form amorphous chains. But some polymers have segments in the polymer chain orientated in parallel bundles to mimic crystal-like domains (Figure 1.1.1). These are called semi-crystalline plastics. However, the two areas are not always completely separate from each other. For example, small defects can occur, which means that breaks can also appear in a crystalline part that lead to amorphous structures and vice versa (Andrady 2017; Bryant 1947; Venkatram *et al.* 2023). The amount of crystalline parts can make the plastic tougher up to a certain point, whereas a higher degree of crystallinity will result in a brittle material. Polymer crystallisation usually takes place under harsh conditions, influenced by cooling rates, shear or extension flows and pressure (Mileva *et al.* 2018). But also the chemical structure of the polymer chain has an influence on crystallisation. Polymers with limited intermolecular interactions, such as PE, crystallize very fast. In contrast to that, polyesters like PET with an additional aromatic ring between repeating ethylene units, slows down crystallization (Mileva *et al.* 2018). In addition to the crystallinity of some polymer fractions, the amorphous parts also influence the mechanical properties of the polymer by having two temperature dependent states. These two phases are separated by the glass transition temperature, which is defined as the temperature at which amorphous polymers or amorphous parts of semi-crystalline polymers starts showing glass-like properties. Above this temperature the polymers become more rubbery. Depending on the application of the polymer, most polymers are used under their Tg, however some are used above their Tg, for example polyisoprenes, such as *cis*-1,4-polyisoprene which is similar to natural rubber and is often used in tyres or footwear (Sanditov *et al.* 2017; Tropin *et al.* 2016). Furthermore, the T_g and the resulting glass-like properties as well as the degree of crystallinity have an influence on the efficiency of some recycling methods, such as enzymatic degradation, and are thus important characteristics of the polymer (Thomsen *et al.* 2022).

1.2. The human crisis of plastic overproduction

Nowadays, it's hard to find a place on the planet that has not been contaminated with plastic. Due to its light weight and long durability, plastic particles are often transported hundreds of miles around the globe. This transport usually starts in rivers, through which the particles enter the oceans and accumulate in huge plastic streams, like the great pacific garbage patch (Lebreton *et al.* 2018). From there, they can either sediment

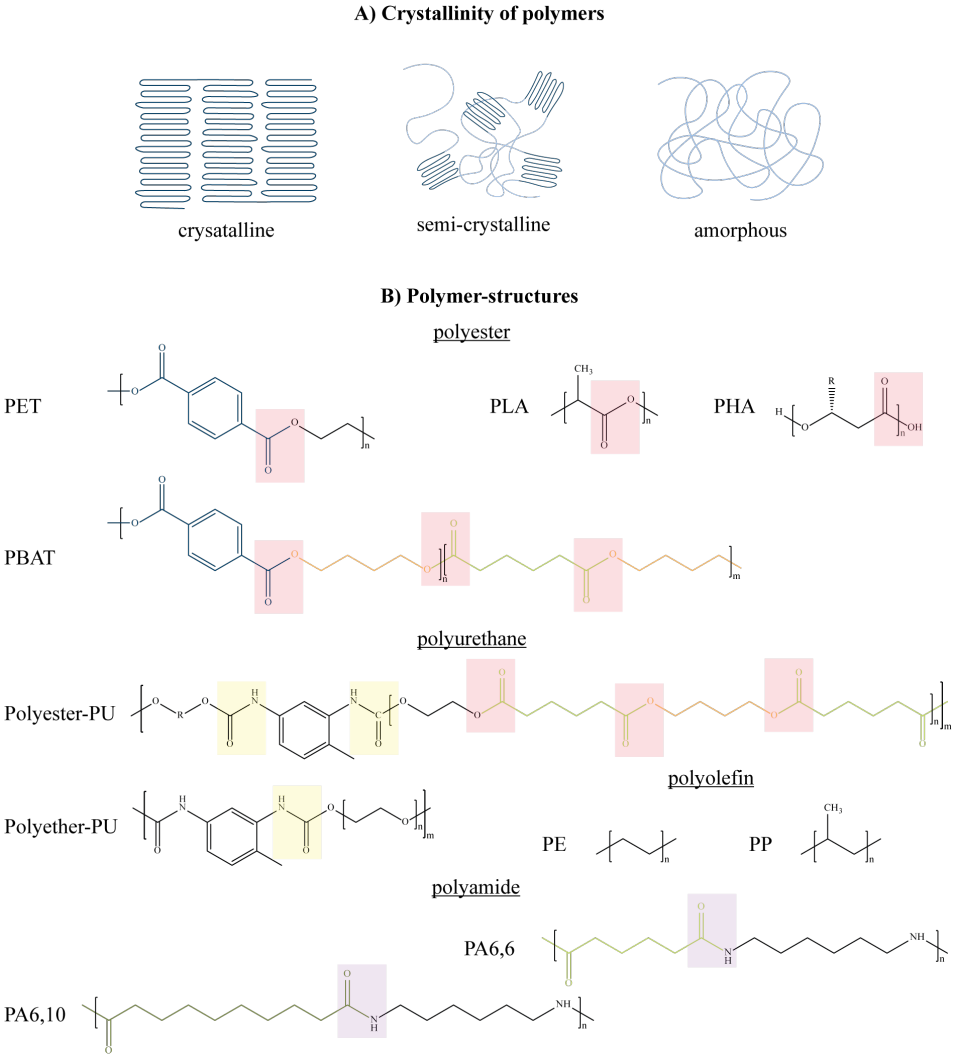

Figure 1.1.1.: Scheme of polymer crystallinity and structure. A) Visualisation of crystalline and amorphous polymer structures. B) Different polymers are grouped according to their functional groups. The yellow boxes show urethane-bonds, the purple boxes show amide-bonds and the red boxes show ester-bonds. Displayed are polyethylene (PE), polypropylene (PP), polyurethane (PU), polyamide (PA), polyethylene terephthalate (PET), polylactic acid (PLA), polyhydroxyalkanoates (PHA), poly(butylene adipate-co-terephthalate) (PBAT).

and reach the deepest layers of the ocean or be emitted into the atmosphere through sea spray and evaporation (Abel *et al.* 2021; Brahney *et al.* 2021). Strong winds can then carry them to the farthest regions of the poles, where no humans are usually present (Caruso *et al.* 2022). All these cases can be traced back to the fact that we have reached a point where we are no longer able to deal with the huge amount of plastic, which is partly due to a lack of awareness of how to deal with plastic and how to recycle it, but also because the existing recycling methods are not being used properly or are simply reaching the end of their capacity. In 2020 European countries stored about 23 % of in total 29.5 Mt of plastic waste on landfills, another 42 % were used for energy recovery and only 35 % were recycled (PlasticsEurope 2022). With about 42 Mt the United States are the largest waste producer. Most of their waste ends up in landfills (75.4 %), about 15.3 % are incinerated and only 9.3 % are recycled (Law *et al.* 2020). Globally, the situation is much worse. In 2016, 91 Mt year^{-1} were produced that had a mismanaged end of life and were not recycled or disposed of properly, representing approximately 42 % of global plastic demand. Lau *et al.* (2020) predict that this number will increase by a further 10 % if current behaviour does not change. This could lead to a production of 240 Mt year^{-1} of mismanaged plastic. Apart from the completely misdirected plastic waste that ends up directly in the environment, the large amount of plastic that ends up in landfills is also a major challenge. On the one hand, landfills require a lot of space, which is becoming increasingly rare in some countries. On the other hand, the collection and transport of the waste has a huge impact on the environment. Especially if the aim is to minimize environmental damage, the location of the landfill should be as close as possible to the consumer and waste producer, but far enough away to minimize health risks (Hopewell *et al.* 2009). Even well-managed landfills carry a high risk of long-term contamination of soil and groundwater through leaching of additives from plastic waste. Some of these additives, such as bisphenol A (BPA) or phthalates, have been shown to have an enormous impact on the development and reproducibility of animals (Oehlmann *et al.* 2009; Parvin *et al.* 2021; Teuten *et al.* 2009).

Besides that, the long-term storage of plastic waste in landfills ties up huge amounts of chemical raw materials and energy that have to be replenished using new fossil resources. In order to avoid at least total energy loss, incineration and energy recovery are the most common ways of disposing of plastic waste in Europe. However, incineration also carries the risk of releasing toxic compounds from plastics into the atmosphere and huge greenhouse gas emissions. The latter, in particular, is a major problem for climate change, as most consumer plastics are still based on fossil fuels. If more biomass were

used to produce substrates for virgin polymers, this could be less unfavourable, as the overall carbon flux would be more or less neutral (Meys *et al.* 2021; Zheng *et al.* 2019).

1.3. Recycling of conventional plastic waste

In order to improve the management of plastic waste at the end of its life cycle, various recycling techniques have been established, each offering different benefits. These include mechanical and chemical recycling methods (Kalali *et al.* 2023). Due to the versatility and ubiquity of plastics, post-consumer waste streams are complex mixtures of polymers and other contaminants. This requires a complex sorting and separation process, as the purity of the recyclate has a major impact on the final quality of the new polymer (Serranti *et al.* 2019). Most of the separation technologies rely on the diverse physical properties exhibited by polymers, such as size, weight, density, or electrostatic characteristics. However, the separation of different polymers with strikingly similar properties, such as low-density PE (LDPE) and high-density PE (HDPE), poses a significant challenge. But also specific colours, especially black and dark colours, pose severe limitations to separation and therefore recycling, as they cannot be detected by near-infrared sensors, a process commonly used in recycling plants (Turner 2018). Apart from foreign contaminants such as aluminium or glass, the use of complex plastic mixtures as a recycling substrate could in the future be a good way to improve or even avoid these complicated separation processes and access those plastic polymers, which are lost in the recycling loop only because of some additives or pigments. But until then, high quality separation is an essential step for the recycling of plastic waste streams.
Mechanical recycling, mostly performed as extrusion, is widely used, cheap and large-scale compatible, but often leads to a reduced quality of the polymer. In case of PET, mechanical recycling leads to a 4-times reduced factor of elongation at break compared to virgin PET, leading to a lower value in packaging industry (Schyns *et al.* 2021). To avoid this loss in value by down-cycling the plastics, another way is the recovery of the monomers or chemical constituents. This is often referred to as chemical or feedstock recycling. It involves the use of catalysts that break the chemical bonds and lead to products that can be purified and recycled back into virgin quality polymers. (Farkas *et al.* 2023; Hopewell *et al.* 2009). Besides that, chemical recycling methods also describe the use of plastic waste in fuel production by gasification or pyrolysis (Meys *et al.* 2020). This refers to the thermal decomposition of polymers in an oxygen-free environment (Maqsood *et al.* 2021. Feedstock recycling could also be achieved by a

process that is becoming increasingly popular, namely biotechnological degradation of plastics based on enzymatic depolymerisation (Wei *et al.* 2020).
In the past, several microorganisms have been isolated and described that can grow on polymers, some of which are described as non-biodegradable (Bollinger *et al.* 2020; Espinosa *et al.* 2020; Khandare *et al.* 2021; Roy *et al.* 2021; Yoshida *et al.* 2016). All of the microorganisms have in common that they use enzymes, such as cutinases or esterases, to depolymerize the polymers. Well-studied examples for degradation of PET for example are the hydrolases from *Ideonella sakaiensis* 201-F6 (Yoshida *et al.* 2016) or TfCut from *Thermobifida fusca* (Kleeberg *et al.* 1998). Since these wildtype enzymes are rather slow and have not been naturally optimised by evolution, there has been growing interest in enhancing them through directed laboratory evolution and enzyme engineering. This resulted in optimized enzymes. Based on the LCC, isolated from a leaf-branch compost (Sulaiman *et al.* 2012), Tournier *et al.* (2020) engineered the enzyme and achieved a 90 % PET depolymerisation in less than 10 h on a pre-treated post-consumer PET, resulting in a productivity of $16.7\,\mathrm{g\,L^{-1}\,h^{-1}}$ at 72 °C. Another engineering target is the increase of the thermostability of the enzymes, which is mostly achieved by adding disulfide bonds to have active enzymes above the T_g of the polymer. This is because the T_g affects the mobility of the amorphous phase of the polymer, and a temperature above the T_g makes the amorphous part much more accessible to enzymatic degradation. However, Thomsen *et al.* (2022) have also demonstrated that an increase in thermostability alone is not sufficient to degrade polymers above their Tg, but that an increase in catalytic efficiency on crystalline parts should also be improved.
Besides PET, other polymers that are not suitable for mechanical recycling, such as PU are more interesting for enzymatic recycling. In case of polyester-polyurethanes polyester hydrolases, such as LCC or TfCut2, also showed good activity on these substrates (Schmidt *et al.* 2017). So far, most of the enzymes described for depolymerizing plastics are hydrolases, which means that only polymers containing hydrolysable bonds are suitable for an enzymatic recycling process. Therefore, in order to develop more sustainable biodegradable polymers, it is important to focus on polymers with hydrolysable backbones (Wei *et al.* 2020).
One possibility to degrade non hydrolysable fossil-based polymers, such as PE, is a pre-treatment step to make the polymer chain enzymatically accessible. Thereby initial oxidation of PE polymers takes place through exposure to UV irradiation in combination with heat or chemicals in the environment leading to carbonyl-groups in the alkane chain (Montazer *et al.* 2020). A similar approach was also demonstrated by

Sanluis-Verdes *et al.* (2022). They isolated a PEase enzyme belonging to the phenol oxidase family that was able to overcome the initial step of PE degradation by oxidizing the carbon-carbon backbone. The resulting functional groups are then hydrolyzed leading to shorter fragments of PE. Smaller fragments of the polymer or oligomers could possibly be degraded *via* pathways similar to degradation pathways of liner *n*-alkanes, such as paraffin or hexadecane (Alvarez 2003; Yoon *et al.* 2012). By pre-treating the polymer chain with a chemical oxidation approach and combining this chemical process with biotechnological degradation of the resulted monomers, Sullivan *et al.* (2022) could demonstrate an efficient way to valorize HDPE. Pre-treatment was also required for the degradation of polyether-polyurethanes by isolated urethanases. In this case, Branson *et al.* (2023) combined a chemical glycolysis step leading to dicarbamates with an enzymatic step using a metagenome-isolated urethanase resulting in the release of CO_2, glycol, and the aromatic diamine.

In addition to chemocatalysis or enzyme catalysis, there is a third possibility, namely whole-cell- or bio-catalysis. In principle, these feedstock recycling methods do not differ greatly in the basic idea of using catalysts to break chemical bonds. The main difference is in the origin and application of the catalysts, with each method having its advantages and disadvantages (Mengers *et al.* 2023). For example, whole-cell catalysis using microorganisms allows for many different enzymatic steps to be carried out in parallel, but only under certain moderate conditions. Chemical catalysts, on the other hand, can use strong solvents, high pressures and temperatures to act quickly, although the use of large amounts of solvent in particular is a disadvantage in terms of sustainability. However, all of the above mentioned studies showed good opportunities for feedstock recycling of conventional, most fossil based, plastics. Nevertheless, there is an ongoing debate about the environmental benefits of feedstock recycling. Geyer *et al.* (2016) showed that closed-loop recycling systems have no inherent environmental benefits compared to open-loop systems. Surprisingly, Shen *et al.* (2010) found that linear recycling pathways for PET through mechanical recycling are environmentally superior to closed-loop pathways with chemical recycling to recover feedstock monomers, even if the mechanically recycled PET is ultimately incinerated. In general, studies could indicate that significant amounts of collected and sorted plastic packaging waste can be effectively materially recycled to achieve material properties suitable for replacing virgin polymers (Meys *et al.* 2020). It is therefore highly desirable to optimise and streamline recycling processes while using sustainable raw materials. These efforts have led to the development of new types of sustainable plastics, known as bioplastics, which

aim to solve the problem of plastic waste and mitigate climate change by replacing fossil resources. To support this goal, the EU Commission has funded several projects under its Horizon2020 program.

1.4. Bioplastic as a potential solution

Despite efforts to collect all waste, the lack of economically viable recycling options hinders the effective retention of carbon in the cycle (Wierckx *et al.* 2015). New technologies are urgently needed to improve the recycling of various plastic waste streams, including impure mixed waste and non-recyclable thermoset polymers such as polyurethane foams. In addition, the continuous release of microplastics from sources such as tyre wear or laundry contributes to environmental pollution. One possible solution to reduce plastic pollution is to develop biodegradable polymers that degrade faster in the environment. However, it is important to consider environmental degradation as a last resort and prioritise other sustainable approaches (Wei *et al.* 2020). As a consequence, one of the most advertised solutions are the so-called bioplastic products, which are becoming more and more popular. However, the use of the term "bioplastic" often encompasses two completely separate product classes, which can lead to consumer confusion. Moreover, the two product classes have different benefits and applications. Bio-based plastics can reduce the carbon footprint, while biodegradable plastics can reduce the environmental impact and may also facilitate bio-recycling (Tiso *et al.* 2022). The *International Union of Pure and Applied Chemistry* (IUPAC) defines bioplastic, as followed:

> "**bioplastic**
> *Biobased polymer* derived from the *biomass* or issued from monomers derived from the biomass and which, at some stage in its processing into finished products, can be shaped by flow.
>
> *Note 1*: Bioplastic is generally used as the opposite of polymer derived from fossil resources.
> *Note 2*: Bioplastic is misleading because it suggests that any polymer derived from the biomass is environmentally friendly.
> *Note 3*: The use of the term "bioplastic" is discouraged. Use the expression "biobased polymer".
> *Note 4*: A biobased polymer similar to a petrobased one does not imply

> any superiority with respect to the environment unless the comparison of respective life cycle assessments is favourable."
> (Vert *et al.* 2012)

Common examples of bioplastic are products made from biopolymers such as polyhydroxyalkanoates (PHA) or polylacticacids (PLA), but also from cellulose or starch (Narancic *et al.* 2020). In addition, fossil-based building blocks are increasingly being replaced by bio-based building blocks. In case of PE, which is usually synthesised from ethylene obtained from petroleum feedstock, it has been successfully demonstrated that ethylene monomers can also be derived from dehydration of bio-ethanol produced from glucose (Alvarenga *et al.* 2013). Although Bio-PE is bio-based and could therefore be called a bioplastic, it does not become a biodegradable polymer (Ghatge *et al.* 2020). Because biodegradable and biodegradation are defined by IUPAC as followed:

> "**biodegradable (biorelated polymer)**
> Qualifier for *macromolecules* or polymeric substances susceptible to *degradation* by *biological activity* by lowering of the molar masses of *macromolecules* that form the substances.
>
> *Note 1*: Adapted from [8] to include the notion of decrease of molar mass in the definition.
> *Note 2*: It is important to note that in the field of *biorelated polymers*, a biodegradable compound is *degradable* whereas a *degradable polymer* is not necessarily biodegradable.
> *Note 3*: Degradation of a polymer in vivo or in the environment resulting from the sole water without any contribution from living elements is not *biodegradation*. The use of *hydrolysis* is recommended. (See also degradation.)"
> (Vert *et al.* 2012)
>
> "**biodegradation (biorelated polymer)**
> *Degradation* of a polymeric item due to cell-mediated phenomena [9].
>
> *Note 1*: The definition given in [2] is misleading because a substance can be degraded by *enzymes* in vitro and never be degraded in vivo or in the environment because of a lack of proper enzyme(s) in situ (or simply a lack

> of water). This is the reason why *biodegradation* is referred to as limited to degradation resulting from cell activity. (See *enzymatic degradation.*) The definition in [2] is also confusing because a compounded *polymer* or a copolymer can include bioresistant additives or moieties, respectively. *Theoretical biodegradation* should be used to reflect the sole organic parts that are *biodegradable.* (See *theoretical degree of biodegradation* and *maximum degree of biodegradation.*).
> *Note 2*: In vivo, degradation resulting solely from hydrolysis by the water present in tissues and organs is not biodegradation; it must be referred to as *hydrolysis* or *hydrolytic degradation.*
> *Note 3*: *Ultimate biodegradation* is often used to indicate complete transformation of organic compounds to either fully oxidized or reduced simple molecules (such as carbon dioxide/methane, nitrate/ammonium, and water. It should be noted that, in case of partial biodegradation, residual products can be more harmful than the initial substance.
> *Note 4*: When biodegradation is combined with another degrading phenomenon, a term com- bining prefixes can be used, such as oxo-biodegradation, provided that both contribu- tions are demonstrated.
> *Note 5*: Biodegradation should only be used when the mechanism is proved, otherwise degra- dation is pertinent.
> *Note 6*: *Enzymatic degradation* processed abiotically in vitro is not biodegradation.
> *Note 7*: Cell-mediated chemical modification without main *chain scission* is not biodegradation. (See *bioalteration.*)"
> (Vert *et al.* 2012)

These definitions highlight one of the current problems with polymers labelled as biodegradable. Although IUPAC is careful in its definition, in many cases plastics are labelled as biodegradable but are instead erodible, hydrodegradable, photodegradable or only partially biodegradable, which can lead to residues in the environment. Another problem in defining biodegradability is the time frame and how to measure it. This is a major challenge in agriculture, where plastics are deliberately used in the soil and where fully biodegradable plastics could be a good solution to minimise environmental damage (Fojt *et al.* 2020; Kyrikou *et al.* 2007).
Biodegradable polymers are ubiquitous in nature and are the most abundant polymers on earth, prominent examples being cellulose or chitin (El Seoud *et al.* 2022). These

polymers are naturally degraded over time by various microorganisms, preventing uncontrolled accumulation on earth. Other natural biodegradable polymers of increasing interest for biotechnological production are PHAs which are accumulated by a wide range of bacteria as a storage compound and are mainly produced during nitrogen, phosphorous and oxygen limitation (Koller *et al.* 2022; Wen *et al.* 2010). PHAs were first described in 1925 by a French scientist in *Bacillus megaterium*, but since then a lot of other Gram-positive as well as Gram-negative bacteria have been described to naturally produce PHAs (Chee *et al.* 2010). Among them, *Cupriavidus necator* is one of the best studied short-chain-length (scl)-PHA producers. It can accumulate up to 90 % of polyhydroxybutyrate (PHB) per cell dry weight via a three-step biosynthetic pathway. As first a 3-ketothiolase, encoded by *phaA*, condenses two molecules of acetyl-CoA to acetoacetyl-CoA. PhaB, an NADH-dependent acetoacetyl-CoA reductase further reduces this to (R)-3-hydroxybutyryl-CoA, which is then polymerized by the PHB synthase PhaC (Schubert *et al.* 1988). In contrast to that, medium-chain-length (mcl)-PHAs are synthesized via the intermediate (R)-3-hydroxyacyl-CoA. This molecule is produced either via β-oxidation when fatty acids or alkanoic acids are used as substrate, or via fatty acid *de novo* synthesis when unrelated carbon sources are used (Mozejko-Ciesielska *et al.* 2018). In *P. putida*, (mcl)-PHA synthesis is organized by two main operons. The first one encodes two (mcl)-PHA synthases PhaC1 and PhaC2, a depolymerase PhaZ, and a transcriptional activator PhaD. The second operon is downstream of the first one in opposite direction and encodes for PhaF and PhaI, two phasins (Mezzina *et al.* 2021). Besides naturally produced biodegradable polymers, nowadays also synthetic biodegradable polymers are becoming more popular. These include, among others, polyesters such as PLA (Avérous 2008) or some PU (Liu *et al.* 2021). The development of biodegradable polymers is limited by the small number of monomers and chemical bonds available and the conflicting requirements for polymer performance, *e.g.* tensile strength and biodegradability. Consequently, there is an urgent need for precise customisation of polymers, achieved by combining different monomers, as in PBAT (Larrañaga *et al.* 2019). Therefore, the focus changed to the development and production of co-polyester of aliphatic and aromatic compounds such as poly(butylene succinate-*co*-terephthalate) (PBST) or PBAT. PBAT is a mainly fossil-based synthetic polymer produced by polycondensation of combinations of diols, such as 1,4-butanediol (BDO), and dicarboxylic acids, such as adipic acid (AA) and terephthalic acid (TA), while some of the components, such as BDO, can already be produced bio-based (Okada 2002; Zhu *et al.* 2022). The exact ratio between AA and TA determines the mechanical and biodegradable

properties (Herrera *et al.* 2002). It is known from several application in packaging material (Jian *et al.* 2020a; Pereira da Silva *et al.* 2017), biomedical fields (de Castro *et al.* 2016; Santana-Melo *et al.* 2017), and the agricultural industries (Nelson *et al.* 2020). In contrast to other polyesters, such as PET or polybutyleneterephthalate (PBT), which are resistant to hydrolysis at low temperatures (Kint *et al.* 1999), PBAT is 100 % biodegradable. In nature, degradation takes place either via enzymatic biodegradation by bacteria, fungi or algae or via abiotic degradation, for example thermal, mechanical or chemical degradation (Shah *et al.* 2008). During enzymatic depolymerization, microorganisms first secrete enzymes such as esterases, cutinases or lipases, which attach to the polymer and catalyze the hydrolysis of the ester bound. As a result, the polymer is broken down into water-soluble monomers and short- or long-chain oligomers, which are further metabolized by microbial cells (Shah *et al.* 2014). These polymers could play a huge role in a circular economy, since they offer a much easier feedstock recycling und thus their monomers could be used as substrate for biotechnological production of various compounds. However, this requires a change in the current recycling industry, which still recycles the majority of plastics through mechanical recycling. Due to the high similarity of the newly introduced biodegradable polymers and the substitution of conventional plastics, as it is the case with PLA and PET, these polymers are considered contaminants in current recycling streams. Mixing PLA and PET waste during recycling could degrade the quality of the recycled PET and prevent the material from being reused (La Mantia *et al.* 2011). This underlines the importance of not only developing new polymers, but also new efficient recycling technologies tailored to each polymer, such as specific enzymatic feedstock recycling with additional bio-upcycling of the resulting monomers.

1.5. Bio-based production and biodegradation of important monomers for bioplastic

On the way to a sustainable bioplastic, as mentioned above, the focus should be on both bio-based production and biodegradation. This also applies to the individual monomers required for polymerisation or those derived from feedstock recycling of waste materials. Therefore, more and more effort is being put into bioproduction based on biocatalysis of conventional monomers, most of which are derived from fossil resources. In addition, complete monomer consumption by microorganisms also plays a key role in the biodegradation of polymers. Sometimes the development of production and

degradation pathways complement each other, as they can run in opposite directions in the cell. In the case of polyester polymers, these monomers are mainly aliphatic and aromatic dicarboxylic acids and diols (Figure 1.5.1).

The α,ω-dicarboxylic acids (DCA), in particular medium chain length (mcl)-DCAs such as AA, are important intermediates in the production of polyesters, PUs, and PAs, such as nylon 6,6 (Debuissy *et al.* 2016; Hai *et al.* 2021). Today, AA is still mainly produced from fossil resources via the nitric oxidation process, with an annual global production volume of more than three million tonnes and an expected market size of more than $ 8 billion by 2025 (Rios *et al.* 2021). This describes a two-step oxidation of cyclohexanone and cyclohexanol mixtures derived from benzene with excess of HNO_3 to AA (Castellan 1991). In particular, the final oxidation step emits the by-product nitrous oxide, which has a huge negative impact on the environment (Rios *et al.* 2021). This could be avoided by a biotransformation approach of cyclohexane to AA by using an engineered *P. taiwanensis* VLB120 strain (Bretschneider *et al.* 2022).

In 2012, AA was selected as a prime candidate for a bio-based production. Therefore, much effort has been put into the development of sustainable production routes of AA (de Jong *et al.* 2012). This could be achieved by different metabolic pathways depending mainly on the substrate. One approach is the production of AA from acetyl-CoA and succinyl-CoA, derived from glucose or other substrates metabolized via the TCA-cycle, via a reverse pathway similar to the AA degradation pathway described in *Acinetobacter baylyi* (Parke *et al.* 2001). By heterologous expression of this synthetic pathway in *E. coli*, Yu *et al.* (2014) were able to produce up to $639 \pm 34\,\mu g\,L^{-1}$ from $10\,g\,L^{-1}$ glucose. By using a similar pathway in the native AA producer *Thermobifida fusca* B6, Deng *et al.* (2015) were able to produce up to $2.23\,g\,L^{-1}$ AA from $50\,g\,L^{-1}$ glucose. Furthermore, production of AA is also described *via cis*, *cis*-muconic acid or glucaric acid, which could be derived from benzoate or glucose (Polen *et al.* 2013). Both compounds are then converted to AA *via* catalytic hydrogenation (Cheong *et al.* 2016; Kohlstedt *et al.* 2018; Kruyer *et al.* 2017). Using longer chain substrates, like fatty acids, it is also possible to produce AA *via* β-oxidation and /or reverse β-oxidation with additional ω-oxidation (Rios *et al.* 2021). A β-oxidation step is also part of the microbial degradation of AA, which was initially described in *A. baylyi*. In this species the responsible genes *dcaAKIJP* and *dcaECHF* are clustered in to separate operons. Both operons are involved in this pathway, whereby AA is first activated to adipyl-CoA by a CoA transferase which is encoded by *dcaIJ* (Parke *et al.* 2001). The following step is a β-oxidation step done by an acyl-CoA dehydrogenase, an enoyl-CoA

hydratase and a hydroxyacyl-CoA dehydrogenase which are encoded by *dcaA*, *dcaE*, and *dcaH*. As a last step the thiolase DcaF degraded 3-oxoadipyl-CoA into acetyl-CoA and succinyl-CoA. DcaK is the transporter, which responsible for AA transport and *dcaP* encodes for a potential porin (Parke *et al.* 2001). Other Gram-negative bacteria like Pseudomonads, which shares some homologs, are not able to natively degrade AA or other mcl-DCAs (Ackermann *et al.* 2021). While AA is the most commonly

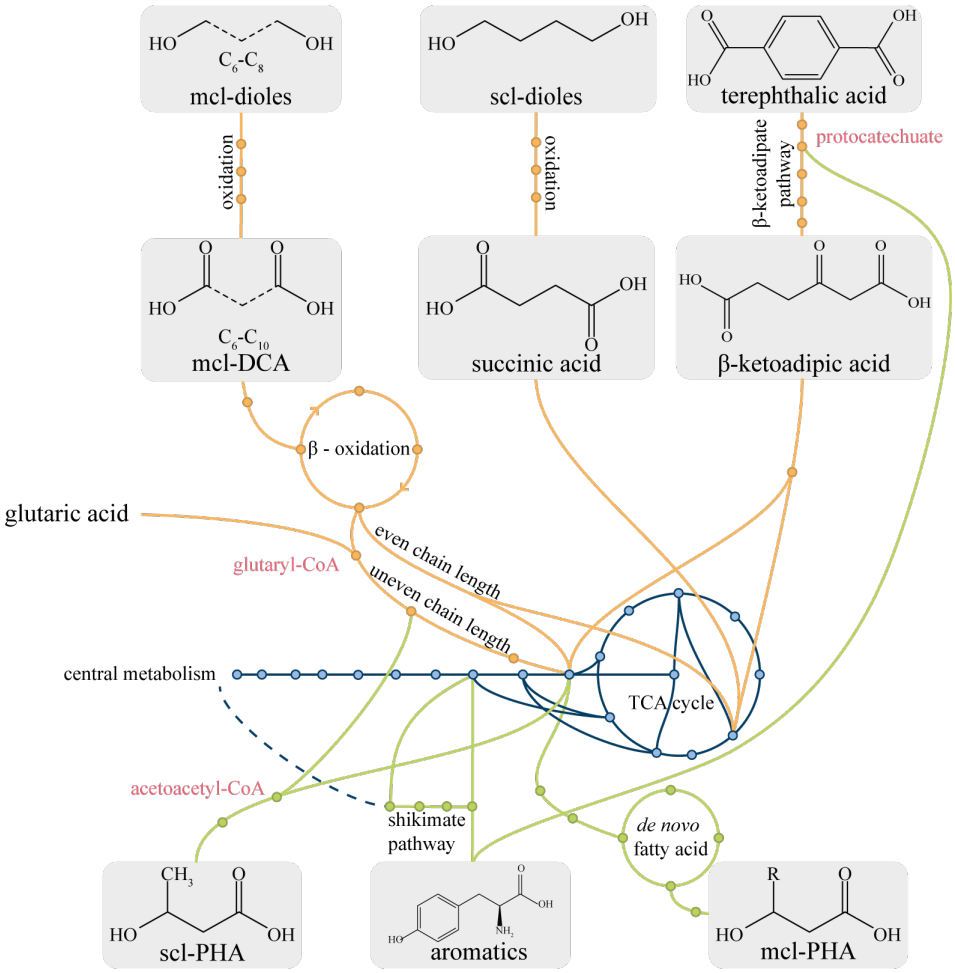

Figure 1.5.1.: Schematic overview of the pathways for degradation and production. Degradation pathways of different plastic monomers are shown in orange. Central metabolism is visualized in blue. Shared intermediates are marked in red. Pathways for production of compounds of interest, such as scl- or mcl-PHAs or aromatic compounds, are shown in green.

used DCA, smaller DCAs such as succinic acid (SA) or glutaric acid (GA) are also important building-blocks and thus part of a potential monomer mixture after depolymerisation. SA is produced by a wide variety of wildtype microorganisms, as it is part of the oxidative tricarboxylic acid (TCA), the glyoxylate and the reductive TCA cycles. However, only the last cycle is able to accumulate succinate efficiently, while the other cycles mostly use SA as an intermediate. The reductive TCA cycle has the advantage of producing two molecules of SA from a C_6-substrate by adding two molecules of CO_2. The other two pathways lose carbon in form of CO_2 and are thus not optimal for fermentation yield (Mancini *et al.* 2019; Nghiem *et al.* 2017; Okino *et al.* 2008). In terms of biodegradation, the oxidative pathways allow a wide variety of bacteria to grow on SA as sole carbon source and allow for rapid degradation of SA. This is similar in the case of glutarate, which is also a metabolic intermediate in bacteria and is part of the degradation of several amino acids such as L-tryptophan or L-lysine (Blázquez *et al.* 2008; Revelles *et al.* 2005). Two different pathways, one CoA-dependent and one independent, have been described in bacteria. For the CoA-independent pathway, glutarate is first hydrolysed to L-2-hydroxyglutarate *via* CsiD, then further oxidized by membrane-associated LhgO to α-ketoglutarate, and finally converted into SA by CsiD (Knorr *et al.* 2018). In addition to that, *via* the CoA-dependent pathway, glutarate is first activated by a CoA-transferase to glutaryl-CoA and then further decarboxylated by GcdH to crotonyl-CoA. Crotonyl-CoA can then be converted *via* acetoacetyl-CoA into two acetyl-CoA molecules (Zhang *et al.* 2019).

Besides the aliphatic DCAs, aromatic DCAs are also important building blocks in the polymer chemistry. They are important for the physical and mechanical properties of the final polymer. TA is the most widely used aromatic DCA and is produced by an oxidation process from fossil *p*-xylene obtained from the fractional distillation of naphtha (Lapa 2023). In order to produce more sustainable polymers, the demand for bio-based TA is increasing. Therefore, different chemical and biotechnological processes are developed. In 2022 Gian *et al.* (2022) were able to show the potential of a biochemical route through the Diels-Alder reaction and a thermochemical route through fast pyrolysis for a more sustainable production of bio-based TA from *Miscanthus* by a comparative life cycle assessment. Both processes aim the production of a bio-based *p*-xylene. Besides the drop-in replacement of the precursor *p*-xylene, Neaţu *et al.* (2016) could successfully demonstrate the production of TA from *p*-cymene, which is produced from biodegradable terpenes, limonene or eucalyptol. Although aromatic compounds inside the polymer chain are important for the polymer properties, this often correlates

with less biodegradability of the polymer. Therefore, towards a more sustainable polymer based on TA, not only a bio-based production but also an environmentally friendly degradation of TA is necessary. In the past, bacterial degradation has been described in several organisms (Choi *et al.* 2005; Narancic *et al.* 2021; Schläfli *et al.* 1994; Wang *et al.* 1995). They all share a similar pathway for the degradation of TA, which starts with the dioxygenation of TA into 1,2-dihydroxy-3,5-cyclohexadiene-1,4-dicarboxylate (DCD) followed by a decarboxylation step to protocatechuate (PCA) (Figure 1.5.1). Three pathways have been described for the degradation of PCA. The most common route is *via* the β-ketoadipate pathway (Stainer *et al.* 1973). Therefore, *ortho*-cleavage of PCA is catalyzed by the protocatechaute 3,4-dioxygenase, encoded by *pcaGH* into β-carboxy-*cis*-*cis*-muconate and then further degraded *via* β-ketoadipate to SA and acetyl-CoA (Harwood *et al.* 1996). The other two pathways include the *meta*-cleavage catalysed by PCA 2,3-dioxygenase (Crawford *et al.* 1979) or the *para*-cleavage catalysed by PCA 4,5-dioxygenase (Dagley *et al.* 1960).

In addition to dicarboxylic acids, α, ω-diols also play a major role in many industrial applications. Like most of the DCAs described above, diols are also produced from fossil resources, hence alternative routes are being developed. Unfortunately, the most common aliphatic diol, 1,4-butanediol, is not naturally produced by any known organism, so synthetic metabolic routes are required for a sufficient biotechnological production (Yim *et al.* 2011). Using these synthetic routes *de novo* synthesis of BDO from renewable feedstock's, such as D-xylose or glucose has been established (Liu *et al.* 2015; Yim *et al.* 2011). The biotechnological degradation of BDO is well described by Li *et al.* (2020). They used adaptive laboratory evolution to optimize the growth of *P. putida* KT2440 on BDO. A direct oxidation of BDO *via* 4-hydroxybutyrate to succinate seems to be the advantageous route, but they also described an alternative β-oxidation pathway leading to glycolyl-CoA and acetyl-CoA that could be active (Li *et al.* 2020) (Figure 1.5.1). However, degradation of longer diols, such as 1,6-hexanediol, 1,7-heptanediol or 1,8-octanediol is still challenging and is focus of the work of this thesis.

The degradation of these plastic monomers, which could be part of a depolymerized mixed plastic waste stream, is the focus of many biotechnological studies, because they have great potential for a bio-upcycling approach that would bring us closer to a circular economy.

1.6. Bio-upcycling of plastic waste streams

The problem with most established industrial recycling processes is that the product loses value during the recycling process. This downcycling results in the need for new virgin polymers and thus new fossil resources. For an efficient circular economy it is important to maintain quality (and thus value) in the product or, in the best case, to increase the industrial value during recycling. This requires, in addition to the degradation of monomers and oligomers after chemical or enzymatic feedstock recycling, the high-yield production of high-value compounds (Figure 1.5.1).

Previous studies have successfully demonstrated the bio-upcycling of PET into high-value aromatic compounds. Kim *et al.* (2019) combined a chemical hydrolysis process with a separation step to obtain high purity ethylene glycol and terephthalic acid (Kim *et al.* 2019). Both monomers were used separately as a carbon source for *Gluconobacter oxydans* and metabolically engineered *E. coli*, to produce either glycolate from ethylene glycol or aromatic compounds derived from protocatechuate or catechol from terephthalate (Kim *et al.* 2019). To avoid the expensive separation step for both monomers, a biological funneling approach may be of interest. This involves the consumption of a variety of monomers by either a single strain or a consortium of different microorganisms through combined metabolic pathways. To this end, Tiso *et al.* (2021) performed an adaptive evolution experiment to enable the growth of the native TA-degrading *P. umsongensis* GO16 on ethylene glycol to produce products of high biotechnological potential, such as PHAs or HAAs form hydrolyzed PET. In combination with chemocatalytic glycolysis, Werner *et al.* (2021) demonstrated the bio-upcycling of PET to β-ketoadipate, which was used to synthesize a nylon 6,6 analogue. They used a genetically engineered *P. putida* strain capable of degrading the monomers resulting from the chemocatalytic process, such as TA and ethylene glycol, but also bis(2-hydroxyethyl) terephthalate (BHET) and mono(hydroxyethyl) terephthalate (MHET). Unlike PET, other polymers may contain some toxic additives or monomers that could limit the bio-upcycling potential. To overcome this, a mixed culture containing a specific strain able to degrade these toxic compounds could be feasible, as Utomo *et al.* (2020) did for the utilization of the toxic PU monomer 2,4-toluenediamine (TDA). Another option to avoid these toxic challenges could be an additional chemical separation process. Eberz *et al.* (2023) were able to selectively separate toxic diamines from a PU hydrolysate, to the point that they were no longer toxic for *P. putida*.

These results suggest the high potential of biological funneling for bio-upcycling of plastic waste material. By broadening the potential substrate spectrum for biological

funneling, this process could not only be feasible for single polymers with different monomers, but also offer a good chance to efficiently recycle mixed plastic waste streams without a complex separation step. In the case of the described quality loss of recycled PET due to PLA contamination, the additional expression or prior addition of PLA degrading enzymes, could funnel both polymers into one product (La Mantia *et al.* 2011; Zaaba *et al.* 2020).
Biological funneling is not an exclusive solution to the plastic waste crisis, but is also well-established in biomass conversion, for example from lignin or cellulose. In the case of lignin valorization, an alkaline pre-treatment is required, resulting in a solid phase consisting of polysaccharides and an alkaline pre-treated liquor. The polysaccharides are converted *via* known routes such as enzymatic hydrolysis and additional fermentation of the released sugar monomers. The alkaline liquor contains a high heterogeneity of different monomers, dimers, and trimers, with the main components being aromatic compounds such as *p*-coumaric acid, vanillic acid, and ferulic acid. All of these compounds were biologically funneled by *P. putida* KT2440 into the aromatic intermediate protocatechuate and then further converted into PHAs (Linger *et al.* 2014).
In addition to upcycling plastic waste into new bioplastics, another interesting product could be aromatic compounds. Aromatic compounds are important bulk and fine chemicals with a wide range of applications in the food, feed and pharmaceutical industries. The majority of aromatics are currently produced from fossil resources, so a raw material substitution represents a major change towards more sustainability. In the past, many bacteria have been successfully engineered to produce aromatic compounds, highlighting their potential for a bio-upcycling approach (Schwanemann *et al.* 2020; Wang *et al.* 2018).

1.7. Pseudomonas as biotechnological chassis

For an efficient bio-upcycling approach, it is important to have a suitable biotechnological host. As shown above, Pseudomonads have already demonstrated their high potential for bio-upcycling in the past, as they are already able to degrade a wide range of plastic monomers (de Witt *et al.* 2023; Franden *et al.* 2018; Li *et al.* 2020; Narancic *et al.* 2021; Utomo *et al.* 2020) and produce high value compounds (Davis *et al.* 2013; Kenny *et al.* 2008; Schwanemann *et al.* 2020; Tiso *et al.* 2020b). The factors resulting in their high potential are manifold and include their robustness, rapid growth, amenability to genetic modification and non-pathogenicity.

The genus Pseudomonas belongs to the Gram-negative γ-proteobacteria and is ubiquitous in a wide variety of niches. Species in this genus are studies for their medical, agricultural, and environmental relevance, with the main focus on the human pathogen *P. aeruginosa* PAO1 (Reynolds *et al.* 2021), the plant pathogen *P. syringae* (Xin *et al.* 2018), the plant growth-promoting *P. stutzeri* (Pham *et al.* 2017) or *P. fluorescens* (Preston 2004) and the non-pathogenic soil bacteria *P. putida* (Volke *et al.* 2020), which is of particular interest in biotechnology. Pseudomonads also include a wide range of highly stress-tolerant species.

One of the reasons for them being of great interest in biotechnological processes is their high chemical stress tolerance, which offers many advantages in approaches such as biodegradation or bio-upcycling of mixed plastic waste. To achieve this high tolerance, Pseudomonads have developed a variety of mechanisms to manage different external stressors in their ecological niche (Bitzenhofer *et al.* 2021). These start at the outer or cytoplasmic membrane to prevent toxic compounds from entering the cell. Thereby Pseudomonads, among other Gram-negative bacteria, use outer membrane vesicles to increase their membrane hydrophobicity. This results in an improved biofilm or microcolony formation and thus increased stress tolerance. Another strategy to prevent penetration of toxic compounds is to modify the cytoplasmic membrane. Thereby, a *cis-trans*-isomerase converts *cis*-unsaturated fatty acids into their *trans* configuration (Eberlein *et al.* 2018; Heipieper *et al.* 2003).

Even in cases where harmful chemicals manage to cross the membrane or are synthesised by the Pseudomonads themselves, possibly by biotechnological means, these organisms have inherent strategies to mitigate the effects of such compounds. This is why different Pseudomonads show variations in their efflux pump systems. An important role in the extrusion of toxic molecules is played by the three efflux pumps TtgABC, TtgDEF and TtgGHI, which belong to the resistance-nodulation-division (RND) family. These so-called toluene tolerance genes have been well studied and are responsible for the majority of toluene resistance in *P. putida* DOT-TIE (Rojas *et al.* 2001). However, TtgABC, which is constitutively expressed and not induced by toluene, is mainly involved in extrusion of several antibiotics. In contrast, TtgDEF, which shows a high similarity on the protein level towards TtgABC, is involved in adaptive toluene tolerance and is able to export toluene from the cell. This pump is linked to the *tod* genes, which encode for a toluene degradation pathway, enabling the cells to grow on toluene as sole carbon source (Rojas *et al.* 2001). In addition, TtgGHI plays a key role in innate and inducible toluene tolerance and the corresponding operon

is highly expressed after induction with toluene (Rojas *et al.* 2001). This is also the reason why the solvent-tolerant *P. taiwanensis* VLB120 strain, which lacks TtgDEF, is able to tolerate aromatic and aliphatic solvents such as toluene, styrene or *n*-octanol (Köhler *et al.* 2013). In contrast, *P. putida* KT2440 lacks TtgDEF and TtgGHI, making this strain solvent-sensitive (Bitzenhofer *et al.* 2021).
In addition, if the cell was not successful in keeping the toxic compounds out of the cells, Pseudomonads can also minimize intracellular damage. Besides the bacterial SOS system, which is essential for DNA damage repair (Maslowska *et al.* 2019), a variety of redox enzymes enable the elimination of reactive compounds. In particular, highly reactive aldehydes, such as 5-hydroxymethylfurfural or vanillin, can be rapidly converted to less reactive alcohols or acids, whereas Pseudomonads mainly use oxidative deactivation (Simon *et al.* 2014; Xu *et al.* 2020).
In order to achieve an optimized biotechnological approach, numerous chassis tailored for diverse applications have been previously engineered, all originating from distinct Pseudomonads. As a first beneficial step, unnecessary biological functions of the cell are often deleted to reduce the metabolic burden and increase energy availability for production of compounds of interest. In 2015 Lieder *et al.* (2015) published a genome-streamlined *P. putida* KT2440 strain that outperformed the parental wildtype strain in many parameters, such as growth rate, biomass yield and amount of compounds produced. A few years later, Wynands *et al.* (2019) engineered a genome-reduced chassis (GRC) strain based on the solvent-tolerant *P. taiwanensis* VLB120. Here, they deleted large proviral segments and the megaplasmid pSTY, as well as genes that allow the cells to swim and form biofilms, resulting in higher growth rates, biomass yields and increased solvent tolerance. Since the solvent efflux pump TtgGHI is encoded on the megaplasmid pSTY, the encoding genes were genomically integrated without (GRC2) and with (GRC3) the regulatory genes (Wynands *et al.* 2019).
Previously, this genome-reduced chassis strain was successfully engineered as a *de novo* producer of phenol (Wynands *et al.* 2019) and other tyrosine-derived aromatics (Wynands *et al.* 2023), demonstrating great potential for a bio-upcycling approach. In order to produce high-value aromatic compounds with Pseudomonads, it is important to delete catabolic pathways, as most Pseudomonads have a high diversity of aromatic degrading pathways (Jimenez *et al.* 2002). This results in a tyrosine-overproducing strain harbouring five deletions (annotated as $\Delta 5$) involved in the (hydro)aromatic degradation pathways. These include the deletion of *hpd* and *pobA*, resulting in strains unable to grow on 4-hydroxybenzoate and tyrosine as sole carbon sources. In addition,

three homologs of 3-dehydroshikimate dehydratase (QuiC) were deleted to prevent the conversion of 3-dehydroshikimate to protocatechuate and thus increase the carbon flux via chorismate. To further increase the supply of phosphoenolpyruvate precursors, the *pykA* gene coding for pyruvate kinase A was deleted (Wynands *et al.* 2019). For an optimized tyrosine accumulation three other amino acid substitutions were described. AroF-1^{P148L} and PheA^{T310I} lead to increased feedback inhibition and thus enhance the flux towards tyrosine (Weaver *et al.* 1990; Wynands *et al.* 2018). On the other hand, the third substitution of an amino acid, namely TrpE^{P290S}, is thought to reduce the activity of anthranilate synthase, the enzyme responsible for an important reaction in tryptophan synthesis. This mutation leads to a reduced consumption of metabolites for the production of unwanted tryptophan and a decrease in intracellular tryptophan levels. The reduced intracellular tryptophan concentration is likely to relieve feedback regulations that inhibit the shikimate pathway. It may also lead to increased transcription of genes involved in the shikimate pathway. Consequently, this could increase the metabolic flow towards tyrosine (Wierckx *et al.* 2008).

1.8. Scope of this thesis

To combine the biotechnological potential for the production of high-value compounds of *P. putida* KT2440 and *P. taiwanensis* VLB120, the overall aim is to extend the substrate spectrum of both strains to efficiently degrade different plastic monomers from mixed plastic waste streams to establish a bio-upcycling approach with a focus on monomers from PBAT.

Therefore, in chapter two the growth of *P. putida* KT2440 on adipate and other (mcl)-DCAs as sole carbon source is enabled by reverse engineering based on whole genome sequencing results of strains selected from an adaptive laboratory evolution experiment. Furthermore, the potential for PHA production from (mcl)-DCAs as a carbon source was analyzed.

Upon enabling growth, in chapter two, it was observed that DCAs of uneven chain length were metabolized much less efficiently. Chapter three therefore focuses on the degradation of (mcl)-DCAs of uneven chain length, with particular emphasis on pimelate. Furthermore, the knowledge gained from uneven chain DCAs will be combined with the degradation pathways of (mcl)-diols to obtain efficient degradation of uneven chain diols. With the resulting strains, monomer mixtures of different DCAs and diols will be degraded and potential PHA production is analyzed.

In addition to bio-upcycling into new polymers, such as PHA, the production of aromatic compounds from plastic monomers is also of interest. Therefore, chapter four focuses on the degradation of adipate and 1,4-butanediol with the aromatic overproducer *P. taiwanensis* GRC3Δ5-TYR2 and the production of tyrosine from these monomers.
To complete the bio-upcycling of all PBAT monomers with *P. taiwanensis*, chapter five focuses on the bioconversion of terephthalate to protocatechuate using adipate or 1,4-butanediol as an additional carbon source. Furthermore, a *de novo* protocatechuate production from glucose as carbon source is established, to also degrade other monomers from widely used PBAT/starch blends.
In general, this thesis will contribute to the efficient bio-upcycling of plastic monomers by characterising different degradation pathways of plastic monomers and producing aromatic precursors, such as tyrosine or protocatechuate, for the production of high-value compounds.

2. Publications and manuscripts

This chapter consists of four manuscripts that have either been published or are about to be published in peer-reviewed journals. The work presented here is the result of collaborations with various working groups within the EU project Mix-UP and other collaborations that have resulted in joint publications.
Contributions of the authors to the respective manuscripts were described using the 'Contributor Roles Taxonomy (CRediT) (Allen *et al.* 2019).

2.1. Engineering adipic acid metabolism in *Pseudomonas putida.*

Yannic S. Ackermann[*], Wing-Jin Li[*], Leonie Op de Hipt, Paul-Joachim Niehoff, William Casey, Tino Polen, Sebastian Köbbing, Hendrik Ballerstedt, Benedikt Wynands, Kevin O'Connor, Lars M. Blank, Nick Wierckx
[*]these authors contributed equally to this study.

Metabolic Engineering, 67 (2021) 29–40, j.ymben.2021.05.001
The online version may be found at: 10.1016/j.ymben.2021.05.001
status: published

CRediT authorship contribution statement:
Yannic S. Ackermann: Methodology, Investigation, Validation, Formal analysis, Data curation, Writing—original draft, Writing—review and editing, Visualization
Wing-Jin Li: Methodology, Investigation, Validation, Formal analysis, Data curation, Writing—review and editing
Leonie Op de Hipt: Investigation, Writing—review and editing
Paul-Joachim Niehoff: Investigation, Writing—review and editing
William Casey: Methodology, Investigation, Validation, Formal analysis, Data curation, Writing—review and editing
Tino Polen: Methodology, Formal analysis, Data curation, Writing—review and editing
Sebastian Köbbing: Methodology, Investigation, Validation, Formal analysis, Data curation, Writing—review and editing
Hendrik Ballerstedt: Methodology, Investigation, Writing—review and editing
Benedikt Wynands: Methodology, Writing—review and editing, Supervision
Kevin O'Connor: Resources, Data curation, Writing—review and editing, Supervision, Project administration, Funding acquisition
Lars M. Blank: Conceptualization, Resources, Data curation, Writing—review and editing, Supervision, Project administration, Funding acquisition
Nick Wierckx: Conceptualization, Resources, Data curation, Writing—original draft, Writing—review and editing, Visualization, Supervision, Project administration, Funding acquisition

Overall, own contribution: 45 %

The presented experimental work was conducted by YSA, WJL, LO, PN, WC, TP, SK, HB. Validation was done by YSA, WJL, WC, TP, SK, BW and NW. Visualization of all data was performed by YSA. The writing of the original draft was done by YSA and WJL, which was reviewed and edited by NW and all co-authors. Funding for the project was acquired by LMB, KO, NW.

2.1.1. Abstract

Bio-upcycling of plastics is an upcoming alternative approach for the valorization of diverse polymer waste streams that are too contaminated for traditional recycling technologies. Adipic acid and other medium-chain-length dicarboxylates are key components of many plastics including polyamides, polyesters, and polyurethanes. This study endows *Pseudomonas putida* KT2440 with efficient metabolism of these dicarboxylates. The *dcaAKIJP* genes from *Acinetobacter baylyi*, encoding initial uptake and activation steps for dicarboxylates, were heterologously expressed. Genomic integration of these *dca* genes proved to be a key factor in efficient and reliable expression. In spite of this, adaptive laboratory evolution was needed to connect these initial steps to the native metabolism of *P. putida*, thereby enabling growth on adipate as sole carbon source. Genome sequencing of evolved strains revealed a central role of a *paa* gene cluster, which encodes parts of the phenylacetate metabolic degradation pathway with parallels to adipate metabolism. Fast growth required the additional disruption of the regulator-encoding *psrA*, which upregulates redundant β-oxidation genes. This knowledge enabled the rational reverse engineering of a strain that can not only use adipate, but also other medium-chain-length dicarboxylates like suberate and sebacate. The reverse engineered strain grows on adipate with a rate of $0.35 \pm 0.01\,\mathrm{h}^{-1}$, reaching a final biomass yield of $0.27\,\mathrm{g_{CDW}\,g_{adipate}}^{-1}$. In a nitrogen-limited medium this strain produced polyhydroxyalkanoates from adipate up to 25 % of its CDW. This proves its applicability for the upcycling of mixtures of polymers made from fossile resources into biodegradable counterparts.

2.1.2. Introduction

Production of plastics reached 359 million tons in 2018 and is almost completely based on fossil resources. By 2050 the plastics industry will have produced an average of 500 million tonnes per year consuming 20 % of total oil production (World Economic Forum *et al.* 2016; Geyer *et al.* 2017). Plastics have a wide range of advantageous properties such as flexibility, durability, and light weight. However, most plastics are extremely stable, and without good end-of-life management they will accumulate in all major terrestrial and aquatic ecosystems on the planet (Andrady *et al.* 2009; Narancic *et al.* 2018; PlasticsEurope 2019). The pollution of plastic has recently been highlighted as a global crisis at every stage, from production to disposal and incineration (RameshKumar *et al.* 2020). Ideally, a fully circular economy is realized where all plastic is recycled with no leakage to the environment. However, this is unrealistic, and surely far from the current reality, in which only a small fraction of plastics is recycled (PlasticsEurope 2019). Even if all waste would be collected, a lack of economically viable recycling options for many plastic waste streams currently limits useful retention of carbon in the cycle. There is therefore a strong need for new technologies especially for the recycling of impure mixed waste streams, as well as for thermoset polymers like polyurethane foams that are not amenable to mechanical recycling. In addition, wear and tear of microplastics from, e.g. tire friction or washing will invariably lead to a certain level of environmental pollution. One possible way to ameliorate the problem of plastic pollution is the development of biodegradable polymers. These likely remain in the environment for a shorter time, although environmental degradation should always be considered an "emergency" last resort (Wei *et al.* 2020). The development of chemical (Meys *et al.* 2020; Rorrer *et al.* 2019; Vollmer *et al.* 2020) and biological (Narancic *et al.* 2020; Wei *et al.* 2020) plastic depolymerization processes has recently enabled a qualitatively new way of recycling. Major advances have been made in the depolymerization of polyesters (Knott *et al.* 2020; Tournier *et al.* 2020; Westhues *et al.* 2018), polyurethanes (Magnin *et al.* 2020) and polyamides (Kumar *et al.* 2020). Biodegradable polymers, like polyhydroxyalkanoate (PHA) and polybutylene adipate terephthalate (PBAT) are especially amenable to this approach, since they are by definition easier to depolymerize. In the case of mixed waste streams, depolymerization of plastic waste will yield a complex mixture of plastic monomers with terminal alcohol, carboxylic acid, and amine groups, the separation and purification of which may not always be economical. In this case, biological funneling is a powerful approach to convert plastic hydrolysates into value-added chemicals (Catur Utomo *et al.* 2020;

Kim *et al.* 2019; Tiso *et al.* 2020b). This bio-upcycling of plastics has recently been heralded as a promising new approach to waste management (Wierckx *et al.* 2015). A prerequisite for the biological funneling of plastic hydrolysates is the efficient microbial metabolism of the contained monomers. In this respect, Pseudomonads are considered highly promising microbial catalysts (Wierckx *et al.* 2015; Wilkes *et al.* 2017). Different non-pathogenic strains of this genus possess favorable intrinsic properties such as high tolerance to chemical stresses and fast and efficient growth (Heipieper *et al.* 2007; Nikel *et al.* 2018; Schwanemann *et al.* 2020; Volmer *et al.* 2014; Wynands *et al.* 2019). The last decade has also seen an explosion of available genetic tools (Aparicio *et al.* 2019; Köbbing 2020; Martínez-García *et al.* 2011; Nikel *et al.* 2014; Zobel *et al.* 2015), enabling deep metabolic engineering for efficient bioproduction (Lenzen *et al.* 2019; Otto *et al.* 2019) and the generation of streamlined chassis strains (Nikel *et al.* 2018; Shen *et al.* 2017; Wynands *et al.* 2019). Pseudomonads are also well known for their metabolic versatility, which already enabled growth on a variety of plastic monomers. *P. putida* KT2440 was naturally capable of growing on diols like ethylene glycol and 1,4-butanediol, but this ability needed to be activated or enhanced by metabolic and/or evolutionary engineering (Li *et al.* 2020; Li *et al.* 2019). Several natural isolates are further capable of degrading styrene (Baggi *et al.* 1983), terephthalate (Narancic *et al.* 2021), and 2,4-toluenediamide (Espinosa *et al.* 2020). One class of compounds that so far cannot be metabolized by Pseudomonads are medium-chain-length (mcl)-dicarboxylates like adipic or sebacic acid. Adipic acid and other mcl-α,ω-dicarboxylates are mainly used in the production of polyamides, polyesters, and polyurethanes. Adipic acid is industrially produced from fossil benzene (Sato 1998), but several microbial production methods have also been developed (Chae *et al.* 2020). Lipids, lignin, and (hemi-)cellulose-derived feedstocks can be utilized to produce muconic or glucaric acid (Bentley *et al.* 2020; Otto *et al.* 2020; Salvachúa *et al.* 2018), which can subsequently be converted to adipic acid via catalytic hydrogenation (Cheong *et al.* 2016; Kohlstedt *et al.* 2018; Kruyer *et al.* 2017; Vardon *et al.* 2015). Further, *E. coli* strains have been developed that can convert glucose directly into adipic acid (Polen *et al.* 2013; Zhao *et al.* 2018). This biosynthesis pathway utilizes a reverse β-oxidation route that is similar to the degradation route for adipic acid (Kallscheuer *et al.* 2017). Microbial degradation of adipic acid and other mcl-dicarboxylates was characterized in *Acinetobacter baylyi* (Parke *et al.* 2001), a robust and versatile Gram-negative soil bacterium used for characterization, evolution, and engineering of enzymes and metabolic pathways (Barbe *et al.* 2004; Pardo *et al.* 2020; Tumen-Velasquez *et al.* 2018). In this species, adipic acid is first activated

to adipyl-CoA, after which it is further metabolized via β-oxidation. The responsible genes are clustered in two operons. One encodes enzymes for the transport (DcaK and DcaP), CoA transferase subunits (DcaIJ), and an acyl-CoA dehydrogenase (DcaA). The other operon (*dcaECHF*) encodes enzymes related to β-oxidation including an enoyl-CoA hydratase, ketoacyl-CoA reductase, hydroxyl-CoA dehydrogenase, and a thiolase (Fischer *et al.* 2008) (Figure 2.1.1).

In this work, the substrate spectrum of *P. putida* KT2440 is expanded to encompass mcl-dicarboxylates like adipic acid. Initial metabolic uptake and activation steps are heterologously inserted using genes from *A. baylyi*, followed by adaptive laboratory evolution to enable and enhance growth. The resulting strains are analyzed by genome re-sequencing and the adipate-metabolizing phenotype is reverse engineered in the wildtype. The resulting strains grow at a rate of $0.31 \pm 0.02\,\mathrm{h}^{-1}$ on adipic acid as sole carbon source, and they can also metabolize other mcl-dicarboxylates like suberic, azelaic, and sebacic acid.

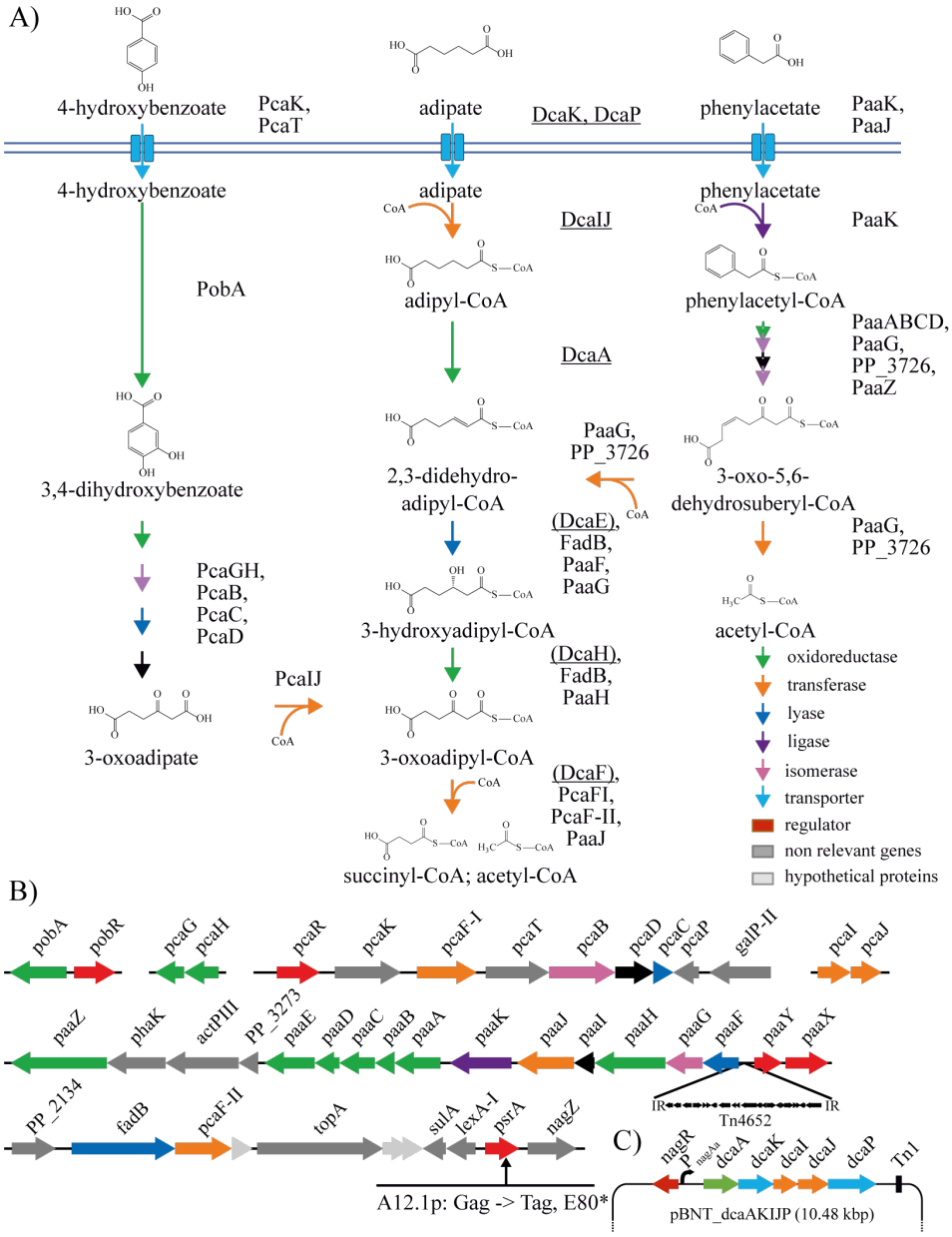

Figure 2.1.1.: Overview of genes and enzymes involved in adipate metabolism. A) Comparison of the adipate metabolic pathway of *A. baylyi* (underlined proteins) with the 4-hydroxybenzoate and phenylacetate pathways from *P. putida* KT2440. B) Genomic organization of genes encoding 4-hydroxybenzoate and phenylacetate pathway enzymes in *P. putida* KT2440. Colors correspond to the encoded enzymes in A. Discovered mutations in ALE strains are shown below the relevant genes. C) Plasmid-based expression cassette of *dcaAKIJP*.

2.1.3. Results and discussion

2.1.3.1. Enabling adipate metabolism by *P. putida* KT2440

Initial growth experiments showed that *P. putida* KT2440 is unable to metabolize adipate as sole carbon source, even after prolonged incubation. In silico comparison of the *P. putida* KT2440 genome to the adipate metabolic enzymes from *A. baylyi* (Parke *et al.* 2001) indicated a partial overlap with the 4-hydroxybenzoate and phenylacetate degradation pathways, starting at the level of 2,3-didehydroadipyl-CoA and 3-oxoadipyl-CoA, respectively (Figure 2.1.1). There are no known *P. putida* homologs of DcaIJ and DcaA. However, a BLAST search with DcaA yielded several hits with putative acyl-CoA dehydrogenases with up to 40 % sequence identity, and the sequences of DcaIJ are 66 % and 62 % identical to the 3 oxoadipyl-CoA transferase PcaIJ of *P. putida* KT2440. The pcaIJ genes are induced by 3-oxoadipate or indirectly by 4-hydroxybenzoate in *P. putida* ATCC12633 (Ornston *et al.* 1976; Parales *et al.* 1993). These metabolites also induce a 3-oxoadipate uptake system that enables adipate import, likely encoded by *pcaT*. However, the same studies also confirm the initial observation that in spite of this, neither the wildtype *P. putida* ATCC12633, nor constitutive transporter mutants, grow on adipate as sole carbon source. Therefore, the *dcaAKIJP* operon from *A. baylyi*, encoding the adipyl-CoA transferase, dehydrogenase, and putative adipate uptake proteins, was overexpressed on vector pBNT-*dcaAKIJP*. In theory, this overexpression completes the genetic inventory of *P. putida* for the metabolism of adipate. However, the resulting *P. putida* KT2440 pBNT-*dcaAKIJP* did not grow on adipate as sole carbon source. This may be attributed to a lack of induction of the native genes encoding the downstream 2,3-didehydroadipyl-CoA metabolic pathway. A similar phenomenon was observed for *P. putida* incubated with ethylene glycol (Li *et al.* 2019). Growth on this substrate was enabled by the addition of the upstream metabolite allantoin, which activated a glyoxylate metabolic pathway fed by the oxidation of ethylene glycol. This misregulation was abolished through adaptive laboratory evolution (ALE), which resulted in mutations that constitutively activated the pathway. We therefore subjected *P. putida* KT2440 pBNT-*dcaAKIJP* to ALE, using a co-feeding scheme of adipate and supporting carbon sources glucose and 4-hydroxybenzoate. 4-Hydroxybenzoate was used to induce the abovementioned *pcaIJ* and *pcaE*, as well as genes like *pcaF-I* and *pcaF-II* via its metabolites protocatechuate and 3-oxoadipate (Parales *et al.* 1993). The latter genes are involved in the degradation of the common intermediate 3-oxoadipyl-CoA (Figure 2.1.1). A stepwise increase in adipate and decrease of supporting carbon sources

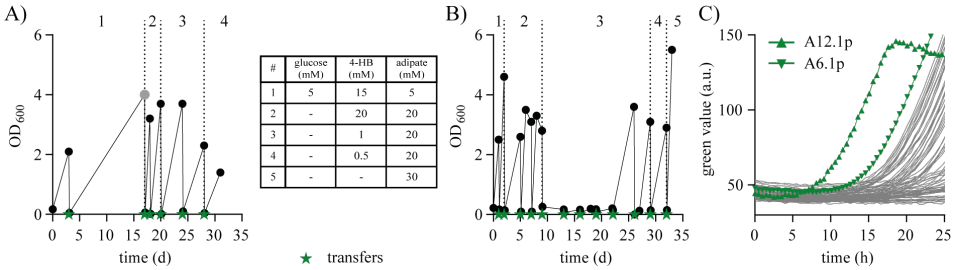

#	glucose (mM)	4-HB (mM)	adipate (mM)
1	5	15	5
2	-	20	20
3	-	1	20
4	-	0.5	20
5	-	-	30

Figure 2.1.2.: Adaptive laboratory evolution of *P. putida* KT2440 pBNT-*dcaAKIJP* on adipate. Sequential batch cultivation to obtain the evolved populations A6p (A) and A12p (B) on MSM medium with the following substrates: (1) 5 mM glucose, 5 mM adipate, 15 mM 4-hydroxybenzoate; (2) 10 mM adipate, 20 mM 4-hydroxybenzoate; (3) 20 mM adipate, 1 mM 4-hydroxybenzoate; (4) 20 mM adipate, 0.5 mM 4-hydroxybenzoate; (5) 30 mM adipate. Each transfer is indicated with a green star. The greyed symbol is an estimated value after visual inspection of a long-term cultivation. C) Growth of 84 single strains isolated from the two ALE batches in two-fold buffered MSM with kanamycin and 30 mM adipate. The strains A12.1p (▲) and A6.1p (▼) were selected for further investigation. Growth was detected via a Growth Profiler using a 96-well plate.

was used to evolve *P. putida* KT2440 with pBNT-*dcaAKIJP* in two individual batches (Figure 2.1.2). No salicylate was added as inducer of the NagR/P_{nagAa} promoter system, which controls the *dcaAKIJP* operon, relying instead on leaky expression of the promoter. This omission provides higher selective pressure on gain-of-function mutations in native genes similar to the heterologously expressed operon, as previous work indicated that an adipate-metabolizing strain might be evolved without the plasmid (Ornston *et al.* 1976) When glucose was supplemented to medium 1 (Figure 2B), the strain grew overnight. The second overnight culture was washed in MSM buffer and used to inoculate medium 2 with 4-hydroxybenzoate and adipate as carbon sources. Growth phases increased to two days reaching OD_{600} 2.6 - 3.5 and could be shortened after three transfers to one day. When 1 mM 4-hydroxybenzoate was co-fed with 20 mM (medium 3) in the A12p culture, optical densities of only 0.16 were reached. This strongly indicates that up to this point adipate was not metabolized. A drastic change was observed after four transfers, which were performed by harvesting the cells and transferring them to fresh medium 3. Subsequent cultures reached high OD_{600} values, which could only be achieved through adipate utilization. The resulting evolved population grew overnight to an OD_{600} of 3.6 on adipate as sole carbon source. Eighty-four strains from evolved cultures were isolated on LB agar plates and tested for growth on adipate (Figure 2.1.2). The fastest growing strains from each batch were selected and called A6.1p and A12.1p (first strain evolved on adipate with 6 or 12 sequential batches harboring a plasmid). Both strains had retained plasmid pBNT-*dcaAKIJP* and were kanamycin resistant. In MSM with

kanamycin, 0.1 mM salicylate as inducer and 30 mM adipate as sole carbon source strain A12.1p grew at a rate of $0.29\,h^{-1}$, which is 2.8-fold faster than A6.1p which grew at a rate of $0.11\,h^{-1}$.

2.1.3.2. Genome sequencing of evolved adipate-metabolizing strains

To understand the molecular basis of the phenotype of the two evolved strains and their plasmids, genome re-sequencing was conducted. Sequencing data are deposited in the NCBI Sequence Read Archive under BioProject number PRJNA464914 with accession numbers SRX9220792 for A6.1p and SRX9220793 for A12.1p. In total 51 mutations were found in A6.1 and 53 mutations in A12.1. As was shown previously for sequenced strains evolved on ethylene glycol and 1,4-butanediol, most of the genomic mutations are also present in our laboratory wildtype and therefore unlikely to contribute to adipate metabolism (Li *et al.* 2020; Li *et al.* 2019). Of the remaining mutations (Table 2.1.1), one prominent phenomenon stood out in both evolved strains. The sequence read coverage for transposon Tn4652 was twice as high as the average genomic coverage. This transposon is known to be activated under stress conditions such as starvation (Ilves *et al.* 2001). It was previously found to play a role in ALE-derived strains growing on ethylene glycol and 1,4-butanediol (Li *et al.* 2020; Li *et al.* 2019). It contains a predicted promoter at its 3´-end and is known for generating novel fusion promoters upon insertion into a new locus (Nurk *et al.* 1993; Teras *et al.* 2000). Arbitrary-primed PCR revealed that this transposon had replicated into a second locus, between *paaFGHIJ* and *paaYX*. The *paa* cluster encodes enzymes responsible for the degradation of phenylacetate, which shows parallel activities to adipate degradation (Figure 2.1.1). In *E.coli*, PaaX is a repressor of *paaZ* and *paaABCDEFGHIJK* (Fernández *et al.* 2014). Phenylacetate is CoA-activated to phenylacetyl-CoA, which binds to PaaX thereby releasing the repression by disassociating from the promoter binding site of PZ and PA (Ferrández *et al.* 2000). The function of PaaY is so far not fully understood. It is thought to inactivate PaaK, the phenylacetate-CoA ligase, by acetylation (Teufel *et al.* 2010).
Additionally, only identified in A12.1p, the *psrA* gene encoding a TetR family transcriptional regulator was mutated (GAG → TAG; E80*). This protein is a homolog to PsrA of P. aeruginosa (protein sequence identity of 85 %), which is a global regulator of β-oxidation that, among others, represses *fadAB* (Fonseca *et al.* 2014; Kang *et al.* 2008). Since *pcaF-II* and *fadB* are close to *psrA*, and these also have high homologies to *fadAB* in *P. aeruginosa*, it is likely that they are also regulated by this transcriptional repressor, and that its disruption activates the expression of these genes (Figure 2.1.1).

Table 2.1.1.: Genomic loci affected by ALE in A6.1p and A12.1p.

Found in strain	affected locus	putative function	mutation (position in genome)	putative effect	Reference
A6.1p, A12.1p	PP_0278	small hypothetical protein	insertion_-_T (336124^336125)	frameshift	Belda *et al.* 2016; Nelson *et al.* 2002
A12.1p	PP_2144	TetR family transcriptional regulator (236 aa)	G→T (2445964)	nonsense E80*	Fonseca *et al.* 2014; Kang *et al.* 2008
A6.1p, A12.1p	PP_2589	aldehyde dehydrogenase	C→T (2958523)	A428V	Kurihara *et al.* 2005
A12.1p	PP_3988	hypothetical protein	deletion_T_-(4498312)	frameshift	Belda *et al.* 2016; Nelson *et al.* 2002
A6.1p, A12.1p	PP_5037	lipocalin family lipoprotein	C→T (5740555)	S175N	Bishop 2000; Flower *et al.* 2000
A6.1p, A12.1p	Tn4652	transposon	17 kb insertion (3719504^3719505)	promoter mutation	Ilves *et al.* 2001; Teras *et al.* 2000

Although *pcaIJ* were induced by 4-hydroxybenzoate during the ALE experiments, no mutations were found in their genomic region. A third mutation found only in A12.1p consists of a frameshift deletion in PP_3988, which affects the last 118 out of the total 682 amino acids of the encoded hypothetical protein of unknown function. However, restoring the wildtype sequence in A12.1 did not affect the growth of this strain on adipate, making it unlikely to be foundational to the phenotype of this strain (Figure S2). Three further mutations were found in both strains (Table 2.1.1), but these were also deemed of lower priority due to their marginal putative effect or the lack of any apparent relation to adipic acid metabolism. Besides genomic mutations, the plasmid of A6.1p contained one missense mutation in the rep gene, which encodes the replication initiator protein of the plasmid (Krüger *et al.* 2014). Mi *et al.* (2016) found similar mutations in the *rep* gene of a related pBBR1 plasmid backbone after ALE with *P. putida*, leading to a lower plasmid copy number which eliminated a plasmid-induced growth defect. Sequence read coverage analysis shows that the plasmid copy number in A6.1p is approximately 3-fold lower than in A12.1p (Figure 2.1.3). Thus, the mutation in

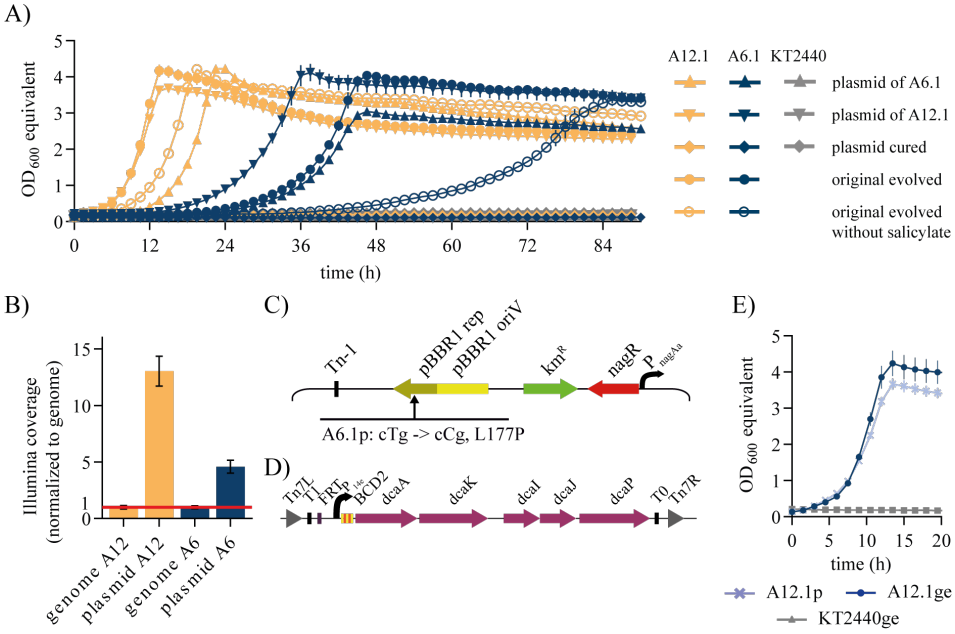

Figure 2.1.3.: Analysis of evolved pBNT-*dcaAKIJP* expression constructs. A) Comparison of growth on adipate of strains A12.1 (orange) and A6.1 (blue) with and without the indicated plasmids. Open symbols indicate omission of salicylate. B) The average sequence read coverage of the plasmids normalized to the genome. C) Mutation in the backbone of plasmid pBNT-*dcaAKIJP*. D) Mini-Tn7 genomic integration construct for constitutive expression of *dcaAKIJP*. E) Growth curves of *P. putida* A12.1 with episomal and genomic expression of the *dcaAKIJP* genes. Growth curves were measured in MSM with 30 mM adipate with the Growth Profiler and the results were converted to an equivalent OD at 600 nm. Error bars indicate the standard error of the mean (n=3 (A), n=5 (E)). (ge = genomically integrated P_{14e}-*dcaAKIJP*; p = pBNT-*dcaAKIJP*).

the *rep* gene of pBNT-*dcaAKIJP* of A6.1p likely reduces the expression of the *dca* operon.

2.1.3.3. Characterization of plasmid effects in evolved adipate-metabolizing strains

The effect of the mutation in the rep gene of the plasmid from A6.1p was investigated by curing the two evolved strains from their plasmids and re-transforming them with plasmids isolated from both strains (Figure 2.1.3A). In the case of A12.1 there is a slight negative effect on growth on adipate from the re-transformation with its own plasmid ($0.26 \pm 0.01\,h^{-1}$) compared to the original evolved strain ($0.29\,h^{-1}$). The growth rate is significantly lower ($0.22\,h^{-1}$) if the plasmid from A6.1p is used. The

opposite effect can be seen in A6.1, whose growth rate increases significantly with the plasmid from A12.1p ($0.12\,h^{-1}$) compared to the original evolved strain ($0.11\,h^{-1}$) and the re-transformed strain ($0.10\,h^{-1}$). However, the A6.1 strain with the plasmid of A12.1 still grew much slower than any of the A12.1 transformants, indicating the effect of additional genomic mutations in the A12 strain background on growth. Omission of salicylate as inducer of the nagR/P_{nagAa} promoter led to much slower growth compared to induced cultures (Figure 2.1.3A). It thus seems that the omission of salicylate in the ALE provided insufficient selective pressure for the emergence of mutations that increased expression or led to gain-of-function of other genes. The mutation in the *rep* gene likely relate to general plasmid instability issues during ALE, as shown by Mi *et al.* (2016), rather than to efficient growth on adipate. In order to avoid the influence of plasmid instability and copy number effects, we therefore opted to integrate the *dcaAKIJP* operon into the genome of *P. putida*. By excluding the variable copy number of the plasmid, the reproducibility and stability of the strain would increase. As additional advantage, no antibiotic selection is needed, thereby providing less metabolic burden. The constitutive synthetic promoter P_{14e} (Zobel *et al.* 2015) was used to drive the expression of the *dca* operon, making salicylate induction unnecessary. The integration of the heterologous genes was carried out using a mini-Tn7 integration construct (Zobel *et al.* 2015), modified to enable marker removal. This provides two main advantages; (I) further genetic modification with the same antibiotic resistance marker is made possible, and (II) application of marker-free strains faces fewer regulatory hurdles in industrial biotechnology. The gentamicin marker in the transposon was replaced by a kanamycin marker flanked by FRT sites, taken from plasmid pBELK (Nikel *et al.* 2013). A second redundant kanamycin marker was removed from the plasmid backbone. Changing the context of synthetic promoters can significantly affect their activity (Köbbing 2020). Therefore, the resulting constructs were validated with different promoters using *msfGFP* as a reporter gene to ensure that the modifications did not affect the activity of downstream promoters (Figure 2.1.4). Indeed, the activity of P_{em7} was decreased by 70 %, in spite of the relatively large distance of 248 bp between the promoter and the modified marker. The activity of the other tested promoters only differed marginally compared to the original construct. In the case of P14e this difference was not significant ($p = 0.2726$), making the generated marker-recycling vector suitable for reliable genomic gene expression. The influence of genomic expression of P_{14e}-*dcaAKIJP* using the Tn7 construct (designated as "ge") was tested in strain A12.1 (Figure 2.1.3). Strain A12.1ge ($0.33 \pm 0.01\,h^{-1}$) grew at a similar

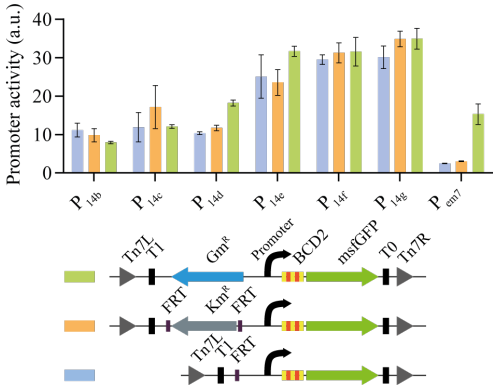

Figure 2.1.4.: Characterization of genomically integrated mini-Tn7 marker recycling constructs in *P. putida* KT2440. The original construct containing a Gm^R marker (green bars) is compared with new versions containing a recyclable Km^R marker flanked by two FRT sites before (orange bars) and after (blue bars) marker recycling. Strains were cultured in a BioLector in minimal medium with 20 mM glucose in a 96 well plate. Identical strains from at least three different transformations were tested, with three biological replicates each. Promoter activity was calculated from the slope of GFP fluorescence to optical density during the exponential phase. Error bars indicate the standard error of the mean (n=9).

rate as the original evolved strain A12.1p induced with salicylate, while a slightly but significantly ($p = 0.0052$) higher final biomass concentration was obtained with A12.1ge. Apparently, the high constitutive expression with the P_{14e} promoter, possibly combined with better translation initiation and mRNA stability caused by the BCD2 element (Zobel *et al.* 2015) was sufficient to counteract the reduced copy number of the genomic construct. Given the additional abovementioned advantages of marker-free genomic integration, the influence of the genomic mutations was further characterized using the genomic expression construct.

2.1.3.4. Characterization and reverse engineering of genomic mutations for adipate metabolism

Plasmid effects alone cannot explain the differences between A6.1 and A12.1, and even with genomic expression of *dcaAKIJP*, wildtype *P. putida* KT2440 cannot grow on adipate as sole carbon source (Figure 2.1.3). This indicates that the discovered genomic mutations are also foundational to efficient growth on adipate. We therefore set out to characterize individual and combined mutations in a reverse engineering approach, starting with wildtype *P. putida* KT2440 with P_{14e}-*dcaAKIJP* integrated into the genome. Because the parallels of adipate and phenylacetate degradation start with

2,3-didehydroadipyl-CoA, initial focus was on the influence of the insertion of transposon Tn4652 between *paaFGHIJK* and *paaYX*. The 17-kb transposon was inserted 104 bp upstream of *paaF*, disrupting a putative P_{paaF} promotor. This disruption leads to the emergence of a putative fusion promoter with the native -10 sequence of P_{paaF} and a -35 sequence located in the mosaic end of the transposon. The putative promotor of *paaYX* remains intact (Figure S1). To mimic the effect of this insertion, the native promotor was exchanged with the strong synthetic constitutive promoter P_{14g} (Zobel *et al.* 2015). Possibly, the large transposon insertion separates the promoter from the unknown binding site of the PaaX repressor. In this case, a promoter exchange alone could still be repressed. To test this hypothesis, a knockout of the *paaYX* regulatory genes, as well as a combined promoter insertion and *paaYX* knockout, was performed. The resulting strains all grow at a similar rate of $0.13\,h^{-1}$ (Δ*paaYX*, ΔP_{paaF}-*paaYX*::P_{14g}) or $0.14\,h^{-1}$ (ΔP_{paaF}::P_{14g}), which is slightly faster than the evolved A6.1p strain but much slower than the reference strain A12.1ge (Figure 2.1.5A). The fact that the knockout of *paaYX*, insertion of P_{14g}, and the combination of both, all enable growth on adipate indicates that either the synthetic promoter P_{14g} is strong enough to drive the transcription of the gene cluster *paaFGHIJK* even in the presence of the PaaX repressor, or that the PaaX binding site overlaps the native P_{paaF} promoter, which was removed during the exchange. The deletion of *paaYX* and/or promoter exchange upstream of *paaF* enable

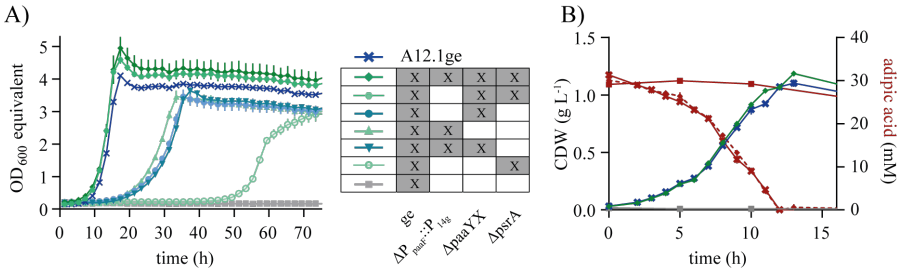

Figure 2.1.5.: Characterization of reverse engineered *P. putida* KT2440ge strains. A) Growth curves measured with the Growth Profiler. KT2440 genotypes are indicated in the table. B) Growth curves of *P. putida* KT2440ge ΔP_{paaF}-*paaYX*::P_{14g} Δ*psrA*, KT2440ge, and A12.1ge measured in 500 mL flasks by offline CDW determination. Adipate concentrations were measured by HPLC (red lines). All strains were cultivated in MSM with 30 mM adipate. Error bars indicate the standard error of the mean (n=3). The abbreviation "ge" denotes genomically integrated marker-free *attTn7*::P_{14e}-*dcaAKIJP*.

growth on adipate, but at a lower rate than that of A12.1ge, indicating that further mutations are necessary to completely mimic the evolved phenotype. As described above, an SNP in *psrA* was only found in A12.1. It is likely that this transcriptional

regulator represses the two genes *fadB* and *pcaF-II*, which may be involved in the metabolism of 2,3-didehydroadipyl-CoA, the common intermediate between adipate and phenylacetate (Figure 2.1.1). The putative repressive effect of PsrA was confirmed by episomal overexpression, which strongly reduced growth of A12.1 on adipic acid (Figure S3). Working on the hypothesis that the nonsense mutation disrupted PsrA, the encoding gene was deleted both in the *P. putida* KT2440ge and in the KT2440ge ΔP_{paaF}-*paaYX*::P_{14g} strains. In the wildtype background, the *psrA* knockout leads to weak growth on adipate. The strain grew at a rate of $0.15 \pm 0.01\,h^{-1}$, but only after a 40-hour long lag phase (Figure 2.1.5A). In contrast, *P. putida* KT2440geΔP_{paaF}-*paaYX*::P_{14g} Δ*psrA* completely mimicked the growth phenotype of the reference strain A12.1ge (Figure 2.1.5A). This result was verified by growth experiments in shake flasks, which also confirmed full metabolism of adipate by both strains (Figure 2.1.5B). Under these conditions the completely reverse engineered strain grew at a rate of $0.35 \pm 0.01\,h^{-1}$, which is similar to that of A12.1ge ($0.34 \pm 0.01\,h^{-1}$). The final biomass reached $1.19 \pm 0.01\,g\,L^{-1}$ after 13 hours (Figure 2.1.5), which corresponds to a yield of $0.27\,g_{CDW}\,{g_{adipate}}^{-1}$.

Taken together, this data show that the degradation pathway of adipate in *P. putida* appears to be a hybrid metabolism involving *dcaAKIJP* from *A. baylyi* and partly redundant downstream β-oxidation pathways encoded by *paaFGHIJK* and *fadB/pcaF-II*. Only the combination of the latter two engineering targets resulted in good growth on adipate as sole carbon source. The requirement of this redundancy fits with RB-TnSeq-analysis of *P. putida* growing on medium chain carboxylates and alcohols (Thompson *et al.* 2020), which could not clearly implicate single enzymes for specific β-oxidation reactions, suggesting that several enzymes may catalyze these steps. Alternatively, the knockout of *psrA* will affect other targets besides *fadB/pcaF-II* (Kang *et al.* 2008), which may also contribute the improved phenotype.

2.1.3.5. Growth of evolved and reverse engineered *P. putida* strains on other mcl-dicarboxylates

A. baylyi can also grow on longer-chain dicarboxylates besides adipate via the DCA pathway (Parke *et al.* 2001). We therefore analyzed the growth of the evolved and reverse engineered *P. putida* strains on glutaric acid (C_5), pimelic acid (C_7), suberic acid (C_8), azelaic acid (C_9), and sebacic acid (C_{10}) (Figure 2.1.6). With the exception of pimelate, good growth was observed for both the ALE strain A12.1ge and the reverse engineered *P. putida* KT2440ge ΔP_{paaF}-*paaYX*::P_{14g} Δ*psrA*. wildtype *P. putida*

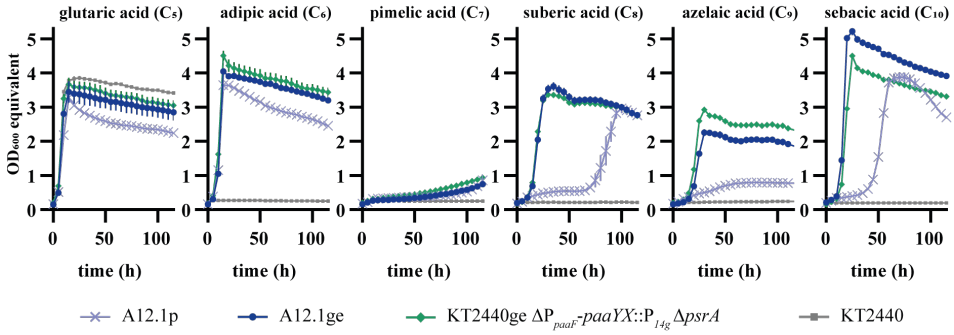

Figure 2.1.6.: Growth of evolved and engineered *P. putida* strains on dicarboxylic acids with different chain lengths. All strains were grown in MSM with the indicated carbon sources at a C-molar equivalent to 30 mM adipate. Cultures of A12.1p further contained 0.1 mM salicylate as inducer. The growth curves were measured with a Growth Profiler and the results were converted to an equivalent OD_{600}. Symbols show every 9th data point. Error bars indicate the standard error of the mean (n=4).

KT2440 only grew on glutaric acid. This C_5 dicarboxylate is converted to succinate via 2-oxoglutarate, and thus not metabolized via β-oxidation (Zhang *et al.* 2018). The fact that only the evolved and/or engineered strains with the heterologous genes from *A. baylyi* grew on the longer-chain dicarboxylates clearly indicates that they are degraded via the same pathway as adipate. In most cases, growth of the strains with the *dca* operon integrated into the genome was similar to that on adipate, although the OD_{max} was higher on sebacate. In contrast, the original ALE-derived strain A12.1p with episomal expression of the dca operon showed impaired growth with an extended lag phase on the longer-chain dicarboxylates, further confirming the detrimental effect of the plasmid-based approach. All strains grew slower and reached lower OD_{max} on the longer uneven chain length azelaate and especially on pimelate, indicating a further misregulation of connecting metabolic pathways, possibly at the point of glutaryl-CoA or malonyl-CoA resulting from β-oxidation of these dicarboxylates (Harrison *et al.* 2005).

2.1.3.6. Production of polyhydroxyalkanoates from adipic acid

Engineering of dicarboxylate-metabolizing *P. putida* strains enables the upcycling of these important plastic monomers into value-added compounds. *P. putida* is an efficient producer of many such compounds (Nikel *et al.* 2018; Schwanemann *et al.* 2020), among which, polyhydroxyalkanoates (PHAs) are a prominent example (Escapa *et al.* 2011; Lee

et al. 2000; Sun *et al.* 2007a). Production of PHAs is especially efficient on substrates, which are metabolized via β-oxidation to yield acetyl-CoA as primary precursor (Fonseca *et al.* 2014; Mezzina *et al.* 2020; Ruiz *et al.* 2019), making them a promising product for the upcycling of adipate and especially longer-chain dicarboxylates. To test the production of PHAs from adipate, the evolved and reverse engineered strains were cultivated in a nitrogen-limited mineral medium (3x buffered) with $3.96\,\mathrm{g\,L^{-1}}$ (27.1 mM) adipic acid (Table 2.1.2). The evolved *P. putida* KT2440 A12.1ge and the engineered KT2440ge $\Delta \mathrm{P}_{paaF}$-*paaYX*::P_{14g} Δ*psrA* reached similar final biomass concentrations. The engineered strain possibly produced more PHA than the evolved strain, but the statistical significance of the difference between these strains is low ($p = 0.086$). Under the conditions tested, the reverse engineered strain produced $25.3 \pm 4.2\,\%$ PHA representing a yield of $9.2\,\%$ ($\mathrm{g\,g^{-1}}$ of carbon) compared with $6.3\,\%$ for the evolved strain. The carbon to PHA yield of the reverse engineered strain compares favorably with previous reported *Pseudomonas* strains grown on 1,4-butandiol (Li *et al.* 2020) and equimolar terephthalic acid and ethylene glycol (Tiso *et al.* 2021) both exhibiting a yield of $3.1\,\%$ ($\mathrm{g\,g^{-1}}$ carbon). The yields are, however, much lower than reported for *P. putida* KT2440 on simple sugars such as glucose under similar flask scale conditions, with greater than $20\,\%$ yield on a carbon basis (Davis *et al.* 2013). The addition of fatty acids, as a cofeed strategy, has been shown to increase PHA productivity and yield in the 1,4 butandiol strains, increasing maximal yield to $9.9\,\%$ with the addition of octanoic acid (Li *et al.* 2020). A similar strategy could be employed to improve PHA production using adipic acid and consequently improve cost efficiency of the process.The original evolved strain A12.1p induced with salicylate performed significantly worse, especially with regard to PHA production, which only reached $8.56\,\%$ of CDW. Unexpectedly, A12.1p performed better without salicylate induction. PHA production was analyzed after 48 h to enable the slower growing uninduced culture to reach maximum production values. However, this also likely caused a longer starvation phase in the other cultures, thereby consuming part of the produced PHA. Previously, the knockout of *psrA* and associated increased β-oxidation activity was shown to cause a shift towards shorter chain lengths in the distribution of PHA monomers (Fonseca *et al.* 2014).
This is likely also the case with the adipate-metabolizing strains. The strain with *psrA* deletion produced a significantly higher fraction of $\mathrm{C_8}$ ($p = 0.029$) and possibly also a lower fraction of $\mathrm{C_{10}}$ ($p = 0.069$) monomers than the control strain *P. putida* KT2440ge $\Delta \mathrm{P}_{paaF}$-*paaYX*::P_{14g} without Δ*psrA*. Since a narrow monomer distribution is important for PHA polymer properties, this information is valuable to guide efficient upcycling,

Table 2.1.2.: Relative monomer composition of PHA polymers produced by strains from adipic acid.

Strain	pH	CDW($g\,L^{-1}$)	PHA (%)	C6 (%)	C8 (%)	C10 (%)	C12 (%)
A12.1p	7.2	0.74 ± 0.02	16.8 ± 3.3	3.6 ± 2.6	30.4 ± 1.3	60.8 ± 2.2	5.2 ± 0.1
A12.1p, induced	7.2	0.65 ± 0.01	8.6 ± 0.8	4.8 ± 0.4	29.5 ± 0.1	60.0 ± 0.4	5.6 ± 0.8
A12.1ge	7.2	0.75 ± 0.01	19.8 ± 0.3	2.8 ± 2.4	33.5 ± 2.3	58.5 ± 2.0	5.2 ± 1.3
KT2440ge ΔP_{paaF}-$paaYX$::P_{14g} $\Delta psrA$	7.2	0.71 ± 0.03	25.3 ± 4.2	4.6 ± 0.9	28.8 ± 4.6	61.2 ± 6.3	5.4 ± 0.7
KT2440ge ΔP_{paaF}-$paaYX$::P_{14g}	7.2	0.69 ± 0.00	22.0 ± 0 4	3.6 ± 0.6	19.8 ± 0.5	70.2 ± 0.3	6.4 ± 0.3

especially in a mixed culture approach aimed at upcycling complex plastic hydrolysates (Catur Utomo *et al.* 2020; Nikodinovic *et al.* 2008)

2.1.4. Conclusion

Biological funneling is a powerful approach to convert mixed-plastic hydrolysates into value-added chemicals. This approach requires microbial biotech workhorses that can efficiently metabolize plastic monomers, which was the focus of this study. The substrate spectrum of *P. putida* KT2440 was expanded to include aliphatic dicarboxylic acids. A combination of metabolic engineering and adaptive laboratory evolution enabled and enhanced growth on adipic acid. Genome sequencing and reverse engineering revealed that a hybrid pathway with partially redundant enzyme activities was required for efficient growth. Besides adipate, the resulting strains can also grow on dicarboxylates of other chain length such as suberate, sebacate, and azelaate. This makes them widely applicable for the upcycling of complex hydrolysates derived from different polyesters. Full conversion will also require the metabolism of terminal diols and aromatic dicarboxylates. This can be achieved by defined microbial communities of available strains (Catur Utomo *et al.* 2020; Li *et al.* 2020; Li *et al.* 2019; Narancic *et al.* 2021) or by consolidation of multiple monomer-metabolizing pathways into engineered chassis strains. In both cases, a detailed understanding of the underlying biochemical pathways and their regulation is paramount, as was also apparent from the differences in PHA production by strains with and without *psrA* mutation.

2.1.5. Experimental procedures

2.1.5.1. Strains and culture conditions

The chemicals used in this work were obtained from Carl Roth (Karlsruhe, Germany), Sigma-Aldrich (St. Louis, MO, USA), or Merck (Darmstadt, Germany) unless stated otherwise. All bacterial strains used in this work are listed in table 2.1.3 or table S1. For quantitative microbiology experiments, *P. putida* KT2440 strains were cultivated in three-fold buffered (11.64 g L^{-1} K_2HPO_4, 4.89 g L^{-1} NaH_2PO_4) MSM (Wierckx *et al.* 2005) unless stated otherwise. Pre-cultures contained 20 mM glucose. For the cultivation with adipic acid, a 300 mM adipic acid stocksolution was dissolved 1:10 in MSM to reach a final concentration of 30 mM. Liquid cultivations were incubated at 30 °C, 200 rpm shaking speed with an amplitude of 50 mm in a Multitron shaker (INFORS, Bottmingen, Switzerland) using 500 mL non-baffled Erlenmeyer flasks with metal caps, containing 50 mL culture volume. For online growth detection without offline sample analysis, a Growth Profiler 960 (Enzyscreen, Heemstede, The Netherlands) was used. This device analyses cultures in microtiter plates with transparent bottoms by image analysis. Pre-cultures containing 2 mL MSM with 20 mM glucose in 14 mL culture tubes (Greiner bio-one, Frickenhausen, Germany) were cultivated in a Multitron shaker (INFORS) with a 220 rpm shaking speed. Main cultures in 96-well plates with 200 µL volume, using MSM with several concentrations of different carbon sources as indicated, were incubated at 30 °C, 225 rpm shaking speed with an amplitude of 50 mm in the Growth Profiler. Pictures were taken every 30 minutes.

2.1.5.2. Adaptive laboratory evolution

Adaptive laboratory evolution was performed as follows: a pre-culture of *P. putida* KT2440, cultivated in MSM with 20 mM glucose, was used to inoculate 250 mL clear glass Boston bottles with Mininert valves (Thermo Fisher Scientific, Waltham, MA, USA) containing different concentrations of adipic acid and alternative carbon sources as indicated (starting OD_{600} of 0.01). Unless stated otherwise, serial transfers were reinoculated with a starting OD_{600} of 0.1 after the cultures reached an OD_{600} of at least 0.5. Single colonies were isolated from ALE cultures by streaking samples on LB agar plates.

2.1.5.3. Plasmid cloning and strain engineering

Plasmids were assembled by Gibson assembly (Gibson *et al.* 2009) using the NEBuilder HiFi DNA Assembly Master Mix (New-England Biolabs, Ipswich, MA, USA). Primers were ordered as unmodified DNA oligonucleotides from Eurofins Genomics (Ebersberg, Germany). As polymerase Q5 High-Fidelity Polymerase was used. Detailed information about utilized primers and plasmid is listed in Table S2 and S3. For the transformation of DNA assemblies and purified plasmids into competent *E. coli* cells a heat chock protocol was used (Hanahan 1983). For *P. putida* either conjugational transfer or electroporation were performed as described by Wynands *et al.* (2018). Knockout strains were obtained using the pEMG system described by Martínez-García *et al.* (2011) with a modified protocol described by Wynands *et al.* (2018). The integration of heterologous genes from *Acinetobacter baylyi* into the *attTn7*-site of the *P. putida* KT2440 genome was achieved by patch-mating of the *E. coli* donor strain holding the respective pBG-plasmid, the helper strain *E. coli* HB101 pRK2013, *E. coli* DH5α λpir pTNS1 providing the required transposase, and the recipient. Evolved plasmids were isolated from indicated *P. putida* strains using the Monarch Plasmid Miniprep Kit (New- England Biolabs, Ipswich, MA, USA) followed by immediate transformation into *E. coli*.

Plasmids containing FRT-FLP marker recycling were generated from plasmid pBG13 (Zobel *et al.* 2015), which was used as a template for the origin of transfer *oriT* and origin of replication *oriR6K* containing fragment. A FRT-flanked kanamycin marker was amplified from pBELK (Nikel *et al.* 2013). Promoters P_{14b} to P_{14g}, BCD2, *msfGFP*, and terminator T0 fragment were amplified from appropriate plasmids pBG14b to pBG14g. A P_{em7} containing fragment was amplified from pBG13 with the same oligonucleotide combination. All fragments were cut out of agarose gels and purified with a DNA Gel Extraction kit (New England Biolabs, Ipswich, Massachusetts, USA). The concentration of purified fragments was measured with a NanoDrop One (Thermo Scientific, Waltham, Massachusetts, USA). Fragments were assembled via Gibson Assembly.

The integration of the novel mini-Tn7 vector was done by patch mating as described above. The kanamycin resistance cassette was removed by flippase activity. pBBFLP was transformed via electroporation into BGX_FRT_Kan bearing *P. putida* KT2440 strains (X stand for different promoters). Afterwards, cells were plated on LB agar plates containing $30\,\mathrm{mg\,L^{-1}}$ tetracycline to maintain pBBFLP. The growth of clones needed up to two days. Colonies were picked on LB agar plates with and without $50\,\mathrm{mg\,L^{-1}}$ kanamycin to identify clones no longer resistant to kanamycin. Verification

was done by colony PCR using OneTaq 2X Master Mix (New England BioLabs, Ipswich, Massachusetts, USA). Plasmid inserts, genome integration and gene deletions were confirmed by Sanger sequencing performed by Eurofins Genomics (Ebersberg, Germany).

Table 2.1.3.: Strains used and generated for adipic acid metabolism.

***P. putida* strain**	**Description**	**Reference**
KT2440	Strain derived of *P. putida* mt-2 cured of the pWW0 plasmid	Bagdasarian *et al.* 1981
A12.1	KT2440 after evolution on adipate, 12 generations, cured from the evolved plasmid pBNT-*dcaAKIJJP*	This work
A12.1p	Evolved KT2440 strain bearing the evolved plasmid pBNT-*dcaAKIJJP*	This work
A12.1ge	A12.1 after genomic integration of *attTn7*::P_{14e}-*dcaAKIJP* and removal of the resistance marker	This work
KT2440ge	KT2440 after genomic integration of *attTn7*::P_{14e}-*dcaAKIJP* and removal of the resistance marker	This work
KT2440ge ΔP_{paaF}::P_{14g}	Exchange of the natural promoter P_{paaF} for the synthetic P_{14g} promoter	This work
KT2440ge ΔP_{paaF}-*paaYX*::P_{14g}	Exchange of the natural promoter P_{paaF} for the synthetic P_{14g} promoter together with knokout of *paaYX*	This work
KT2440ge Δ*paaYX*	Knockout of *paaYX* without promoter exchange	This work
KT2440ge Δ*psrA*	Knockout of *psrA*	This work
KT2440ge Δ*paaYX* Δ*psrA*	Knockout of *paaYX*, knockout of *psrA*	This work
KT2440ge ΔP_{paaF}-*paaYX*::P_{14g} Δ*psrA*	Exchange of the natural promoter P_{paaF} for the synthetic P_{14g} promoter together with knockout of *paaYX*, knockout of *psrA*	This work

* All strains for molecular biological procedures and the marker recycling experiments are shown in S1

2.1.5.4. Analytical methods

Bacterial growth was monitored as optical density at a wavelength of $\lambda = 600\,\mathrm{nm}$ (OD_{600}) with an Ultrospec 10 Cell Density Meter (GE Healthcare, Little Chalfront, Buckinghamshire, United Kingdom). Cell dry weight values were derived from OD_{600} using a separate calibration. The conversion factor for OD_{600} to CDW is 0.3121. The online analysis of growth using the Growth Profiler was analysed using the Growth Profiler Control software V2_0_0. Resulting G-values were converted to an equivalent OD_{600} according to the manufacturer's instructions. All growth curves from Growth Profiler experiments of each well was smoothed (window: 5 points) before calculating mean values and standard error of the mean and symbols show every 3rd data point for better visibility, unless stated otherwise. Characterization of promoter activities were determined with a Biolector (M2P Labs, Baesweiler, Germany) in clear bottom 96 well plates (Greiner Bio-One) with a filling volume of 200 µL MSM medium supplemented with 20 mM glucose as sole carbon source. Biomass was measured at 620 nm and GFP fluorescence with ex488 nm/em520 nm. The activity was calculated as a slope of GFP fluorescence over optical density during the exponential phase. A more detailed protocol is described by Köbbing (2020).

2.1.5.5. PHA analysis

Single colonies were picked and used to inoculate 2 mL overnight cultures in mineral medium ($9\,\mathrm{g\,L^{-1}}$ $Na_2HPO_4 \cdot 12\,H_2O$, $1.5\,\mathrm{g\,L^{-1}}$ K_2HPO_4, $0.2\,\mathrm{g\,L^{-1}}$ $MgSO_4 \cdot 7\,H_2O$, $1\,\mathrm{g\,L^{-1}}$ NH_4Cl and $1\,\mathrm{mL\,L^{-1}}$ trace elements solution prepared according to Sun *et al.* (2007b) (Schlegel *et al.* 1961). The medium was supplemented with $3.96\,\mathrm{g\,L^{-1}}$ of adipic acid (as a sodium salt). Kanamycin and salicylic acid were added to overnight cultures as appropriate. Strains were incubated for 24 h at 30 °C in an orbital shaker at 200 rpm. Overnight cultures were used to inoculate (1 % (v/v), inclusion) 250 mL Erlenmeyer flasks containing 50 mL altered mineral medium with reduced nitrogen concentration and a higher buffer capacity ($27\,\mathrm{g\,L^{-1}}$ $Na_2HPO_4 \cdot 12\,H_2O$, $4.5\,\mathrm{g\,L^{-1}}$ K_2HPO_4, $0.2\,\mathrm{g\,L^{-1}}$ $MgSO_4 \cdot 7\,H_2O$, $0.25\,\mathrm{g\,L^{-1}}$ NH_4Cl and $1\,\mathrm{mL\,L^{-1}}$ trace elements solution). This medium was supplemented with $3.96\,\mathrm{g\,L^{-1}}$ of adipic acid to achieve a carbon to nitrogen ratio of 30:1. pH was adjusted to 6.5 with 3 M sodium hydroxide. Strains were incubated for 48 h at 30 °C in an orbital shaker at 200 rpm. Flasks were harvested at 48 h for determination of CDW and PHA quantification by acid methanolysis and GC analysis as described in Li *et al.* (2020).

2.1.5.6. Extracellular metabolites

For measuring extracellular metabolites, samples taken from liquid cultivation were centrifuged for 3 min at 17,000×g to obtain supernatant for High-Performance Liquid Chromatography (HLPC) analysis using a 1260 Infinity II HPLC equipped with a 1260 Infinity II Refractive Index Detector (Agilent, Santa Clara, California, USA). Analytes were eluted using a 300 x 8 mm organic acid resin column (Metab-AAC, Isera, Düren, Germany) together with a 40 x 8 mm organic acid resin precolumn with 5 mM H_2SO_4 as mobile phase at a flow rate of 0.6 mL min^{-1} at 40 °C.

2.1.5.7. Genome sequencing

Genomic DNA for sequencing was isolated through a High Pure PCR Template Preparation Kit (ROCHE life science, Basel, Switzerland). Sequencing was performed by GATC (Konstanz, Germany) using Illumina technology as paired-end reads of 2x 150 base pairs. The read data (FASTQ files) were processed with the CLC Genomics Workbench software (Qiagen Aarhus A/S) for base quality filtering and read trimming. For each sample, the output was mapped to the GenBank accession AE015451 as the *P. putida* KT2440 reference genome sequence and to the pBNT-*dcaAKIJP* plasmid reference sequence. The resulting mappings were used for the gene coverage analysis and the quality-based SNP and structural variant detection with the CLC Genomics Workbench. The detected SNPs were consolidated in one list for sample comparison and inspected regarding their relevance. The mapping was also visualized and inspected with the Integrative Genomics Viewer (IGV) (Thorvaldsdottir *et al.* 2013).
Sequencing data are deposited in the NCBI Sequence Read Archive under BioProject number PRJNA464914 with accession numbers SRX9220792 for A6.1p and SRX9220793 for A12.1p.

2.2. Bio-upcycling of even and uneven medium-chain-length diols and dicarboxylates to polyhydroxyalkanoates using engineered *Pseudomonas putida*

Yannic S. Ackermann[*], Jan de Witt[*], Mariella P. Mezzina, Christoph Schroth, Tino Polen, Pablo I. Nikel, Benedikt Wynands, Nick Wierckx
[*]these authors contributed equally to this study.

Microbial Cell Factories, 23 (2024)
The online version may be found at: 10.1186/s12934-024-02310-7
status: published

CRediT authorship contribution statement:

Yannic S. Ackermann:Methodology, Investigation, Validation, Formal analysis, Data curation, Writing—original draft, Writing—review and editing, Visualization

Jan de Witt: Methodology, Investigation, Validation, Formal analysis, Data curation, Writing—original draft, Writing—review and editing, Visualization

Mariella P. Mezzina: Investigation, Writing—review and editing

Christoph Schroth: Investigation, Writing—review and editing

Tino Polen: Methodology, Formal analysis, Data curation, Writing—review and editing

Pablo I. Nikel: Resources, Writing—review and editing, Supervision, Funding acquisition

Benedikt Wynands: Methodology, Writing—review and editing, Supervision

Nick Wierckx: Conceptualization, Resources, Data curation, Writing—original draft, Writing—review and editing, Visualization, Supervision, Project administration, Funding acquisition

Overall, own contribution: 42 %

The presented experimental work was conducted by YSA (dicarboxylic acid part), JDW and CS (diol part), MPM cloning of plasmid for PHB production. Validation was done by YSA, JdW, TP, BW and NW. Visualization of all data was performed by YSA and JdW. The writing of the original draft was done by YSA and JdW, which was reviewed and edited by NW and all co-authors. Funding for the project was acquired by PIN and NW.

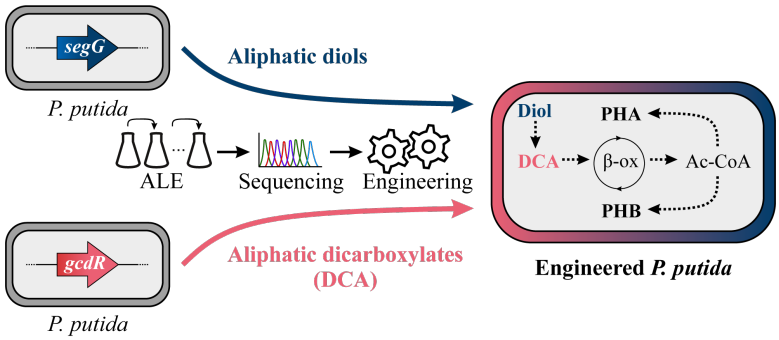

2.2.1. Abstract

Bio-upcycling of plastics is an emerging alternative process that focuses on extracting value from a wide range of plastic waste streams. Such streams are typically too contaminated to be effectively processed using traditional recycling technologies. Medium-chain-length (mcl) diols and dicarboxylates (DCA) are major products of chemically or enzymatically depolymerized plastics, such as polyesters or polyethers. In this study, we enabled the efficient metabolism of mcl-diols and -DCA in engineered *Pseudomonas putida* as a prerequisite for subsequent bio-upcycling. We identified the transcriptional regulator GcdR as target for enabling metabolism of uneven mcl-DCA such as pimelate, and uncovered amino acid substitutions that lead to an increased coupling between the heterologous β-oxidation of mcl-DCA and the native degradation of short-chain-length DCA. Adaptive laboratory evolution and subsequent reverse engineering unravelled two distinct pathways for mcl-diol metabolism in *P. putida*, namely *via* the hydroxy acid and subsequent native β-oxidation or *via* full oxidation to the dicarboxylic acid that is further metabolized by heterologous β-oxidation. Furthermore, we demonstrated the production of polyhydroxyalkanoates from mcl-diols and -DCA by a single strain combining all required metabolic features. Overall, this study provides a powerful platform strain for the bio-upcycling of complex plastic hydrolysates to polyhydroxyalkanoates and leads the path for future yield optimizations.

2.2.2. Introduction

The plastic crisis is a pressing environmental issue facilitated by an increasing plastic production that reached about 390 million metric tons in 2021, of which 90 % was based on fossil raw materials. More than half of the plastics produced are polyolefins such as polypropylene, low- or high-density polyethylene, and polyesters like PET (PlasticsEurope 2022). Especially mixed plastics are a major challenge for mechanical and chemical recycling as they typically require pure feedstocks or the costly purification of individual building blocks (Ellis *et al.* 2021; Idumah *et al.* 2019; Wei *et al.* 2020). Bio-upcycling is a promising strategy to overcome the drawbacks of conventional end-of-life solutions (Tiso *et al.* 2022). This describes the process of biologically converting plastic waste into valuable products or materials through (bio-)depolymerization and subsequent microbial cultivation. Such conversion could provide better end-of-life options for hard-to-recycle polymers and composites because biology is uniquely capable to work with complex mixtures and materials (Wierckx *et al.* 2015). Furthermore, significant efforts were invested in the past to combine enzymatic or chemical depolymerisation with microbial metabolization by using genetic and metabolic engineering (Ellis *et al.* 2021). For example, pyrolysis was used to produce hydrocarbon wax from PE polymers, which was subsequently oxidized to a mixture of fatty acids. This mixture could then serve as substrate for polyhydroxyalkanoate (PHA) production in *Pseudomonas* (Guzik *et al.* 2021). Furthermore, Sullivan *et al.* (2022) combined a chemical auto-oxidation step to break down the carbon bonds of high-density PE or PET with a microbial bioconversion step to further metabolize the resulted monomers into new compounds. Unfortunately, both chemical and enzymatic degradation processes sometimes lead to unfavourable by-products such as toxic monomers or require harmful solvents (Magnin *et al.* 2020). Although in some cases it is possible to separate toxic compounds, such as aromatic diamines (Eberz *et al.* 2023; Utomo *et al.* 2020), this will not always be economically feasible. Therefore, it is important to use robust microbial hosts. One promising candidate is the widely used biotechnological host *Pseudomonas putida* KT2440 (Bitzenhofer *et al.* 2021; Schwanemann *et al.* 2020). Besides a high tolerance to chemical stress and rapid growth, in previous studies *P. putida* was already enabled to grow on different plastic monomers such as 1,4-butanediol (BDO), adipic acid (AA), ethylene glycol, or itaconate (Ackermann *et al.* 2021; de Witt *et al.* 2023; Franden *et al.* 2018; Li *et al.* 2020; Utomo *et al.* 2020). Moreover, *P. putida* KT2440 was engineered to serve as platform organism for the production of several value-added molecules including aromatic compounds (Schwanemann *et al.* 2020), rhamnolipids (Tiso

et al. 2020b), and medium-chain-length (mcl) polyhydroxyalkanoates (PHA), consisting of C_6-C_{12} monomers (Dalton *et al.* 2022; Mezzina *et al.* 2020; Prieto *et al.* 2016).
Mcl-aliphatic diols, such as BDO and 1,6-hexanediol (HDO), are prevalent monomers of polyurethanes or polyesters. Previous studies enhanced metabolism of BDO in *P. putida* KT2440 (Li *et al.* 2020). A mutation in a transcriptional regulator, encoded by PP_2046, activated the downstream operon PP_2047-51, thereby greatly enhancing the rate of BDO metabolism. Since this operon encodes enzymes involved in β-oxidation, it is likely that BDO is converted to glycolyl-CoA and acetyl-CoA, although direct oxidation to succinate could not be excluded. A relevant group of intermediates within this pathway are the partly oxidized hydroxy acids (HA) such as 6-hydroxyhexanoate which is the monomer of polycaprolactone. The production of PHA from BDO by *P. putida* was successfully shown (Li *et al.* 2020). Nevertheless, several other mcl-diols including HDO can currently not be funneled into the central metabolism of *P. putida* for bio-upcycling.
Together with mcl-aliphatic diols, mcl-dicarboxylates (DCA) are mainly used for the synthesis of polyesters but also to produce polyamides and polyurethanes. Furthermore, mcl-DCA are products from chemical oxidation of longer polyolefins (Sullivan *et al.* 2022). Growth on single mcl-DCA was already achieved with the engineered *P. putida* KT2440ge ΔP_{paaF}-$paaYX$::P_{14g} $\Delta psrA$ (KT2440-AA) strain expressing the heterologous *dcaAKIJP* cluster from *Acinetobacter baylyi* (Ackermann *et al.* 2021). However, metabolism of especially uneven-chain-length (ucl) DCA is still rather inefficient, especially in the case of pimelate (C_7). An exception to this is glutarate (C_5), which is a favorable native carbon source for *P. putida* and is metabolized through two independent pathways. One is regulated by the GntR family regulator CsiR, which induces a CoA-independent pathway with glutarate hydroxylase (CsiD) and L-2-hydroxyglutarate oxidase (LhgO) as key enzymes (Zhang *et al.* 2018). Furthermore, *P. putida* contains a CoA-dependent pathway, in which glutarate is activated by a CoA-transferase (PP_0159) to glutaryl-CoA and then further decarboxylated by glutaryl-CoA dehydrogenase (GcdH) to crotonyl-CoA (Zhang *et al.* 2019). Crotonyl-CoA can then be converted *via* acetoacetyl-CoA into two acetyl-CoA molecules.
In this study, we aimed to extend the substrate range of *P. putida* KT2440 with prevalent polyethylene and polyester hydrolysate constituents, namely mcl-diols and –DCA, using metabolic engineering and laboratory evolution. Especially metabolism of substrates of uneven chain-length is limited and needs to be addressed. The combination of unravelled pathways should result in a mutant that is able to funnel a complex

polyester mock hydrolysate into its central metabolism providing it as substrate for bio-upcycling. To demonstrate such an approach, PHA and poly(3-hydroxybutyrate) (PHB) production from mcl-diols and -DCA as pure substrates and in a mock hydrolysate is envisioned. Altogether, this study leads the path for future bio-upcycling of mixed plastic hydrolysates that currently are a burden to conventional recycling.

2.2.3. Results and discussion

2.2.3.1. Engineering metabolism of aliphatic diols

Aliphatic mcl-diols are prevalent monomers in a variety of polymers such as polyesters or polyurethanes. In previous work, *P. putida* KT2440 was engineered to metabolize BDO as sole carbon source (Li *et al.* 2020). The metabolic pathway for BDO was predicted to occur *via* its partial oxidation to 4-hydroxybutyrate followed either by CoA-activation and subsequent β-oxidation resulting in acetyl-CoA and glycolyl-CoA, or by full oxidation to succinate. In contrast to succinate, longer chain-length DCA and thus the corresponding diols cannot be directly funneled into the central metabolism but require the heterologous β-oxidation for DCA (Ackermann *et al.* 2021). Consequently, two different pathways might enable metabolism of aliphatic diols, in which either the partly oxidized HA (HA-CoA-activating) or the further oxidized DCA is CoA-activated (DCA-CoA-activating) (Figure 2.2.1). As the wild type strain is not capable of metabolizing mcl-DCAs, engineering its background might only enable degradation *via* the HA-CoA-activating pathway. In contrast, engineering of *P. putida* KT2440-AA, which is able to metabolize mcl-DCA, could lead to degradation *via* both pathways.
To enable growth on HDO *via* the HA-CoA-activating pathway, adaptive laboratory evolution (ALE) of the *P. putida* KT2440 wild type was performed on HDO (Figure S4). Subsequent whole-genome sequencing of ALE mutants and reverse engineering resulted in the triple mutant PP_2046$^{\mathrm{A257T}}$, PP_2790$^{\mathrm{A220V}}$, *ttgG*$^{\Delta 4\mathrm{bp}}$ that metabolized HDO and 1,8-octanediol (ODO) but not 1,7-heptanediol (Figure 2.2.1). Interestingly, the transcriptional activator encoded by PP_2046 that was already involved in BDO metabolism, was revealed to be involved in HDO metabolism as well. Hence, HDO was likely metabolized by the HA-CoA-activating pathway encoded by PP_2047-51. Additionally, a mutation within a second regulator, more specifically a sigma factor 54-dependent sensory box protein encoded by PP_2790, was found to be involved in HDO metabolism. This regulator might activate expression of orthologs of this pathway

with higher affinities for HDO than BDO. Moreover, a frameshift mutation within *ttgB* (PP_1385) encoding an efflux pump membrane protein increased growth on HDO. Possibly, the intact TtgABC efflux pump reduces intracellular HDO concentrations thereby hindering its metabolism.

In addition to the HA-CoA-activating pathway, HDO might also be metabolized by the DCA-CoA-activating pathway *via* adipate (AA). Therefore, *P. putida* KT2440-AA that was recently engineered to metabolize AA and other even chain-length DCA was chosen as a starting point for enabling mcl-diol metabolism. Although this strain was not able to grow on HDO as sole carbon source (Figure 2.2.1), ALE resulted in the isolation of mutants able to metabolize 15 mM HDO within 24 h (Figure S4). Whole-genome sequencing of the fastest-growing ALE mutant revealed two single nucleotide variants (SNV). The first SNV occurred in PP_5423 encoding a putative membrane protein causing arginine 29 to be replaced by proline (PP_5423^{R29P}). The second mutation caused the exchange of glycine 70 to arginine in the protein translocase subunit SecG encoded by PP_5706 (*secG*^{G70R}). Both positions are highly conserved among Pseudomonads. Reverse engineering of the unevolved *P. putida* KT2440-AA revealed that the *secG*^{G70R} mutation alone could reproduce the growth phenotype of the isolated ALE mutant. Reverse engineering of the PP_5423^{R29P} mutation enabled growth on HDO, albeit much slower and with a long lag phase. Combination of both *secG*^{G70R} and PP_5423^{R29P} in one strain did not further enhance growth compared to the *secG*^{G70R} mutant (Figure S5), indicating the mutated SecG protein as most important for HDO metabolism. SecG is an auxiliary protein that recognizes pre-protein signal sequences and builds the core of the protein translocation apparatus SecABCDEFGY (Crane *et al.* 2017). Deletion of *secG* in the unevolved *P. putida* KT2440-AA mimicked the phenotype of the *secG*^{G70R} mutant on HDO as sole carbon source indicating that the SNV likely caused a loss of function (Figure S6). We speculate that this mutation could affect the subcellular localisation of oxidoreductases, thereby influencing the transport of HDO and/or its intermediates into the cytoplasm. However, global effects on other proteins, such as transporters, or signalling pathways are also conceivable but further investigations are required to unravel the exact mechanisms. Because the metabolism of 6-hydroxyhexanoate was found to not require the *secG*^{G70R} mutation, we conclude that this mutation affects the first oxidation steps of the diol to the HA (Figure S7). In addition to DCA-CoA-activating pathway, 6-hydroxyhexanoate was also metabolized *via* the HA-CoA-activating pathway in the reverse engineered KT2440 wild type-based strain. Hence, 6-hydroxyhexanoate can be directed into the central metabolism *via* both

pathways enabling future bio-upcycling processes of polycaprolactone hydrolysates.
In addition to HDO, the reverse engineered *secG*^{G70R} mutant was also able to utilize ODO as sole carbon source, whereas 1,7-heptanediol was poorly metabolized by the strain (Figure 2.2.1). These results are in agreement with the ability of the parent strain *P. putida* KT2440-AA to metabolize the corresponding dicarboxylate suberate (C_8) much better than pimelate (C_7) (Ackermann *et al.* 2021). To test whether HDO and ODO were metabolized *via* the DCA-CoA-activating pathway, the *dcaAKIJP* operon, enabling growth on mcl-DCA, was deleted in *P. putida* KT2440-AA *secG*^{G70R}. Indeed, the *secG*^{G70R} Δ*dcaAKIJP* mutant showed decreased growth with HDO and ODO indicating that both substrates were metabolized *via* their mcl-DCA (Figure 2.2.1). However, this indicated that the HA-CoA-activating pathway was also active in the *P. putida* KT2440-AA-based strain. Although the *secG*^{G70R} Δ*dcaAKIJP* mutant showed an increased lag-phase with ODO compared to HDO, the observed growth indicated that ODO is the favoured substrate for the HA-CoA-activating pathway. Deletion of PP_2051 encoding a 3-ketoacyl-CoA thiolase that is involved in the degradation of BDO, did not alter the phenotypes of the *secG*^{G70R} Δ*dcaAKIJP* mutant with HDO and ODO, likely due to the presence of isozymes (Liu *et al.* 2023) (Figure S6). Hence, both pathways can be used to metabolize mcl-diols but they result in different central metabolites as end products namely acetyl-CoA and glycolyl-CoA for the HA-CoA-activating or acetyl-CoA and succinyl-CoA for the DCA-CoA-activating pathway (Figure 2.2.1). In contrast to succinyl-CoA, the metabolic route for glycolyl-CoA is unknown, but a conversion to glyoxylate is likely. This can be funneled into the glyoxylate shunt (Li *et al.* 2019), or it might also be metabolized *via* tartronate semialdehyde yielding 2-phosphoglycerate that is an intermediate of glycolysis (Franden *et al.* 2018). Since degradation of glycolyl-CoA can be associated with the release of CO_2 and consumption of NAD(P)H, the HA-CoA-activating pathway might be energetically inferior compared to the DCA-CoA-activating pathway. In addition to this, the deletion of *dcaAKIJP* within the DCA-CoA-activating pathway might enable the consolidation of a mixture containing diols and DCA to a single group of monomers. Such bioconversion using a Δ*dcaAKIJP* mutant would enhance the economic viability of monomer recycling from PE hydrolysates as not a heterogeneous mixture of monomers but only a single type of building blocks needs to be purified from the hydrolysate.

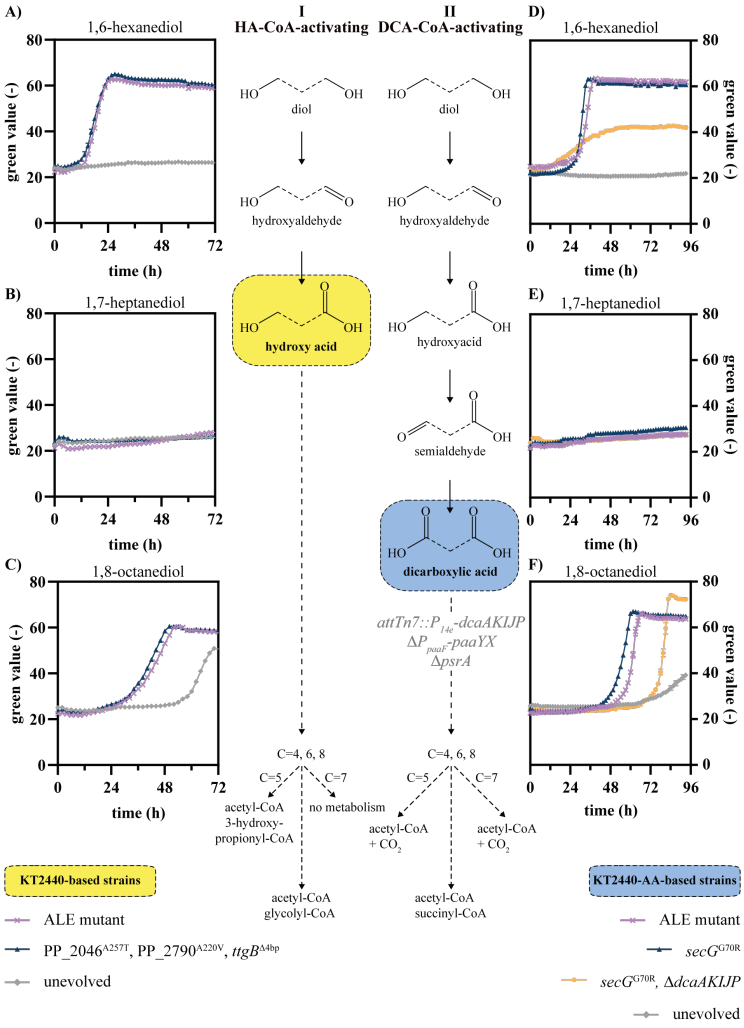

Figure 2.2.1.: Metabolic pathways of aliphatic diols in engineered *P. putida* KT2440. *P. putida* KT2440 wild type-based strains (A-C) and *P. putida* KT2440-AA-based strains (D-F) were cultivated in mineral salts medium (MSM) supplemented with 1,6-hexanediol, 1,7-heptanediol, or 1,8-octanediol in concentrations that are C-mol equivalent to 30 mM 1,6-hexanediol. Depending on the background strain, the mcl-diols are either metabolized *via* the HA-CoA-activating (I) or DCA-CoA-activating (II) pathway which required the expression of the heterologous *dcaAKIJP* cluster in *P. putida* KT2440-AA (genomic modifications in grey). Depending on the chain-length of the diol (dashed lines), namely C=4 (1,4-butanediol), C=5 (1,5-pentanediol), C=6 (1,6-hexanediol), C=7 (1,7-heptanediol), and C=8 (1,8-octanediol) and the respective pathway, different central metabolites are obtained. The results of single mutant cultivation are shown in Figure S5. Growth was monitored using a Growth Profiler. Error bars indicate the standard error of the mean (n=3).

2.2.3.2. Engineering metabolism of ucl-DCA

Given that *P. putida* KT2440-AA grows very poorly on ucl-DCA, the inability of the $secG^{G70R}$ mutant to metabolize ucl-diols likely stems from this downstream limitation. Hence, the next step was to optimize catabolism of ucl-DCA. Sullivan *et al.* (2022) demonstrated the upcycling of a DCA mixture from plastic waste containing polyesters. Even when growth was enabled on the mixture containing C_4-C_{17} DCA and all substrates were degraded over time, growth inhibition was observed on the single monomers with uneven-chain-length, especially pimelate (C_7). This suggested a further misregulation of connecting metabolic pathways, possibly at the point of glutaryl-CoA, resulting from β-oxidation of these DCA (Harrison *et al.* 2005). Since it is known that pimelate cannot act as an inducer of GcdR, the absence of glutarate could explain the difference in growth between a monomer mixture and pimelate as sole carbon source (Thompson *et al.* 2019). To further investigate this misregulation, an evolution experiment was performed. *P. putida* KT2440-AA and the corresponding evolved strains *P. putida* A12.p and A12.1ge (Ackermann *et al.* 2021), were cultivated in MSM containing pimelate as sole carbon source to provoke stable mutations. After 70-80 hours of cultivation, weak growth was detectable (Figure 2.2.2). The cultures of all replicates were spread on LB agar plates and single colonies were re-inoculated in MSM containing pimelate as sole carbon source. This re-inoculation resulted in a significantly shorter lag phase and better growth, suggesting that stable mutations had occurred.

Whole-genome sequencing of two of the *P. putida* A12.1ge strains re-inoculated on pimelate revealed mutations in the regulator *gcdR*. One strain (PA1.2) contained a C→T mutation in *gcdR* resulting in a G148D substitution, while the other strain (PA1.1) contained a C→T mutation resulting in a G154D substitution. Among Pseudomonads, both positions are highly conserved and the emerged amino acid exchanges are located in the substrate binding domain of GcdR. This LysR family regulator governs the expression of *gcdH*, encoding a glutaryl-CoA dehydrogenase, and PP_0159, encoding a family III CoA-transferase (Madhuri Indurthi *et al.* 2016; Zhang *et al.* 2019). Glutarate is the effector of GcdR (Thompson *et al.* 2019; Zhang *et al.* 2019), but since pimelate is degraded *via* glutaryl-CoA and not glutarate, the reason for the poor growth is likely the lack of induction of *gcdH*. We hypothesized that the mutations found in *gcdR* ameliorate this lack of induction, hence enhancing growth on longer- ucl-DCA.

To investigate the impact of the regulator GcdR on the degradation of ucl-DCA, a *gcdR*

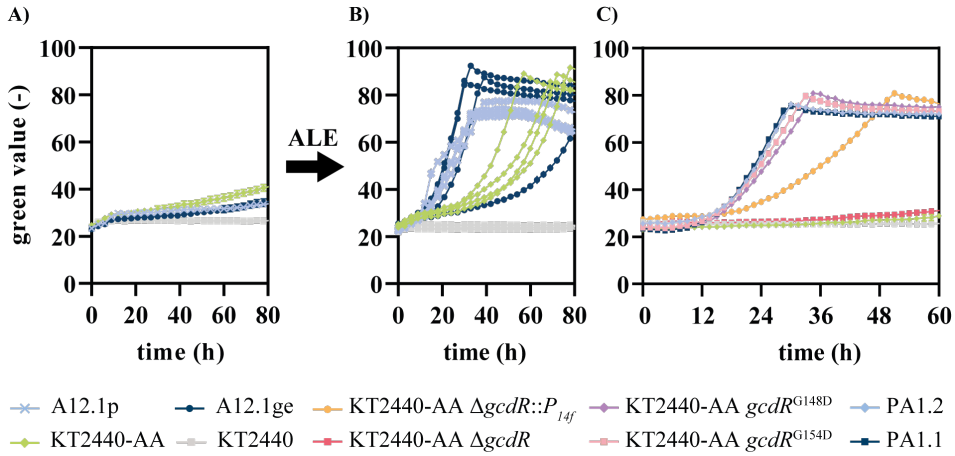

Figure 2.2.2.: Adaptive laboratory evolution and reverse engineering for growth on pimelate. All strains were cultivated in three-fold buffered MSM containing 25.7 mM pimelate as sole carbon source. A) Long-term cultivation of strains that are not able to grow on pimelate to induce adaptive mutations. B) Growth of single strains which were isolated on LB agar plates after 80 h from the experiment shown in A. C) Growth of reverse engineered strains based on mutations found after whole-genome sequencing of evolved *P. putida* A12.1ge strains. Growth was monitored using a Growth Profiler. Error bars indicate the standard error of the mean, but errors are sometimes so small that they are not visible behind the lines (n=3).

knockout strain was compared to a strain harbouring the synthetic promoter P_{14f} for constitutive expression of *gcdH*-PP_0159 (Figure 2.2.2). Since *P. putida* KT2440-AA Δ*gcdR* was not able to grow on pimelate as sole carbon source, it is likely that GcdR activates the transcription of *gcdH*-PP_0159. Growth on glutarate was not decreased by the deletion of *gcdR* probably due to the second CoA-independent degradation pathway of *P. putida* (Figure S8). In contrast, constitutive expression of *gcdH*-PP_0159 enabled growth on pimelate, but at a lower rate than in the two evolved strains, indicating that activation of the native promoter mediated by the mutated GcdR is stronger than the expression obtained using a constitutive synthetic promoter. This was confirmed by genomic insertion of the mutations encoding the amino acid exchanges found in the evolved strains. Growth of these reverse engineered strains was much better compared to the constitutive P^{14f} expression, almost completely mimicking the growth phenotype of the evolved strains (Figure 2.2.2).

2.2.3.3. SNV's in *gcdR* may cause changes in ligand binding

To comprehend the effects of the G148D and G154D mutations on GcdR, RT-qPCR experiments were performed to analyze expressions levels of *gcdH* in the *gcdR* mutants on different ucl-DCA and on glucose (Figure 2.2.3). In the $GcdR^{G154D}$ mutant, the expression levels of *gcdH* are the same on all substrates. Hence, this mutation likely led to a strong constitutive activation, at a level similar to the wild type induced by glutarate. In contrast, in the $GcdR^{G148D}$ mutant, expression levels of *gcdH* are much higher on glutarate and pimelate than on glucose or azelate, indicating that this mutant is induced by both ucl-DCA, in contrast to the wild type regulator which is only induced by glutarate. This indicates that the G148D mutation increased the spectrum of possible ligands of GcdR. ColabFold protein structure simulations and YASARA docking studies (Krieger *et al.* 2014; Mirdita *et al.* 2022) indicate a structural impact of G148D and G154D on the effector binding pocket of GcdR (Figure 2.2.3, S6). The G148D substitution is more distal from the pocket, which appears to be larger compared to the wild type. The G154D mutation is closer to the pocket, where the negatively charged aspartic acid might lead to a conformational change that is not easily modelled by this in silico method. This would support the RT-qPCR results, although these are only simulations that need further confirmation. The expression levels of *gcdH* with the wild type regulator induced by glutarate, the G148D mutant induced by glutarate or azelate, and the constitutive G154D mutant, are similarly high, significantly exceeding that of the constitutive P_{14f} promoter exchange strain. This supports that the slow growth of the latter strain was caused by the relatively weak expression driven by the promoter exchange.

With this knowledge, the strains containing the SNVs were compared to *P. putida* KT2440-AA in terms of growth on different mcl-DCA. This confirmed the improvement of growth of the $GcdR^{G154D}$ strain on ucl-DCA compared to the starting strain (Figure 2.2.3). The most conspicuous difference can be seen on azelate. The parent strain with wild type *gcdR* grew reasonably well on this C_9-DCA, possibly as a result of the two acetyl-CoA released from β-oxidation of this longer chain length. However, growth on azelate was enhanced by the G154D mutation but inhibited by G148D. This indicated that the G148D mutation altered the effector binding pocket such that pimelate causes induction, while azelate causes repression.

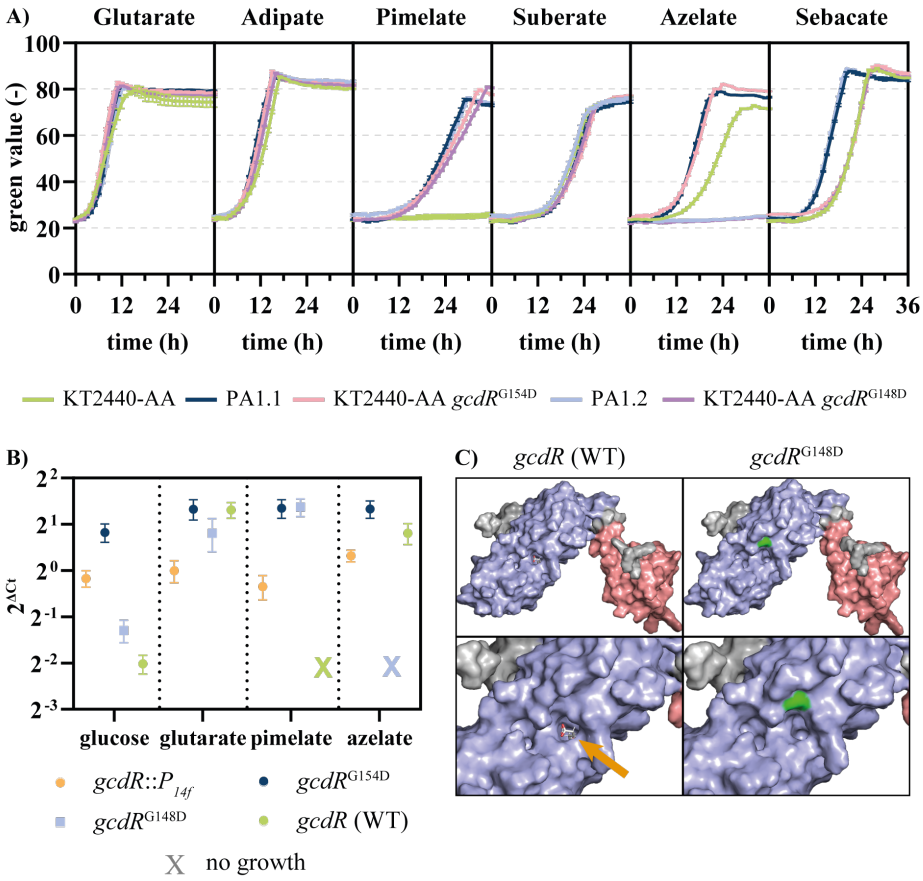

Figure 2.2.3.: Characterization of growth of engineered and evolved strains of *P. putida* on dicarboxylic acids of varying chain lengths. A) All strains were cultured in MSM containing the specified carbon source, that are C-mol equivalent to 30 mM adipate. The growth was monitored using a Growth Profiler. Error bars indicate the standard error of the mean (n=3). B) Relative expression levels of *gcdH* in cells of *P. putida* with wild type or mutated versions of the regulator GcdR on different C-sources were determined by RT-qPCR. The Ct values were normalized to the Ct of *rpoD*. Standard errors of the means were calculated using three technical replicates of two biological replicates. Expression levels in cells that did not grow on certain substrates were set equal to unexpressed values and are indicated with "X". C) Three-dimensional structures were predicted with ColabFold and visualized with PyMOL. Docking of glutaric acid in the wild type regulator was calculated using YASARA (orange arrow). The mutated amino acid (D148) is marked in green. The blue surface color indicates the effector binding domain and the red surface color indicates the DNA binding domain. The visualization of the mutant gcdRG154D is shown in Figure S9.

2.2.3.4. Enabling growth on ucl 1,7-heptanediol

P. putida KT2440-AA *secG*^{G70R} metabolized diols of even chain-length *via* the DCA-CoA-activating pathway, whereas the ucl 1,7-heptanediol was poorly metabolized by this strain due to its inability to utilize pimelate. Since introducing the *gcdR*^{G154D} mutation into *P. putida* KT2440-AA enabled metabolism of pimelate as sole carbon source, it was introduced into *P. putida* KT2440-AA *secG*^{G70R}. Indeed, the resulting *secG*^{G70R}, *gcdR*^{G154D} mutant metabolized 1,7-heptanediol and deletion of the *dcaAK-IJP* cluster confirmed its metabolism *via* the DCA-CoA-activating pathway (Figure 2.2.4). The *gcdR*^{G154D} mutation was also introduced into the wild type-based *ttgG*$^{\Delta 4bp}$, PP_2046^{A257T}, PP_2790^{A220V} mutant that metabolized HDO and ODO *via* the HA-CoA-activating pathway. However, the resulting mutant was not able to metabolize 1,7-heptanediol (data not shown). This highlights the DCA-CoA-activating pathway as most suitable pathway for funneling aliphatic even and uneven mcl-DCA and -diols into the central metabolism of the engineered *P. putida* KT2440-AA *secG*^{G70R}, *gcdR*^{G154D}. A mixture consisting of C_6-C_{10} DCA and C_6-C_8 diols was fully consumed by this strain confirming the successful funneling of all substrates from a complex mixture into the central metabolism (Figure 2.2.4).

2.2.3.5. Towards bio-upcycling of complex aliphatic mixtures

Although growth on single monomers is useful to elucidate the genetic and biochemical basis of mcl-DCA metabolism, for bio-upcycling purposes it is necessary to metabolize mixtures of complex plastic hydrolysates. For example, auto-oxidation of high-density polyethylene (HDPE) yields a mixture of C_4-C_{22} dicarboxylic acids (Sullivan *et al.* 2022). This mixture was successfully degraded by Sullivan *et al.* (2022) by strain AW162 comparable to *P. putida* KT24440-AA described above. Strain AW162 lacks the mutations in *gcdR* and is not able to grow on pimelate as sole carbon source (Sullivan *et al.* 2022). However, AW162 was able to metabolize ucl-DCA in a mixture, likely due to the presence of glutarate to induce *gcdH*-PP_0159. We hypothesized that the relatively low concentration of glutarate might lead to sub-optimal expression that might be ameliorated by the *gcdR* mutation. Indeed, comparison of growth of our reverse engineered strain with and without *gcdR*^{G154D} on a mixture of C_4-C_{10} DCA reveals a much better growth for the strain harbouring the mutation (Figure 2.2.5). This was the case for mixtures with and without glutarate.

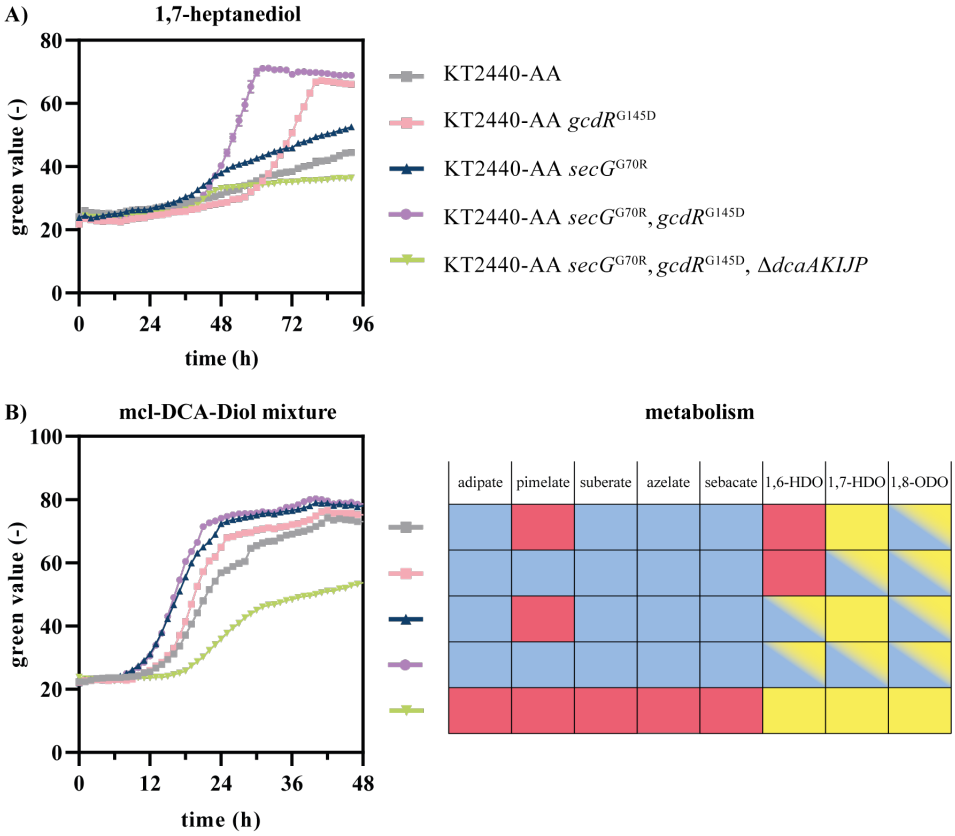

Figure 2.2.4.: Growth of KT2440-AA strains on 1,7-heptanediol and on a mcl-DCA -diol mixture. All strains were cultivated in MSM containing 25.7 mM 1,7-heptanediol (A) or a mixture consisted of adipate, pimelate, suberate, azelate, sebacate, 1,6-hexanediol (HDO), 1,7-heptanediol, and 1,8-octanediol (ODO) with concentrations of 3 mM each (B). Red indicates the inability of the strain to metabolize the substrate. Yellow indicates metabolism *via* the HA-CoA-activating pathway, whereas blue indicates that the substrate was metabolized *via* the DCA-CoA-activating pathway. Potential activity of both pathways is indicated as color gradient. All mutations shown are in the KT2440-AA strain. Error bars indicate the standard error of the mean (n=3).

The successful funneling of DCA and diols of even and uneven chain lengths into the central metabolism of our engineered *P. putida* KT2440-AA *secG*^{G70R}, *gcdRG*^{G154D} paves the way for investigating their bio-upcycling. As target product, polyhydroxyalkanoates (PHA) were selected that are biodegradable polyesters with increasing industrial applications (Blanco *et al.* 2021; Dalton *et al.* 2022). In nitrogen-limited media, *P. putida* KT2440 natively produces mcl-PHA providing (*R*)-3-hydroxyacyl-CoA,

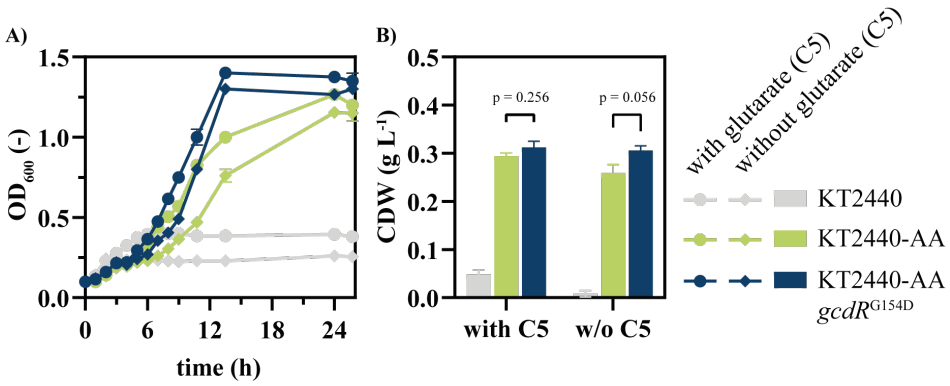

Figure 2.2.5.: Growth of strains on a mixture of various (mcl)-dicarboxylic acids. All strains were cultivated in three-fold buffered MSM containing 1 mM of each DCA (C_4-C_{10}) with and without glutarate to compare the influence of inducer. For offline growth measurements, samples were taken at several time points (A). Final consumption of all monomers was confirmed by HPLC (data not shown). After 26 hours sample were taken for final cell dry weight determination (B). Error bars indicate the standard error of the mean (n=2).

the primary precursor, *via* two pathways (Liu et al., 2023). By this, related substrates such as fatty acids are converted to (*R*)-3-hydroxyacyl-CoA *via* β-oxidation, whereas unrelated substrates such as glucose are funneled *via* malonyl-CoA into fatty acid *de novo* synthesis resulting in the production of the precursor. To test if the engineered *P. putida* KT2440-AA *secG*^{G70R}, *gcdR*^{G154D} is able to produce mcl-PHA from mcl-DCA and -diols, the strain was cultivated in nitrogen-limited medium with a C:N ratio of 30:1 using substrate concentrations that are C-mol equivalent to 30 mM adipate. Although all mcl-DCA are metabolized *via* the *dcaAKIJP*-encoded β-oxidation, PHA production was clearly dependent on the chain-length of the substrate (Table 2.2.1). Using adipate as substrate, mcl-PHA were produced to 15.7 ± 1.0% of the cell dry weight (CDW) with 3-hydroxydecanoic acid as the dominant monomer (57.8 ± 3.2 %). In contrast to this, only 3.3 ± 0.1 % mcl-PHA were produced from pimelate and less than 1 % mcl-PHA were produced from suberate, azelate, and sebacate. The same trend was observed when different mcl-diols were tested for mcl-PHA production. In total, 10.0 ± 0.6 % mcl-PHA were produced from HDO and 4.3 ± 0.1 % from 1,7-heptanediol. As observed for suberate, mcl-PHA production from ODO was below 1 %. Although the relative monomer composition of adipate and pimelate compared to HDO and 1,7-heptanediol was similar, the total amount of mcl-PHA was higher when the mcl-DCA were used as substrates (Table 2.2.1). This can be explained by the presence of the HA-CoA-activating pathway for mcl-diol metabolism in the Δ*dcaAKIJP* mutants.

Hence, less carbon was likely funneled from the diols into the DCA-CoA-activating pathway yielding less favourable precursors for mcl-PHA production. When a mock hydrolysate consisting of C_6-C_{10}-DCA and C_6-C_{10}-diols with 5 mM each was used as substrate, 0.3 ± 0.0 % mcl-PHA were produced. This low yield can be explained by the relative high amount of C_8-C_{10} substrates that were identified to be barely suitable for mcl-PHA production. Our results fit into the observations of Sullivan *et al.* (2022) that reported a yield of 11.8 ± 2.9 % mcl-PHA from a mixture containing benzoate, acetate, and C_4-C_{17}-mcl-DCA. When a polystyrene hydrolysate was tested, only 0.8 ± 0.2 % mcl-PHA were produced indicating that only fractions of complex mixtures can be used to produce PHA. In contrast to C_8-C_{10}-fatty acids that are well-suited for mcl-PHA production in *P. putida* KT2440 (Prieto *et al.* 2016), C_8-C_{10}-DCA were not appropriate for mcl-PHA production. This likely results from the fact that mcl-DCA such as adipate and pimelate are metabolized *via* β-oxidation, but unlike fatty acids they are not directly used as PHA precursors. Rather they are broken down to acetyl-CoA, and then shunted back into fatty acid *de novo* synthesis, which is linked back to β-oxidation through the action of PhaG. Possibly, the longer-chain DCA, which match the typical PHA monomer chain length, induce components of β-oxidation that interfere with PHA synthesis by degrading the hydroxyacyl-CoA precursor. Moreover, the ratio between succinyl-CoA and acetyl-CoA increases with increasing chain-length using C-molar equivalent concentrations of the substrate. The changing ratio might influence PHA production (Figure 2.2.6). This could also be an explanation for the variation in CDWs when different substrates are metabolized (Table 2.2.1).

To avoid the abovementioned hypothesized conflict, we investigated whether PHB might be a favoured product for the bio-upcycling of the described substrates. This short-chain polymer is produced from acetoacetyl-CoA, which is converted to (*R*)-3-hydroxybutyryl-CoA as substrate for PHB synthesis. To produce PHB in *P. putida* KT2440, the ability to produce mcl-PHA was abolished by deleting the PP_5003-6 gene cluster including the PHA (de-)polymerases. Since *P. putida* KT2440 is not a natural PHB producer, a PHB biosynthesis pathway from *C. necator* H16 was expressed in the KT2440-AA $secG^{G70R}$ $gcdR^{G154D}$ mutant. The synthetic pathway comprises *phaCAB*, encoding (i) PhaA, a thiolase that condenses 2 acetyl- CoA moieties into acetoacetyl-CoA, (ii) PhaB, a reductase that converts acetoacetyl-CoA into (*R*)-3-hydroxybutyryl-CoA and (iii) PhaC, a short-chain-length (scl)-PHA synthase that polymerizes 3-hydroxybutyryl-CoA monomers (C_4) to yield PHB. We constructed a synthetic operon with these genes under the transcriptional control of the ChnR/P_{chnB} expression system, inducible by

cyclohexanone (Benedetti *et al.* 2016), and a synthetic ribosome binding site (5'-AGG AGG AAA AAC AT-3') upstream of each gene. This construct was assembled in the pSEVA631 vector by USER cloning, resulting in plasmid pS6311·PHB.

Table 2.2.1.: Production of mcl-PHAs by engineered *P. putida* KT2440-AA *secG*^{G70R}, *gcdR*^{G154D} from different substrates. The CDW, PHA content, and relative monomer composition of mcl-PHA are shown. The strain was cultivated in MSM supplemented with C-mol equimolar concentrations to 30 mM of adipate using a C:N ratio of 30:1. The mock hydrolysate consisted of 5 mM of each individual substrate. Error values are calculated as standard deviations (n=2). Exemplary GC chromatograms are shown in Figure S10.

substrates	CDW(gL^{-1})	PHA (%)	C_6 (%)	C_8 (%)	C_{10} (%)	C_{12} (%)
adipate	0.62 ± 0.05	15.7 ± 1.05	14.3 ± 3.2	24.1 ± 0.2	57.8 ± 3.2	3.8 ± 0.2
pimelate	0.62 ± 0.02	4.3 ± 0.12	14.2 ± 0.2	32.3 ± 0.3	47.9 ± 0.2	5.6 ± 0.0
suberate	0.47 ± 0.00	0.4 ± 0.01	n. d.	5.0 ± 1.1	48.4 ± 1.6	46.6 ± 3.4
azelate	0.47 ± 0.01	0.4 ± 0.02	n. d.	n. d.	48.8 ± 3.4	51.2 ± 3.4
sebacate	0.52 ± 0.03	0.6 ± 0.01	n. d.	9.9 ± 0.2	55.8 ± 0.7	34.3 ± 0.4
1,6-hexanediol	0.57 ± 0.03	10.0 ± 0.6	10.0 ± 0.5	33.4 ± 0.2	52.9 ± 0.1	3.8 ± 0.2
1,7-heptanediol	0.57 ± 0.01	3.4 ± 0.01	12.8 ± 0.7	30.0 ± 0.0	49.7 ± 0.2	7.5 ± 0.5
1,8-octanediol	0.43 ± 0.01	0.5 ± 0.00	4.7 ± 0.5	7.2 ± 0.1	49.1 ± 2.8	39.0 ± 2.0
mock hydrolysate	0.89 ± 0.02	0.3 ± 0.01	n. d.	n. d.	60.9 ± 1.1	39.1 ± 1.1

Heterologous expression of the *phaCAB* cluster indeed enabled production of PHB by *P. putida* KT2440-AA *secG*^{G70R}, *gcdR*^{G154D} carrying pS6311·PHB under nitrogen-sufficient conditions (Table 2.2.2). In contrast to native mcl-PHA production, uneven substrates such as pimelate (15.14 ± 0.05 %) and 1,7-heptanediol (21.86 ± 2.77 %) were preferred for PHB accumulation. This can be explained by the formation of acetoacetyl-CoA as intermediate that is directly used for PHB synthesis. Hence less carbon is available for biomass formation yielding lower CDWs (Table 2.2.2). When azelate was used as substrate, less PHB (6.53 ± 0.92 %) was produced compared to pimelate likely caused by the formation of an additional molecule of acetyl-CoA that was used for the production of biomass as indicated by the CDW.

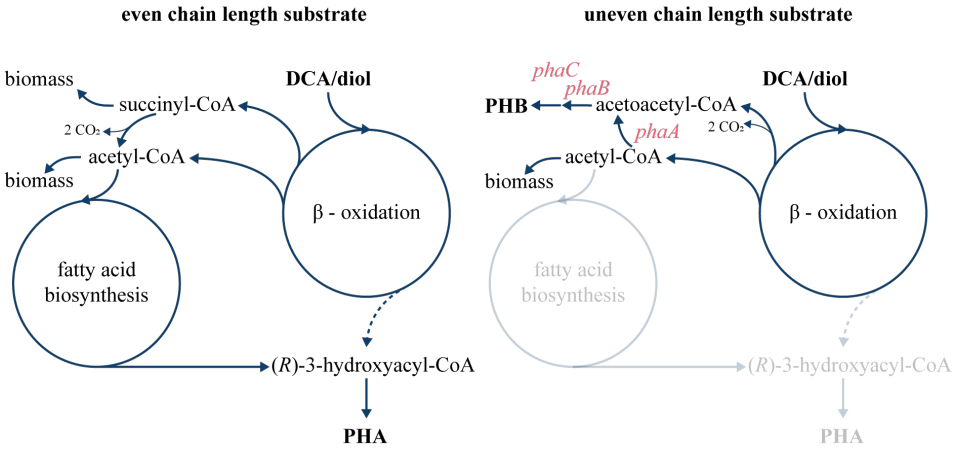

Figure 2.2.6.: Comparison between PHA and PHB synthesis from even- and uneven-chain aliphatic diols and dicarboxylates. The heterologous enzymes from *C. necator* responsible for PHB production are shown in red.

Although mcl-PHA were produced from adipate, this substrate as well as suberate and sebacate were not suited for the production of PHB as acetyl-CoA was likely used for biomass formation (Table 2.2.2). Moreover, HDO and ODO also resulted in lower amounts of PHB. In all, these results indicate that the produced PHB was mainly derived from acetoacetyl-CoA as intermediate of ucl-DCA or -diol metabolism. Consequently, our results indicate that acetyl-CoA from substrates with even chain length are predominantly utilized for the production of biomass rather than converted to acetoacetyl-CoA for PHB synthesis. To enable efficient upcycling of substrates with even and uneven chain lengths present in mixed hydrolysates, future studies could investigate the combination of scl- with mcl-PHA synthesis pathways in a single strain. By this both mcl- and ucl-substrates can be converted to scl-co-mcl-PHA that features enhanced physical properties compared to homopolymeric PHAs (Wang *et al.* 2023).

Table 2.2.2.: Production of PHB by engineered *P. putida* KT2440-AA *secG*^{G70R}, *gcdR*^{G154D} carrying plasmid pS6311·PHB from different substrates. The CDW and PHB content are shown. The strain was cultivated in MSM supplemented with C-equimolar concentrations of pure substrates and 1 mM cyclohexanone as inducer for *phaCAB* expression. The strain was cultivated in MSM supplemented with C-mol equimolar concentrations to 30 mM of adipate using a C:N ratio of 30:1. The mock hydrolysate consisted of 5 mM of each individual substrate. Error values are calculated as standard deviations (n=2). Exemplary GC chromatograms are shown in Figure S10.

substrates	**CDW(g L^{-1})**	**PHB (%)**
adipate	1.52 ± 0.05	1.16 ± 0.06
pimelate	0.23 ± 0.01	15.14 ± 0.05
suberate	1.52 ± 0.04	1.56 ± 0.19
azelate	1.47 ± 0.01	6.53 ± 0.92
sebacate	1.52 ± 0.02	2.35 ± 0.07
1,6-hexanediol	1.29 ± 0.14	3.59 ± 0.01
1,7-heptanediol	0.26 ± 0.01	21.86 ± 2.77
1,8-octanediol	0.56 ± 0.01	2.20 ± 0.76
mock hydrolysate	1.16 ± 0.01	3.59 ± 0.01

2.2.4. Conclusion

Bio-upcycling of complex monomer mixtures, either from a single polymer or from mixed plastic waste streams, is a promising approach for the establishment of a circular economy. In order to achieve an efficient bio-upcycling approach, the funneling of different monomers into the value-added products is crucial. We successfully engineered the combined degradation of diols and dicarboxylic acids in a single platform strain of *P. putida* KT2440. Using this strain, we demonstrated the conversion of monomer mixtures into different PHA, which are of increasing interest in the polymer industry. Although PHA yields are currently relatively low (± 0.03 g_{PHA} $g_{substrate}^{-1}$), our study provides fundamental insights into the different metabolic pathways available for aliphatic α, ω-functionalized molecules and how their central metabolic products affect product formation. This leads the path for future PHA yield optimizations and increased the range of potential substrates for PHA production.

2.2.5. Experimental procedures

2.2.5.1. Strains and culture conditions

The chemicals used in this work were obtained from Carl Roth (Karlsruhe, Germany), Sigma-Aldrich (St. Louis, MO, USA), or Merck (Darmstadt, Germany) unless stated otherwise.
All bacterial strains used in this work are listed in table 2.2.3. Unless otherwise stated, *P. putida* KT2440 strains were cultivated for quantitative microbiology experiments in three-fold buffered (11.64 g L^{-1} K_2HPO_4, 4.89 g L^{-1} NaH_2PO_4) mineral salt medium (MSM) (Hartmans *et al.* 1989). Pre-cultures contained 20 mM glucose. For cultivation experiments, the final concentrations of diols or dicarboxylates were C-molar equivalent to 30 mM adipate. For online growth measurements cultures were grown and analyzed with the Growth Profiler 960 (Enzyscreen, Heemstede, The Netherlands) by image analysis. Main cultures were cultivated in transparent bottom 96-well microtiter plates (CR1496dg) with a volume of 200 µL at 30 °C and 225 rpm shaking speed.
Adaptive laboratory evolution (ALE) on HDO was performed in 96-well microtiter plates by iterative inoculation of fresh medium after the stationary phase was reached. For *P. putida* KT2440-AA, 30 mM HDO was used as sole carbon source. Since *P. putida* KT2440 did not grow with HDO as sole carbon source at the start of the ALE, 15 mM HDO and 15 mM BDO were used for the first two batches of the ALE. This concentration was shifted to 20 mM HDO and 10 mM BDO (batches 3-5), and to 30 mM HDO (batches 6-14). After ALE, single clones were isolated on LB agar plates and screened for growth on HDO as sole carbon source. The best growing strains were selected for whole genome sequencing.
Liquid cultivations with additional analysis were incubated at 30 °C, with a shaking speed of 200 rpm and an amplitude of 50 mm using Climo-Shaker ISF1-X (Kuhner Shaker, Birsfelden, Switzerland) in 500 mL non-baffled Erlenmeyer flasks with metal caps, containing 50 mL culture volume. For PHA production experiments, cells were cultivated in three-fold buffered and nitrogen-limited MSM. For this, a C:N ratio of 30:1 was used. PHB production was carried out in three-fold buffered MSM with 1 mM of cyclohexanone as inducer and 10 µg mL^{-1} gentamicin to maintain the pS6311·PHB plasmid. Cultivations were performed in 500 mL shake flasks with 50 mL of culture volume at 30 °C and 200 rpm until the stationary phase was reached.

2.2.5.2. Plasmid cloning and strain engineering

Cloning primers were ordered as unmodified DNA oligonucleotides from Eurofins Genomics (Ebersberg, Germany) and are listed in table S3. The Q5 High-Fidelity 2X Master Mix (New-England Biolabs, Ipswich, MA, USA) was used for the amplification of cloning fragments, while the One*Taq* Quick-Load 2X Master Mix (New-England Biolabs, Ipswich, MA, USA) was used for screening together with a pre-lysis step in alkaline PEG200 (Chomczynski *et al.* 2006). Plasmids used in this study were assembled by Gibson assembly (Gibson *et al.* 2009) using the NEBuilder HiFi DNA assembly Master Mix (New-England Biolabs, Ipswich, MA, USA) or USER cloning (Cavaleiro *et al.* 2015) and are listed with more details in table S2. In order to bestow PHB biosynthesis to *P. putida* strains, plasmid pS6311·PHB was constructed as follows. First, plasmid pS648::(sRBS)*phaCAB* was constructed in order to introduce synthetic RBSs upstream of each gene comprising the PHB operon. Such sRBSs sequences were introduced in the USER primers and *phaCAB* from *Cupriavidus necator* H16 was amplified from pS341·PHA (Durante-Rodríguez *et al.* 2018). The resulting plasmid, bearing sRBSs upstream of each of the three genes comprising the *pha* operon, was then used as template for the amplification of this construction. Lastly, pSEVA2311 (Silva-Rocha *et al.* 2013) was used as template for PCR amplification of the ChnR/P_{chnB} expression system. These two USER fragments were used to assemble plasmid pS6311·PHB.
Transformation of *E. coli* with assembled DNA and purified plasmids was performed by a heat chock protocol (Hanahan 1983). Transformation of *P. putida* was performed by electroporation and conjugational transfer of mobilized plasmids by patch mating as described by Wynands *et al.* (2018). Knockouts, promoter exchanges and point mutations were obtained using either a modified pSNW2 system from Volke *et al.* (2020) based on the pEMG system described by Martínez-García *et al.* (2011) or the original system with a modified protocol described by Wynands *et al.* (2018). Antibiotics were added to the medium as needed to support plasmid maintenance and to select for genomic recombination events (final concentration: Kanamycin sulfate $50\,\mathrm{mg\,L^{-1}}$; Gentamicin $25\,\mathrm{mg\,L^{-1}}$).
Plasmids, gene deletions and point mutations were confirmed by Sanger sequencing performed by Eurofins Genomics (Ebersberg, Germany).

Table 2.2.3.: Strains used and generated for this study.

Micat no.	*P. putida* strain	Description	Reference
30	**KT2440**	Strain derived from *P. putida* mt-2 cured of the pWW0 plasmid	Bagdasarian *et al.* 1981
586	**A12.1p**	Evolved KT2440 strain bearing the evolved plasmid pBNT-*dcaAKIJJP*	Ackermann *et al.* 2021
607	**A12.1ge**	A12.1 after genomic integration of *attTn7*::P_{14e}-*dcaAKIJP* and removal of the resistance marker	Ackermann *et al.* 2021
618	**KT2440ge** $\Delta P_{paaF\text{-}paaYX}$**::**$P_{14g}$ Δ***psrA* **(KT2440-AA)**	Exchange of the natural promoter P_{paaF} for the synthetic P_{14g} promoter together with knockout of *paaYX*, knockout of *psrA*	Ackermann *et al.* 2021
2230	**PA1.1**	Evolved A12.1ge strain for growth on pimelate with $gcdR^{\mathrm{G154D}}$	This work
2231	**PA1.2**	Evolved A12.1ge strain for growth on pimelate with $gcdR^{\mathrm{G148D}}$	This work
1447	**KT2440-AA** Δ***gcdR***	Knockout of *gcdR*	This work
1446	**KT2440-AA** Δ***gcdR*****::**P_{14f}	Exchange of the regulator gene *gcdR* for the synthetic P_{14f} promoter	This work
1459	**KT2440-AA** $gcdR^{\mathrm{G154D}}$	$gcdR^{\mathrm{G154D}}$	This work
1454	**KT2440-AA** $gcdR^{\mathrm{G148D}}$	$gcdR^{\mathrm{G148D}}$	This work
1558	**KT2440-AA ALE HDO**	Evolved KT2440ge $\Delta P_{paaF\text{-}paaYX}$::$P_{14g}$ $\Delta psrA$ strain for growth on 1,6-hexanediol	This work
1560	**KT2440 ALE HDO**	Evolved KT2440 wildtype on 1,6-hexanediol	This work
1675	**KT2440 PP_2046**$^{\mathrm{A257T}}$	Partly reverse engineered, PP_2046$^{\mathrm{A257T}}$	This work
1712	**KT2440 PP_2790**$^{\mathrm{A220V}}$	Partly reverse engineered, PP_2790$^{\mathrm{A220V}}$	This work
1713	**KT2440** ***ttgB*****Δ4bp**	Partly reverse engineered, PP_1385$^{\Delta 4\mathrm{bp}}$	This work

Table 2.2.3.: Strains used and generated for this study. (followed)

Micat no.	*P. putida* strain	Description	Reference
1717	**KT2440 PP_2046^{A257T}, PP_2790^{A220V}, *ttgB*$^{\Delta 4bp}$**	Fully reverse engineered strain	This work
1678	**KT2440-AA *secG*^{G70R}**	Fully reverse engineered strain, PP_5706 *secG*^{G70R}	This work
1677	**KT2440-AA PP_5243^{R29P}**	Partly reverse engineered, PP_5243^{R29P}	This work
1718	**KT2440-AA *secG*^{G70R} PP_5243^{R29P}**	*secG*^{G70R}, PP_5243^{R29P} combined	This work
1758	**KT2440-AA *secG*^{G70R} ΔP$_{14e}$-*dcaAKIJP***	Deletion of *dcaAKIJP* in KT2440-AA *secG*^{G70R}	This work
1834	**KT2440-AA *secG*^{G70R} *gcdR*^{G154D}**	Final strain for (u)mcl-DCA and -diol metabolism	This work
2174	**KT2440-AA *secG*^{G70R} *gcdR*^{G154D} ΔPP_5003-6, pS6311·PHB**	Strain for PHB production using pS6311·PHB, containing *phaCAB*, PHB biosynthesis pathway from *C. necator* H16	This work

* All strains for molecular biological procedures are shown in table S1.

2.2.5.3. RT-qPCR

To analyze gene expression levels, RT-qPCR was performed. Therefore, pre-cultures of *P. putida* strains were used to inoculate 50 mL shake flask main-cultures in three-fold buffered MSM containing either glutarate (36 mM), pimelate (25.7 mM), azelate (20 mM) or glucose (20 mM) as sole carbon source to an initial OD600 of 0.1. After incubation to mid-exponential growth phase, cells were harvested from 2 mL of cell culture by centrifugation (21,000 × g for 2 min) and immediately resuspended in 1 mL RNAlater (Thermo Fisher Scientific, Massachusetts, USA) and stored at −20 °C until further analysis. RNA extraction was performed using the Quick-RNA Miniprep Kit (Zymo Research, Irvine, CA, USA) and cDNA was prepared from the purified RNA using the LunaScript RT superMix Kit (New England Biolabs, Ipswich, MA, USA). The expression levels of *gcdH* and *rpoD* were analysed using primer designed by qPCR assay design tool from Eurofins Genomics and listed in table S3. Quantita-

tive RT-PCR was performed using Luna Universal qPCR Master Mix (New England Biolabs, Ipswich, MA, USA) in 96-well plates by the qTOWER 2.2 (Analytik Jena, Jena, Germany). The reaction conditions were used as described in the manufacturer's instructions. Experiments were performed in technical triplicates of biological duplicates. Gene expression levels were evaluated by comparing the Ct values of the housekeeping gene *rpoD* (Wang *et al.* 2010) with the Ct value of *gcdH* using the following equation:

$$\text{Gene expression level} = 2^{\text{Ct(rpoD)-Ct(target)}}$$

2.2.5.4. Genome sequencing

Genomic DNA from selected strains was purified using a Monarch Genomic DNA Purification Kit (NEB) from an overnight LB culture. Afterwards, 1 µg of DNA was used for library preparation using the NEBNext® Ultra™ II DNA Library Prep Kit for Illumina® (New England Biolabs, Ipswich, MA, USA). The library was evaluated by qPCR using the KAPA library quantification kit (Peqlab, Erlangen, Germany). Afterwards, normalization for pooling was done and paired-end sequencing with a read length of 2 × 150 bases was performed on a MiSeq (Illumina, San Diego, CA, USA). The sequencing output (base calls) were received as demultiplexed fastq files. The data (e.g. trimming, mapping, coverage extraction) were processed using the CLC Genomic Workbench software (Qiagen Aarhus A/S, Aarhus, Denmark). For each sample, the output was mapped to the GenBank accession AE015451.2 as the *P. putida* KT2440 reference genome with further modifications for previous genetic engineering (Ackermann *et al.* 2021). Sequencing data are deposited in the NCBI Sequence Read Archive under BioProject number PRJNA987418.

2.2.5.5. Analytical methods

In shake flask experiments, bacterial growth was monitored as optical density at a wavelength of 600 nm (OD_{600}) with an Ultrospec 10 cell Density Meter (Ge Healthcare, Little Chalfront, Buckinghamshire, United Kingdom). Online analysis of growth was measured by the Growth Profiler and analyzed using the Growth Profiler Control software V2_0_0. The corresponding green values are derived from image analysis of the image taken from the bottom of microtiter plates. For measuring extracellular mcl-diols and DCA metabolites, samples were harvested from liquid cultivation by centrifugation (21,000 × g for 2 min) and the supernatant was analysed using a 1260

Infinity II HPLC equipped with a 1260 Infinity II Refractive Index Detector (Agilent, Santa Clara, California, USA). Analytes were eluted using a 150 x 7.80 mm organic acid resin column (Rezex ROA – organic acid H+ (8 %), Phenomenex, Torrance, CA, USA) together with a 40 × 8 mm organic acid resin pre-column with 5 mM H_2SO_4 as mobile phase at a flow rate of 0.7 mL min^{-1} at 80 °C. Metabolites were quantified using HPLC-grade chemicals.

2.2.5.6. PHA and PHB analysis *via* gas chromatography

PHA and PHB quantification was performed using acidic methanolysis and gas chromatography (GC) analysis as described in Li *et al.* (2020). For this, cells were harvested by centrifugation at 5000 × g for 10 min and washed with H_2O_{MilliQ}. Prior to analysis, samples were lyophilized overnight in a Christ LT-105 freeze drier (Martin Christ Gefriertrocknungsanlagen, Osterode am Harz, Germany). Next, 5-15 mg of lyophilized cells were mixed with 2 mL acidified methanol (15 % (v/v) H_2SO_4) and 2 mL chloroform containing methyl benzoate as internal standard in a 15 mL Pyrex tube. The tube was sealed and incubated at 100 °C for 3 h. After cooling the tubes on ice for 2 min, 1 mL of H_2O_{MilliQ} was added to each tube and the solution was mixed by vortexing. The phases were allowed to separate and the organic phase (lower phase) was filtered through cotton wool before further analysis. The 3-hydroxyalkanoic acid methyl esters were quantified using an Agilent 7890A Gas Chromatograph equipped with a HP Innowax column (30 m x 0.25 mm x 0.5 µm) and a flame ionization detector (FID). An oven ramp cycle was employed as follows: 120 °C for 5 min, increasing by 3 °C min^{-1} to 180 °C, 180 °C for 10 min. A 10:1 split was used with helium as the carrier gas and an inlet temperature of 250 °C. Commercially available 3-hydroxyalkanoic acids (C_4-C_{12}) were methylated as described above and used as standards to quantify PHA monomers.

Declaration of competing interest
The authors declare no competing interest

Funding
This project has received funding from the European Union's Horizon 2020 research and innovation programme under Grant Agreements No. 870294 for the project MIX-UP to N.W. This project has received funding from the Bio-based Industries Joint Undertaking (JU) under the European Union's Horizon 2020 research and innovation programme under grant agreement No 887711 to N.W. The JU receives support from the European

Union's Horizon 2020 research and innovation programme and the Bio-based Industries Consortium. This project was also partially supported by The Novo Nordisk Foundation through grants NNF20CC0035580, LiFe (NNF18OC0034818) and TARGET (NNF21OC0067996) and the European Union's Horizon 2020 Research and Innovation Programme under grant agreement No. 814418 (SinFonia) to P.I.N.

2.3. Engineering of 1,4-butanediol and adipic acid metabolism in *P. taiwanensis* for upcycling to aromatic compounds.

Leonie Op de Hipt*, **Yannic S. Ackermann***, Hannah de Jong, Tino Polen, Benedikt Wynands, Nick Wierckx
*these authors contributed equally to this study.

manuscript in preparation
status: unpublished

CRediT authorship contribution statement:

Leonie Op de Hipt:Methodology, Investigation, Validation, Formal analysis, Data curation, Writing—original draft, Writing—review and editing, Visualization

Yannic S. Ackermann: Methodology, Investigation, Validation, Formal analysis, Data curation, Writing—original draft, Writing—review and editing, Visualization

Hannah de Jong: Investigation, Writing—review and editing

Tino Polen: Methodology, Formal analysis, Data curation, Writing—review and editing

Benedikt Wynands: Methodology, Writing—review and editing, Supervision

Nick Wierckx: Conceptualization, Resources, Data curation, Writing—original draft, Writing—review and editing, Visualization, Supervision, Project administration, Funding acquisition

Overall, own contribution: 45 %

The presented experimental work was conducted by LO and HdJ (diol part), YSA and LO (dicarboxylic acid part). Validation was done by LO, YSA, TP, BW and NW. Visualization of all data was performed by LO and YSA. The writing of the original draft was done by LO and YSA, which was reviewed and edited by NW and all co-authors. Funding for the project was acquired by NW.

2.3.1. Abstract

The overwhelming amount of plastic produced is an unprecedented challenge for humanity especially due to the lack of end-of-life solutions for heterogeneous plastic wastes that cannot be recycled conventionally. One possibility is feedstock recycling of mixed plastics and complex polymers, combined with subsequent biological funneling and upcycling. Common depolymerization products include aliphatic dicarboxylic acids or diols such as adipic acid (AA) and 1,4-butanediol (BDO). In this work, the substrate spectrum of an aromatic overproducing *P. taiwnanensis* was extended to AA and BDO to enable upcycling of these compounds. For this purpose, adaptive laboratory evolution followed by genome sequencing was used and key growth-enabling mutations were discovered. In the case of AA, in addition to expression of the heterologous *dcaAKIJP* genecluster and the *paa* genes, mutations in the ribosomal protein encoding gene *rpmE* were identified that are thought to affect production and thus growth. In contrast to *P. putida* KT2440, knockout the repressor gene *psrA* regulating expression of genes involved in β-oxidation had no positive effect on growth on AA. Growth on BDO was enabled *via* a point mutation enabling expression of PVLB_10545 encoding a dehydrogenase. This dehydrogenase likely catalyzes the oxidation of BDO to 4-hydroxybutyrate thus substituting for PedI, which is present in *P. putida* but not *P. taiwanensis*. Two additional mutations further enhanced growth most likely by speeding up steps downstream 4-hydrxybutyrate. The first mutation was identified in PVLB_12690 encoding a LysR dependent transcriptional regulator, whose homologue was also mutated in *P. putida* KT2440 after evolution on BDO. Both strains were then characterized for growth and production of aromatic compounds such as tyrosine and phenylalanine as model compounds with AA and BDO as carbon source.

2.3.2. Introduction

The plastic crisis presents one of the biggest challenges of modern society. Plastics themselves are an important cornerstone of today's life due to their beneficial properties and versatile applications (Andrady *et al.* 2009). Therefore, production has increased exponentially in the last 50 years and is predicted to further rise (Geyer *et al.* 2017). Since, the current state of plastic economy is up to date mostly linear with 90 % of new materials being produced from fossil feedstocks and only 8.3 % post-consumer recycled plastics in 2021, this enormous increase is accompanied by huge negative consequences (PlasticsEurope 2022). Firstly, plastic production significantly contributes to fossil resource depletion due to their mainly petrochemical production. About 15 % of the global oil demand was used as petrochemical feedstock in 2020 with the biggest fraction of 70 % being used for the production of plastics (10 mb/d) (International Energy Agency (IEA), 2022). Secondly, most of resulting plastic waste is not managed properly. In 2015 about 12 % was incinerated for energy gain and 79 % percent were deposited in landfills eventually ending up in the environment where it accumulates due to the extreme stability of most plastic materials (Geyer *et al.* 2017; Worm *et al.* 2017). Several million tons of plastics enter the sea each year further resulting in widespread pollution of the oceans (Lebreton *et al.* 2018). Even when potential efforts to reduce plastic pollution are taken into account the amount is expected to further rise in the future (Borrelle *et al.* 2020; Jambeck *et al.* 2015; Law *et al.* 2023; Ostle *et al.* 2019). Moreover, the linear plastic economy is associated with emission of huge amounts of greenhouse gasses during their whole life from manufacturing to potential incineration. Today plastics are already responsible for 4.5 %of global greenhouse gas emissions (Cabernard *et al.* 2021; Stegmann *et al.* 2022). To stop this extremely harmful and unsustainable trend, solutions leading to a more circular plastics economy are needed. Bioplastics could present a promising approach to help solve this problem (Narancic *et al.* 2020). One interesting candidate is the biodegradable aliphatic aromatic co–polyester poly(butylene adipate-*co*-terephthalate) (PBAT), which is synthesized by esterifying 1,4 butanediol (BDO) with terephthalate and successive polycondensation with adipate (AA) (Wu *et al.* 2023). It has similar properties to non-biodegradable polyolefins such as LDPE, while being much more prone to biological degradation (Ferreira *et al.* 2019). However, it is also a more complex polymer, consisting of a mix of three different monomers. This makes the material an interesting target for biological re- or upcycling. Moreover, in a worst-case scenario, in which the polymer ends up in the environment due to improper disposal, the biodegradability reduces the overall accumulation of plastic waste, which is associated

with many hazardous effect on wildlife and nature (Wei *et al.* 2020). For those reasons, PBAT has already been industrially produced and introduced to the market as a more sustainable and eco-friendlier alternative to polyolefines more than 20 years ago and is mostly used as mulch-foils or as packaging material in various sectors (Jian *et al.* 2020b). Furthermore, although currently mostly produced from fossil resources, biological production pathways exist for AA (Kallscheuer *et al.* 2017) and BDO, with the latter already being produced at industrial scale (Burgard *et al.* 2016). This further underlines the high potential that PBAT has as a candidate for a more sustainable circular plastic economy. However, to ensure full circularity, suitable end-of-life options in form of recycling must be developed. These should be suited for the enormous heterogeneity of plastic waste, usually containing a variety of different polymers consisting of different monomers with various bond types as well as additives. Here a combination of chemical approaches as well as enzymatic depolymerization might be necessary for degradation of all polymers (Ellis *et al.* 2021; Jehanno *et al.* 2022; Sullivan *et al.* 2022). Hydrolysates resulting from such depolymerization will be chemically diverse, which would make the purification of single monomers difficult and expensive. A very promising and cost-effective solution here could be to use these hydrolysates as a carbon source for microbial biotechnology (Ellis *et al.* 2021; Wierckx *et al.* 2015). The monomers are funneled into the central carbon metabolism of a pure or a mixed culture of microorganism that use them as energy source to grow and more importantly produce a desired compound that eventually can be more easily purified from the culture broth such as polyhydroxyalkanoates (PHAs), bio-polyurethane and β-ketoadipic acid (Linger *et al.* 2014; Merchan *et al.* 2022). Pseudomonads are very promising hosts for such a metabolic funneling approach as they have a very broad substrate spectrum as well as a high resistance to harsh conditions such as high concentration of the plastic monomers (Bitzenhofer *et al.* 2021). The substrate spectrum of *Pseudomonas putida* KT2440 has already been broadened to include several plastic monomers (Ackermann *et al.* 2021; Franden *et al.* 2018; Li *et al.* 2019; Li *et al.* 2020). Moreover, Pseudomonads have also been developed to synthesize a variety of products ranging from bioplastics to biosurfactants (Loeschcke *et al.* 2015; Narancic *et al.* 2021; Tiso *et al.* 2020a). One especially interesting strain is *Pseudomonas taiwanensis* VLB120, which has been shown to have a high resistance to various solvents and has already been used to produce interesting aromatic compounds (Schwanemann *et al.* 2020). Wynands *et al.* (2019) have created a genome reduced chassis strain with enhanced flux into the shikimate pathway, which has been shown to be a superior platform strain for the production of

aromatics. Among these are 4-coumarate and derived *para*-hydroxy aromatics which in turn can be used as building blocks for new synthetic polymers (Wynands *et al.* 2023). To enable metabolic funneling of plastic monomers into the central carbon metabolism of these aromatics-producing strains, engineering of corresponding catabolic pathways is necessary. For this purpose, two helpful approaches can be followed. In both cases, the first step is, if necessary, heterologous expression of genes encoding enzymes with functions that are not natively present and that cannot be easily gained by modification or activation of native genes. Next, Adaptive Laboratory Evolution (ALE) has been shown to be a powerful tool to enable growth on plastic monomers (Franden *et al.* 2018; Li *et al.* 2019). Alternatively, the mutations found after an ALE can be genetically reconstructed in the unevolved strain. In this work, the substrate spectrum of a tyrosine producing *P. taiwanensis* strain was expanded to the PBAT-monomers AA and BDO by ALE and by targeted reconstruction of mutations that emerged during the ALE. These were largely diverging from the mutations identified in *P. putida* evolved on 1,4-butanediol, which underlines the differences between the two strains but also the high potential of ALE to identify new genetic targets and thereby enable unbiased engineering. The effect of the mutations was investigated in more detail contributing to a wider knowledge about the degradation pathways. Furthermore, the influence of both approaches on tyrosine and potentially derived aromatics production was investigated.

2.3.3. Results and discussion

2.3.3.1. Engineering growth on adipate and 1,4-butanediol *via* adaptive laboratory evolution

Growth of *P. putida* KT2440 on AA could only be achieved with additional heterologous expression of the *dcaAKIJP* cluster from *Acinetobacter baylyi* complementing the phenylacetate degradation pathway with the enzymes enabling uptake and initial conversion of AA to the common metabolite 2,3 didehydroadipyl-CoA (Ackermann *et al.* 2021; Parke *et al.* 2001). Additionally, an ALE was performed resulting in a constitutive expression of the phenylacetate degradation cluster (Ackermann *et al.* 2021). Based on this knowledge, the *dcaAKIJP* was genomically integrated into the *attTn7*-site (Zobel *et al.* 2015) of *P. taiwanensis* GRC3Δ5-TYR2, a tyrosine overproducing genome reduced chassis strain, to enable its constitutive expression. With this strain, six parallel ALE runs were performed with AA as sole carbon source (Figure 2.3.1).

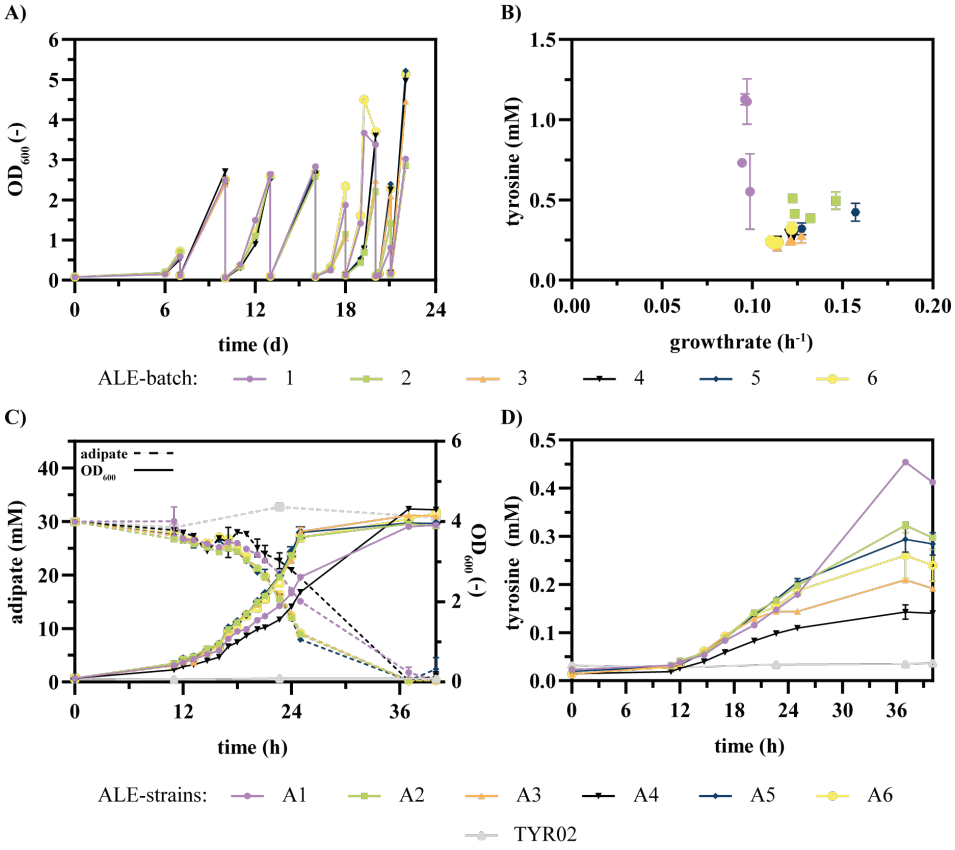

Figure 2.3.1.: ALE of *P. taiwanensis* GRC3Δ5-TYR2 *attTn7*::P_{14e}-*dcaAKIJP* on AA. A) Sequential batch cultivation of the strain *P. taiwanensis* GRC3Δ5-TYR2 *attTn7*::P_{14e}-*dcaAKIJP* in 10 mL MSM with 30 mM AA as sole carbon source in Boston bottles. Six runs were performed in parallel. B) End concentrations of tyrosine measured *via* HPLC analysis plotted against growth rate of single strains isolated from all six ALE-batches. The strains were cultivated in the GP while online-monitoring growth *via* green values (GV). To calculate the growth rates GV were converted into OD_{600} equivalents using a calibration. The growth rates were calculated for all cultures with the OD_{600} equivalents in the range from 0.5 to 0.9. C) OD_{600}, AA concentrations and D) tyrosine concentrations measured at different timepoints during the cultivation of six selected evolved strains in shake flasks. Error bars derive from three technical replicates and indicate the SEM.

In all runs growth on AA could be detected after a long lag phase of six days. After several reinoculation steps, higher OD_{600} values were achieved in shorter time spans. The ALE was terminated on day 22 after approximately 32 to 37 generations, when all six cultures reached an OD_{600} above 3 within a day. In contrast to the evolution of *P. putida* KT2440 on adipate, no additional carbon source was necessary. This is probably due to the fact that a stable and good expression of the *dcaAKIJP* cluster right at the beginning of the ALE was ensured *via* Tn7 integration (Zobel *et al.* 2015). In *P. putida* KT2440, a plasmid-based expression of *dcaAKIJP* was used, which may have presented an additional bottleneck at the beginning of the ALE that prevented growth without further carbon source. This hypothesis is supported by mutations affecting the copy number of the plasmid that emerged during ALE (Ackermann *et al.* 2021). For selection of the strains with the most beneficial mutations, singling smear from all six batches on LB-agar plates was performed and single colonies were tested for growth and tyrosine production from AA (Figure 2.3.1). One strain with the best combination of growth and production was chosen from each ALE run for further investigation. The selected strains differ in growth rate and amount of produced tyrosine indicating that different mutations occurred. Moreover, the amount of tyrosine produced is approximately ten times lower compared to the amount produced by the original strain from 20 mM glucose, with a carbon yield of 0.02 ± 0.00 C_{mol} C_{mol}^{-1} and 0.21 ± 0.01 C_{mol} C_{mol}^{-1} respectively (Otto *et al.* 2019). One reason for this could be that AA is channeled into the central carbon metabolism *via* the TCA-cycle. Therefore, the precursors for tyrosine production must be formed *via* gluconeogenic reactions instead of glycolysis resulting in a higher energetic expense. Therefore, AA is a less beneficial substrate for tyrosine production compared to glucose. A similar effect has been observed before for production of 4-hydroxybenzoate and phenol from xylose *via* the TCA-cycle through the oxidative Weimberg pathway (Lenzen *et al.* 2019; Wynands *et al.* 2018). Furthermore, mutations impairing the production might have occurred during the ALE, considering that aromatics production likely poses a metabolic burden which provides selective pressure favoring repressor mutations.

In contrast to AA as carbon source, for BDO no heterologous genes are necessary to enable growth of *P. putida* KT2440 and it can be degraded *via* several oxidation steps catalyzed by different native dehydrogenases. In specific, the cluster PP_2047-2051 as well as the *ped*-cluster have been shown to be involved in the oxidation of BDO (Li *et al.* 2020). However, the *ped*-cluster is absent in *P. taiwanensis* VLB120 and alternative dehydrogenases oxidizing BDO and intermediates need to be identified. Therefore, an

ALE was carried out with the tyrosine over producer *P. taiwanensis* TYR2 and the same strain evolved on AA, *P. taiwanensis* A1. During the first two weeks, almost no growth on BDO was detected. As before for the ALE on AA, an increase in the measured OD_{600} values and a simultaneous decrease in the required cultivation durations could be seen with increasing number of ALE steps. For identification of advantageous mutations, single strains were isolated from the ALE and tested for their growth and tyrosine production from BDO. For more detailed insights in improvement between different ALE steps, the best strains from two different timepoints were chosen (Figure 2.3.2). The strains *P. taiwanensis* AB1 and AB2, which originated from *P. taiwanensis* A1, were isolated after 4 and 9 rounds of cultivation, resulting in respective growth rates of 0.065 ± 0.002 h^{-1} and 0.114 ± 0.001 h^{-1}. The increase in the growth rates between the two timepoints indicates the appearance of additional mutations.
The strain *P. taiwanensis* B1 that was not evolved on AA before grew with a similar growth rate of 0.111 ± 0.002 h^{-1}. Moreover, this strain produced 1.4 ± 0.02 mM tyrosine corresponding to a carbon yield of 0.09 ± 0.00 C_{mol} C_{mol}^{-1}. Compared to the original strain on glucose it is still smaller, which is likely due to the disadvantageous carbon source, but compared to the strain that was evolved on AA before, which produced amounts of tyrosine in the range of 0.01 ± 0.00 C_{mol} C_{mol}^{-1} and 0.02 ± 0.00 C_{mol} C_{mol}^{-1}, the carbon yield on BDO is still considerably higher, promoting the earlier explained hypothesis that mutations might have occurred during the ALE on AA that impair tyrosine production.
To further expand the substrate spectra for the diols analogously to the dicarboxylic acids up to a chain length of six carbon atoms the growth of the evolved strains on 1,5-pentanediol and 1,6-hexanediol was also tested. All strains were able to grow on 1,5-pentanediol. Interestingly, only the strain that has also been evolved on AA was able to grow on 1,6-hexanediol indicating metabolization of 1,6-hexandiol *via* AA. Upon knockout of the *dcaAKIJP* cluster in this strain, growth on 1,6-hexanediol was significantly reduced, which further promotes this hypothesis. However, some growth could still be detected indicating that an additional route for metabolization of 1,6-hexanediol is present (Figure S11).

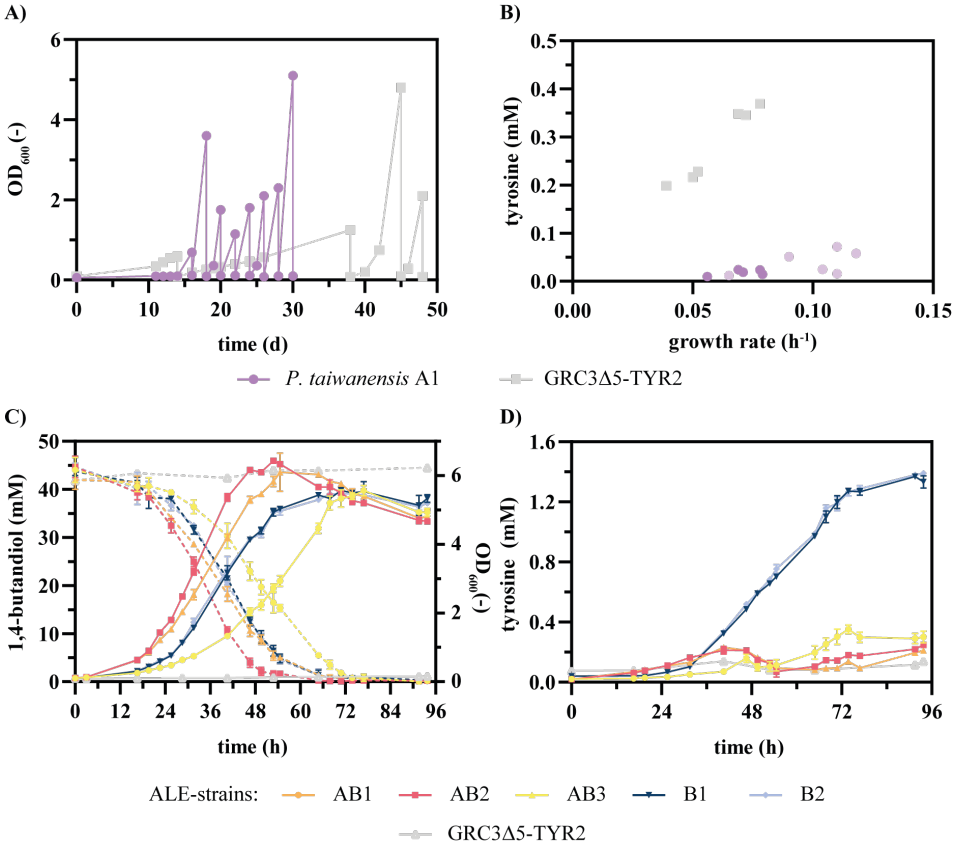

Figure 2.3.2.: ALE of *P. taiwanensis* A1.6 and *P. taiwanensis* GRC3Δ5-TYR2 *attTn7*::P_{14e}-*dcaAKIJP* on BDO. A) Sequential batch cultivation of the strain *P. taiwanensis* A1.6 and *P. taiwanensis* GRC3Δ5-TYR2 in 10 mL MSM with 45 mM BDO as sole carbon source in Boston bottles. B) End concentrations of tyrosine measured *via* HPLC analysis plotted against growth rate of different strains isolated from both ALE-batches. The strains were cultivated in the GP while online-monitoring growth *via* GV. To calculate the growth rates GV were converted into OD_{600} equivalents using a calibration. The growth rates were calculated for all cultures with the OD_{600} equivalents in the range from 0.5 to 0.9. C) OD_{600}, BDO concentrations and D: tyrosine concentrations measured at different timepoints during the cultivation of five selected evolved strains in shake flasks. Error bars derive from three technical replicates and indicate the SEM.

2.3.3.2. Characterization and reverse engineering of causal mutations for 1,4-butanediol and adipic acid metabolism

Adaptive laboratory evolution is a very powerful and promising approach to enable growth on non-preferred substrates. However, the mutations are random and may have unfavorable effects on the strains with regard to production or growth under other conditions. Therefore, a promising next step is to apply the knowledge gained from ALE and subsequent whole genome sequencing to a well-defined parental strain. This way, only known and beneficial modifications are used and a defined strain background can be guaranteed. Considering the enhanced growth rate of all selected strains with BDO as sole carbon source, mutations were expected in all five strains (Table 2.3.1). The only mutation that could be identified in the strain *P. taiwanensis* AB1 was a SNV in PVLB_10540 encoding hypothetical protein without known function that resulted in a silent mutation. *In silico* analysis of the corresponding genomic area revealed no indications for a regulatory role of the mutated sequence, but an increased expression of the downstream gene, which encodes an ethanol-active dehydrogenase, could be detected within the reverse engineered strain *via* RT-qPCR (Figure S12). Moreover,

Table 2.3.1.: Genomic loci affected by ALE on BDO.

Found in strain	affected locus	putative function	mutation (position in genome)	putative effect
AB1, AB2, AB3	PVLB_10540	Small hypothetical protein	G → A (2316640)	Missense, alteration of regulatory region
AB2, AB3	PVLB_12690	LysR family transcriptional regulator	C → T (2802833)	A247V
B1, B2	PVLB_13305	Sigma factor dependent transcriptional regulator	T → C (2946894)	S141P
B1, B2	PVLB_10765	Diguanylate cyclase	C → T (2368691)	G179D
B1, B2	PVLB_02465 and intergenic region between PVLB_02465 and *putA*	Acyl-CoA-dehydrogenase	Deletion (567672-568117)	alteration of regulatory region

upon reconstruction of this mutation in the unevolved strain, growth on BDO could be

recovered (Figure 2.3.3). It can be concluded that the mutation activates expression of PVLB_10545, encoding the ethanol active dehydrogenase, which in turn is responsible for oxidation of BDO and/or its oxidation products and thereby enables its degradation. However, growth is still decreased compared to the evolved strains, indicating that further beneficial mutations have occurred. One mutation, which was present in the strain isolated at a later timepoint is a SNV in PVLB_12690 resulting in an amino acid exchange in a LysR family transcriptional regulator. Interestingly, the homologue with 79 % sequence identity was also mutated in a *P. putida* KT2440 evolved on BDO. In context of *P. putida* KT2440, the encoded regulator was shown to be an activator of the downstream gene cluster PP_2047-51 and the mutation resulted in constant expression of the corresponding genes encoding among others for several dehydrogenases. The ion active dehydrogenase encoded by PP_2049 in particular was shown to be involved in BDO metabolization (Li *et al.* 2020). In contrast to *P. putida* KT2440, reconstruction of this mutation alone did not enable the growth on BDO, which can be explained by the lack of the *ped*-cluster. PedI was shown to oxidize BDO to 4-hydroxybutyrate in *P. putida* KT2440 (Li *et al.* 2020). Since this cluster is missing in *P. taiwanensis* VLB120 this first step is not catalyzed and therefore no growth is possible. In combination with the silent mutation however growth is enabled indicating that the silent mutation is responsible for the initial conversion of BDO. Therefore, it can be concluded that the ethanol active dehydrogenase encoded by PVLB_10545 substitutes for PedI in the evolved *P. taiwanensis* strains and oxidizes BDO to 4-hydroxybutyrate. When the mutation in PVLB_10540 is combined with the mutation in PVLB_12690 an increase in growth rate is achieved, proving a positive influence of the mutation in PVLB_12690 on BDO metabolism. It is therefore likely that this mutation accelerates a limiting step downstream of the initial oxidation of BDO. This hypothesis was also strengthened by the fact that growth on 4-hydroxybutyrate is influenced by the reconstruction of PVLB_12690^{A247V}. Initial slow growth followed by a rapid increase was observed, which can be explained by initial accumulation of succinate semialdehyde, suggesting that the dehydrogenases encoded by the PVLB_12665-12685 gene cluster catalyze the oxidation of 4-hydroxybutyrate to succinate semialdehyde (Figure S13). The aldehyde in turn might have a growth inhibitory effect causing the slow growth on 4-hydroxybutyrate in the beginning of cultivation (Bitzenhofer *et al.* 2021; Jayakody *et al.* 2018). However, once the aldehyde has been further metabolized to succinate in sufficient concentration, rapid growth occurs due to quick succinate metabolization. A similar aldehyde inhibition delay has also been observed during engineering of *P. putida* KT2440 metabolism of

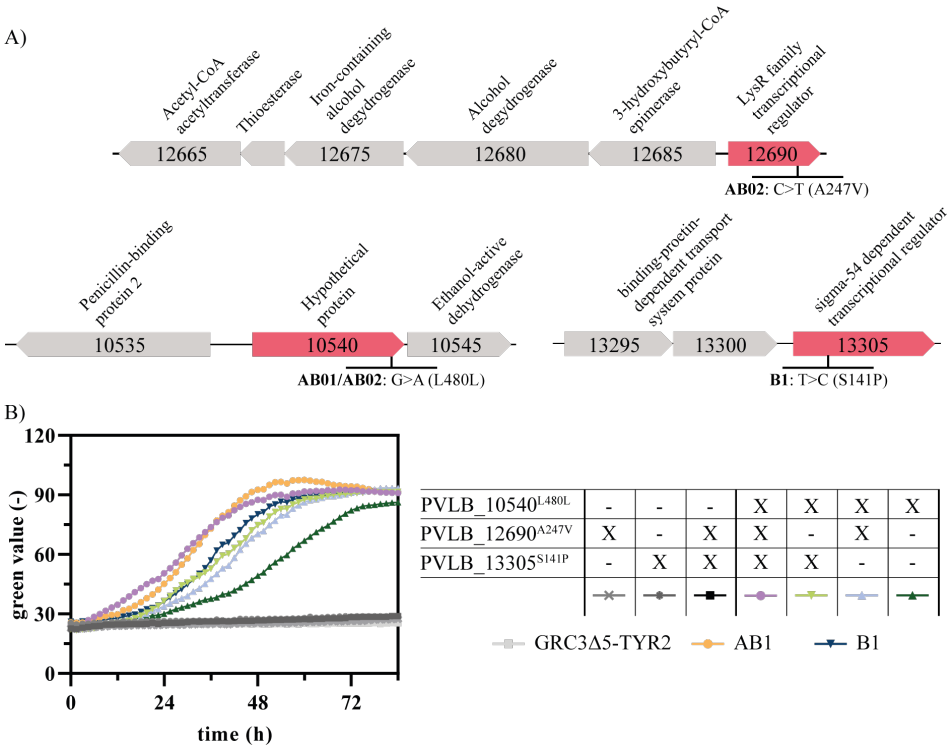

Figure 2.3.3.: Reverse engineering of *P. taiwanensis* GRC3Δ5-TYR2 strains for growth on BDO. A) Genomic context of mutations identified in the evolved strains with positive effect on growth on BDO. B) Growth curves of engineered strains carrying different mutations found during the whole genome sequencing of the ALE on BDO. All strains are cultivated in three-fold buffered MSM medium containing 45 mM of BDO as sole carbon source. Error bars represent the standard error of the mean (n=3).

ethylene glycol (Franden *et al.* 2018). In contrast, the strain *P. taiwanensis* B1 does not harbor any of the two described mutations but instead one in PVLB_13350 encoding a sigma factor dependent transcriptional regulator and one in PVLB_10765 encoding a diguanylate cyclase, both resulting in amino acid exchanges. Additionally, a deletion of 445 bp was identified in the intergenic region between PVLB_02465 encoding an acyl-CoA dehydrogenase and *putA*. Upon reverse engineering of the two first mutations no growth could be restored indicating that there is still a limiting step in the metabolism of BDO. This step could be circumvented by reconstruction of the silent mutation in PVLB_10540 from the strain *P. taiwanensis* AB1. When the mutation of the strain *P. taiwanensis* B1 in the sigma factor dependent transcriptional regulator encoded by

PVLB_13350 was combined with the silent mutation and the mutation in PVLB_12690 the resulting strain mimicked the growth phenotype of *P. taiwanensis* AB1. Hence, a positive effect of the mutation in PVLB_13350 on the growth on BDO can be concluded, resulting in the best growing reverse engineered strain. In contrast, combining the silent mutation in PVLB_10540 with the mutation in the gene encoding the diguanylate cyclase had no effect and in combination with all three other mutations a negative effect can be seen (Figure S14). Therefore, the diguanylate cyclase is probably not directly involved in BDO metabolism. Although ALE-like growth could be restored *via* reverse engineering, the question remains unanswered how the evolved strain *P. taiwanensis* B1 can grow without the silent mutation in PVLB_10540. The most likely hypothesis is that growth is enabled by the deletion of 445 bp between PVLB_02465 and *putA*, but this mutation could not be reverse engineered. In addition, the original growth rate of the evolved strain AB1 could only be achieved by reconstructing an additional mutation from strain B1 suggesting that there are other effects within AB1 that positively affect growth. Possibly, these effects are related with the reduced tyrosine production that occurred after the primary evolution of the strain on AA.

In all evolved strains isolated from the ALE on AA, mutations were identified within the genomic region of *paaXY* as well as *rpmE*. In a previous study where *P. putida* KT2440 was evolved on AA, a transposon insertion upstream of *paaXY* led to the overexpression of the *paa* gene cluster through the formation of a fusion promoter. Furthermore heterologous expression of *dcaAKIJP* on the one hand and activated expression of the *paa* gene cluster due to knockout of the repressor genes on the other hand enabled growth of *P. putida* KT2440 on AA as sole carbon source, suggesting the importance of the activated phenylacetate degradation pathway. It was concluded that DcaAKIJP enable uptake and activation of AA to 2,3-didehydroadipyl-CoA, which is a common metabolite to the phenylacetate degradation pathway that encoded by the *paa* cluster. Moreover, ALE of *P. putida* reveals the advantage of a higher β-oxidation activity induced by the deletion of the gene *psrA*, which encodes for the repressor of *fadAB* (Ackermann *et al.* 2021). The mutations identified in the six *P. taiwanensis* strains evolved on AA in this study range from a deletion of 402 bp in *paaX* to SNVs in *paaX* as well as in the intergenic region between *paaF* and *paaX*. Therefore, *paaYX* was deleted in the unevolved strain harbouring the *dcaAKIJP* genes at the *attTn7* site. This resulted in a strain capable of growing on AA as sole carbon source, although this growth was much worse and the strain took twice as long to reach stationary phase as the ALE strain A1 (Figure 2.3.4). Since this strain will later be used for a bio-upcycling approach

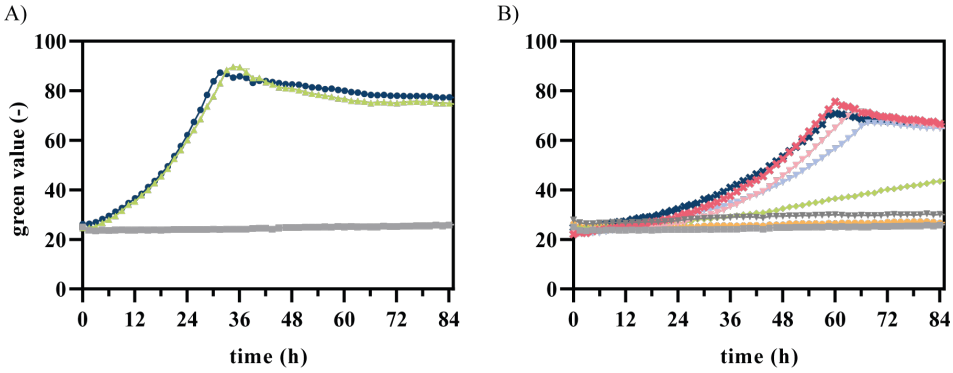

Strain background	A1		GRC3Δ5-TYR2							
dcaAKIJP	*attTn7*	*attTn7*	*ΔpaaYX*	*ΔpaaYX*	*attTn7*	*attTn7*	*attTn7*	*attTn7*	-	-
ΔpaaYX	mutated	mutated	-	-	X	X	-	-	-	-
ΔpsrA	-	X	X	-	X	-	X	-	X	-

Figure 2.3.4.: Characterization of growth of reverse engineered *P. taiwanensis* GRC3Δ5-TYR2 strains on AA. All strains are cultivated in three-fold buffered MSM medium containing 30 mM of AA as sole carbon source. A) Analysis of the growth of the evolved strain A1 on AA and the influence of the deletion of *psrA*. B) Growth curves of engineered strains carrying different mutations found during the whole genome sequencing of the ALE strains. Error bars represent the standard error of the mean (n=3).

and will therefore require further metabolic engineering and heterologous integration of production clusters, it is advantageous to keep well-established integration sites, such as *attTn7*, empty. For this purpose, the *dcaAKIJP* expression cassette was integrated directly into the position of the regulatory genes *paaYX*, deleting the latter genes in the process. The resulting strain GRC3Δ5-TYR2 Δ*paaYX*::P_{14e}-*dcaAKIJP* was also able to grow on AA as sole carbon source. Furthermore, growth could be slightly increased compared to the integration at the *attTn7*-site, suggesting that the integration at *paaYX* seems to be beneficial, perhaps due to a higher expression rate of the *dcaAKIJP* cluster. However, growth was still not comparable to that of the evolved strains. Previously, it was shown that an increased β-oxidation could enhance growth of *P. putida* KT2440 on AA as sole carbon source, induced by a deletion of *psrA* (Ackermann *et al.* 2021). It was striking that unlike in *P. putida*, the gene encoding the β-oxidation regulator PsrA was not mutated in any of the evolved *P. taiwanensis* strains, nor were any other mutations found that could plausibly affect β-oxidation. To investigate this difference, *psrA* was deleted in the evolved strain A1 and in the reverse engineered strains. Deletion

of *psrA* in the ALE-strain has no effect on growth, suggesting that β-oxidation does not limit growth on AA in the ALE-background. In contrast, deletion of *psrA* could indeed slightly increase growth in the strain expressing the *dcaAKIJP* genes from *attTn7*-site, although growth was not comparable to the evolved strain. This effect was not visible, when *psrA* was deleted in strain GRC3Δ5-TYR2 Δ*paaYX*::P_{14e}-*dcaAKIJP*. Deletion of *psrA* without deletion of *paaYX* also resulted in weak growth, showing that Δ*psrA* is at least not negative for growth on AA, but that β-oxidation is not the limiting step in AA degradation in this strain. This difference between *P. putida* and the *P. taiwanensis* strains tested here can likely be attributed to the production of aromatic compounds. The GRC3Δ5-TYR2 strain studied here contains many genetic modifications (Wynands *et al.* 2019), which reduce the growth rate of *P. taiwanensis* to the point where β-oxidation catalyzed by the *paa* cluster-encoded enzymes alone is likely sufficient. Another possible cause of the enhanced growth rate of the evolved strains compared to the reverse engineered strain, are the mutations found in the genomic region around *rpmE* (PVLB_01635). These mutations were either a deletion of 236 bp of *rpmE* or point-mutations in the intergenic region (IGR) between *priA* and *rpmE* or in *rpmE* itself (Figure 2.3.5). Downstream of *rpmE*, a putative nuclease and the malic enzyme MaeB are encoded. Hence, these mutations may have an influence on the ribosomal protein bL31 encoded by *rpmE* or on the malate dehydrogenase which is part of the central metabolism. To clarify the effects on growth on AA, all *rpmE* mutations were repaired back to the wildtype sequence in the evolved strains. This resulted in strains that grew much worse, similar to the reverse engineered strain (Figure 2.3.5). This strongly suggests that the mutations around *rpmE* were the reason for the different growth of the strains. To further investigate the reason for the observed phenotype a RT-qPCR was performed to detect changes in the expression levels of *rpmE*, the nuclease (PVLB_01640), *maeB* and *priA*, which is located upstream of *rpmE*. This analysis showed no significant difference in the expression levels of *maeB* or *priA*. The same is true for *maeB* in the strains harboring a mutation within the gene suggesting that the phenotype is rather caused by mis-functional version of the encoded ribosomal protein bL31 than due to changed expression levels. In case of the mutation in the IGR, more precisely in the putative promoter of *rpmE*, the RT-qPCR results show a lower expression level in the mutated strain compared to the repaired version. Surprisingly, in both cases, the ALE strain (strain A3) containing the potential promoter mutation and the repaired strain have higher expression levels of the nuclease-encoding gene than the parental strain harbouring the wildtype genes. Overall, these results suggested a

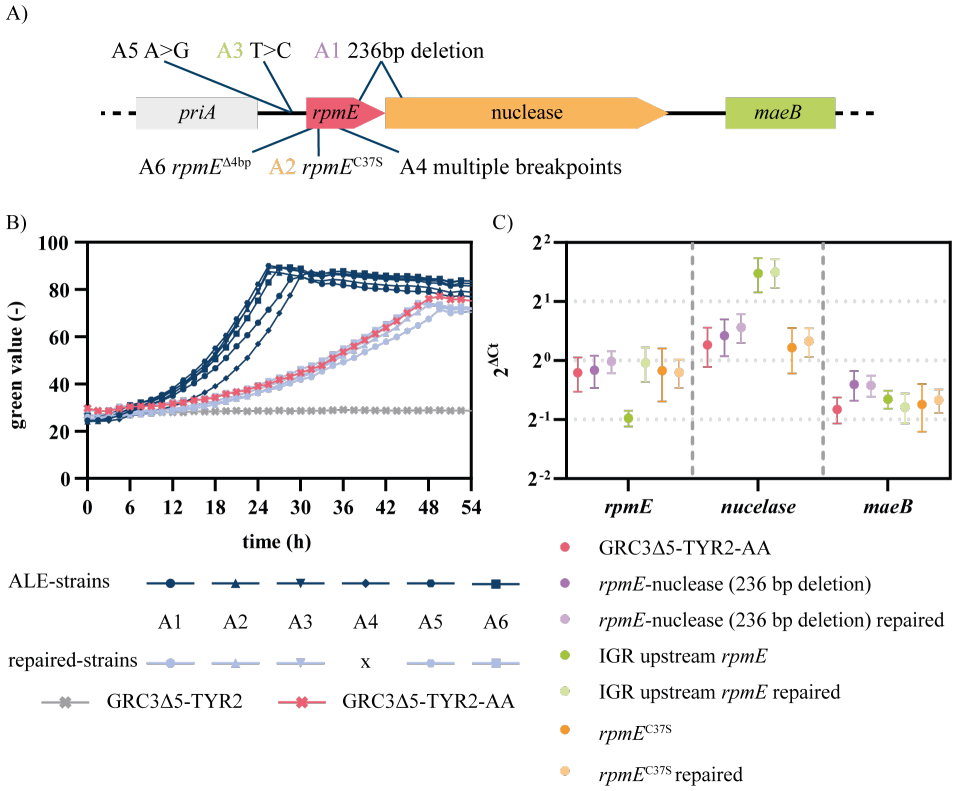

Figure 2.3.5.: Analysis of different mutations in *rpmE* found in all ALE strains. A) Schematic overview of the genomic region of *rpmE* and the mutations of each ALE strain. Arrow size does not correspond to gene size. B) Comparison of growth of ALE strains with corresponding strains, which contain the wildtype sequence of *rpmE* (repaired strains). Growth curves were measured in three-fold buffered MSM medium containing 30 mM of AA with the Growth Profiler. Error bars represent the standard error of the mean (n=3). C) Relative expression levels of *rpmE*, nuclease, and *maeB* in cells of evolved strains and strains with the repaired sequence were determined by RT-qPCR. The Ct values were normalized to *rpoD*. Standard errors of the means were calculated using three technical replicates of two biological replicates.

potential effect of the ribosomal protein bL31 on growth on non-native carbon sources such as AA. The *rpmE* gene encodes the non-essential bacteria-specific (C+) ribosomal protein L31. Many bacteria like *B. subtilis*, *E. coli* or *P. aeruginosa* possess one or more Zn-independent (C-) paralogs (Hensley *et al.* 2012), but these were not found in the genome of *P. taiwanensis*. In *E. coli*, deletion of these paralogs leads to a decreased growth (Aseev *et al.* 2020). In this study, attempts to knock out *rpmE* by homologous recombination were unsuccessful, confirming the absence of a paralog of

RpmE in *P. taiwanensis*. The presence of paralogs of the ribosomal protein in other species is connected to zinc availability. *P. aeruginosa* produces the C- protein when zinc deficiency occurs, although the C+ paralog (which requires zinc as cofactor) is still present. It is assumed that the presence of both ribosomal proteins enables the strain to rapidly switch metabolism as soon as Zn^{2+} is available again (Hensley *et al.* 2012). Even though no paralogs were identified in *P. taiwanensis*, the role of these proteins in *P. aeruginosa* suggests an involvement of zinc availability. To test this hypothesis a growth experiment containing different zinc concentrations was performed (Figure 2.3.6).

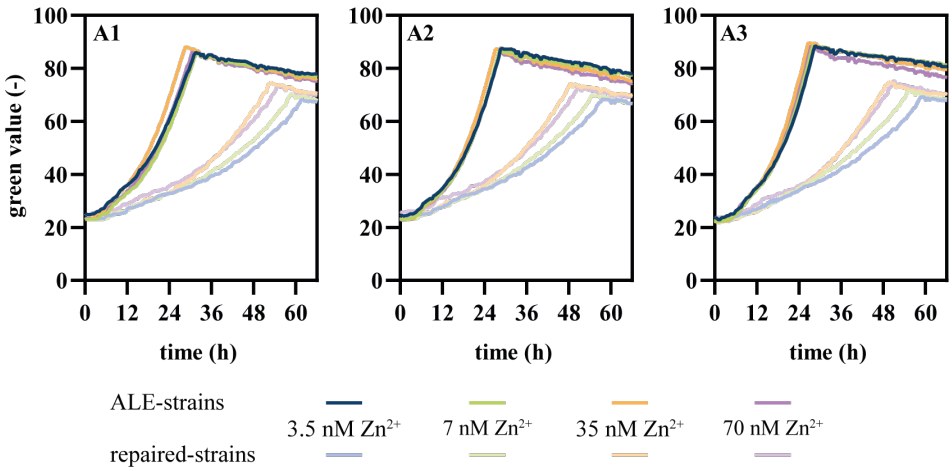

Figure 2.3.6.: Growth of ALE strains and the corresponding repaired *rpmE* strains with different zinc concentrations. All strains were cultivated in three-fold buffered MSM medium containing 30 mM AA and different zinc concentration as shown in the figure. Shaded areas indicate the standard error of the mean, but they are so small, that they are covert by the lines (n=3).

On the one hand, these results indicate a positive effect of higher zinc concentrations in the medium. Our standard MSM medium contains 7 nM Zn^{2+}. Increasing this concentration by five-fold leads to a visible improvement in strains bearing the wildtype *rpmE* sequence, whereas a ten-fold increase does not further optimize growth. These differences are much smaller in the strains harbouring the mutated version of *rpmE*, suggesting a higher tolerance of these strains to zinc limitation in the medium. However, even the highest zinc concentration did not restore growth of the reverse engineered strain to the level of the ALE strains, suggesting that zinc availability is not the primary reason for the growth difference. Nevertheless, the fact that restoration of the

wildtype *rpmE* sequence reduced growth of the evolved strain to the level of the reverse engineered strain clearly indicates the importance of this gene. Hence as alternative hypothesis the production of tyrosine might have been affected by the *rpmE* mutations, which could indirectly improve growth by alleviating the metabolic burden of production.

2.3.3.3. Tyrosine production from adipate and 1,4-butanediol by the evolved and reverse engineered strains

The development of an efficient bio-upcycling approach as part of a circular economy requires besides a well-established consumption of waste stream substrates, such as monomers from plastic waste hydrolysates, also a good production of compounds of higher value. In this study, we aimed to enable the conversion of AA and BDO into aromatic compounds by implementation of monomer metabolism in the tyrosine-producing aromatics platform strain *P. taiwanensis* GRC3Δ5-TYR2 (Wynands *et al.* 2023; Wynands *et al.* 2019) This strain harbours deletions of aromatic catabolic pathways (Δ*hpd*, Δ*quiC*, Δ*quiC1*, Δ*quiC2*, Δ*pobA*) and four modifications (TrpE^{P290S}, AroF-1^{P148L}, PheAT^{310I}, Δ*pykA*) to increase the carbon flux trough the shikimate pathway towards tyrosine (Wynands *et al.* 2019). To test tyrosine production, cultivations were performed on 30 mM glucose and C-equimolar concentrations of AA and BDO, and endpoint measurements were taken at the respective early stationary phases (Figure 2.3.7). On glucose, the parental strain GRC3Δ5-TYR2 accumulates 2.4 ± 0.23 mM tyrosine and 1.7 ± 0.19 mM phenylalanine after 28 h. After 48 h no phenylalanine was detectable and about 3.0 ± 0.18 mM of tyrosine accumulates, suggesting that the phenylalanine is partly converted to tyrosine *via* PhhAB. The difference in the total amount of aromatics produced could be due to separate cultivations and needs to be further investigated in the future. The transient accumulation of phenylalanine was previously also observed by Otto *et al.* (2019) and is probably caused by a bottleneck activity of PhhAB. As this strain is unable to metabolize AA, no growth or tyrosine production on AA took place. In contrast, small amounts of tyrosine/phenylalanine accumulated after 72 h during the cultivation on BDO. In line with this, an increase in biomass was detected within the growth profiler after about60 h (data not shown). Although this was unexpected, the previous ALE shows that this strain can spontaneously mutate to enable BDO metabolism. Likely, this mutation occurred earlier in this culture, causing the slow growth observed here.

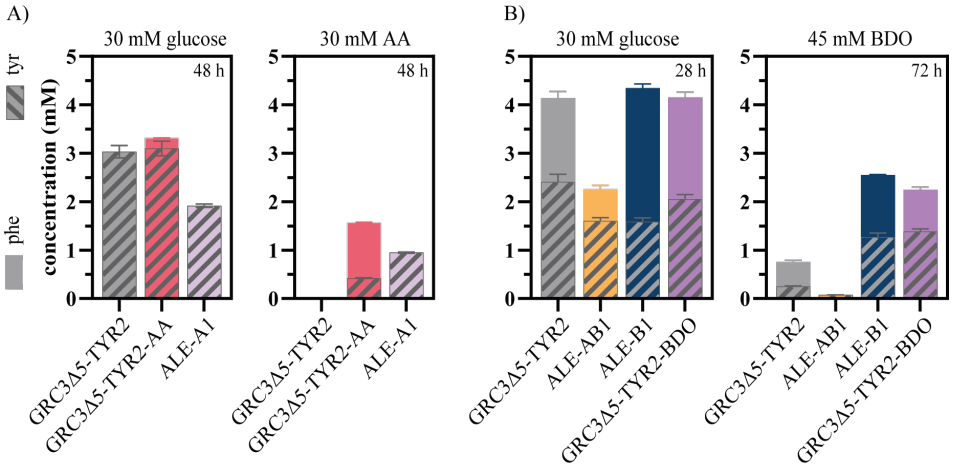

Figure 2.3.7.: Comparison of tyrosine production of evolved strains with reverse engineered strains. All strains were cultivated in three-fold buffered MSM medium containing c-equimolar concentrations of glucose, AA (A) and BDO (B). The amount of tyrosine or phenylalanine are added in the bar chars. Error bars represent the standard error of the mean (n=3).

Both the reverse engineered GRC3Δ5-TYR2-BDO and the ALE-B1 strain produced a similar total of approximately 2.39 ± 0.10 mM aromatics from 45 mM BDO after 72 h, of which 1.33 ± 0.07 mM tyrosine and 1.07 ± 0.04 mM phenylalanine. This constitutes a total yield of 12 % C_{mol} C_{mol}^{-1}. These strains show a similar production from glucose compared to the parental strain with titers approximately twice as high compared to BDO as substrate. This difference was expected, considering that BDO is metabolized *via* succinate, acetyl-CoA, or glycosyl-CoA, which is probably converted to succinyl-CoA *via* the glyoxylate shunt in the TCA cycle, resulting in precursor formation for aromatic production by gluconeogenic reactions (Li *et al.* 2020). Previous work on aromatics production with a comparable strain from xylose metabolized *via* the TCA cycle also resulted in much lower yields, which are comparable to those achieved here (Lenzen *et al.* 2019). The reverse engineered GRC3Δ5-TYR2-AA produced 1.57 ± 0.02 mM aromatics from AA in 48 h, of which 1.15 ± 0.01 mM phenylalanine and 0.42 ± 0.01 mM tyrosine. Growth on AA was faster compared to the BDO strains, but the yield of 7.8 % C_{mol} C_{mol}^{-1} was significantly lower. Using glucose as substrate, the tyrosine production of GRC3Δ5-TYR2-AA (3.1 ± 0.21 mM) is comparable to that of the parental strain after 48 h. However, a small amount of phenylalanine (0.2 ± 0.00 mM) accumulates at this time and is likely to be converted afterwards. Interestingly, the ALE-A1 strain produced significantly less aromatics on both AA and glucose. A

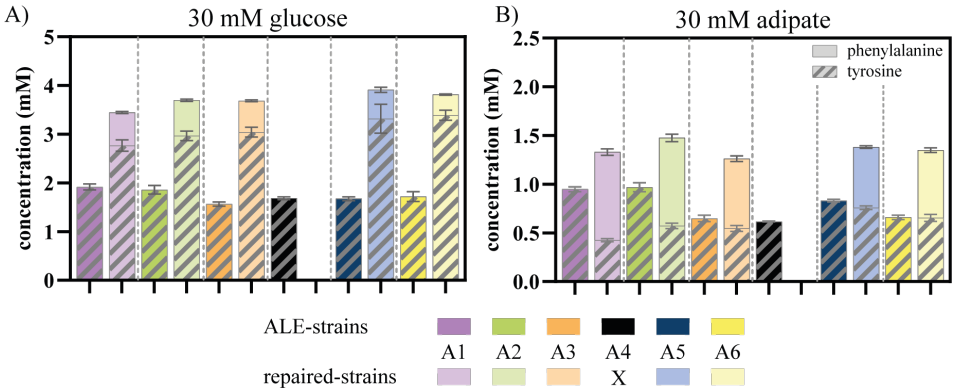

Figure 2.3.8.: Analysis of the influence of mutated *rpmE* on production of tyrosine. All strains were cultivated in three-fold buffered MSM medium containing c-equimolar concentrations of glucose and AA. The amount of tyrosine or phenylalanine are added in the bar chars. Error bars represent the standard error of the mean (n=3).

similar performance was observed for ALE-AB1, which is derived from ALE-A1, on both glucose and BDO. This strongly indicates that a mutation occurred during the ALE on AA that negatively affects production. To test whether the mutations in *rpmE* were responsible for these differences in production, the previously repaired strains were compared with the corresponding ALE strains on glucose and AA. Indeed, all ALE strains only produced about half as much aromatics as the corresponding repaired strains (Figure 2.3.8). This clearly confirms a link between the mutations in *rpmE* and the production of aromatics, although it is currently not clear how the mutation in this ribosomal protein exerts this effect. The *rpmE* mutations likely affect ribosomal activity (Lilleorg *et al.* 2017), which might have an indirect global effect on intracellular amino acid pools due to altered protein synthesis rates. This could in turn affect tyrosine and phenylalanine production directly, or indirectly *via* allosteric inhibition effects in the tyrosine biosynthesis pathway, but this is mere speculation which requires further study. Nevertheless, these results demonstrate the high potential of the bio-upcycling approach.

2.3.4. Conclusion

In this study, we extended the substrate spectrum of a tyrosine-overproducing *P. taiwanensis* strain to the monomers AA and BDO, enabling microbial upcycling to of these PBAT monomers. The two strategies of ALE and reverse engineering proved

to be very useful and each showed different advantages. The ALE enabled fast and unbiased optimization of plastic monomers metabolism, providing clear leads for rational strain engineering and highlighting differences between *P. putida* and *P. taiwanensis*. However, this work also exemplified a drawback of ALE-based optimization for substrate metabolism in the presence of a secondary objective of product formation. This highlights the importance of rational reverse engineering, which in this case restored lost production capacity. The *P. taiwanensis* GRC3Δ5-TYR2 platform can readily be extended with other production modules, enabling production of a wide range of value-added aromatics (Schwanemann *et al.* 2020; Wynands *et al.* 2018; Wynands *et al.* 2023) from plastic monomers. This makes this platform widely applicable for plastic hydrolysate upcycling, which can be further extended by implementation of other monomer-metabolism pathways.

2.3.5. Experimental procedures

2.3.5.1. Strains and culture conditions

The chemicals used in this work were obtained from Carl Roth (Karlsruhe, Germany), Sigma-Aldrich (St. Louis, MO, USA), or Merck (Darmstadt, Germany) unless stated otherwise. All bacterial strains are listed in table 2.3.2.

Table 2.3.2.: Strains used and generated for this study.

Micat no.	*P. putida* strain	Description	Reference
58	**GRC3Δ5-TYR2**	Genome reduced chassis strain optimized for production of tyrosine, harbours trpEP290S and pheAP144S	Wynands *et al.* 2023
1211	**AB1**	GRC3Δ5-TYR2 A1 evolved on 1,4-butanediol as sole carbon source	This work
2507	**AB2**	GRC3Δ5-TYR2 A1 evolved on 1,4-butanediol as sole carbon source	This work
2508	**AB3**	GRC3Δ5-TYR2 A1 evolved on 1,4-butanediol as sole carbon source	This work
1478	**B1**	GRC3Δ5-TYR2 evolved on 1,4-butanediol as sole carbon source	This work
2509	**B2**	GRC3Δ5-TYR2 evolved on 1,4-butanediol as sole carbon source	This work

Table 2.3.2.: Strains used and generated for this study. (followed)

Micat no.	*P. putida* strain	Description	Reference
1148	**AB1** Δ***attTn7*::P_{14e}-*dcaAKIJP***	Restored Tn7 site by knockout of *dcaAKIJP*	This work
1508	**GRC3Δ5-TYR2 PVLB_10540^{L480L}**	Reconstruction of SNV in PVLB_10540	This work
1481	**GRC3Δ5-TYR2 PVLB_12690^{A247V}**	Reconstruction of SNV in PVLB_12690	This work
1480	**GRC3Δ5-TYR2 PVLB_13305^{S141P}**	Reconstruction of SNV in PVLB_13305	This work
1567	**GRC3Δ5-TYR2 PVLB_10765^{G179D}**	Reconstruction of SNV in PVLB_10765	This work
1530	**GRC3Δ5-TYR2 PVLB_10540^{L480L} PVLB_12690^{A247V}**	Combination of SNV in PVLB_10540 and PVLB_12690	This work
1509	**GRC3Δ5-TYR2 PVLB_10540^{L480L} PVLB_13305^{S141P}**	Combination of SNV in PVLB_10540 and PVLB_13305	This work
1482	**GRC3Δ5-TYR2 PVLB_12690^{A247V} PVLB_13305^{S141P}**	Combination of SNV in PVLB_12690 and PVLB_13305	This work
1579	**GRC3Δ5-TYR2 PVLB_12690^{A247V} PVLB_13305^{S141P} PVLB_10765^{G179D}**	Combination of SNV in PVLB_12690, PVLB_13305 and PVLB_10765	This work
1486	**GRC3Δ5-TYR2 PVLB_10540^{L480L} PVLB_12690^{A247V} PVLB_13305^{S141P}**	Combination of SNV in PVLB_10540, in PVLB_12690 and PVLB_13305	This work
1580	**GRC3Δ5-TYR2 PVLB_10540^{L480L} PVLB_12690^{A247V} PVLB_13305^{S141P} PVLB_10765^{G179D}**	Combination of SNV in PVLB_10540 and PVLB_10540, in PVLB_12690, PVLB_13305 and PVLB_10765	This work
623	**GRC3Δ5-TYR2 *attTn7*::P_{14e}-*dcaAKIJP***	Genome integrated *dcaAKIJP* cluster under the control of P_{14e}	This work

Table 2.3.2.: Strains used and generated for this study. (followed)

Micat no.	*P. putida* strain	Description	Reference
1323	**A1**	GRC3Δ5-TYR2 *attTn7*::P_{14e}-*dcaAKIJP* evolved on adipate as sole carbon source	This work
1324	**A2**	GRC3Δ5-TYR2 *attTn7*::P_{14e}-*dcaAKIJP* evolved on adipate as sole carbon source	This work
1325	**A3**	GRC3Δ5-TYR2 *attTn7*::P_{14e}-*dcaAKIJP* evolved on adipate as sole carbon source	This work
1326	**A4**	GRC3Δ5-TYR2 *attTn7*::P_{14e}-*dcaAKIJP* evolved on adipate as sole carbon source	This work
1327	**A5**	GRC3Δ5-TYR2 *attTn7*::P_{14e}-*dcaAKIJP* evolved on adipate as sole carbon source	This work
1328	**A6**	GRC3Δ5-TYR2 *attTn7*::P_{14e}-*dcaAKIJP* evolved on adipate as sole carbon source	This work
1426	**GRC3Δ5-TYR2 Δ*psrA***	Knockout of *psrA*	This work
1427	**GRC3Δ5-TYR2 *attTn7*::P_{14e}-*dcaAKIJP* Δ*psrA***	Knockout of *psrA* in addition to genomic integration of *dcaAKIJP*	This work
1428	**A1 Δ*psrA***	Knockout of *psrA* in evolved strain A1	This work
1434	**GRC3Δ5-TYR2 Δ*paaYX*::P_{14e}-*dcaAKIJP* Δ*psrA***	Combined integration of *dcaAKIJP* at the position of *paaYX* by deleting *paaYX*, knockout of *psrA*	This work
1443	**GRC3Δ5-TYR2 *attTn7*::P_{14e}-*dcaAKIJP* Δ*paaYX* Δ*psrA***	Knockout of *paaYX* and *psrA* in addition to genomic integration of *dcaAKIJP*	This work
1978	**GRC3Δ5-TYR2 Δ*paaYX*::P_{14e}-*dcaAKIJP***	Combined integration of *dcaAKIJP* at the position of *paaYX* by deleting *paaYX*	This work
2399	**GRC3Δ5-TYR2 *attTn7*::P_{14e}-*dcaAKIJP* Δ*paaYX***	Knockout of *paaYX* in addition to genomic integration of *dcaAKIJP*	This work
2233	**A1 *rpmE* (repaired)**	Repaired *rpmE* region with wildtype sequence	This work
2234	**A2 *rpmE* (repaired)**	Repaired *rpmE* region with wildtype sequence	This work

Table 2.3.2.: Strains used and generated for this study. (followed)

Micat no.	*P. putida* strain	Description	Reference
2235	**A3 *rpmE* (repaired)**	Repaired *rpmE* region with wildtype sequence	This work
2244	**A5 *rpmE* (repaired)**	Repaired *rpmE* region with wildtype sequence	This work
2245	**A6 *rpmE* (repaired)**	Repaired *rpmE* region with wildtype sequence	This work

* All strains for molecular biological procedures are shown in table S1.

All strains were routinely cultured in lysogeny broth (LB) medium prepared with premixed LB medium (Carl Roth, Karlsruhe, Germany) or on LB agar plates prepared with a respective mixture (Carl Roth, Karlsruhe, Germany). To select for *Pseudomonas* strains after mating procedures, 25 mg mL irgasan was added. For the selection for delivered genetic elements, antibiotics corresponding to the transferred resistance genes were added in the following concentrations: 50 mg mL kanamycin sulfate, 25 mg mL gentamicin, 100 mg mL ampicillin. Experiments involving the measurement of growth on plastic monomers, their utilization, and the production of aromatic compounds were conducted using a mineral salt medium (MSM) according to Hartmans *et al.* (1989). Pre-cultures were performed in MSM with one-fold buffer and 20 mM of glucose whereas the main cultures were performed with three-fold buffer unless stated otherwise and the plastic monomers instead of glucose. All plastic monomers were added in a C-equimolar concentration to 45 mM 1,4-butanediol. In general, liquid cultures were performed in 500 mL non-baffled Erlenmeyer flasks with a filling volume of 10 %, at 200 rpm shaking speed with an amplitude of 50 mm and a humidity of 80 % using a ISF1-X Climo-Shaker (Kuhner shaker, Birsfelden, Switzerland). All *Pseudomonas* strains were cultivated at 30 °C and all *E. coli* strains at 37 °C. For online monitoring of growth, liquid cultivations were performed in a 96-microwell plate with transparent polystyrene bottom (Enzyscreen, Heemstedem, The Netherlands) within the Growth Profiler (Enzyscreen, Heemstedem, The Netherlands) at 224 rpm with an amplitude of 50 mm and 30 °C.

2.3.5.2. Adaptive laboratory evolution

ALE was performed in 100 mL Boston bottles filled with 10 mL MSM. The first ALE step was inoculated with an overnight culture grown on glucose. As soon as the cultures were turbid, the cultures were sampled and OD_{600} was measured. If OD_{600} was above 1, fresh medium was inoculated for the next ALE step. Starting OD_{600} of every ALE step was 0.1. Cells used for inoculation were washed with sterile 0.9 % NaCl to prevent transfer of media components and allow cultivation under constant conditions. The ALE experiment was stopped when the cultures reached an OD_{600} above 2.8 overnight. At the end of ALE, single colonies were isolated on LB agar plates and subsequently analyzed for their growth and tyrosine production from adipate. For this they were grown in the Growth Profiler (Enzyscreen, Heemstedem Netherlands). Depending on growth and tyrosine production, at least one strain from each ALE batch was selected for whole genome sequencing and further analysis in shake flask cultivations.

2.3.5.3. Plasmid cloning and strain engineering

All primers and plasmids utilized in this work are listed in table S2 and table S3. The primers were ordered from Eurofins Genomics (Ebersberg, Germany) and used in combination with Q5 High-Fidelity Polymerase to amplify DNA fragments *via* PCR. The fragments were assembled to plasmids by Gibson assembly (Gibson *et al.* 2009) using the NEBuilder HiFi DNA Assembly Master Mix (New-England Biolabs, Ipswich, MA, USA). Constructed plasmids were transformed into competent *E. coli* cells *via* heat shock. Subsequently, the plasmids were transferred from *E. coli* into the desired *Pseudomonas* strain through conjugational transfer using *E. coli* HB101 pRK2013 as helper strain as described by Wynands *et al.* (2018). For genomic integration of heterologous genes into the *attTn7* site a pBG mini-Tn7 vector harboring the genetic module of interest and the pTNS1 providing the required transposase were introduced by mating (Zobel *et al.* 2015). A variant of the pBG14 plasmid containing FRT sites for a recyclable kanamycin marker was used as described by Ackermann *et al.* (2021). SNVs and knockouts were obtained using the pEMG system described by Martínez-García *et al.* (2011) with a modified protocol described by Wynands *et al.* (2018). All constructed plasmids and genomic modifications were verified *via* colony PCR using OneTaq 2X Master Mix (New England BioLabs, Ipswich, Massachusetts, USA) followed by Sanger sequencing performed by Eurofins Genomics (Ebersberg, Germany). For

this purpose, template colonies were pre-lyzed with alkaline PEG200, according to Chomczynski *et al.* 2006.

2.3.5.4. RT-qPCR

Gene expression levels were analyzed by RT-qPCR. For this purpose, 50 mL shake flask main-cultures were carried out as previously described. After reaching mid-exponential growth phase, cells were harvested and promptly suspended in 1 mL of RNAlater (Thermo Fisher Scientific, Massachusetts, USA). The samples were then stored at −20 °C for subsequent analysis. RNA extraction was performed using the Quick-RNA Miniprep Kit (Zymo Research, Irvine, CA, USA) and cDNA was prepared from the purified RNA using the LunaScript RT superMix Kit (New England Biolabs, Ipswich, MA, USA). The expression levels of the house keeping gene *rpoD* (Wang *et al.* 2010) as well as the gene of interest were analysed using oligonucleotides designed by qPCR assay design tool from Eurofins Genomics that are listed in table S3. Quantitative RT-PCR was performed using Luna Universal qPCR Master Mix (New England Biolabs, Ipswich, MA, USA) in 96-well plates by the qTOWER 2.2 (Analytik Jena, Jena, Germany). The reaction conditions were used as described in the manufacturer's instructions. Experiments were performed in triplicates with biological duplicates or triplicates. Gene expression levels were evaluated by comparing the Ct values of the housekeeping gene *rpoD* (Wang *et al.* 2010) with the Ct value of genes of interest using the following equation:

$$\text{Gene expression level} = 2^{\text{Ct(rpoD)-Ct(target)}}$$

2.3.5.5. Analytical methods

In shake flask cultivations, growth was detected by measuring the optical density at 600nm (OD_{600}) with an Ultrospec 10 Cell Density Meter (GE Healthcare, Little Chalfront, Buckinghamshire, United Kingdom). Online growth monitoring was performed in the growth profiler via bottom-up images of transparent-bottom microtiter plates taken every 30 min and image analysis using the Growth Profiler Control software V2_0_0. Where indicated, resulting green values were converted to an equivalent OD_{600} *via* a non-linear correlation.

2.3.5.6. HPLC analysis

Concentrations of extracellular metabolites were detected *via* HPLC analysis. For this purpose, samples were prepared by centrifugation for 3 min at 17,000×g and filtration of the supernatant through an AcroPrep™ 96-well filter plate (Pall Corporation, Port Washington, NY, USA). All measurements were performed with the 1260 Infinity II HPLC (Agilent, Santa Clara, California, USA). For analysis of glucose, adipate and 1,4-butanediol concentrations the column Metab-AAC (Isera, Düren, Germany) or Phenomenex Rezex ROA-organic Acid H+ (150x 7.8 mm) (Phenomenex, Torrance, California, United States of America) were used together with a 40 × 8 mm organic acid resin precolumn with 5 mM H_2SO_4 as mobile phase at 0.6 mL min^{-1} and column temperature of 40 °C. All tree compounds were detected with a 260 Infinity II Refractive Index Detector (Agilent, Santa Clara, California, USA). Tyrosine and phenylalanine were detected with a method involving the derivatization of the amino group with *ortho*-phthalaldehyde *via* the 1260 Infinity II Fluorescence Detector (Agilent, Santa Clara, California, USA). For this method, the utilized column was Phenomenex Kinetex 2.6µm EVO C18 100 A (Phenomenex, Torrance, California, United States of America) with methanol and borate buffer (14.2 g L^{-1} Na_2HPO_4, 28.1 g L^{-1} $Na_2B_4O_7$, pH at 8.2) as running agents. A constant flow of 0.42 mL min^{-1} and a gradient from 95 % borate puffer and 5 % methanol to 100 % methanol during the first 10 minutes and back to the starting ratio during the last 2 minutes was applied. The column temperature is 40 °C.

2.3.5.7. Genome sequencing

For whole-genome sequencing, genomic DNA was isolated using the Monarch® Genomic DNA Purification Kit (New-England Biolabs, Ipswich, MA, USA) following the manufacturer's instructions. For library preparation, the NEBNext® Ultra™ II DNA Library Prep Kit for Illumina® (New England Biolabs, Ipswich, Massachusetts, USA) was utilized. All steps were performed according to the manufacturer's protocol. For validation of the library, qPCR was carried out with the KAPA PROBE FORCE Kit (Sigma-Aldrich, Munich, Germany). Subsequently, the concentrations of the library samples were calculated. Samples were diluted to the desired concentration 3 mM with 10 mM Tris/HCl containing 0.1 % tween (pH of 8.5). Next, denaturation of the DNA was achieved by mixing 5 µL of the library sample with 5 µL 0.2 N NaOH, short vortexing, centrifugation and incubation for 5 minutes at room temperature. After incubation,

990 µL of cold hybridization buffer HT1 from the MiSeq reagent kit (Illumina, San Diego, California, USA) used for sequencing, was added. 600 µL of the prepared samples were loaded onto the prefilled cartridge and sequencing was started in the MiSeq-System (Illumina, San Diego, California, USA). After the sequencing run, *de novo* assembly of the resulting sequencing followed by alignment to the reference genome was carried out.

Declaration of competing interest

The authors declare no competing interest

Funding

This project has received funding from the European Union's Horizon 2020 research and innovation programme under Grant Agreements No. 953073 for the project UPLIFT and under Grant Agreements No. 870294 for the project MIX-UP.

2.4. Bio-upcycling of PBAT mock hydrolysates by defined mixed cultures into PCA.

Yannic S. Ackermann, Benedikt Wynands, Nick Wierckx

Manuscript in preparation

CRediT authorship contribution statement:
Yannic S. Ackermann: Conceptualization, Methodology, Validation, Formal analysis, Investigation, Writing - Original Draft, Visualization
Benedikt Wynands: Methodology, Writing - Review & Editing, Supervision
Nick Wierckx: Conceptualization, Validation, Resources, Writing - Review & Editing, Supervision, Funding acquisition, Project administration

Overall, own contribution: 90 %

The presented experimental work was conducted by YSA. Validation was done by YSA, BW and NW. Visualization of all data was performed by YSA. The writing of the original draft was done by YSA, which was reviewed and edited by BW, NW. Funding for the project was acquired by NW.

2.4.1. Abstract

The overproduction of plastics and the rapidly increasing greenhouse gas emissions are two of the major crises of our time. In some ways, plastics and the climate crisis are inextricably linked: the massive overproduction of virgin plastics from fossil sources leads to enormous greenhouse gas emissions. One way to avoid this is to replace fossil fuels with bio-based, renewable raw materials. In addition, more efficient recycling technologies should be developed and implemented. The enormous amount of post-consumer plastic waste offers a huge source of feedstock for the production of new plastics, preventing the extraction of new fossil raw materials and also protecting renewable agricultural land.

In addition to the production of new bio-based plastics such as polyhydroxyalkanoates, post-consumer plastic waste can also serve as a substrate for other chemically important building blocks. Therefore, this work focuses on the production of protocatechuic acid (PCA), an aromatic precursor of interest in many industries. For the production of bio-based PCA, a tyrosine-producing *Pseudomonas taiwanensis* GRC3 streamlined chassis strain is first optimized for the production of PCA. Several metabolic pathways are used. By combining QuiC, a feedback-resistant version of UbiC, and the expression of RpcTAL-*ech-vdh-fcs*, Carbon/Carbon yields of 22.5 ± 0.04 % are obtained from glucose. This glucose can come from agricultural waste streams or be a by-product of the depolymerization of PBAT/starch blends. These PBAT/starch blends can also be used to combine biological funneling of plastic hydrolysates with biotransformation. One of the monomers of a PBAT hydrolysate is terephthalate. This terephthalate can be degraded by expressing the *tph* operon of *P. umsongensis* GO16 *via* PCA and is therefore a good substrate for the production of PCA. Only an additional carbon and energy source is needed. This can be one of the other monomers of PBAT or glucose resulting from starch.

By using defined mixed cultures of strains capable of degrading the respective monomers, a realistic PBAT and a PBAT/starch mock hydrolysate were successfully degraded in this work and also used as a substrate for the biotransformation of TA to PCA. Overall, this work could demonstrate the potential of bio-upcycling of mixed substrates. This will be particularly important in the recycling of mixed wastes or complex substrates, where purification is very costly or not possible.

2.4.2. Introduction

In today's world, conventional plastics have become one of the most important materials due to their exceptional properties and affordability. This had led to very high production capacities and huge resource consumption (PlasticsEurope 2022). In particular, the fossil feedstock of most of the plastics used poses a major challenge, not only in terms of the plastic pollution crisis, but also in terms of climate change (Wei *et al.* 2020). Therefore, more and more efforts are being made to build a circular economy (Kawashima *et al.* 2019; Meys *et al.* 2020). One promising solution is the biotechnological upcycling of waste streams, either from agricultural waste, such as molasses or starch, or directly from plastic waste into high-value compounds, to keep the carbon fixed in the loop of the circular economy (Blank *et al.* 2020; Wierckx *et al.* 2018). One building block with increased usage in the polymer and pharmaceutical industry is 3,4-dihydroxybenzoate (protocatechuate, PCA).

PCA is a secondary metabolite in various plants and serves as an antifungal or nematicidal agent. In addition, PCA exhibits antibacterial, anticancer, and antioxidant activities, making it very interesting for pharmaceutical applications (Kakkar *et al.* 2014; Nguyen *et al.* 2013). Moreover, PCA has been used as a natural antioxidant on film for food packaging materials (Liu *et al.* 2017). Besides these properties, PCA is also of interest for the polymer industry. It has been shown that PCA could be an alternative to bisphenol A for the production of epoxy resins (Chen *et al.* 2020; Tao *et al.* 2020). Within a circular economy, there are two ways to produce PCA, one is a bio-based approach of *de novo* production from glucose or other sugars that derive from agricultural waste streams (Takkellapati *et al.* 2018). In previous studies, different microorganisms, such as *Corynebacterium glutamicum*, *Pseudomonas putida*, or *Saccharomyces cerevisiae*, have been successfully used for the biosynthesis of PCA (Labib *et al.* 2021; Li *et al.* 2021; Weber *et al.* 2012).

The other option is biotransformation, in which one compound is converted to another in a few enzymatic steps. This approach is well established in the valorization of lignin. As PCA is a key intermediate in the aromatic catabolic pathways of many organisms, it provides a promising target for the biotransformation of various aromatic compounds from lignin. After the biotransformation of various aromatic compounds to PCA, it is metabolized to high-value products, such as muconic acid or polyhydroxyalkanoates (PHA) via the β-ketoadipate pathway (Linger *et al.* 2014; Salvachúa *et al.* 2018). Given that PCA is part of the degradation pathway of terephthalic acid (TA), a widely used monomer of various polymers such as PET or PBAT, TA could also be a good

compound for a biotransformation approach. In the past, several microorganism, such as *Comamonas* sp. *Rhodococcus* sp. and *P. umsongensis* GO16 have been found to be able to degrade TA via PCA naturally (Choi *et al.* 2005; Narancic *et al.* 2021; Sasoh *et al.* 2006).
One limitation that often arises when biotransformation approaches, such as the conversion of PCA to muconic acid, do not proceed via the TCA cycle is the need for an additional source of carbon and energy to maintain the metabolism of the cell (Salvachúa *et al.* 2018). However, this fits to another challenge of the plastic crisis, which is the recycling of mixed plastic wastes streams or the issue that most plastic polymers consist of different monomers. For example, poly(butylene adipate co-terephthalate) (PBAT) is a promising and widely used aliphatic-aromatic co-polyester due to its development potential in various applications, which is obtained by polycondensation of 1,4-butanediol (BDO), adipic acid (AA) and terephthalic acid (TA) (Jian *et al.* 2020a). Therefore, a combination of bio-degradation of AA or BDO with the biotransformation of TA could offer a great bio-upcycling approach. In addition, fossil polyesters are often blended with other sustainable polymers such as starch or PLA to reduce resource consumption and production costs or to optimise the physical properties of the product, resulting in a waste plastic blend with additional starch components or lactic acid polymers that could be degraded by enzymatic hydrolysis to glucose or lactic acid monomers. These monomers could then also serve as a potential carbon source in a biotransformation approach (Aversa *et al.* 2022; Thothong *et al.* 2013).
One promising candidate for this approach is the solvent tolerant *P. taiwanensis* strain. This strain already confirmed its huge potential in the production of aromatic compounds of high interest (Lenzen *et al.* 2019; Otto *et al.* 2019; Otto *et al.* 2020; Schwanemann *et al.* 2020; Wynands *et al.* 2018). In the past, Wynands *et al.* (2019) developed a genome-reduced *P. taiwanensis* chassis (GRC) to improve growth rates, biomass yields and solvent tolerance. Due to the removal of the megaplasmid pSTY, it was necessary to genetically integrate the solvent efflux pump TtgGHI into the genome, resulting in strain GRC3 (Wynands *et al.* 2019).

In this study, we follow two different approaches for the production of PCA within a circular economy. The first step is the *de novo* production of bio-based PCA from glucose as a feedstock, potentially derived from agricultural waste streams. This will be achieved by metabolic engineering and heterologous gene expression in which a tyrosine overproducing strain *P. taiwanensis* GRC3Δ5-TYR1 will be transformed into a PCA

producer. In a second approach, we aim to convert TA into PCA by using different additional carbon and energy sources derived from PBAT hydrolysates. To achieve this, TA metabolism is enabled in *P. taiwanensis* and combined with previous knowledge of AA and BDO degradation. Finally, we bio-upcycle a realistic PBAT mock hydrolysate with defined mixed cultures into the aromatic compound PCA.

2.4.3. Results and discussion

2.4.3.1. Engineering a tyrosine-producing *P. taiwanensis* strain for *de novo* production of PCA

The production of bio-based PCA, an important building block for novel polymers, is of increasing interest to reduce the use of fossil resources and move towards a circular economy. In recent years significant effort was put into the production of aromatic compounds with non-pathogenic Pseudomonads (Schwanemann *et al.* 2020). A promising candidate for the production of PCA is the solvent tolerant *P. taiwanensis* VLB120, which has already been optimised as a genome reduced chassis for the production of aromatic compounds *via* phenylalanine and tyrosine (Otto *et al.* 2019; Wynands *et al.* 2019). For the production of PCA, we initially used two different strains. First, GRC3Δ5-TYR1, which has an SNV in *tprE* (P290S) that reduces the flux towards tryptophan and leads to tryptophan bradytrophy, and a deletion of *pykA* for an increased precursor supply, both of which result in higher tyrosine production (Figure 2.4.1). In addition, a previous version of GRC3Δ5-TYR1 without the SNV in trpE (GRC3Δ5-aΔ) was used, resulting in a normal carbon flux towards anthranilate and thus not limiting the tryptophan supply of the cell (Wynands *et al.* 2018). In a first step, the knockout of *pobA* was "repaired" by re-inserting the *pobA* gene into its native locus (strains from now on denoted as Δ4). This gene encodes a 4-hydroxybenzoate 3-monooxygenase that converts 4-hydroxybenzoate (4-HB) into PCA. Almost the same approach was used as for the *pobA* knockout, except that the native gene was left in between the homologous recombination flanks. The resulting strain is able to grow on 4-HB again. To prevent PCA from being further metabolized, the *pcaGH* genes encoding protocatechuate 3,4-dixoygenase were knocked out (Wynands *et al.* 2018). This knockout disabled growth on 4-HB. These modifications were verified by a growth experiment on MSM agar-plate containing 5 mM of 4-HB as sole carbon source (Figure S15). However, the production experiments showed that these modifications were not sufficient to enable PCA accumulation (data not shown), probably due to the prior optimization for tyrosine production,

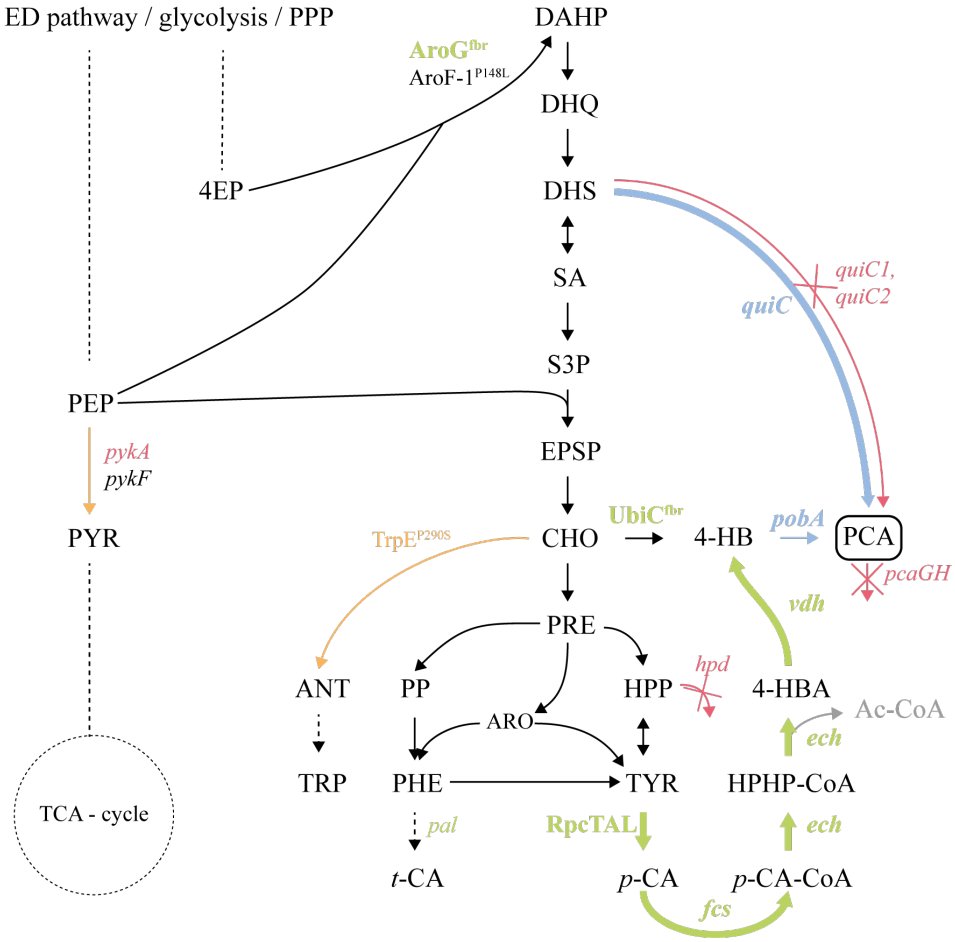

Figure 2.4.1.: Schematic overview of the PCA production pathways. Genes that are deleted priory deleted are marked in red. Blue arrows indicated reintegrated genes, which were initially deleted. Reduced fluxes are shown in orange. Heterologous pathways and enzymes are illustrated in green. Abbreviations: ED, Entner-Doudoroff; PPP, pentose phosphate pathway; TCA, tricarboxylic acid; PEP, phosphoenolpyruvate; PYR, pyruvate; E4P, erythrose 4-phosphate; DAHP, 3-deoxy-D-arabino-heptulosonate 7-phosphate; DHQ, 3-dehydroquinate; DHS, 3-dehydroshikimate; SH, shikimate; S3P, shikimate 3-phosphate; EPSP, 5-enolpyruvyl- shikimate 3-phosphate; CHO, chorismate; 4-HB, 4-hydroxybenzoate; PCA, protocatechuate; ANT, anthranilate; TRP, tryptophan; PRE, prephenate; PP, phenylpyruvate; HPP, 4-hydroxyphenylpyruvate; ARO, arogenate; TYR, tyrosine; PykA/PykF, pyruvate kinase isozymes; AroGfbr, DAHP synthase isozyme; QuiC/QuiC1/QuiC2, 3-dehydroshikimate dehydratase isozymes; PobA, 4-hydroxybenzoate 3-monooxygenase; PcaGH, protocatechuate 3,4-dioxygenase; Hpd, 4-hydroxyphenylpyruvate dioxygenase; TrpEP290S, anthranilate synthase component I; Figure adapted from (Wynands *et al.* 2018).

so adding a side pathway without redirecting the carbon flux is not enough. A further reason could be feedback inhibition by phenylalanine and/or tyrosine as byproducts. The first step of the shikimate pathway, catalyzed by the DAHP synthase isozymes and encoded by *aroF*, *aroG* and *aroH*, is a major step in the production of aromatic compounds and is feedback regulated by different aromatic compounds such as tyrosine, phenylalanine or tryptophan (Brown 1968). To avoid tyrosine feedback inhibition both strains already contain a feedback-resistant version of *aroF-1* (P148L) (Wynands *et al.* 2018). In addition, a feedback-resistant version of AroG from *E. coli*, which is natively inhibited by phenylalanine, was genomically integrated via the mini-Tn7 system. Previous studies have already shown a beneficial effect on the production of aromatic compounds (Kikuchi *et al.* 1997; Wynands *et al.* 2018). Besides the regulation of the shikimate pathway, another feedback inhibition limits the accumulation of PCA by a decreased precursor supply of 4-HB. In this case the chorismate pyruvate-lyase (UbiC), which catalyzes the conversion of chorismate into 4-HB, is directly inhibited by its product (Holden *et al.* 2002). To overcome this limitation, Jha *et al.* (2019) engineered a reduced product inhibited version of UbiC by using a specific biosensor and mutagenesis approach. Thereby two amino acid substitution (E31Q and M34V) showed the best results. This engineered $ubiC^{fbr}$ from *E. coli* was heterologously expressed in GRC3Δ5-aΔ as well as GRC3Δ5-TYR1. Especially in combination with $trpE^{\mathrm{P290S}}$ the use of $ubiC^{\mathrm{fbr}}$ leads already to a production of 2.1 mM of PCA (Figure 2.4.2).
To further increase the flux to PCA by overexpression of the endogenous *quiC*, another pathway were investigated in more detail. Previously, all three versions of *quiC* were knocked out to avoid degradation of the aromatic precursors 3-dehydroshikimate (DHS) (Otto *et al.* 2019; Wynands *et al.* 2018). It appears that the overexpression of *quiC* alone only allows the production of low amounts of PCA independent of the SNV in *trpE*. This is somewhat surprising at first, since previous studies have shown that it is important to delete all three 3-dehydroshikimate dehydratase-encoding genes (*quiC*, *quiC1*, *quiC2*) for the production of phenol and other aromatic compounds. Otherwise, *P. taiwanensis* is still able to grow on quinate and thus convert the shikimate pathway intermediate 3-dehydroshikimate to PCA (Peek *et al.* 2017; Wynands *et al.* 2018). The combination of the two pathways in the strain without $\mathrm{TrpE}^{\mathrm{P290S}}$ further increased the production. This shows that the integration of *quiC*, especially in combination with $ubiC^{\mathrm{fbr}}$, has a positive effect on the production. The strains with the mutation in *trpE*, that leads to a reduced flux to anthranilate and increased the production of tyrosine, also showed the advantages of both pathways. This strain produced up to 3.4 mM PCA.

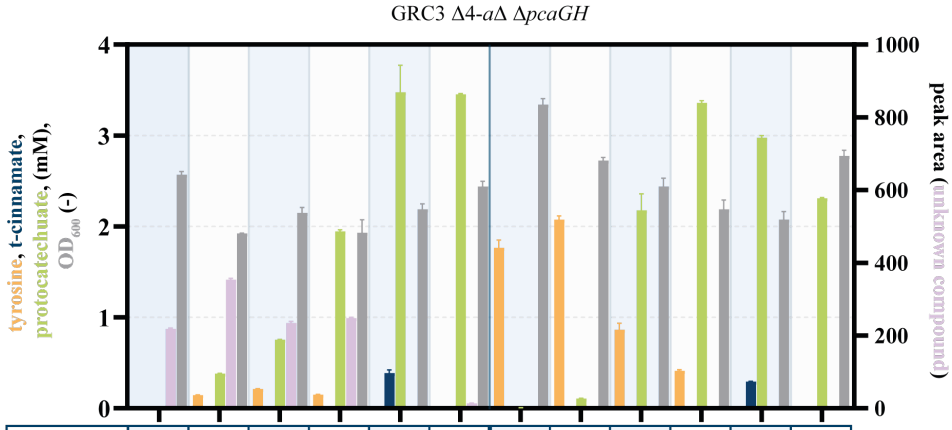

trpE^{P290S}	-	-	-	-	-	-	X	X	X	X	X	X
quiC-aroG^{fbr}	-	X	-	X	X	X	-	X	-	X	X	X
ubiC^{fbr}*-aroG*^{fbr}	-	-	X	X	X	X	-	-	X	X	X	X
RtPAL-fg	-	-	-	-	X	-	-	-	-	-	X	-
RpcTAL-fg	-	-	-	-	-	X	-	-	-	-	-	X

Figure 2.4.2.: Characterization of different genomic modifications for *de novo* PCA production from glucose. All Strains were grown in 24-well microtiter plates using mineral salt medium (MSM) with 20 mM glucose as sole carbon source for 75 h to ensure glucose depletion. "fg" denotes for ferulic genes. Error bars indicate the standard error of the mean (n=2).

However, the strains with TrpE^{P290S} still produced up to 2.1 mM tyrosine when only *quiC* was overexpressed. Even the best producing PCA strain still produces 0.4 mM tyrosine. Furthermore, strains lacking *trpE*^{P290S} accumulate an undefined compound that was detected by a DAD detector during HPLC measurement. To increase the production of PCA in the future, it could be beneficial to integrate again the other two 3-dehydroshikimate dehydratases (PVLB_10935, PVLB_13075).

In order to prevent tyrosine accumulation and increase PCA production, one alternative would be the deletion of chorismate mutase/prephenate dehydrogenase, but this would lead to phenylalanine and tyrosine auxotrophy, which is a cost-increasing issue for industrial purposes. Therefore, the conversion of tyrosine to PCA *via* 4-HB was targeted by integrating an additional third pathway. Therefore, a phenylalanine/tyrosine ammonia lyase from *Rhodosporidium toruloides* (RtPAL) (Nijkamp *et al.* 2007) which converts tyrosine to *p*-coumerate was integrated. This ammonia lyase showed good properties in converting phenylalanine or tyrosine in contrast to other specific tyrosine ammonia lyases, probably due to a higher V_{max} (Wynands *et al.* 2023). In addition to that the ferulic acid metabolic genes, consisting of *ech*, *vdh* and *fcs* from *P. putida* KT2440 were

used to metabolize *p*-coumerate into 4-hydroxybenzoate (4-HB) (Lenzen *et al.* 2019). 4-HB is then converted *via* PobA into PCA. Depending on the use of $TrpE^{P290S}$ these pathway further increase the amount of PCA. The strain GRC3Δ4-*a*Δ now produces about 3.5 mM of PCA (Figure 4.2). In contrast to that, the amount of PCA is slightly reduced after the integration of RtPAL-*ech-vdh-fcs* in GRC3Δ4-TYR1.
The use of the ammonia lyase could indeed prevent tyrosine accumulation, but unfortunately the activity towards phenylalanine led to the production of up to 0.4 mM of *trans*-cinnamate, which could not be further metabolized. One option to prevent this is the hydroxylation of *trans*-cinnamate to 4-coumerate via a plant cytochrome P450 cinnamate 4-hydroxylase (C4H). However, its functional expression in bacteria is very challenging (Li *et al.* 2018). Therefore, a better approach could be the use a specific tyrosine ammonia lyase without any side activity for phenylalanine. In order to achieve this, the recently characterized RpcTAL from *Rivularia* sp. with high tyrosine conversion activity was used instead of RtPAL (Brack *et al.* 2022). In contrast to the construction of the plasmid for the integration of P_{14f}-RtPAL-*ech-vdh-fcs*, the cloning of P_{14f}-RpcTAL-*ech-vdh-fcs*, was not possible using the usual methods, instead another terminator upstream of the promoter sequence was required to obtain plasmids without mutations in the genes. In addition to these modifications, a random mutation occurred at the end of P_{14f} in *E. coli*, and because no other positive plasmids were obtained, the combination with the promoter mutation (P_{14fm}) was used for genomic integration in *P. taiwanensis*. The integration of RpcTAL indeed abolished trans-cinnamate accumulation after 48 h. The final yield achieved with the best producing strain *P. taiwanensis* GRC3Δ4-*a*Δ Δ*pcaGH attTn7*::P_{14f}-*quiC-ubiC*^{fbr}-*aroG*^{fbr} PVLB_02480::P_{14fm}-RpcTAL-*ech-vdh-fcs* (henceforth denoted as GRC3Δ4-PCA) was 22.50 ± 0.04 % (C_{mol} C_{mol}^{-1}) with the strains without the modification in *trpE* (Table 2.4.1). In combination with $trpE^{P290S}$ the final yield was 16.00 ± 0.04 % (C_{mol} C_{mol}^{-1}). These result suggested a good *de novo* production of PCA from a renewable carbon source, which can be derived from sugar-rich waste streams, or as component of a PBAT/starch hydrolysate.

Table 2.4.1.: Overview of the C_{mol} C_{mol}^{-1} yields of PCA from glucose from different *P. taiwanensis* strains engineered in this study.

	Genotype	Yield C_{mol} C_{mol}^{-1}
without $trpE^{P290S}$	GRC3Δ4-*a*Δ Δ*pcaGH*	0.0 ± 0.00
	+ *quiC*-*aroG*^{fbr}	2.1 ± 0.01
	+ *ubiC*^{fbr}-*aroG*^{fbr}	5.0 ± 0.02
	+ *quiC*-*ubiC*^{fbr}-*aroG*^{fbr}	13.0 ± 0.08
	+ *quiC*-*ubiC*^{fbr}-*aroG*^{fbr} RtPAL-*ech*-*vdh*-*fcs*	19.9 ± 1.39
	+ *quiC*-*ubiC*^{fbr}-*aroG*^{fbr} RpcTAL-*ech*-*vdh*-*fcs*	22.5 ± 0.04
with $trpE^{P290S}$	GRC3Δ4-*a*Δ Δ*pcaGH*	0.0 ± 0.02
	+ *quiC*-*aroG*^{fbr}	0.7 ± 0.01
	+ *ubiC*^{fbr}-*aroG*^{fbr}	13.5 ± 0.92
	+ *quiC*-*ubiC*^{fbr}-*aroG*^{fbr}	21.5 ± 0.12
	+ *quiC*-*ubiC*^{fbr}-*aroG*^{fbr} RtPAL-*ech*-*vdh*-*fcs*	15.5 ± 0.11
	+ *quiC*-*ubiC*^{fbr}-*aroG*^{fbr} RpcTAL-*ech*-*vdh*-*fcs*	16.0 ± 0.04

2.4.3.2. Engineering terephthalate metabolism in *P. taiwanensis* GRC3Δ5

Besides producing bio-based PCA as a building block for polymers, it is also important to use carbon that is already in the loop of a circular economy in form of plastic polymers. Therefore, in a next approach we want to combine our knowledge of monomer consumption with the production of PCA. In this case we use PBAT as the polymer and the corresponding monomers adipic acid, 1,4-butanediol and terephthalic acid. Previous studies have successfully enabled the metabolism of AA and BDO in *P. taiwanensis* (Op de Hipt, unpublished, Chapter 2.3). Thus, a first step would be the conversion of TA. For this purpose, three different producing strains, *P. taiwanensis* GRC3Δ5-*a*Δ, GRC3Δ5-TYR1 and GRC3Δ5-TYR2, were used in order to exclude negative effects of the producing background, induced by $trpE^{P290S}$ (Otto *et al.* 2019; Wynands *et al.* 2018; Wynands *et al.* 2023). Since *P. taiwanensis* is naturally able to grow on protocatechuate as the sole carbon source, the engineering focused on the first two enzymatic steps

from TA to PCA (Figure 2.4.3). The genes encoding the dioxygenase TphA1A2A3 and the dehydrogenase TphB, were previously described in *P. umsongensis* GO16 and heterologous expressed using the mini-Tn7 integration system, with an additional marker recycling step (Ackermann *et al.* 2021), together with the transporter TphK and the native regulatory gene *iclR*. This construct enabled growth on terephthalate as sole carbon source. After integration of the *tph*-operon all used strains are able to grow, but the strain without the point mutations in *trpE* and *pheA* grows far better than the others. After around 20 h this strain reached the stationary phase, which is almost as fast as the native TA degrader *P. umsongensis* GO16. The difference in growth between the tested strains is probably caused by the mutations made for optimized tyrosine production. The two other strains needed three times longer, which is likely due to the point mutations in *trpE*, which causes a tryptophan bradytrophy (Wynands 2018). In contrast to that, the influence of $pheA^{T310I}$ seems to be much lower, as the strain

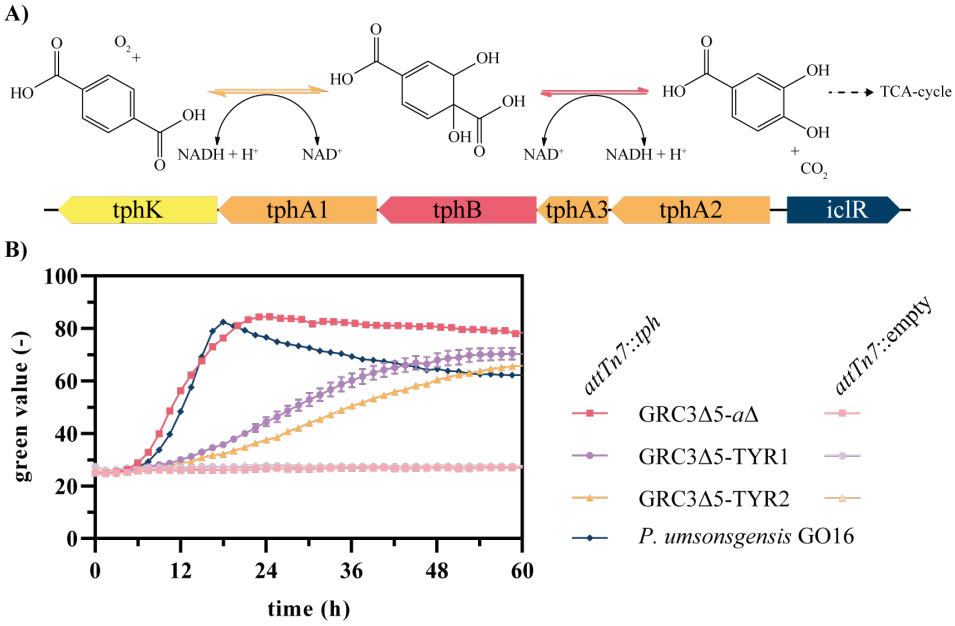

Figure 2.4.3.: Enabling growth on terephthalate as sole carbon source. A) Two step reaction from TA to PCA via the intermediate DCD and corresponding genes from *tph*-operon from *P. umsongensis* GO16. B) Characterization of growth on TA after genomic integration of *tph* genes in different aromatic producing *P. taiwanensis* strains. All strains were cultivated in three-fold buffered MSM medium containing 22.5 mM TA in the Growth Profiler. Symbols show every 2nd data point. Error bars indicate the standard error of the mean (n=3).

containing both *trpE*^{P290S} and *pheA*^{T310I} grows only slightly worse than the strain with just *trpE*^{P290S}.

2.4.3.3. Enabling biotransformation of TA into PCA with *P. taiwanensis*

For upcycling of waste plastic materials into compounds of higher value, TA as one of the most commonly used aromatic diacids in plastic polymers is an important compound to develop a bio-upcycling approach. As mentioned TA is degraded via PCA, a compound of high interest and thus a good target for the biotransformation. Since, the previously engineered *P. taiwanensis* strains can already grow and metabolise TA, it is only required to prevent PCA from being further metabolised by knocking out the genes *pcaGH* encoding for the protocatechuate 3,4-dioxygenase. This resulted in strains, which can no longer grow on TA as sole carbon source (Figure 2.4.4). Therefore, an additional substrate as carbon and energy source is required. On the one hand, this could be another plastic monomer that occurs in a plastic hydrolysate, such as ethylene glycol from a PET hydrolysate or adipate and 1,4-butanediol from a PBAT hydrolysate. However, it can also be other additives from the plastic polymer. For better physical properties, PBAT is often mixed with starch or poly lactic acid (Aversa *et al.* 2022; Nayak 2010). If also an amylase or PLase is used in the enzymatic hydrolysis, the resulting hydrolysate would also consist of glucose or lactic acid besides the PBAT monomers (Thothong *et al.* 2013; Zaaba *et al.* 2020). These substrates could then serve as carbon and energy source for the cells. In the case of the used aromatic producing strains, it is also possible to convert the glucose into high value aromatic compound, like tyrosine. To enable the biotransformation of TA to PCA, *pcaGH* was first knocked out in the aromatic producer strains GRC3Δ5-TYR1 and GRC3Δ5-TYR2 and their progenitor strain GRC3Δ5-*a*Δ, and glucose was used as the carbon and energy source. Online growth measurements of these strains confirm that *pcaGH* is essential for growth on TA (Figure 2.4.4). However, they can grow on glucose as the sole carbon source and on a substrate mixture of glucose and TA. Only a slightly decrease is observed when TA and glucose are used together, indicating that the concentrations of TA applied here are not toxic. In a first biotransformation approach, 10 mM of TA was used in combination with the standard setup of 3-fold buffered MSM medium containing 20 mM of glucose. The experiment was performed in System Duetz plates for sampling for offline analytics, and in parallel in the Growth Profiler to determine online growth curves. All three strains grew very similarly and completely consumed the glucose after

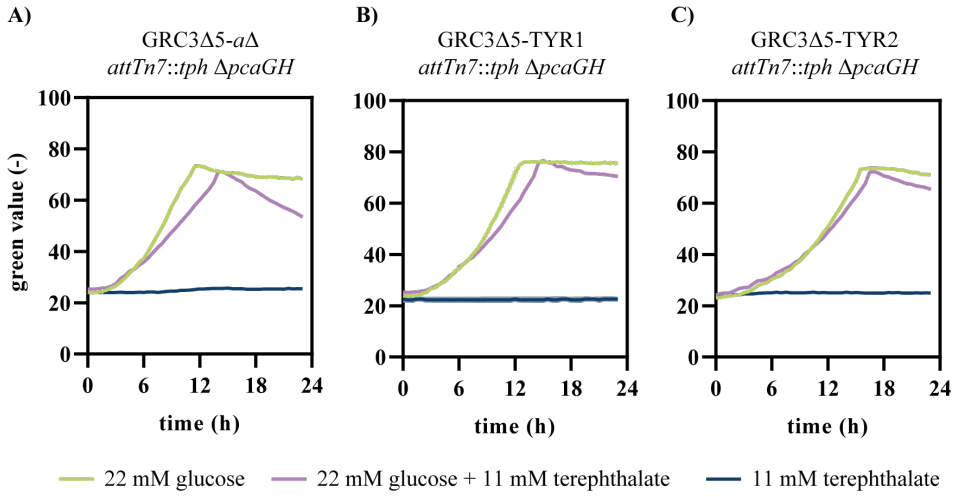

Figure 2.4.4.: Characterization of strains for biotransformation of TA and glucose. A) All strains were cultivated separately in MSM medium containing terephthalate and/or glucose as mentioned in the figure. Online growth curves were measured using the Growth Profiler. Error bars indicate the standard error of the mean (n=3).

24 h (Figure S16). In addition, all three strains converted some of the TA into PCA. The ratio between the consumed TA and the produced PCA is in all strains almost 100 %, which shows that no by-products or intermediates such as 1,2-dihydroxy-3,5-cyclohexadiene-1,4-dicarboxylate (DCD) are accumulating (Figure 2.4.5). However, there are still about 5 mM TA left after 24 h in the GRC3Δ5-*a*Δ *attTn7*::*tph* Δ*pcaGH* and the GRC3Δ5-TYR1 *attTn7*::*tph* Δ*pcaGH* strains, and this was not further converted upon prolonged incubation. The GRC3Δ5-TYR2 *attTn7*::*tph* Δ*pcaGH* strain performed slightly better, converting 68 % of TA into PCA and leaving about 3 mM TA. Besides the biotransformation, both aromatic-producing strains produced up to 1.77 mM (TYR1) or 1.61 mM (TYR2) of tyrosine with a corresponding C_{mol} C_{mol}^{-1} yield of 11 %. This is a little less than previous studies, where the GRC3Δ5-TYR2 strain produced a bit more than 2 mM after 24 h, but still quite good considering that the strains express another gene cluster and produce additional enzymes that require other co-factors (Otto *et al.* 2019). Overall it seems that the biotransformation is coupled to the consumption of glucose, hence in a next step, higher glucose and different TA to glucose ratios where tested. Therefore, the glucose concentration was increased to 30 mM or 40 mM and further the TA concentration was reduced to 5 mM in combination with 20 mM of glucose, to exclude any toxicity or inhibitory effects of TA. In all cases,

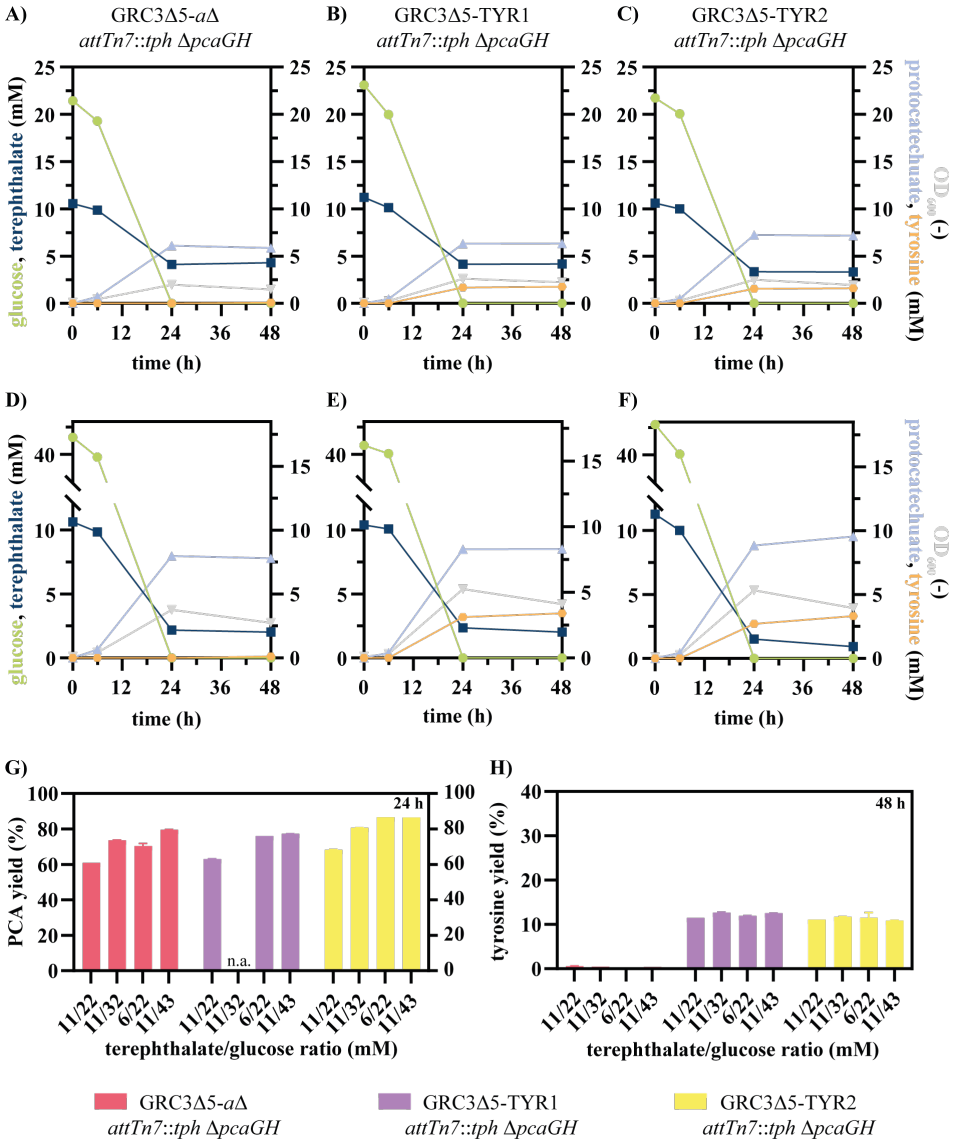

Figure 2.4.5.: Biotransformation of TA into PCA with glucose as additional carbon source. All strains were cultivated separately in MSM medium containing TA and glucose as mentioned in the figure. Samples were taken over time from separate System Duetz plates, which were all inoculated from the same master mix. (A-C) HPLC data from cultivations with 10 mM TA and 20 mM glucose. (D-F) HPLC data from cultivations with 10 mM TA and 40 mM glucose. (G) Calculated PCA yield from TA after 24 h of different strains with different ratios of TA and glucose. (H) Calculated final tyrosine yields (C_{mol} C_{mol}^{-1}) from glucose. Error bars indicate the standard error of the mean (n=2).

the strains grew in a comparable manner, with different final biomasses due to the different amounts of carbon available (Figure 2.4.5/Figure S17). Even the double amount of glucose is consumed after 24 h with comparable growth in all three strains. This shows that the strains did not lack other medium components such as nitrogen or trace elements due to the higher carbon ratio. Indeed, by increasing the glucose/TA ratio, the amounts of TA converted are higher compared to the lower ratios. However, even at the highest glucose/TA ratio tested, not all TA could be converted to PCA. This was the case for both TA concentrations, suggesting that there is no negative effect of the TA, but rather that the amounts of glucose provide an insufficient carbon and energy source for biotransformation. This trend was observed for all three strains tested. Nevertheless, all three tested strains are able to convert TA into PCA when glucose is present. The GRC3Δ5-TYR2 *attTn7*::*tph* Δ*pcaGH* strain seems to be the best converting strain, which could be explained by its slightly slower growth. However, neither the Growth Profiler growth curves nor the conversion data show large differences between the strains, so it is difficult to say, whether the strains perform differently. Besides the conversion of TA into PCA, the GRC3Δ5-TYR1 *attTn7*::*tph* Δ*pcaGH* and GRC3Δ5-TYR2 *attTn7*::*tph* Δ*pcaGH* strains are also able to produce tyrosine from glucose. Both strains reached a tyrosine yield of 11 to 12 % of $C_{mol(tyrosine)}$ $C_{mol(glucose)}^{-1}$ after 48 h regardless of the concentration glucose in the medium at the beginning of the cultivation.

As mentioned above a hydrolysate of PBAT/starch could not only harbour glucose as additional carbon source but also AA or BDO. Furthermore, when only PBAT is hydrolysed there is no glucose at all present in the hydrolysate. That is why in a next step we enabled the AA and BDO degrading strains GRC3Δ5-TYR2-AA and GRC3Δ5-TYR2-BDO strains to grow on TA and further convert TA into PCA (Op de Hipt *et al.*, chapter 2.3). Therefore, the *tph* operon from *P. umsongensis* GO16 under the control of the native regulation was genomically integrated into the *attTn7* site of both strains (Figure 2.4.6). This enabled both strains to grow on TA as sole carbon source after a lag-phase. To prevent PCA from being further metabolized, *pcaGH* was knocked out. This leads to two strains that were no longer be able to grow on TA as sole carbon source (Figure S18). Based on the knowledge from the glucose experiment, the biotransformation was performed with different concentrations of adipate (20 mM, 30 mM, 40 mM) or BDO (30 mM, 45 mM, 60 mM) and 5 mM or 10 mM of TA in System Duetz plates. Samples for OD_{600} and HPLC measurements were taken after 19 h, 47 h and 72 h. Furthermore, for online growth measurements

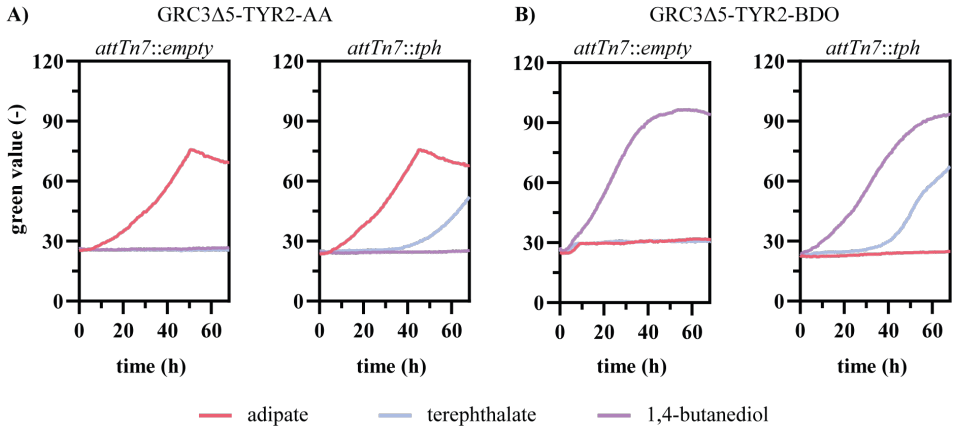

Figure 2.4.6.: Characterization of strains for biotransformation of TA on monomers of PBAT. All strains were cultivated separately in MSM medium containing 22.5 mM TA, 30 mM AA or 45 mM BDO. Online growth curves were measured using the Growth Profiler. A) GRC3Δ5-TYR2-AA strain with and without genomically integrated *tph* genes. B) GRC3Δ5-TYR2-BDO strain with and without genomically integrated *tph* genes. Error bars indicate the standard error of the mean, but these are so small that they are not visible behind the lines (n=3).

Growth Profiler experiments were performed in parallel with the same cultures. The strain GRC3Δ5-TYR2-AA *attTn7*::*tph* Δ*pcaGH* consumed all adipate after 72 h except for the highest concentrations of 40 mM (Figure 2.4.7). This could be due to a rather low-initial pH of 6.30. At this low pH, the strain grew a little slower and consumed only half of the initial amount of adipate after 72 h. At this point, the pH already shifted to 6.97. Endpoint HPLC measurements from the corresponding Growth Profiler experiment showed a complete consumption of 40 mM adipate after 120 h, and the growth curves suggested complete degradation by 96 h, when this strain reached the stationary phase.

To avoid this short growth lag in future experiments, higher buffer concentrations could be beneficial. Overall, the biotransformation of TA into PCA is lower compared to the previous results on glucose. This could be due to the slower growth and therefore lower biomass in the first hours. After 72 h, when using 5 mM of TA and 20 mM of adipate, only 26.8 % of TA were converted into PCA, this ratio did not change in the Growth Profiler experiment after 120 h, suggesting that at 72 h the biotransformation already stopped. Interestingly the conversion percentage is higher at the ratio of 10 mM to 20 mM TA/AA. In this setup, about 40 % of TA were converted. The difference between the two setups could be explained by a slightly higher initial adipate concentration and thus more biomass for the conversion. Next, the adipate concentration was increased to

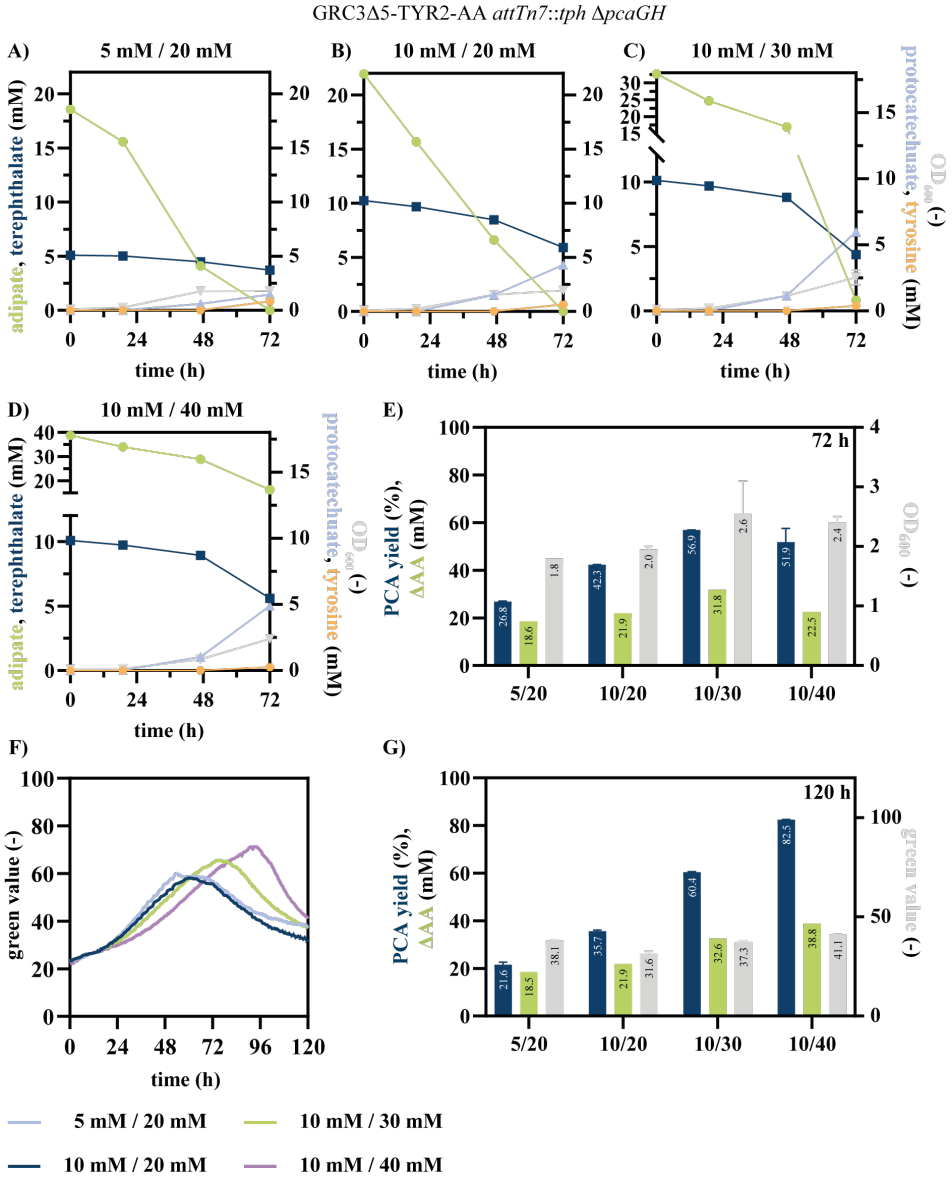

Figure 2.4.7.: Biotransformation of TA into PCA with AA as additional carbon source. All strains were cultivated separately in MSM medium containing TA and AA as mentioned in the figure. Samples were taken over time from separate System Duetz plates, which were all inoculated from the same master mix. (A-D) HPLC data from cultivations with different TA/AA ratios. (E) Calculated PCA yields from TA after 72 h of different strains with different ratios of TA/AA and the amount of consumed AA (ΔAA). (F) Online growth curves measured in the Growth Profiler and (G) corresponding PCA yields from TA calculated from HPLC samples taken after 120 h. Error bars indicate the standard error of the mean, for F these are so small that they are not visible behind the lines (A-E n=2; F-G n=3).

30 mM as the initial concentration. This resulted in a higher final OD_{600} of 2.6, but was not high enough to convert the complete amount of TA. Looking at the highest adipate concentration of 40 mM adipate, also the highest conversion rate was achieved. Due to slower growth described above, the strains converted less TA at 72 h compared to the lower adipate concentrations, but after 120 h in the Growth Profiler a conversion rate of 82.5 % was achieved. Overall, these results showed that adipate could be used as carbon and energy source, although it seems important to have a much higher adipate concentration compared to TA. Considering PBAT as a substrate, this could be disadvantageous since a high amount of aliphatic monomers, such as adipate, compared to aromatic monomers makes the physical properties of the polymer much weaker and thus unfavourable for most of the industrial approaches (Herrera *et al.* 2002).
Since the ratio of dicarboxylic acids to the diol in PBAT is approximately 1:1, regardless of the ratio of adipate to TA, a hydrolysate of PBAT will contain more BDO than TA. Therefore, BDO was also tested as an additional carbon source. First, the strains grew much slower on BDO in the presence of TA (Figure 2.4.8). This was true for all approaches, depending on the BDO concentrations. The online growth curves from the Growth Profiler experiment show growth limitations at different initial BDO concentrations. A pH effect, as with adipate, could be excluded, as all initial pH-values were between 7.01 and 7.07. Interestingly, at 30 mM BDO the growth was better after 72 h in the 5 mM TA cultivation compared to 10 mM. From the corresponding System Duetz cultivation, we know that the 5 mM TA are completely converted in contrast to the 10 mM TA. It seems that TA inhibts growth on BDO specifically, as this was not observed with adipate or glucose as co-substrates. One possible explanation for this could be a chelating effect of metal ions by TA. In particular, the binding of zinc ions could inhibit growth. In chapter 2.3 we could show that the first step of BDO metabolism in *P. taiwanensis* is catalysed by a zinc-dependent alcohol dehydrogenase (PVLB_10545). We also observed that another iron-dependent alcohol dehydrogenase (PVLB_12675) is part of the degradation pathway. However, zinc as a limiting factor seems more likely, since the mineral salt medium has a higher iron content (18 nM $FeSO_4$) compared to zinc (7 nM $ZnSO_4$).

It was also observed that zinc deficiency slightly limited growth on AA as sole carbon source. Thus, metal ion limitation could perhaps explain the growth limitation in the presence of TA, but not the growth dependence on the BDO concentration. One explanation for this could be a limiting step in the transport of BDO into the cells. The mechanism of BDO transport in Pseudomonas is still unclear. Although, Li *et al.* (2020)

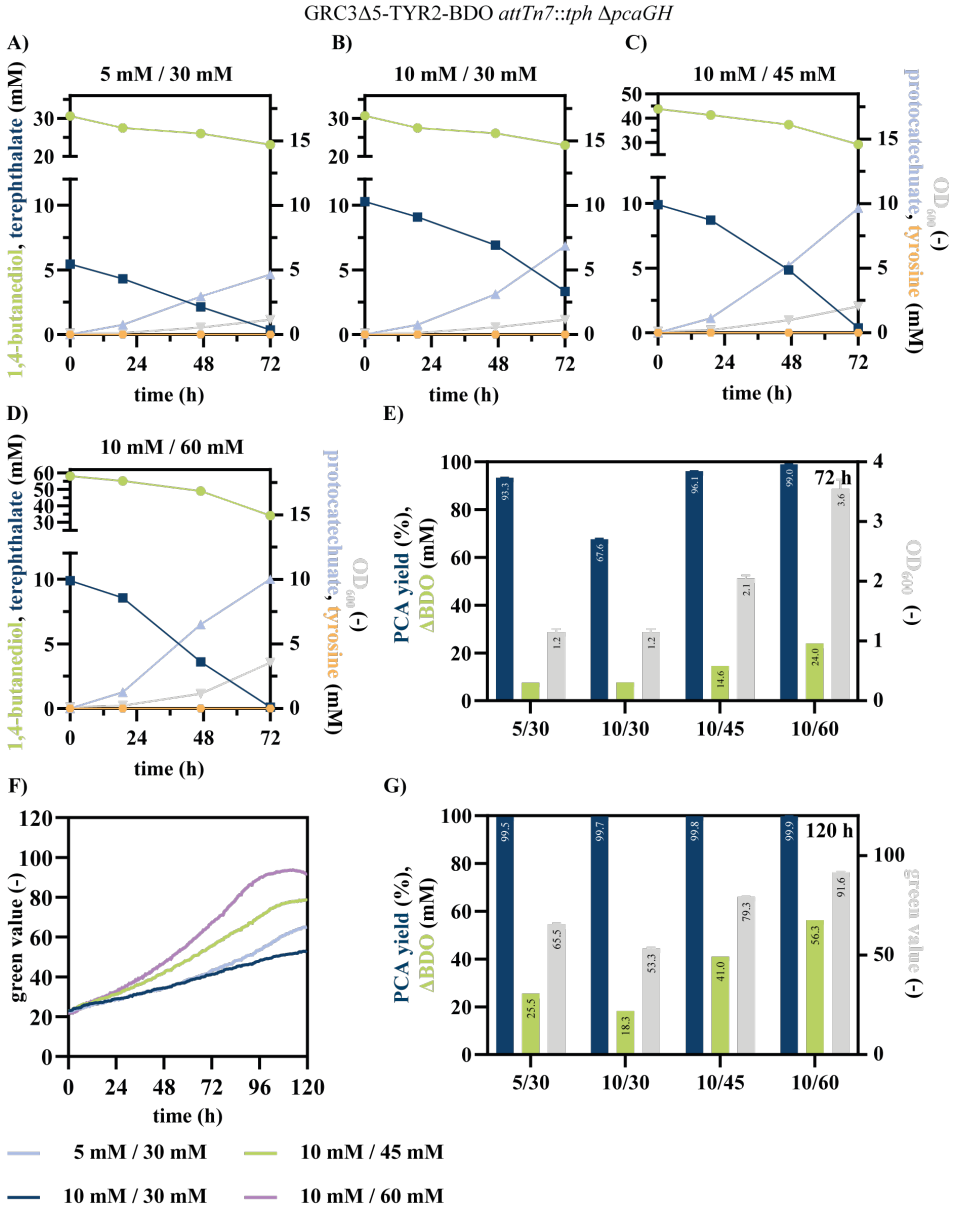

Figure 2.4.8.: Biotransformation of TA into PCA with BDO as additional carbon source. All strains were cultivated separately in MSM medium containing TA and BDO as mentioned in the figure. Samples were taken over time from separate System Duetz plates, which were all inoculated from the same master mix. (A-D) HPLC data from cultivations with different TA/BDO ratios. (E) Calculated PCA yields from TA after 72 h of different strains with different ratios of TA/BDO and the amount of consumed BDO (ΔBDO). (F) Online growth curves measured in the Growth Profiler and (G) corresponding PCA yields from TA calculated from HPLC samples taken after 120 h. Error bars indicate the standard error of the mean, for F these are so small that they are not visible behind the lines (A-E n=2; F-G n=3).

observed that an amine transporter in *P. putida* was upregulated when an evolved strain was grown on BDO as a carbon source, but a knockout of this transporter did not affect gorwth on BDO. The results rather indicate a passive transport trough the membrane, which is concentration-dependent. Besides growth limitations, the results showed a very good conversion rate of TA into PCA. Except for the cultivation with 10 mM TA and 30 mM BDO, all other cultivations achieved ratios above 90 % after 72 h. In the Growth Profiler, complete conversion of TA into PCA was achieved after 120 h in all cultivations. Although some unclear effects of TA on growth with BDO are still present, it seems that BDO could be a good additional carbon source for efficient biotransformation of TA into PCA.

2.4.3.4. Degradation of PBAT mock hydrolysates with defined Mixed Cultures

As shown above, different strains have been successfully engineered to grow on different plastic monomers and further convert them into aromatic compounds. However, all these strains only metabolize one or two monomers, but one of the major problems in the plastics crisis is the mixture of different monomers coming from a complex polymer or from a mixture of different polymers (Kalali *et al.* 2023). Since separating of the different monomers is very costly, it would be beneficial to be able to degrade more than one or two monomers in one step. One way to solve this problem is to combine all the genetic modifications in a single strain and enable it to grow on a wide variety of plastic monomers. However, this could lead to a high metabolic load, elaborate development and less flexibility in changing the substrate mixture, so a bacterial consortium could be a good alternative (Vinuselvi *et al.* 2012). We therefore applied a mixed culture of different monomer-degrading strains. As a representative monomer mixture a mock hydrolysate was prepared based on a monomer ratio of a real PBAT hydrolysate from enzymatic hydrolysis (C. Siracusa, BOKU University Vienna, personal communication). The mock hydrolysate medium contains 9 mM adipate, 12 mM terephthalate and 27.5 mM mM 1,4-butanediol in three-fold buffered (108 mM) mineral salt medium. Furthermore, a mock hydrolysate based on PBAT/starch blends was also used, containing additional 4 mM glucose. Usually these blends consist of 10 % starch (C. Siracusa, BOKU University Vienna, personal communication).
At first, the three previously engineered strains GRC3Δ5-TYR2-AA, GRC3Δ5-TYR2-BDO and GRCΔ5-*a*Δ *attTn7*::*tph* were used to grow on the mock hydrolysates. In the

case of the PBAT/starch hydrolysate, all strains should first metabolise the glucose in parallel and then the respective specific monomers. Online measurements suggested good growth on the mixtures (Figure 2.4.9). Due to the additional glucose monomers in the PBAT/starch mock hydrolysate, the strains grew slightly faster compared to the PBAT mock medium, resulting in faster biomass accumulation and thus these strains reached their stationary phase much earlier. Because of the different monomer concentrations and growth of the respective strains, different growth rates are visible. After 14-18 h in both cases the growth decreases, probably due to the complete consumption of adipate, increase in green value afterwards is only from the slower growing strains on BDO and TA. To confirm these results, samples were taken over time from

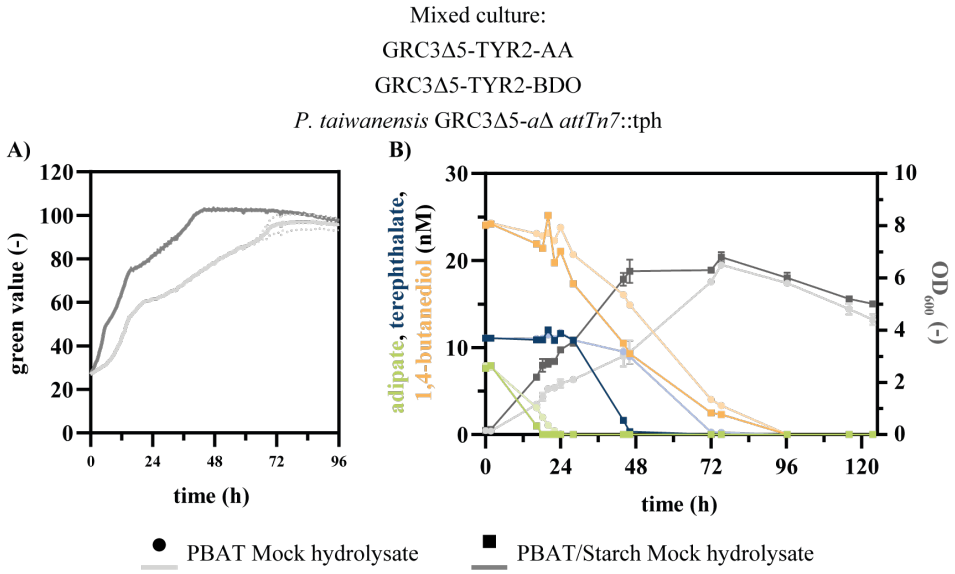

Figure 2.4.9.: Growth and monomer consumption of a defined mixed culture on PBAT and PBTA/starch mock hydrolysates. A) For online growth measurements in the Growth Profiler, all strains were cultivated in MSM medium containing a PBAT and PBAT/starch mock hydrolysate as substrate. B) Growth and monomer consumption in shake flask cultivation, samples were taken over time. Error bars indicate the standard error of the mean (A n=3; B n=2).

cultures grown in System Duetz plates and analysed by HPLC. First, glucose from the PBAT/starch mock medium was consumed after a few hours. As observed previously, the growth of both cultures on PBAT and on PBAT/starch is slowed down after 24 h. At this point, the adipate is completely consumed. The next carbon source utilized is TA. Due to a higher difference in biomass on PBAT compared to PBAT/starch mock media, TA is consumed much faster in cultures with added glucose. BDO is finally consumed

after 96 h. These results confirm the previous results on a mixture of TA and BDO. It indicates a general effect of TA on BDO metabolism and not just a growth limitation due to the inability of GRC3Δ5-TYR2-BDO *attTn7*::*tph* Δ*pcaGH* to degrade TA. The fact that the biomass seems to remain constant after 48 h and does not increase, even in the presence of BDO, could be due to the long stationary phase of the adipate degrading strains. Sometimes a decrease in biomass is observed in the end, probably due to cell lysis. This effect could counteract the increase in biomass of the BDO and TA degrading strains. To overcome this, it may be beneficial to inoculate the cultures with different initial strain concentrations. Another possibility is to change the monomer mixture by increasing AA and decreasing TA, which would lead to longer growth of the AA degrading strains and could eliminate negative TA effects at an earlier stage. However, to get as close as possible to a realistic process, we decided to mimic a real hydrolysate and are therefore limited in the monomer composition. A further challenge is posed by the differences in substrate consumption rates, which greatly affect the efficiency of the conversion. Although the use of single specialized strains for the degradation of mixed substrates has some advantages, such as greater flexibility in changing the substrate mixture or faster and less laborious development, the use of a single strain that consumes all substrates could be an option for faster degradation (Figure 2.4.10). Consuming all substrates at different rates in one superstrain strain, assuming that the substrates are consumed sequentially, would result in a higher initial biomass when the less favourable monomer is consumed. This higher biomass would then reduce the time for degradation. In addition, an "in-between" solution could be the use of a defined mixed culture with strains that can consume more than one substrate, but not all substrates, to improve the outcome of such biological funneling approaches. When the mixed cultures are combined with a biotransformation approach to produce high-value compounds, it is necessary to combine different substrate consumptions in one cell, since an additional carbon source is required. Nevertheless, these results successfully demonstrated the complete consumption of monomer mixtures adapted to PBAT and PBAT/starch hydrolysate, thus demonstrating the potential for bio-upcycling. Since the bacterial mixed culture above mostly resulted in biomass production from mixed plastic monomers and thus did not produce any product of higher value. In the next approach, the consumption of plastic monomers in a mixed culture were combined with the biotransformation of TA into PCA (Figure 2.4.10). Therefore, either the sole AA degrading strain GRC3Δ5-TYR2-AA was combined with a BDO and TA degrading strain, or the sole BDO degrading strain GRC3Δ5-TYR2-BDO was combined with an AA and

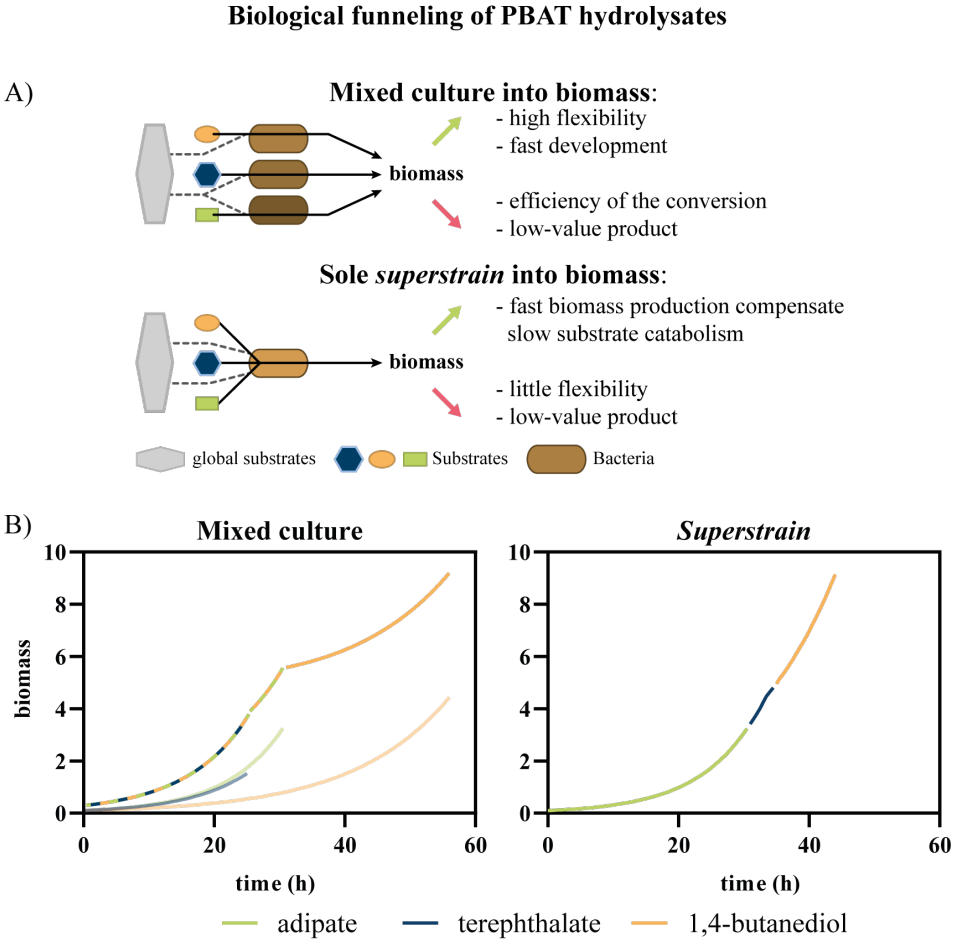

Figure 2.4.10.: Simulated comparison of biological funneling with mixed cultures or *superstrains*. A) Overview of the consumption of different substrates by either a defined mixed culture or a single *superstrain*. B) Growth visualization of a defined mixed culture or a *superstrain* on a substrate mixture containing three different monomers (AA, TA, BDO), which are degraded separately. For mixed cultures, all biomass values were added for combined consumption and for the *superstrain* growth was then calculated with different initial biomasses resulting from the previous substrate. Growth rates and final biomass values for the simulation were calculated from a shake flask growth experiment on a c-equimolar ratio of all monomers (AA $\mu = 0.1141$; TA $\mu = 0.1088$; BDO $\mu = 0.0677$) (de Jong 2022).

TA degrading strain and cultivated on the PBAT and PBAT/starch mock hydrolysates. This results in a cultivation where either AA or BDO acts as the carbon source, while TA is converted to PCA by the strain with the additional *tph* operon and the deletion of *pcaGH*, and further either AA or BDO is degraded by the additional single specialist strain, leading to complete utilisation of AA and BDO and accumulation of PCA from TA. Initially, the growth of these mixtures was measured online to see if any growth effects occurred during the cultivation (Figure 2.4.11). To rule out any negative effect caused by the biotransformation of TA into PCA, strains without the knockout of *pcaGH* were also tested. Regardless of which single degrading strain, GRC3Δ5-TYR2-AA or GRC3Δ5-TYR2-BDO was used, both cultures grew quite fast at the beginning. As observed above, the cultivation on PBAT/starch mock grew faster in the beginning, probably due to the additional glucose. When using GRC3Δ5-TYR2-BDO *attTn7*::*tph* in combination with GRC3Δ5-TYR2-AA, in contrast to the three-strain mixed culture above, no growth interruption is observed. This is probably due to the fact that this strain can now also use TA as a carbon and energy source, which is consumed faster than the BDO. Indeed, when GRC3Δ5-TYR2-BDO *attTn7*::*tph* Δ*pcaGH* is used a growth inhibition is observed after 24 h. This is caused by the fact that the strain can no longer use TA as carbon and energy source and thus only biomass production from BDO is measured. In contrast to that, when the single BDO degrading strain is used in combination with GRC3Δ5-TYR2-AA *attTn7*::*tph* or GRC3Δ5-TYR2-AA *attTn7*::*tph* Δ*pcaGH* this second slower growth phase after 24 h is not observed. The reason for this could be the complete degradation of TA, when GRC3Δ5-TYR2-AA *attTn7*::*tph* Δ*pcaGH* reaches its stationary phase, and thus no limiting effect of TA occurs anymore, allowing a faster growth of GRC3Δ5-TYR2-BDO. Looking at the previous results of biotransformation with AA this is rather unlikely as even after 72 h, TA was still present in the medium. Nevertheless, it seems that no larger limitation occurs by combining the biotransformation with the mixed cultures. Therefore, in a last step mixed culture of both biotransformation strains GRC3Δ5-TYR2-AA *attTn7*::*tph* Δ*pcaGH* and GRC3Δ5-TYR2-BDO *attTn7*::*tph* Δ*pcaGH* were prepared in shake flask. In this case, the complete amount of TA should be converted into PCA and not biomass. In general, the mixed cultivation takes longer than the cultivation with a single degrading strain. As expected, AA is consumed first and completely degraded after 72 h. After 72 h, when AA is consumed, half of the TA is still present in the medium. This is then consumed together with BDO as a carbon source. After 6 days, 100 % of the TA in the medium is converted into PCA. At this point, there are still 5 mM of BDO from

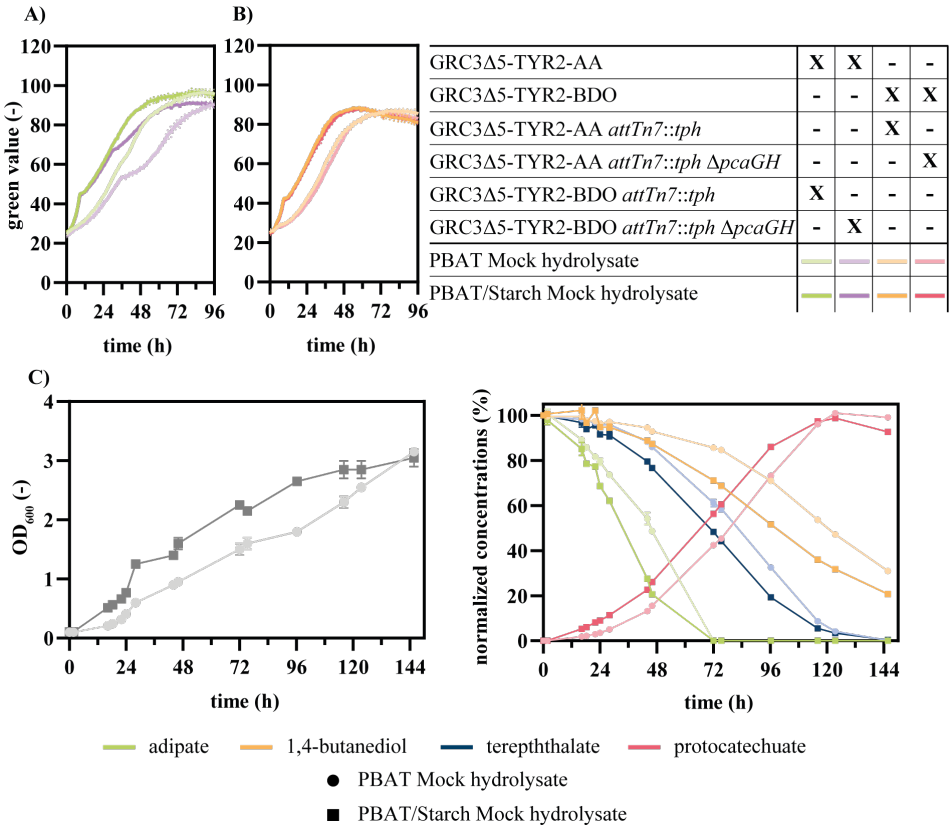

Figure 2.4.11.: Biotransformation of PBAT and PBTA/starch mock hydrolysates into PCA with a defined mixed culture.. (A/B) Growth Profiler measurement of a defined mixed culture consisting of either a TA and AA or a TA and BDO degrading strain and a strain that only converts the other monomer to biomass. All mixed cultures were cultivated on MSM medium containing a PBAT or PBAT/starch mock hydrolysate. "X" indicates the presence of the strain in the defined mixed culture. C) Growth and monomer consumption of a defined mixed culture consisting of GRC3Δ5-TYR2-AA *attTn7::tph* Δ*pcaGH* and GRC3Δ5-TYR2-BDO *attTn7::tph* Δ*pcaGH* in shake flask cultivation, samples were taken over time. Monomer concentrations are normalized to their initial concentration (9 mM AA, 12 mM TA, 27.5 mM BDO). Error bars indicate the standard error of the mean (A,B n=3; C n=2).

the PBAT/starch and about 7 mM from the PBAT hydrolysate in the medium. If the cultivation is prolonged, this BDO should also be degraded, probably much faster in the end when no TA is left. However, the economic viability of this biotransformation approach needs to be validated in the future, e.g. through a techno-economic analysis. Due to the high amount of AA and BDO required to convert TA to PCA, it should be evaluated whether a separate purification step of the remaining TA after degradation of AA and BDO might be more useful for an efficient degradation of PBAT monomers (Ling *et al.* 2019). In this case, AA or BDO could simply be consumed by the cells or, as previously demonstrated with *P. putida* KT2440, used for PHA production (Ackermann *et al.* 2021; Li *et al.* 2020). The purified TA could easily be used as a substrate for new polymerisation. However, to address the plastic waste crisis, it is important to pursue different approaches and validate them accurately. In view of this, this experiment successfully demonstrated the biotransformation of a realistic mock hydrolysate from PBAT or PBAT/starch mixtures into an aromatic precursor of great interest, such as PCA.

2.4.3.5. Conclusion

The substitution of fossil substrates with renewable raw materials or waste streams plays a key role in the future circular economy. In particular, bio-upcycling of these substrates into high-value compounds using efficient microorganisms is important. In this study, we enabled the production of a bio-based aromatic compound, protocatechuate, which is an important precursor for many industrial and pharmaceutical approaches. To do this, we converted a previously optimized tyrosine overproducing strain into a PCA producer using metabolic engineering and heterologous expression of optimized genes. Besides feeding new renewable carbon into the plastics circular economy, it is also of increasing interest to better re- or up-cycle plastic waste streams. Therefore, we successfully combined a biotransformation approach, where we convert TA into PCA, with a defined mixed culture growing on different monomers of PBAT or PBAT/starch hydrolysates. In the end, we were able to produce bio-based PCA either from renewable feedstock such as glucose or from plastic waste hydrolysates. For an efficient future approach and higher PCA production, it could be interesting to combine the knowledge gained in the *de novo* production from glucose with the degradation of AA and BDO. This would lead to PCA production not only from TA but also from AA and BDO, thus increasing the value of the degradation of the other monomers. Furthermore, the

biotransformation step could also be optimised by changing various parameters. It is known that the second step, catalysed by TphB, is zinc-dependent, so an increase in the supply of co-factors could be beneficial. Fed-batch fermentation, where substrates are added systematically over time, could also be an option by increasing the biomass at the beginning of the fermentation and then continuing to feed the high biomass (Qin *et al.* 2023).

2.4.4. Experimental procedures

2.4.4.1. Strains and culture conditions

The chemicals used in this work were obtained from Carl Roth (Karlsruhe, Germany), Sigma-Aldrich (St. Louis, MO, USA), or Merck (Darmstadt, Germany) unless stated otherwise.

All bacterial strains used in this section are listed in table 2.4.2. For quantitative microbial experiments, *P. taiwanensis* were cultivated in three-fold buffered (108 mM phosphate buffer) mineral salt medium (MSM). Pre-cultures were prepared in MSM medium containing 20 mM of glucose. Unless stated otherwise, final substrate concentrations in main-cultures were C-equimolar to 30 mM adipic acid. The concentrations mentioned for the biotransformation experiments are the averaged concentrations of the values measured by HPLC. Liquid cultivations were incubated at 30 °C, with a shaking speed of 200 rpm and an amplitude of 50 mm using Multitron shaker (INFORS) in either 500 mL non-baffled Erlenmeyer flasks with metal caps, containing 50 mL culture volume or 24 well System Duetz plates containing 1.5 mL culture volume. For online growth measurements cultures were analysed with the Growth Profiler^{9}60 (Enzyscreen, Heemstede, The Netherlands) by image analysis. Main cultures were cultivated in transparent bottom 96-well microtiterplates (CR1496dg) with a volume of 200 µL at 30 °C and 225 rpm shaking speed.

Table 2.4.2.: Strains used and generated for this study.

Micat no.	*P. putida* strain	Description	Reference
39	**GRC3Δ5-*a*Δ**	Genome reduced chassis strain optimized for production of tyrosine	Wynands *et al.* 2019
660	**GRC3Δ5-TYR1**	Genome reduced chassis strain optimized for production of tyrosine, harbours $trpE^{P290S}$	Wynands *et al.* 2023

Table 2.4.2.: Strains used and generated for this study. (followed)

Micat no.	*P. putida* strain	Description	Reference
58	**GRC3Δ5-TYR2**	Genome reduced chassis strain optimized for production of tyrosine, harbours $trpE^{P290S}$ and $pheA^{T310I}$	Wynands *et al.* 2023
1407	**GRC3Δ4-*a*Δ**	Reintegration of *pobA*	This work
1408	**GRC3Δ4-TYR1**	GRC3Δ4-TYR1 with reintegrated *pobA*	This work
1412	**GRC3Δ4-*a*Δ Δ*pcaGH***	Additional knockout of *pcaGH*	This work
1413	**GRC3Δ4-TYR1 Δ*pcaGH***	Additional knockout of *pcaGH*	This work
1417	**GRC3Δ4-*a*Δ Δ*pcaGH attTn7*::km^R-P$_{14f}$-*quiC*-*aroG*^{fbr}**	Genomic integration of *quiC*-*aroG*^{fbr} under the control of the synthetic promoter P$_{14f}$	This work
1422	**GRC3Δ4-TYR1 Δ*pcaGH attTn7*::km^R-P$_{14f}$-*quiC*-*aroG*^{fbr}**	Genomic integration of *quiC*-*aroG*^{fbr} under the control of the synthetic promoter P$_{14f}$	This work
1418	**GRC3Δ4-*a*Δ Δ*pcaGH attTn7*::km^R-P$_{14f}$-*ubiC*^{fbr}-*aroG*^{fbr}**	Genomic integration of *ubiC*^{fbr}-*aroG*$_{fbr}$ under the control of the synthetic promoter P$_{14f}$	This work
1421	**GRC3Δ4-TYR1 Δ*pcaGH attTn7*::km^R-P$_{14f}$-*ubiC*^{fbr}-*aroG*^{fbr}**	Genomic integration of *ubiC*^{fbr}-*aroG*^{fbr} under the control of the synthetic promoter P$_{14f}$	This work
1441	**GRC3Δ4-*a*Δ Δ*pcaGH attTn7*::P$_{14f}$-*quiC*-*ubiC*^{fbr}-*aroG*^{fbr}**	Genomic integration of *quiC*-*ubiC*^{fbr}-*aroG*^{fbr} under the control of the synthetic promoter P$_{14f}$	This work
1442	**GRC3Δ4-TYR1 Δ*pcaGH attTn7*::P$_{14f}$-*quiC*-*ubiC*^{fbr}-*aroG*^{fbr}**	Genomic integration of *quiC*-*ubiC*^{fbr}-*aroG*^{fbr} under the control of the synthetic promoter P$_{14f}$	This work
1444	**GRC3Δ4-*a*Δ Δ*pcaGH attTn7*::P$_{14f}$-*quiC*-*ubiC*^{fbr}-*aroG*^{fbr} PVLB_02480::P$_{14f}$-RtPAL-*ech*-*vdh*-*fcs***	Genomic integration of P$_{14f}$-RtPAL-*ech*-*vdh*-*fcs* at landig pad PVLB_02480-PVLB_02485	This work

Table 2.4.2.: Strains used and generated for this study. (followed)

Micat no.	*P. putida* strain	Description	Reference
1445	**GRC3Δ4-TYR1 Δ*pcaGH* *attTn7*::P$_{14f}$-*quiC*-*ubiC*^{fbr}-*aroG*^{fbr} PVLB_02480::P$_{14f}$-RtPAL-*ech*-*vdh*-*fcs***	Genomic integration of P$_{14f}$-RtPAL-*ech*-*vdh*-*fcs* at landig pad PVLB_02480-PVLB_02485	This work
2251	**GRC3Δ4-*a*Δ Δ*pcaGH* *attTn7*::P$_{14f}$-*quiC*-*ubiC*^{fbr}-*aroG*^{fbr} PVLB_02480::P$_{14f}$-RpcTAL-*ech*-*vdh*-*fcs***	Genomic integration of P$_{14f}$-RpcPAL-*ech*-*vdh*-*fcs* at landig pad PVLB_02480-PVLB_02485, additional promotermutation in P$_{14f}$	This work
2250	**GRC3Δ4-TYR1 Δ*pcaGH* *attTn7*::P$_{14f}$-*quiC*-*ubiC*^{fbr}-*aroG*^{fbr} PVLB_02480::P$_{14f}$-RpcTAL-*ech*-*vdh*-*fcs***	Genomic integration of P$_{14f}$-RpcPAL-*ech*-*vdh*-*fcs* at landig pad PVLB_02480-PVLB_02485, additional promotermutation in P$_{14f}$	This work
2261	**GRC3Δ5-*a*Δ *attTn7*::tph**	Genomic integration of tph operon from *P. umsongensis* GO16	This work
2263	**GRC3Δ5-TYR1 *attTn7*::tph**	Genomic integration of tph operon from *P. umsongensis* GO16	This work
2262	**GRC3Δ5-TYR2 *attTn7*::tph**	Genomic integration of tph operon from *P. umsongensis* GO16	This work
2268	**GRC3Δ5-*a*Δ *attTn7*::tph Δ*pcaGH***	Knockout of *pcaGH* to enable biotransformation into PCA	This work
2270	**GRC3Δ5-TYR1 *attTn7*::tph Δ*pcaGH***	Knockout of *pcaGH* to enable biotransformation into PCA	This work
2269	**GRC3Δ5-TYR2 *attTn7*::tph Δ*pcaGH***	Knockout of *pcaGH* to enable biotransformation into PCA	This work
1434	**GRC3Δ5-TYR2-AA**	Reverse engineered *P. taiwanensis* GRC3Δ5-TYR2 paaYX::P14e-dcaAKIJP Δ*psrA* for growth on AA	Op de Hipt, unpublished
1486	**GRC3Δ5-TYR2-BDO**	Reverse engineered *P. taiwanensis* GRC3Δ5-TYR2 PVLB_10540^{L480L} PVLB_12690^{A247V} PVLB_13305^{S141P} for growth on BDO	Op de Hipt, unpublished

Table 2.4.2.: Strains used and generated for this study. (followed)

Micat no.	*P. putida* strain	Description	Reference
2265	**GRC3Δ5-TYR2-AA *attTn7*::tph**	AA reverse engineered strain able to grow on TA	This work
2264	**GRC3Δ5-TYR2-BDO *attTn7*::tph**	BDO reverse engineered strain able to grow on TA	This work
2272	**GRC3Δ5-TYR2-AA *attTn7*::tph Δ*pcaGH***	Strain for biotransformation of TA into PCA with AA as additional carbon source	This work
2271	**GRC3Δ5-TYR2-BDO *attTn7*::tph Δ*pcaGH***	Strain for biotransformation of TA into PCA with BDO as additional carbon source	This work

* All strains for molecular biological procedures are shown in table S1.

2.4.4.2. Plasmid cloning and strain engineering

Cloning primer were ordered as unmodified DNA oligonucleotides from Eurofins Genomics (Ebersberg, Germany) and are listed in table S3. The Q5 High-Fidelity Polymerase Master Mix was used for the amplification of cloning fragments, while the Taq DNA Polymerase Master Mix for used for screenings (New-England Biolabs, Ipswich, MA, USA). Plasmids used were assembled by Gibson assembly (Gibson *et al.* 2009) using NEBuilder HiFi DNA assembly Master Mix (New-England Biolabs, Ipswich, MA, USA) and are listed in more detail in Table S2. Transformation of *E.coli* with assembled DNA and purified plasmid was performed by a heat chock protocol (Hanahan 1983). Transformation of *P. taiwanensis* was performed by electroporation and conjugational transfer of mobilized plasmids was performed by patch mating as described by Wynands *et al.* (2018). Knockouts, promoterexchange and point mutations were obtained using either a modified pSNW2 system from Volke *et al.* (2020) based on the pEMG system described by Martínez-García *et al.* (2011) or the original system with a modified protocol described by Wynands *et al.* (2018). Integration of heterologous genes into the *attTn7*-site of the *P. taiwanensis* VLB120 genome was achieved by patch-mating of the *E. coli* donor strain harbouring the respective pBG-plasmid, the helper strain *E. coli* HB101 pRK2013, *E. coli* DH5α λpir pTNS1 providing the required transposase, and the recipient, which are listed in table 2.4.2. Marker recycling was performed as described

in Ackermann *et al.* (2021).Genomic integration of the RpcTAL-*ech-vdh-fcs* cassette downstream of PVLB_02480 was only possible with an additional terminator sequence upstream of the P_{14f} promoter sequence on the integration plasmid. Additionally, a mutation (A→C) at the end of P_{14f} that occurred during integration, resulting in sequence GCCCGTTGACATGACATGGTTTTGAGGGTATAATGTGGCG**C**.
Plasmids, gene deletions and point mutations were verified by colony PCR using the One*Tag* 2x Master Mix (New England BioLabs, Ipswich, Massachusetts, USA) with an additional pre-lysis step in alkaline PEG 200 (Chomczynski *et al.* 2006) and confirmed by Sanger sequencing performed by Eurofins Genomics (Ebersberg, Germany).

2.4.4.3. Analytical methods

In shake flask experiments, bacterial growth was monitored as optical density at a wavelength of 600 nm (OD600) with an Ultrospec 10 cell Density Meter (Ge Healthcare, Little Chalfront, Buckinghamshire, United Kingdom). Online analysis of growth was measured by the Growth Profiler and analysed using the Growth Profiler Control software V2_0_0. The corresponding green values are derived from image analysis of the image taken from the bottom of microtiter plates.

2.4.4.4. Extracellular metabolites

For measuring extracellular metabolites, samples were harvested from liquid cultivation by centrifugation and the supernatant was analysed using a 1260 Infinity II HPLC equipped with a 1260 Infinity II Refractive Index Detector (Agilent, Santa Clara, California, USA). Analytes (AA and BDO) were eluted using a 150 x 7.8 mm organic acid H+ resin column (Rezex™ ROA-Organic Acid H+ (8 %), LC Column 150 x 7.8 mm) together with a 40 x 8 mm organic acid resin pre-column with 5 mM H_2SO_4 as mobile phase at a flow rate of 0.6 mL min^{-1} at 60 °C. TA and PCA were analyzed using a reversed-phase C18-HPLC column (InfinityLab Poroshell 120 EC-C18,3.0 x 150 mm, 2.7 µm, Agilent Technologies, P.N. 693975-302T) together with a pre-column (Agilent Technologies; P.N.: 615 823750-911) and eluted by using a gradient of 0.1 % (v/v) trifluoroacetic acid (TFA, Sigma Aldrich) and acetonitrile (Th. Geyer) at a flow rate of 0.8 mL min^{-1} and a temperature of 40 °C. Primary amines, such as tyrosine, were separated and quantified as *ortho*-phthalaldehyde derivatives using a Kinetex 2,6 µm EVO C18 (100Å, 100 x 2,1 mm) HPLC column, equipped with SecurityGuard ULTRA cartridges (Phenomenex) and a gradient of a mobile phase consisting of 10 mM Na_2HPO_4, 10 mM $Na_2B_4O_7$ (pH 8.2) at a flow rate of 0.42 mL min^{-1}.

3. General discussion and outlook

The overproduction of plastics and the environmental impact caused by improper disposal are major global challenges for our present and future. Since plastics have many advantages over traditional materials such as steel, glass or cement in terms of flexibility, weight and manufacturing, and are indispensable in modern society, their complete elimination is not a viable solution. Instead, it is imperative to explore the development of new and efficient processes to solve this dilemma. One part of the solution, to which the work of this thesis will contribute, in the complex system of plastics recycling could be biological treatment and upcycling.

3.1. Biodegradation of monomers enables plastic waste to be used as feedstock for biotechnological approaches

The transition to a circular economy for plastics has encountered several obstacles, including the depolymerization of polyolefins such as PE or PP. These polyolefins have beneficial properties but are difficult to degrade due to their strong carbon-carbon backbone. The majority of these often single-use plastics are not recycled and end up in landfills or the environment, causing ecological and environmental damage (Rorrer *et al.* 2021). Therefore, to tackle the issue of efficient recycling, interdisciplinary approaches are necessary. These approaches should integrate highly efficient thermochemical or catalytic depolymerization methods with microbial metabolization (Tiso *et al.* 2022). Pyrolysis, which is an example of such an efficient depolymerization method, holds promise in this regard. Under the absence of oxygen, products of pyrolysis can be mixtures of n-alkanes, which then could be further oxidized to fatty acids. The resulting fatty acids being a promising feedstock for microbial production of PHAs by different Pseudomonads strains (Guzik *et al.* 2021). Besides pyrolysis, also the oxidation of the polyolefine backbone demonstrate a promising combined approach. These oxidation could either be done by enzymatical oxidation, e.g. by phenoloxidases (Sanluis-Verdes *et al.* 2022), by chemical autooxidation (Sullivan *et al.* 2022) or by microwave-assisted oxidation (Bäckström *et al.* 2017). Such oxidations of PE can yield mixtures of medium-

and long-chain α,ω-diacids.
Another challenge has been the utilization of the resulting monomers from these depolymerization approaches. To solve this open part towards a circular economy, different Pseudomonads have been engineered in this thesis for the efficient microbial degradation of a variety of plastic monomers, ranging from medium- to long-chain aliphatics, such as α,ω-alcohols (Chapter 2.2,2.3) and α,ω-acids (Chapter 2.1,2.2), from PE to complex aromatics from PET or PBAT (Chapter 2.4). The chain length of the products from oxidation of PE is often depending on the process parameters like temperature, recycling time or used catalyst and thus have an influence on the sustainability of the process (Bäckström *et al.* 2017). The broad substrate spectrum of the engineered *P. putida* provides a good opportunity for a more sustainable process, as it is not necessary to degrade the PE chain to the smallest fraction, but it becomes possible to stop the reaction earlier and accept longer chains of even and uneven length.
Once both depolymerization and subsequent funneling of the monomers into the central carbon metabolism have taken place, almost all common sugar-based biotechnological processes can be used and combined to produce new products from plastic waste (Wierckx *et al.* 2018). Here, the substrate spectrum of an aromatics-producing *P. taiwanensis* was switched from glucose to adipate and 1,4-butanediol. Thereby, carbon/carbon yields of 12 % from BDO and 7.8 % from adipate were achieved, which is only slightly worse than previous yields from glucose (Otto *et al.* 2019). For the future approach and an economically feasible bio-upcycling process, it will be important to move beyond from tyrosine, which is mainly used as a feed additive, to aromatic compounds with higher value (Schwanemann *et al.* 2020; Wynands *et al.* 2023).
Initially, the focus was on single monomers, such as mcl-dicarboxylic acids and diols, but this could later be extended to mixed substrates. To achieve high quality end products, mechanical and physicochemical recycling demand waste feedstocks that are pure and free from impurities through resource-intensive sorting. At this point the high potential of bio-degradation and further biological funneling of mixtures of monomers resulting from mixed plastic waste underlines the usage of these approaches. This was also demonstrated by Reifsteck *et al.* (2023). They performed a techno-economic assessment (TEA) and compared the monomer recovery after enzymatic recycling with a further microbial conversion. Thereby the advantage of using all of the resulting monomers from a plastic waste mixture as microbial feedstocks compared to the recovery of only lactic acid, which led to a huge loss of carbon in case of TA and EG, become clear. They also calculated a decreased carbon foot print of microbial conversion against recovery,

due to less freshwater usage and wastewater production (Reifsteck *et al.* 2023).

3.2. Future applications of biotechnological recycling

In addition to the recycling of solid post-consumer plastic waste, the recycling and removal of micro- and nano-plastic particles from industrial, domestic, and municipal wastewater is becoming increasingly important. Wastewater treatment plants are a major source of plastic pollution because most treatment processes are poor at separating, filtering or degrading the small plastic particles. They either accumulate in the final sludge and could thus end up on agricultural land or are pumped directly into rivers *via* the effluent water (Okoffo *et al.* 2019). Since wastewater is often even more contaminated than solid collected plastic waste, a further purification step by means of selective biological degradation of the plastic fraction could be beneficial (Hou *et al.* 2021). Recycling steps that require a high degree of purity, such as mechanical recycling, are rather unsuitable at this point, since this would first require a costly separation process. Here, the strains of this work could also be useful and used in a combined process involving a prior catalytic depolymerization process. Either only for degradation of the plastic particles and production of biomass or for upcycling of the wastewater into new bio-based plastic. However, it should be noted that this is a separate closed treatment step and the microorganisms cannot simply be added to the conventional biological active sludge treatment step because they are GMOs. Nevertheless, this step could be worthwhile, since most non-GMOs microorganisms isolated so far are often very slow to degrade plastic and would then potentially take longer than the wastewater stays in the treatment plant. Especially for microplastic-rich point sources, such as plastic production plants, this approach could prove economical or even essential in the face of ever stricter environmental norms and legislation. The situation differs when considering other waste treatment processes, such as composting plants. Composting plants today also often have the problem that the circulation time within the plant is too short to break down plastics completely, this is often the case even when it is biodegradable plastic, such as PLA or PBAT (Millican *et al.* 2021). Since high temperatures are often generated within the process, usually around the glass transition temperatures of the polymers (Azim *et al.* 2018), the use of naturally isolated thermophilic strains growing under high temperature conditions could be advantageous compared to engineered mesophilic microorganisms. Using isolated or genetically

modified thermophilic strains is also one approach to tackle the challenge of combined enzymatic and biological degradation of plastics. The enzymes currently used for degradation are most effective at higher temperatures above the T_g of the polymer (Wei *et al.* 2017), making direct fermentation of hydrolysates with engineered Pseudomonads in the same reactor impossible. Lowering the temperature to room temperature would significantly reduce the enzymatic activity (Wei *et al.* 2017). Nevertheless, a combined approach, in which the same organism responsible for degrading the resulting monomers also produces and releases the necessary enzymes, has some advantages due to the direct metabolism of the released monomers. On the one hand, it could avoid product inhibition or toxicity effects that would reduce enzyme activity. Secondly, it would reduce the need to add expensive acids or bases, as the acids, such as adipic acid or terephthalic acid, are consumed immediately. (Ellis *et al.* 2021). However, this approach would still be limited by different optimal temperatures and would require an additional carbon source at the beginning to ensure efficient production of sufficient biomass and enzymes. At this point, thermophilic organisms that thrive at around 60 °C, such as *Geobacillus thermoleovorans* (Dinsdale *et al.* 2011), could be advantageous as they have similar optimal temperatures to the enzymes. To overcome the problem of low initial biomass and associated low enzyme concentration, continuous processes could be considered in the future, where enzymes are partially recycled if this allows their activity. Otherwise, the process would have a much longer lag phase than if a larger amount of purified enzymes were used. A disadvantage of using thermophilic bacteria for an up-cycling approach is that only a few thermophilic production hosts have been described so far. In contrast, Pseudomonads are known for their broad production spectrum, as was also shown in this work. Whether a better compromise would be an initial enzymatic degradation at an optimal temperature, followed by a temperature reduction for further processing, has to be proven in the future, but the costs of reducing acid and base in the combined process should not be neglected. In addition to expanding the substrate spectrum of Pseudomonads for efficient metabolism of plastic monomers and production of bio-based polymers such as PHAs, this work also focused on biological funneling and the production of new bio-based compounds such as tyrosine and protocatechuate. These efforts aim to address not only the plastics crisis, but also the climate crisis by conserving resources, replacing fossil feedstocks, and reducing greenhouse gas emissions. Walker *et al.* (2022) have shown that the choice of materials and their disposal play a critical role in determining the net impact on greenhouse gas emissions. By using biomass as a substrate, bio-based plastics can

sequester atmospheric CO_2 during their lifecycle, which can lead to negative emissions if renewable energy is used (Walker *et al.* 2022). Considering plastics and the climate crisis together, this thesis succeeded in the *de novo* production of key precursors and building blocks, including protocatechuate. The combination of *de novo* production of PCA from glucose or later from plastic hydrolysates with biotransformation of terephthalate could be a good way to efficiently utilize and biologically funnel mixed substrate and thus enable a sustainable recycling of mixed plastic waste. However, more research is needed to determine whether a mixed culture approach or the use of a single strain is the better option. Although a defined mixed culture would shorten the development time, this work shows some limitations in terms of biotransformation and high-energy catabolism, which stops once the carbon and energy source is consumed. For this case, a single "superstrain" that can utilize several to all substrates might be better. On the one hand, preferred substrates such as glucose, which is produced during the degradation of PBAT/starch blends, can be used to produce sufficient biomass in the first place. The subsequent consumption of less suitable substrates would consequently start at higher biomass concentrations, leading to an overall more rapid biotransformation (Figure 2.4.10). If the strain is also a *de novo* producer, the excess substrates can also be used for the production of PCA. However, especially in the development of such processes, it is also important to know and understand each individual degradation and production pathway, and therefore it is necessary to test separate strains, to which this work contributes. In conclusion, the solution to the plastics crisis lies in weighing up the most efficient solution (Bachmann *et al.* 2023). This will involve a mix of technologies. For pure and easily separable plastics, mechanical recycling, as is already partly the case today, will probably make the most economic sense. If plastic incineration is used in combination with energy recovery to avoid the use of fossil resources such as gas, coal or oil, this technology could also be an initial alternative and reduce the huge amount of plastic. For much else, pyrolysis is currently the most mature technology. All processes are easily scalable in terms of volume, which is an advantage given the huge volume of plastic waste. However, pyrolysis in particular requires large amounts of energy, which can lead to high greenhouse gas emissions in some regions, depending on the energy mix. This, together with the fact that there are still many waste streams that are not very pure or difficult to sort, gives biotechnological recycling methods a niche that cannot be ignored. This work has contributed to the success of this technique by broadening the substrate spectrum of different Pseudomonads and showing the conversion into chemical molecules of increasing interest.

Bibliography

Abel, S. M., S. Primpke, I. Int-Veen, A. Brandt, and G. Gerdts (01/2021). "Systematic identification of microplastics in abyssal and hadal sediments of the Kuril Kamchatka trench." In: *Environmental Pollution* 269, p. 116095. DOI: 10.1016/J.ENVPOL.2020.116095.

Ackermann, Y. S., W.-J. Li, L. Op de Hipt, P.-J. Niehoff, W. Casey, T. Polen, S. Köbbing, H. Ballerstedt, B. Wynands, K. O'Connor, L. M. Blank, and N. Wierckx (09/2021). "Engineering adipic acid metabolism in *Pseudomonas putida*." In: *Metabolic Engineering* 67, pp. 29–40. DOI: 10.1016/j.ymben.2021.05.001.

Allen, L., A. O'Connell, and V. Kiermer (01/2019). "How can we ensure visibility and diversity in research contributions? How the Contributor Role Taxonomy (CRediT) is helping the shift from authorship to contributorship." In: *Learned Publishing* 32.1, pp. 71–74. DOI: 10.1002/leap.1210.

Alvarenga, R. A. and J. Dewulf (11/2013). "Plastic vs. fuel: Which use of the Brazilian ethanol can bring more environmental gains?" In: *Renewable Energy* 59, pp. 49–52. DOI: 10.1016/j.renene.2013.03.029.

Alvarez, H. M. (07/2003). "Relationship between β-oxidation pathway and the hydrocarbon-degrading profile in actinomycetes bacteria." In: *International Biodeterioration & Biodegradation* 52.1, pp. 35–42. DOI: 10.1016/S0964-8305(02)00120-8.

Andrady, A. L. (2017). "The plastic in microplastics: A review." In: *Marine Pollution Bulletin* 119.1, pp. 12–22. DOI: 10.1016/j.marpolbul.2017.01.082.

Andrady, A. L. and M. A. Neal (07/2009). "Applications and societal benefits of plastics." In: *Philosophical Transactions of the Royal Society B: Biological Sciences* 364.1526, pp. 1977–1984. DOI: 10.1098/rstb.2008.0304.

Aparicio, T., V. Lorenzo, and E. Martínez-García (09/2019). "CRISPR/Cas9-enhanced ssDNA recombineering for *Pseudomonas putida*." In: *Microbial Biotechnology* 12.5, pp. 1076–1089. DOI: 10.1111/1751-7915.13453.

Aseev, L. V., L. S. Koledinskaya, and I. V. Boni (2020). "Autogenous regulation in vivo of the *rpmE* gene encoding ribosomal protein L31 (bL31), a key component of the protein-protein intersubunit bridge B1b." In: *Rna* 26.7, pp. 814–826. DOI: 10.1261/rna.074237.119.

Avérous, L. (2008). "Polylactic Acid: Synthesis, Properties and Applications." In: *Monomers, Polymers and Composites from Renewable Resources*. Elsevier, pp. 433–450. DOI: 10.1016/B978-0-08-045316-3.00021-1.

Aversa, C., M. Barletta, G. Cappiello, and A. Gisario (06/2022). "Compatibilization strategies and analysis of morphological features of poly(butylene adipate-co-terephthalate) (PBAT)/poly(lactic acid) PLA blends: A state-of-art review." In: *European Polymer Journal* 173, p. 111304. DOI: 10.1016/j.eurpolymj.2022.111304.

Azim, K., B. Soudi, S. Boukhari, C. Perissol, S. Roussos, and I. Thami Alami (06/2018). "Composting parameters and compost quality: a literature review." In: *Organic Agriculture* 8.2, pp. 141–158. DOI: 10.1007/s13165-017-0180-z.

Bachmann, M., C. Zibunas, J. Hartmann, V. Tulus, S. Suh, G. Guillén-Gosálbez, and A. Bardow (03/2023). "Towards circular plastics within planetary boundaries." In: *Nature Sustainability* 6.5, pp. 599–610. DOI: 10.1038/s41893-022-01054-9.

Bäckström, E., K. Odelius, and M. Hakkarainen (12/2017). "Trash to Treasure: Microwave-Assisted Conversion of Polyethylene to Functional Chemicals." In: *Industrial & Engineering Chemistry Research* 56.50, pp. 14814–14821. DOI: 10.1021/acs.iecr.7b04091.

Bagdasarian, M., R. Lurz, B. Rückert, F. Franklin, M. Bagdasarian, J. Frey, and K. Timmis (12/1981). "Specific-purpose plasmid cloning vectors II. Broad host range, high copy number, RSF 1010-derived vectors, and a host-vector system for gene cloning in *Pseudomonas*." In: *Gene* 16.1-3, pp. 237–247. DOI: 10.1016/0378-1119(81)90080-9.

Baggi, G., M. M. Boga, D. Catelani, E. Galli, and V. Treccani (01/1983). "Styrene catabolism by a strain of *Pseudomonas fluorescens*." In: *Systematic and Applied Microbiology* 4.1, pp. 141–147. DOI: 10.1016/S0723-2020(83)80042-3.

Barbe, V., D. Vallenet, N. Fonknechten, A. Kreimeyer, S. Oztas, L. Labarre, S. Cruveiller, C. Robert, S. Duprat, P. Wincker, L. N. Ornston, J. Weissenbach, P. Marlière, G. N. Cohen, and C. Médigue (10/2004). "Unique features revealed by the genome sequence of *Acinetobacter* sp. ADP1, a versatile and naturally transformation competent bacterium." In: *Nucleic Acids Research* 32.19, pp. 5766–5779. DOI: 10.1093/nar/gkh910.

Belda, E., R. G. A. van Heck, M. José Lopez-Sanchez, S. Cruveiller, V. Barbe, C. Fraser, H.-P. Klenk, J. Petersen, A. Morgat, P. I. Nikel, D. Vallenet, Z. Rouy, A. Sekowska, V. A. P. Martins dos Santos, V. de Lorenzo, A. Danchin, and C. Médigue (10/2016). "The revisited genome of *Pseudomonas putida* KT2440 enlightens its value as a robust metabolic chassis." In: *Environmental Microbiology* 18.10, pp. 3403–3424. DOI: 10.1111/1462-2920.13230.

Benedetti, I., V. de Lorenzo, and P. I. Nikel (01/2016). "Genetic programming of catalytic *Pseudomonas putida* biofilms for boosting biodegradation of haloalkanes." In: *Metab. Eng.* 33, pp. 109–118. DOI: 10.1016/j.ymben.2015.11.004.

Bentley, G. J., N. Narayanan, R. K. Jha, D. Salvachúa, J. R. Elmore, G. L. Peabody, B. A. Black, K. Ramirez, A. De Capite, W. E. Michener, A. Z. Werner, D. M. Klingeman, H. S. Schindel, R. Nelson, L. Foust, A. M. Guss, T. Dale, C. W. Johnson, and G. T. Beckham (05/2020). "Engineering glucose metabolism for enhanced muconic acid production in *Pseudomonas putida* KT2440." In: *Metabolic Engineering* 59, pp. 64–75. DOI: 10.1016/j.ymben.2020.01.001.

Bîrcă, A., O. Gherasim, V. Grumezescu, and A. M. Grumezescu (2019). "Introduction in thermoplastic and thermosetting polymers." In: *Materials for Biomedical Engineering*. Elsevier, pp. 1–28. DOI: 10.1016/B978-0-12-816874-5.00001-3.

Bishop, R. E. (10/2000). "The bacterial lipocalins." In: *Biochimica et Biophysica Acta (BBA) - Protein Structure and Molecular Enzymology* 1482.1-2, pp. 73–83. DOI: 10.1016/S0167-4838(00)00138-2.

Bitzenhofer, N. L., L. Kruse, S. Thies, B. Wynands, T. Lechtenberg, J. Rönitz, E. Kozaeva, N. T. Wirth, C. Eberlein, K.-E. Jaeger, P. I. Nikel, H. J. Heipieper, N. Wierckx, and A. Loeschcke (07/2021). "Towards robust Pseudomonas cell factories to harbour novel biosynthetic pathways." In: *Essays in Biochemistry* 65.2. Ed. by D. Mattanovich and P. Ivan Nikel, pp. 319–336. DOI: 10.1042/EBC20200173.

Blanco, F. G., N. Hernández, V. Rivero-Buceta, B. Maestro, J. M. Sanz, A. Mato, A. M. Hernández-Arriaga, and M. A. Prieto (06/2021). "From Residues to Added-Value Bacterial Biopolymers as Nanomaterials for Biomedical Applications." In: *Nanomaterials* 11.6, p. 1492. DOI: 10.3390/nano11061492.

Blank, L. M., T. Narancic, J. Mampel, T. Tiso, and K. O'Connor (2020). "Biotechnological upcycling of plastic waste and other non-conventional feedstocks in a circular economy." In: *Current Opinion in Biotechnology* 62, pp. 212–219. DOI: 10.1016/j.copbio.2019.11.011.

Blázquez, B., M. Carmona, J. L. García, and E. Díaz (2008). "Identification and analysis of a glutaryl-CoA dehydrogenase-encoding gene and its cognate transcriptional regulator from *Azoarcus* sp . CIB." In: 10, pp. 474–482. DOI: 10.1111/j.1462-2920.2007.01468.x.

Bollinger, A., S. Thies, N. Katzke, and K.-E. Jaeger (01/2020). "The biotechnological potential of marine bacteria in the novel lineage of *Pseudomonas pertucinogena*." In: *Microbial Biotechnology* 13.1, pp. 19–31. DOI: 10.1111/1751-7915.13288.

Borrelle, S. B., J. Ringma, K. L. Law, C. C. Monnahan, L. Lebreton, A. McGivern, E. Murphy, J. Jambeck, G. H. Leonard, M. A. Hilleary, M. Eriksen, H. P. Possingham, H. De Frond, L. R. Gerber, B. Polidoro, A. Tahir, M. Bernard, N. Mallos, M. Barnes, and C. M. Rochman (09/2020). "Predicted growth in plastic waste exceeds efforts to mitigate plastic pollution." In: *Science* 369.6510, pp. 1515–1518. DOI: 10.1126/science.aba3656.

Boyer, H. W. and D. Roulland-dussoix (05/1969). "A complementation analysis of the restriction and modification of DNA in *Escherichia coli*." In: *Journal of Molecular Biology* 41.3, pp. 459–472. DOI: 10.1016/0022-2836(69)90288-5.

Brack, Y., C. Sun, D. Yi, and U. T. Bornscheuer (05/2022). "Discovery of Novel Tyrosine Ammonia Lyases for the Enzymatic Synthesis of p -Coumaric Acid." In: *ChemBioChem* 23.10, pp. 1–7. DOI: 10.1002/cbic.202200062.

Brahney, J., N. Mahowald, M. Prank, G. Cornwell, Z. Klimont, H. Matsui, and K. A. Prather (04/2021). "Constraining the atmospheric limb of the plastic cycle." In: *Proceedings of the National Academy of Sciences* 118.16. DOI: 10.1073/pnas.2020719118.

Branson, Y., S. Söltl, C. Buchmann, R. Wei, L. Schaffert, C. P. Badenhorst, L. Reisky, G. Jäger, and U. T. Bornscheuer (2023). "Urethanases for the Enzymatic Hydrolysis of Low Molecular Weight Carbamates and the Recycling of Polyurethanes." In: *Angewandte Chemie - International Edition* 62.9. DOI: 10.1002/anie.202216220.

Bretschneider, L., I. Heuschkel, K. Bühler, R. Karande, and B. Bühler (03/2022). "Rational orthologous pathway and biochemical process engineering for adipic acid production using *Pseudomonas taiwanensis* VLB120." In: *Metabolic Engineering* 70.November 2021, pp. 206–217. DOI: 10.1016/j.ymben.2022.01.014.

Brown, K. D. (09/1968). "Regulation of aromatic amino acid biosynthesis in *Escherichia coli* K12." In: *Genetics* 60.1, pp. 31–48. DOI: 10.1093/genetics/60.1.31.

Bryant, W. M. D. (12/1947). "Polythene fine structure." In: *Journal of Polymer Science* 2.6, pp. 547–564. DOI: 10.1002/pol.1947.120020601.

Burgard, A., M. J. Burk, R. Osterhout, S. Van Dien, and H. Yim (12/2016). "Development of a commercial scale process for production of 1,4-butanediol from sugar." In: *Current Opinion in Biotechnology* 42, pp. 118–125. DOI: 10.1016/j.copbio.2016.04.016.

Cabernard, L., S. Pfister, C. Oberschelp, and S. Hellweg (12/2021). "Growing environmental footprint of plastics driven by coal combustion." In: *Nature Sustainability* 5.2, pp. 139–148. DOI: 10.1038/s41893-021-00807-2.

Caruso, G., E. Bergami, N. Singh, and I. Corsi (05/2022). "Plastic occurrence, sources, and impacts in Antarctic environment and biota." In: *Water Biology and Security* 1.2, p. 100034. DOI: 10.1016/j.watbs.2022.100034.

Castellan, A. (05/1991). "Industrial production and use of adipic acid." In: *Catalysis Today* 9.3, pp. 237–254. DOI: 10.1016/0920-5861(91)80049-F.

Catur Utomo, R. N., W.-J. Li, T. Tiso, C. Eberlein, M. Doeker, H. J. Heipieper, A. Jupke, N. Wierckx, and L. M. Blank (11/2020). "Defined microbial mixed culture for utilization of polyurethane monomers." In: *ACS Sustainable Chemistry & Engineering* 8.47, pp. 17466–17474. DOI: 10.1021/acssuschemeng.0c06019.

Cavaleiro, A. M., S. H. Kim, S. Seppälä, M. T. Nielsen, and M. H. H. Nørholm (09/2015). "Accurate DNA Assembly and Genome Engineering with Optimized Uracil Excision Cloning." In: *ACS Synth. Biol.* 4.9, pp. 1042–1046. DOI: 10.1021/acssynbio.5b00113.

Chae, T. U., J. H. Ahn, Y.-S. Ko, J. W. Kim, J. A. Lee, E. H. Lee, and S. Y. Lee (03/2020). "Metabolic engineering for the production of dicarboxylic acids and diamines." In: *Metabolic Engineering* 58, pp. 2–16. DOI: 10.1016/j.ymben.2019.03.005.

Chee, J.-y., S.-s. Yoga, N.-s. Lau, S.-c. Ling, R. M. M. Abed, and K. Sudesh (2010). "Bacterially produced polyhydroxyalkanoate (PHA): Converting renewable resources into bioplastics." In: *Current research, technology and education topics in Applied Microbiology and Microbial Biotechnology*. Ed. by A. Mendez-Vilas. 2, pp. 1395–1404.

Chen, X., J. Hou, Q. Gu, Q. Wang, J. Gao, J. Sun, and Q. Fang (09/2020). "A non-bisphenol-a epoxy resin with high Tg derived from the bio-based protocatechuic acid: Synthesis and properties." In: *Polymer* 205.April, p. 122726. DOI: 10.1016/j.polymer.2020.122726.

Cheong, S., J. M. Clomburg, and R. Gonzalez (05/2016). "Energy- and carbon-efficient synthesis of functionalized small molecules in bacteria using non-decarboxylative Claisen condensation reactions." In: *Nature Biotechnology* 34.5, pp. 556–561. DOI: 10.1038/nbt.3505.

Choi, K. Y., D. Kim, W. J. Sul, J.-C. Chae, G. J. Zylstra, Y. M. Kim, and E. Kim (11/2005). "Molecular and biochemical analysis of phthalate and terephthalate degradation by Rhodococcus sp. strain DK17." In: *FEMS Microbiology Letters* 252.2, pp. 207–213. DOI: 10.1016/j.femsle.2005.08.045.

Chomczynski, P. and M. Rymaszewski (04/2006). "Alkaline polyethylene glycol-based method for direct PCR from bacteria, eukaryotic tissue samples, and whole blood." In: *BioTechniques* 40.4, pp. 454–458. DOI: 10.2144/000112149.

Crane, J. M. and L. L. Randall (04/2017). "The Sec System: Protein Export in *Escherichia coli*." In: *EcoSal Plus* 7.2. Ed. by S. T. Lovett and H. D. Bernstein. DOI: 10.1128/ecosalplus.ESP-0002-2017.

Crawford, R. L., J. W. Bromley, and P. E. Perkins-Olson (03/1979). "Catabolism of protocatechuate by Bacillus macerans." In: *Applied and Environmental Microbiology* 37.3, pp. 614–618. DOI: 10.1128/aem.37.3.614-618.1979.

Dagley, S., W. C. Evans, and D. W. Ribbons (11/1960). "New Pathways in the Oxidative Metabolism of Aromatic Compounds by Micro-Organisms." In: *Nature* 188.4750, pp. 560–566. DOI: 10.1038/188560a0.

Dalton, B., P. Bhagabati, J. De Micco, R. B. Padamati, and K. O'Connor (03/2022). "A Review on Biological Synthesis of the Biodegradable Polymers Polyhydroxyalkanoates and the Development of Multiple Applications." In: *Catalysts* 12.3, p. 319. DOI: 10.3390/catal12030319.

Davis, R., R. Kataria, F. Cerrone, T. Woods, S. Kenny, A. O'Donovan, M. Guzik, H. Shaikh, G. Duane, V. K. Gupta, M. G. Tuohy, R. B. Padamatti, E. Casey, and K. E. O'Connor (12/2013). "Conversion of grass biomass into fermentable sugars and its utilization for medium chain length polyhydroxyalkanoate (mcl-PHA) production by Pseudomonas strains." In: *Bioresource Technology* 150, pp. 202–209. DOI: 10.1016/j.biortech.2013.10.001.

De las Heras, A., C. A. Carreño, and V. de Lorenzo (12/2008). "Stable implantation of orthogonal sensor circuits in Gram-negative bacteria for environmental release." In: *Environmental Microbiology* 10.12, pp. 3305–3316. DOI: 10.1111/j.1462-2920.2008.01722.x.

Debuissy, T., E. Pollet, and L. Avérous (2016). "Synthesis of potentially biobased copolyesters based on adipic acid and butanediols: Kinetic study between 1,4- and 2,3-butanediol and their influence on crystallization and thermal properties." In: *Polymer* 99, pp. 204–213. DOI: 10.1016/j.polymer.2016.07.022.

De Castro, J. G., B. V. M. Rodrigues, R. Ricci, M. M. Costa, A. F. C. Ribeiro, F. R. Marciano, and A. O. Lobo (2016). "Designing a novel nanocomposite for bone tissue engineering using electrospun conductive PBAT/polypyrrole as a scaffold to direct nanohydroxyapatite electrodeposition." In: *RSC Advances* 6.39, pp. 32615–32623. DOI: 10.1039/C6RA00889E.

De Jong, E., A. Higson, P. Walsh, and M. Wellisch (2012). "Bio-based Chemicals: Value added products from biorefineries." In: *IEA Bioenergy, Task42 Biorefinery*, p. 36.

De Jong, H. (2022). "Reverse engineering of 1,4-butanediol metabolism in *Pseudomonas taiwanensis* for the bio-upcycling of plastic monomers with defined mixed culture." PhD thesis. Fachhochschule Aachen.

Deng, Y. and Y. Mao (10/2015). "Production of adipic acid by the native-occurring pathway in *Thermobifida fusca* B6." In: *Journal of Applied Microbiology* 119.4, pp. 1057–1063. DOI: 10.1111/jam.12905.

De Witt, J., P. Ernst, J. Gätgens, S. Noack, D. Hiller, B. Wynands, and N. Wierckx (01/2023). "Characterization and engineering of branched short-chain dicarboxylate metabolism in Pseudomonas reveals resistance to fungal 2-hydroxyparaconate." In: *Metabolic Engineering* 75, pp. 205–216. DOI: 10.1016/j.ymben.2022.12.008.

Dinsdale, A. E., G. Halket, A. Coorevits, A. Van Landschoot, H.-J. Busse, P. De Vos, and N. A. Logan (08/2011). "Emended descriptions of *Geobacillus thermoleovorans* and *Geobacillus thermocatenulatus*." In: *International Journal of Systematic and Evolutionary Microbiology* 61.8, pp. 1802–1810. DOI: 10.1099/ijs.0.025445-0.

Durante-Rodríguez, G., V. de Lorenzo, and P. I. Nikel (11/2018). "A Post-translational Metabolic Switch Enables Complete Decoupling of Bacterial Growth from Biopolymer Production in Engineered *Escherichia coli*." In: *ACS Synth. Biol.* 7.11, pp. 2686–2697. DOI: 10.1021/acssynbio.8b00345.

Eberlein, C., T. Baumgarten, S. Starke, and H. J. Heipieper (2018). "Immediate response mechanisms of Gram-negative solvent-tolerant bacteria to cope with environmental stress: cis-trans isomerization of unsaturated fatty acids and outer membrane vesicle secretion." In: *Applied Microbiology and Biotechnology* 102.6, pp. 2583–2593. DOI: 10.1007/s00253-018-8832-9.

Eberz, J., M. Doeker, Y. S. Ackermann, D. Schaffeld, N. Wierckx, and A. Jupke (04/2023). "Selective Separation of 4,4'-Methylenedianiline, Isophoronediamine and 2,4-Toluenediamine from Enzymatic Hydrolysis Solutions of Polyurethane." In: *Solvent Extraction and Ion Exchange* 41.3, pp. 358–373. DOI: 10.1080/07366299.2023.2193229.

El Seoud, O. A., K. Jedvert, M. Kostag, and S. Possidonio (06/2022). "Cellulose, chitin and silk: the cornerstones of green composites." In: *Emergent Materials* 5.3, pp. 785–810. DOI: 10.1007/s42247-021-00308-0.

Eling, B., Ž. Tomović, and V. Schädler (07/2020). "Current and Future Trends in Polyurethanes: An Industrial Perspective." In: *Macromolecular Chemistry and Physics* 221.14, p. 2000114. DOI: 10.1002/macp.202000114.

Ellis, L. D., N. A. Rorrer, K. P. Sullivan, M. Otto, J. E. McGeehan, Y. Román-Leshkov, N. Wierckx, and G. T. Beckham (2021). "Chemical and biological catalysis for plastics recycling and upcycling." In: *Nature Catalysis* 4.7, pp. 539–556. DOI: 10.1038/s41929-021-00648-4.

Escapa, I. F., V. Morales, V. P. Martino, E. Pollet, L. Avérous, J. L. García, and M. A. Prieto (03/2011). "Disruption of β-oxidation pathway in *Pseudomonas putida* KT2442 to produce new functionalized PHAs with thioester groups." In: *Applied Microbiology and Biotechnology* 89.5, pp. 1583–1598. DOI: 10.1007/s00253-011-3099-4.

Espinosa, M. J. C., A. C. Blanco, T. Schmidgall, A. K. Atanasoff-Kardjalieff, U. Kappelmeyer, D. Tischler, D. H. Pieper, H. J. Heipieper, and C. Eberlein (03/2020). "Toward biorecycling: isolation of a soil bacterium that grows on a polyurethane oligomer and monomer." In: *Frontiers in Microbiology* 11, p. 404. DOI: 10.3389/fmicb.2020.00404.

Farkas, V., M. Nagyházi, P. T. Anastas, J. Klankermayer, and R. Tuba (04/2023). "Making Persistent Plastics Degradable." In: *ChemSusChem*, pp. 1–23. DOI: 10.1002/cssc.202300553.

Fernández, C., E. Díaz, and J. L. García (06/2014). "Insights on the regulation of the phenylacetate degradation pathway from *Escherichia coli*." In: *Environmental Microbiology Reports* 6.3, pp. 239–250. DOI: 10.1111/1758-2229.12117.

Ferrández, A., J. L. García, and E. Díaz (04/2000). "Transcriptional regulation of the divergent *paa* catabolic operons for phenylacetic acid degradation in *Escherichia coli*." In: *Journal of Biological Chemistry* 275.16, pp. 12214–12222. DOI: 10.1074/jbc.275.16.12214.

Ferreira, F. V., L. S. Cividanes, R. F. Gouveia, and L. M. Lona (03/2019). "An overview on properties and applications of poly(butylene adipate-co-terephthalate)-PBAT based composites." In: *Polymer Engineering & Science* 59.s2, E7–E15. DOI: 10.1002/pen.24770.

Figurski, D. H. and D. R. Helinski (04/1979). "Replication of an origin-containing derivative of plasmid RK2 dependent on a plasmid function provided in trans." In: *Proceedings of the National Academy of Sciences* 76.4, pp. 1648–1652. DOI: 10.1073/pnas.76.4.1648.

Fischer, R., F. S. Bleichrodt, and U. C. Gerischer (10/2008). "Aromatic degradative pathways in *Acinetobacter baylyi* underlie carbon catabolite repression." In: *Microbiology* 154.10, pp. 3095–3103. DOI: 10.1099/mic.0.2008/016907-0.

Flower, D. R., A. C. North, and C. E. Sansom (10/2000). "The lipocalin protein family: structural and sequence overview." In: *Biochimica et Biophysica Acta (BBA) - Protein Structure and Molecular Enzymology* 1482.1-2, pp. 9–24. DOI: 10.1016/S0167-4838(00)00148-5.

Fojt, J., J. David, R. Přikryl, V. Řezáčová, and J. Kučerík (11/2020). "A critical review of the overlooked challenge of determining micro-bioplastics in soil." In: *Science of The Total Environment* 745, p. 140975. DOI: 10.1016/j.scitotenv.2020.140975.

Fonseca, P., F. de la Peña, and M. A. Prieto (11/2014). "A role for the regulator PsrA in the polyhydroxyalkanoate metabolism of *Pseudomonas putida* KT2440." In: *International Journal of Biological Macromolecules* 71, pp. 14–20. DOI: 10.1016/j.ijbiomac.2014.04.014.

Franden, M. A., L. N. Jayakody, W.-J. Li, N. J. Wagner, N. S. Cleveland, W. E. Michener, B. Hauer, L. M. Blank, N. Wierckx, J. Klebensberger, and G. T. Beckham (07/2018). "Engineering *Pseudomonas putida* KT2440 for efficient ethylene glycol utilization." In: *Metabolic Engineering* 48, pp. 197–207. DOI: 10.1016/j.ymben.2018.06.003.

Geyer, R., J. R. Jambeck, and K. L. Law (07/2017). "Production, use, and fate of all plastics ever made." In: *Science Advances* 3.7, e1700782. DOI: 10.1126/sciadv.1700782.

Geyer, R., B. Kuczenski, T. Zink, and A. Henderson (2016). "Common Misconceptions about Recycling." In: *Journal of Industrial Ecology* 20.5, pp. 1010–1017. DOI: 10.1111/jiec.12355.

Ghatge, S., Y. Yang, J. H. Ahn, and H. G. Hur (2020). "Biodegradation of polyethylene: a brief review." In: *Applied Biological Chemistry* 63.1. DOI: 10.1186/s13765-020-00511-3.

Gian, M., C. García-Velásquez, and Y. van der Meer (09/2022). "Comparative life cycle assessment of the biochemical and thermochemical production routes of biobased

terephthalic acid using *Miscanthus* in the Netherlands." In: *Cleaner Environmental Systems* 6.December 2021, p. 100085. DOI: 10.1016/j.cesys.2022.100085.

Gibson, D. G., L. Young, R.-Y. Chuang, J. C. Venter, C. A. Hutchison, and H. O. Smith (05/2009). "Enzymatic assembly of DNA molecules up to several hundred kilobases." In: *Nature Methods* 6.5, pp. 343–345. DOI: 10.1038/nmeth.1318.

Goodyear, C. (1844). *Improvment in India-Rubber Farbrics*.

Guzik, M. W., T. Nitkiewicz, M. Wojnarowska, M. Sołtysik, S. T. Kenny, R. P. Babu, M. Best, and K. E. O'Connor (11/2021). "Robust process for high yield conversion of non-degradable polyethylene to a biodegradable plastic using a chemo-biotechnological approach." In: *Waste Management* 135, pp. 60–69. DOI: 10.1016/j.wasman.2021.08.030.

Hai, T. A. P., M. Tessman, N. Neelakantan, A. A. Samoylov, Y. Ito, B. S. Rajput, N. Pourahmady, and M. D. Burkart (2021). "Renewable polyurethanes from sustainable biological precursors." In: *Biomacromolecules* 22.5, pp. 1770–1794. DOI: 10.1021/acs.biomac.0c01610.

Hanahan, D. (06/1983). "Studies on transformation of *Escherichia coli* with plasmids." In: *Journal of Molecular Biology* 166.4, pp. 557–580. DOI: 10.1016/S0022-2836(83)80284-8.

Harrison, F. H. and C. S. Harwood (03/2005). "The *pimFABCDE* operon from *Rhodopseudomonas palustris* mediates dicarboxylic acid degradation and participates in anaerobic benzoate degradation." In: *Microbiology* 151.3, pp. 727–736. DOI: 10.1099/mic.0.27731-0.

Hartmans, S., J. P. Smits, M. J. van der Werf, F. Volkering, and J. A. M. de Bont (11/1989). "Metabolism of Styrene Oxide and 2-Phenylethanol in the Styrene-Degrading Xanthobacter Strain 124X." In: *Applied and Environmental Microbiology* 55.11, pp. 2850–2855. DOI: 10.1128/aem.55.11.2850-2855.1989.

Harwood, C. S. and R. E. Parales (10/1996). "The β-ketoadipate pathway and the biology of self-identity." In: *Annual Review of Microbiology* 50.1, pp. 553–590. DOI: 10.1146/annurev.micro.50.1.553.

Heipieper, H. J., F. Meinhardt, and A. Segura (12/2003). "The cisâ€“trans isomerase of unsaturated fatty acids in Pseudomonas and Vibrio : biochemistry, molecular biology and physiological function of a unique stress adaptive mechanism." In: *FEMS Microbiology Letters* 229.1, pp. 1–7. DOI: 10.1016/S0378-1097(03)00792-4.

Heipieper, H. J., G. Neumann, S. Cornelissen, and F. Meinhardt (04/2007). "Solvent-tolerant bacteria for biotransformations in two-phase fermentation systems." In: *Applied Microbiology and Biotechnology* 74.5, pp. 961–973. DOI: 10.1007/s00253-006-0833-4.

Hensley, M. P., T. S. Gunasekera, J. A. Easton, T. K. Sigdel, S. A. Sugarbaker, L. Klingbeil, R. M. Breece, D. L. Tierney, and M. W. Crowder (2012). "Characterization of Zn(II)-responsive ribosomal proteins YkgM and L31 in E. coli." In: *Journal of Inorganic Biochemistry* 111, pp. 164–172. DOI: 10.1016/j.jinorgbio.2011.11.022.

Herrera, R., L. Franco, A. Rodríguez-Galán, and J. Puiggalí (12/2002). "Characterization and degradation behavior of poly(butylene adipate- co -terephthalate)s." In: *Journal*

of Polymer Science Part A: Polymer Chemistry 40.23, pp. 4141–4157. DOI: 10.1002/pola.10501.

Herrero, M., V. de Lorenzo, and K. N. Timmis (11/1990). "Transposon vectors containing non-antibiotic resistance selection markers for cloning and stable chromosomal insertion of foreign genes in gram-negative bacteria." In: *Journal of Bacteriology* 172.11, pp. 6557–6567. DOI: 10.1128/JB.172.11.6557-6567.1990.

Holden, M., M. Mayhew, D. Gallagher, and V. Vilker (01/2002). "Chorismate lyase: kinetics and engineering for stability." In: *Biochimica et Biophysica Acta (BBA) - Protein Structure and Molecular Enzymology* 1594.1, pp. 160–167. DOI: 10.1016/S0167-4838(01)00302-8.

Hopewell, J., R. Dvorak, and E. Kosior (2009). "Plastics recycling: Challenges and opportunities." In: *Philosophical Transactions of the Royal Society B: Biological Sciences* 364.1526, pp. 2115–2126. DOI: 10.1098/rstb.2008.0311.

Hou, L., D. Kumar, C. G. Yoo, I. Gitsov, and E. L. Majumder (02/2021). "Conversion and removal strategies for microplastics in wastewater treatment plants and landfills." In: *Chemical Engineering Journal* 406.Feb 2021, p. 126715. DOI: 10.1016/j.cej.2020.126715.

Idumah, C. I. and I. C. Nwuzor (11/2019). "Novel trends in plastic waste management." In: *SN Applied Sciences* 1.11, p. 1402. DOI: 10.1007/s42452-019-1468-2.

Ilves, H., R. Hõrak, and M. Kivisaar (09/2001). "Involvement of ςS in starvation-induced transposition of *Pseudomonas putida* transposon Tn4652." In: *Journal of Bacteriology* 183.18, pp. 5445–5448. DOI: 10.1128/JB.183.18.5445-5448.2001.

Jambeck, J. R., R. Geyer, C. Wilcox, T. R. Siegler, M. Perryman, A. Andrady, R. Narayan, and K. L. Law (02/2015). "Plastic waste inputs from land into the ocean." In: *Science* 347.6223, pp. 768–771. DOI: 10.1126/science.1260352.

Jayakody, L. N., C. W. Johnson, J. M. Whitham, R. J. Giannone, B. A. Black, N. S. Cleveland, D. M. Klingeman, W. E. Michener, J. L. Olstad, D. R. Vardon, R. C. Brown, S. D. Brown, R. L. Hettich, A. M. Guss, and G. T. Beckham (2018). "Thermochemical wastewater valorization: Via enhanced microbial toxicity tolerance." In: *Energy and Environmental Science* 11.6, pp. 1625–1638. DOI: 10.1039/c8ee00460a.

Jehanno, C., J. W. Alty, M. Roosen, S. De Meester, A. P. Dove, E. Y.-X. Chen, F. A. Leibfarth, and H. Sardon (03/2022). "Critical advances and future opportunities in upcycling commodity polymers." In: *Nature* 603.7903, pp. 803–814. DOI: 10.1038/s41586-021-04350-0.

Jha, R. K., N. Narayanan, N. Pandey, J. M. Bingen, T. L. Kern, C. W. Johnson, C. E. M. Strauss, G. T. Beckham, S. P. Hennelly, and T. Dale (04/2019). "Sensor-Enabled Alleviation of Product Inhibition in Chorismate Pyruvate-Lyase." In: *ACS Synthetic Biology* 8.4, pp. 775–786. DOI: 10.1021/acssynbio.8b00465.

Jian, J., Z. Xiangbin, and H. Xianbo (2020a). "An overview on synthesis, properties and applications of poly(butylene-adipate-co-terephthalate)–PBAT." In: *Advanced Industrial and Engineering Polymer Research* 3.1, pp. 19–26. DOI: 10.1016/j.aiepr.2020.01.001.

Jian, J., Z. Xiangbin, and H. Xianbo (01/2020b). "An overview on synthesis, properties and applications of poly(butylene-adipate-co-terephthalate)–PBAT." In: *Advanced*

Industrial and Engineering Polymer Research 3.1, pp. 19–26. DOI: 10.1016/j.aiepr.2020.01.001.

Jimenez, J. I., B. Minambres, J. L. Garcia, and E. Diaz (12/2002). "Genomic analysis of the aromatic catabolic pathways from *Pseudomonas putida* KT2440." In: *Environmental Microbiology* 4.12, pp. 824–841. DOI: 10.1046/j.1462-2920.2002.00370.x.

Kakkar, S. and S. Bais (03/2014). "A Review on Protocatechuic Acid and Its Pharmacological Potential." In: *ISRN Pharmacology* 2014, pp. 1–9. DOI: 10.1155/2014/952943.

Kalali, E. N., S. Lotfian, M. E. Shabestari, S. Khayatzadeh, C. Zhao, and H. Y. Nezhad (2023). "A critical review of the current progress of plastic waste recycling technology in structural materials." In: *Current Opinion in Green and Sustainable Chemistry* 40, p. 100763. DOI: 10.1016/j.cogsc.2023.100763.

Kallscheuer, N., J. Gätgens, M. Lübcke, J. Pietruszka, M. Bott, and T. Polen (03/2017). "Improved production of adipate with *Escherichia coli* by reversal of β-oxidation." In: *Applied Microbiology and Biotechnology* 101.6, pp. 2371–2382. DOI: 10.1007/s00253-016-8033-3.

Kang, Y., D. T. Nguyen, M. S. Son, and T. T. Hoang (06/2008). "The *Pseudomonas aeruginosa* PsrA responds to long-chain fatty acid signals to regulate the *fadBA5* β-oxidation operon." In: *Microbiology* 154.6, pp. 1584–1598. DOI: 10.1099/mic.0.2008/018135-0.

Kawashima, N., T. Yagi, and K. Kojima (09/2019). "How do bioplastics and fossil-based plastics play in a circular economy?" In: *Macromolecular Materials and Engineering* 304.9, p. 1900383. DOI: 10.1002/mame.201900383.

Keen, N., S. Tamaki, D. Kobayashi, and D. Trollinger (10/1988). "Improved broad-host-range plasmids for DNA cloning in Gram-negative bacteria." In: *Gene* 70.1, pp. 191–197. DOI: 10.1016/0378-1119(88)90117-5.

Kenny, S. T., J. N. Runic, W. Kaminsky, T. Woods, R. P. Babu, C. M. Keely, W. Blau, and K. E. O'Connor (10/2008). "Up-Cycling of PET (Polyethylene Terephthalate) to the Biodegradable Plastic PHA (Polyhydroxyalkanoate)." In: *Environmental Science & Technology* 42.20, pp. 7696–7701. DOI: 10.1021/es801010e.

Khandare, S. D., D. R. Chaudhary, and B. Jha (04/2021). "Marine bacterial biodegradation of low-density polyethylene (LDPE) plastic." In: *Biodegradation* 32.2, pp. 127–143. DOI: 10.1007/s10532-021-09927-0.

Kikuchi, Y., K. Tsujimoto, and O. Kurahashi (02/1997). "Mutational analysis of the feedback sites of phenylalanine-sensitive 3-deoxy-D-arabino-heptulosonate-7-phosphate synthase of *Escherichia coli*." In: *Applied and Environmental Microbiology* 63.2, pp. 761–762. DOI: 10.1128/aem.63.2.761-762.1997.

Kim, H. T., J. K. Kim, H. G. Cha, M. J. Kang, H. S. Lee, T. U. Khang, E. J. Yun, D.-H. Lee, B. K. Song, S. J. Park, J. C. Joo, and K. H. Kim (12/2019). "Biological valorization of poly(ethylene terephthalate) monomers for upcycling waste PET." In: *ACS Sustainable Chemistry & Engineering* 7.24, pp. 19396–19406. DOI: 10.1021/acssuschemeng.9b03908.

Kint, D. and S. Muñoz-Guerra (05/1999). "A review on the potential biodegradability of poly(ethylene terephthalate)." In: *Polymer International* 48.5, pp. 346–352. DOI: 10.1002/(SICI)1097-0126(199905)48:5<346::AID-PI156>3.0.CO;2-N.

Kleeberg, I., C. Hetz, R. M. Kroppenstedt, R.-J. Müller, and W.-D. Deckwer (05/1998). "Biodegradation of Aliphatic-Aromatic Copolyesters by Thermomonospora fusca and Other Thermophilic Compost Isolates." In: *Applied and Environmental Microbiology* 64.5, pp. 1731–1735. DOI: 10.1128/AEM.64.5.1731-1735.1998.

Knorr, S., M. Sinn, D. Galetskiy, R. M. Williams, C. Wang, N. Müller, O. Mayans, D. Schleheck, and J. S. Hartig (2018). "Widespread bacterial lysine degradation proceeding via glutarate and L -2-hydroxyglutarate." In: *Nature Communications*, pp. 2–11. DOI: 10.1038/s41467-018-07563-6.

Knott, B. C., E. Erickson, M. D. Allen, J. E. Gado, R. Graham, F. L. Kearns, I. Pardo, E. Topuzlu, J. J. Anderson, H. P. Austin, G. Dominick, C. W. Johnson, N. A. Rorrer, C. J. Szostkiewicz, V. Copié, C. M. Payne, H. L. Woodcock, B. S. Donohoe, G. T. Beckham, and J. E. McGeehan (10/2020). "Characterization and engineering of a two-enzyme system for plastics depolymerization." In: *Proceedings of the National Academy of Sciences* 117.41, pp. 25476–25485. DOI: 10.1073/pnas.2006753117.

Köbbing, S. (2020). "Development of synthetic biology tools for *Pseudomonas putida*." PhD thesis. RWTH Aachen.

Köhler, K. A., C. Rückert, S. Schatschneider, F.-J. Vorhölter, R. Szczepanowski, L. M. Blank, K. Niehaus, A. Goesmann, A. Pühler, J. Kalinowski, and A. Schmid (12/2013). "Complete genome sequence of Pseudomonas sp. strain VLB120 a solvent tolerant, styrene degrading bacterium, isolated from forest soil." In: *Journal of Biotechnology* 168.4, pp. 729–730. DOI: 10.1016/j.jbiotec.2013.10.016.

Kohlstedt, M., S. Starck, N. Barton, J. Stolzenberger, M. Selzer, K. Mehlmann, R. Schneider, D. Pleissner, J. Rinkel, J. S. Dickschat, J. Venus, J. B.J.H. van Duuren, and C. Wittmann (05/2018). "From lignin to nylon: cascaded chemical and biochemical conversion using metabolically engineered *Pseudomonas putida*." In: *Metabolic Engineering* 47, pp. 279–293. DOI: 10.1016/j.ymben.2018.03.003.

Koller, J., U. Baumer, and D. Mania (01/2001). "High-tech in the middle Palaeolithic: Neandertal-manufactured pitch identified." In: *European Journal of Archaeology* 4.3, pp. 385–397. DOI: 10.1179/eja.2001.4.3.385.

Koller, M. and A. Mukherjee (02/2022). "A New Wave of Industrialization of PHA Biopolyesters." In: *Bioengineering* 9.2, p. 74. DOI: 10.3390/bioengineering9020074.

Krieger, E. and G. Vriend (10/2014). "YASARA View—molecular graphics for all devices—from smartphones to workstations." In: *Bioinformatics* 30.20, pp. 2981–2982. DOI: 10.1093/bioinformatics/btu426.

Krüger, R., S. A. Rakowski, and M. Filutowicz (04/2014). "Participating elements in the replication of iteron-containing plasmids." In: *Plasmid Biology*. Ed. by B. Funnell and G. Phillipps. Washington, DC, USA: ASM Press. Chap. 2, pp. 23–45. DOI: 10.1128/9781555817732.ch2.

Kruyer, N. S. and P. Peralta-Yahya (06/2017). *Metabolic engineering strategies to bio-adipic acid production*. DOI: 10.1016/j.copbio.2017.03.006.

Kumar, A., N. von Wolff, M. Rauch, Y.-Q. Zou, G. Shmul, Y. Ben-David, G. Leitus, L. Avram, and D. Milstein (08/2020). "Hydrogenative depolymerization of nylons." In: *Journal of the American Chemical Society* 142.33, pp. 14267–14275. DOI: 10.1021/jacs.0c05675.

Kurihara, S., S. Oda, K. Kato, H. G. Kim, T. Koyanagi, H. Kumagai, and H. Suzuki (02/2005). "A novel putrescine utilization pathway involves γ-glutamylated intermediates of *Escherichia coli* K-12." In: *Journal of Biological Chemistry* 280.6, pp. 4602–4608. DOI: 10.1074/jbc.M411114200.

Kyrikou, I. and D. Briassoulis (2007). "Biodegradation of agricultural plastic films: A critical review." In: *Journal of Polymers and the Environment* 15.2, pp. 125–150. DOI: 10.1007/s10924-007-0053-8.

La Mantia, F., L. Botta, M. Morreale, and R. Scaffaro (11/2011). "Effect of small amounts of poly(lactic acid) on the recycling of poly(ethylene terephthalate) bottles." In: *Polymer Degradation and Stability* 97.1, pp. 21–24. DOI: 10.1016/j.polymdegradstab.2011.10.017.

Labib, M., J. Görtz, C. Brüsseler, N. Kallscheuer, J. Gätgens, A. Jupke, J. Marienhagen, and S. Noack (02/2021). "Metabolic and Process Engineering for Microbial Production of Protocatechuate from Xylose with *Corynebacterium glutamicum*." In: *bioRxiv*, p. 2021.02.12.430943. DOI: 10.1101/2021.02.12.430943.

Lapa, H. M. (2023). "p -Xylene Oxidation to Terephthalic Acid : New Trends p -Xylene Oxidation to Terephthalic Acid : New Trends." In.

Larrañaga, A. and E. Lizundia (12/2019). "A review on the thermomechanical properties and biodegradation behaviour of polyesters." In: *European Polymer Journal* 121, p. 109296. DOI: 10.1016/j.eurpolymj.2019.109296.

Lau, W. W. Y., Y. Shiran, R. M. Bailey, E. Cook, M. R. Stuchtey, J. Koskella, C. A. Velis, L. Godfrey, J. Boucher, M. B. Murphy, R. C. Thompson, E. Jankowska, A. Castillo Castillo, T. D. Pilditch, B. Dixon, L. Koerselman, E. Kosior, E. Favoino, J. Gutberlet, S. Baulch, M. E. Atreya, D. Fischer, K. K. He, M. M. Petit, U. R. Sumaila, E. Neil, M. V. Bernhofen, K. Lawrence, and J. E. Palardy (09/2020). "Evaluating scenarios toward zero plastic pollution." In: *Science* 369.6510, pp. 1455–1461. DOI: 10.1126/science.aba9475.

Law, K. L. and C. M. Rochman (07/2023). "Large-scale collaborations uncover global extent of plastic pollution." In: *Nature* 619.7969, pp. 254–255. DOI: 10.1038/d41586-023-02175-7.

Law, K. L., N. Starr, T. R. Siegler, J. R. Jambeck, N. J. Mallos, and G. H. Leonard (10/2020). "The United States' contribution of plastic waste to land and ocean." In: *Science Advances* 6.44. DOI: 10.1126/sciadv.abd0288.

Lebreton, L., B. Slat, F. Ferrari, B. Sainte-Rose, J. Aitken, R. Marthouse, S. Hajbane, S. Cunsolo, A. Schwarz, A. Levivier, K. Noble, P. Debeljak, H. Maral, R. Schoeneich-Argent, R. Brambini, and J. Reisser (03/2018). "Evidence that the Great Pacific Garbage Patch is rapidly accumulating plastic." In: *Scientific Reports 2018 8:1* 8.1, pp. 1–15. DOI: 10.1038/s41598-018-22939-w.

Lee, S. Y., H. H. Wong, J.-i. Choi, S. H. Lee, S. C. Lee, and C. S. Han (05/2000). "Production of medium-chain-length polyhydroxyalkanoates by high-cell-density cultivation of *Pseudomonas putida* under phosphorus limitation." In: *Biotechnology and Bioengineering* 68.4, pp. 466–470. DOI: 10.1002/(SICI)1097-0290(20000520)68:4<466::AID-BIT12>3.0.CO;2-T.

Lenzen, C., B. Wynands, M. Otto, J. Bolzenius, P. Mennicken, L. M. Blank, and N. Wierckx (06/2019). "High-yield production of 4-hydroxybenzoate from glucose or glycerol by an engineered *Pseudomonas taiwanensis* VLB120." In: *Frontiers in Bioengineering and Biotechnology* 7. DOI: 10.3389/fbioe.2019.00130.

Li, J. and B.-C. Ye (01/2021). "Metabolic engineering of *Pseudomonas putida* KT2440 for high-yield production of protocatechuic acid." In: *Bioresource Technology* 319, p. 124239. DOI: 10.1016/j.biortech.2020.124239.

Li, W.-J., L. N. Jayakody, M. A. Franden, M. Wehrmann, T. Daun, B. Hauer, L. M. Blank, G. T. Beckham, J. Klebensberger, and N. Wierckx (10/2019). "Laboratory evolution reveals the metabolic and regulatory basis of ethylene glycol metabolism by *Pseudomonas putida* KT2440." In: *Environmental Microbiology* 21.10, pp. 3669–3682. DOI: 10.1111/1462-2920.14703.

Li, W.-J., T. Narancic, S. T. Kenny, P.-J. Niehoff, K. O'Connor, L. M. Blank, and N. Wierckx (03/2020). "Unraveling 1,4-butanediol metabolism in *Pseudomonas putida* KT2440." In: *Frontiers in Microbiology* 11, p. 382. DOI: 10.3389/fmicb.2020.00382.

Li, Y., J. Li, B. Qian, L. Cheng, S. Xu, and R. Wang (2018). "*de novo* biosynthesis of p-coumaric acid in E. Coli with a trans-Cinnamic Acid 4-Hydroxylase from the Amaryllidaceae Plant Lycoris aurea." In: *Molecules* 23.12, pp. 1–19. DOI: 10.3390/molecules23123185.

Lieder, S., P. I. Nikel, V. de Lorenzo, and R. Takors (12/2015). "Genome reduction boosts heterologous gene expression in *Pseudomonas putida*." In: *Microbial Cell Factories* 14.1, p. 23. DOI: 10.1186/s12934-015-0207-7.

Lilleorg, S., K. Reier, J. Remme, and A. Liiv (04/2017). "The Intersubunit Bridge B1b of the Bacterial Ribosome Facilitates Initiation of Protein Synthesis and Maintenance of Translational Fidelity." In: *Journal of Molecular Biology* 429.7, pp. 1067–1080. DOI: 10.1016/j.jmb.2017.02.015.

Ling, C., S. Shi, W. Hou, and Z. Yan (03/2019). "Separation of waste polyester/cotton blended fabrics by phosphotungstic acid and preparation of terephthalic acid." In: *Polymer Degradation and Stability* 161, pp. 157–165. DOI: 10.1016/j.polymdegradstab.2019.01.022.

Linger, J. G., D. R. Vardon, M. T. Guarnieri, E. M. Karp, G. B. Hunsinger, M. A. Franden, C. W. Johnson, G. Chupka, T. J. Strathmann, P. T. Pienkos, and G. T. Beckham (08/2014). "Lignin valorization through integrated biological funneling and chemical catalysis." In: *Proceedings of the National Academy of Sciences* 111.33, pp. 12013–12018. DOI: 10.1073/pnas.1410657111.

Liu, H. and T. Lu (05/2015). "Autonomous production of 1,4-butanediol via a *de novo* biosynthesis pathway in engineered *Escherichia coli*." In: *Metabolic Engineering* 29, pp. 135–141. DOI: 10.1016/j.ymben.2015.03.009.

Liu, J., J. He, R. Xue, B. Xu, X. Qian, F. Xin, L. M. Blank, J. Zhou, R. Wei, W. Dong, and M. Jiang (05/2021). "Biodegradation and up-cycling of polyurethanes: Progress, challenges, and prospects." In: *Biotechnology Advances* 48.December 2020, p. 107730. DOI: 10.1016/j.biotechadv.2021.107730.

Liu, J., C.-g. Meng, S. Liu, J. Kan, and C.-h. Jin (02/2017). "Preparation and characterization of protocatechuic acid grafted chitosan films with antioxidant activity." In: *Food Hydrocolloids* 63, pp. 457–466. DOI: 10.1016/j.foodhyd.2016.09.035.

Liu, S., T. Narancic, J.-L. Tham, and K. E. O'Connor (03/2023). "β-oxidation–polyhydroxyalkanoates synthesis relationship in *Pseudomonas putida* KT2440 revisited." In: *Applied Microbiology and Biotechnology* 107.5-6, pp. 1863–1874. DOI: 10.1007/s00253-023-12413-7.

Loeschcke, A. and S. Thies (08/2015). "*Pseudomonas putida*—a versatile host for the production of natural products." In: *Applied Microbiology and Biotechnology* 99.15, pp. 6197–6214. DOI: 10.1007/s00253-015-6745-4.

Madhuri Indurthi, S., H.-T. Chou, and C.-D. Lu (05/2016). "Molecular characterization of lysR-lysXE, gcdR-gcdHG and amaR-amaAB operons for lysine export and catabolism: a comprehensive lysine catabolic network in *Pseudomonas aeruginosa* PAO1." In: *Microbiology* 162.5, pp. 876–888. DOI: 10.1099/mic.0.000277.

Magnin, A., E. Pollet, V. Phalip, and L. Avérous (03/2020). "Evaluation of biological degradation of polyurethanes." In: *Biotechnology Advances* 39, p. 107457. DOI: 10.1016/j.biotechadv.2019.107457.

Mancini, E., S. S. Mansouri, K. V. Gernaey, and J. Luo (2019). "Technology From second generation feed-stocks to innovative fermentation and downstream techniques for succinic acid production." In: *Critical Reviews in Environmental Science and Technology* 0.0, pp. 1–45. DOI: 10.1080/10643389.2019.1670530.

Maqsood, T., J. Dai, Y. Zhang, M. Guang, and B. Li (10/2021). "Pyrolysis of plastic species: A review of resources and products." In: *Journal of Analytical and Applied Pyrolysis* 159.August, p. 105295. DOI: 10.1016/j.jaap.2021.105295.

Martínez-García, E. and V. de Lorenzo (10/2011). "Engineering multiple genomic deletions in Gram-negative bacteria: analysis of the multi-resistant antibiotic profile of *Pseudomonas putida* KT2440." In: *Environmental Microbiology* 13.10, pp. 2702–2716. DOI: 10.1111/j.1462-2920.2011.02538.x.

Martínez-Garćía, E., T. Aparicio, A. Goñi-Moreno, S. Fraile, and V. De Lorenzo (01/2015). "SEVA 2.0: An update of the Standard European Vector Architecture for de-/re-construction of bacterial functionalities." In: *Nucleic Acids Research* 43.D1, pp. D1183–D1189. DOI: 10.1093/nar/gku1114.

Maslowska, K. H., K. Makiela-dzbenska, and I. J. Fijalkowska (2019). "Review The SOS System : A Complex and Tightly Regulated Response to DNA Damage." In: 384.November 2018, pp. 368–384. DOI: 10.1002/em.22267.

Mengers, H. G., N. Guntermann, W. Graf von Westarp, A. Jupke, J. Klankermayer, L. M. Blank, W. Leitner, and D. Rother (04/2023). "Three Sides of the Same Coin: Combining Microbial, Enzymatic, and Organometallic Catalysis for Integrated Conversion of Renewable Carbon Sources." In: *Chemie Ingenieur Technik* 95.4, pp. 485–490. DOI: 10.1002/cite.202200169.

Merchan, A. L., T. Fischöder, J. Hee, M. S. Lehnertz, O. Osterthun, S. Pielsticker, J. Schleier, T. Tiso, L. M. Blank, J. Klankermayer, R. Kneer, P. Quicker, G. Walther, and R. Palkovits (2022). "Chemical recycling of bioplastics: technical opportunities

to preserve chemical functionality as path towards a circular economy." In: *Green Chemistry* 24.24, pp. 9428–9449. DOI: 10.1039/D2GC02244C.

Meys, R., F. Frick, S. Westhues, A. Sternberg, J. Klankermayer, and A. Bardow (11/2020). "Towards a circular economy for plastic packaging wastes – the environmental potential of chemical recycling." In: *Resources, Conservation and Recycling* 162, p. 105010. DOI: 10.1016/j.resconrec.2020.105010.

Meys, R., A. Kätelhön, M. Bachmann, B. Winter, C. Zibunas, S. Suh, and A. Bardow (10/2021). "Achieving net-zero greenhouse gas emission plastics by a circular carbon economy." In: *Science* 374.6563, pp. 71–76. DOI: 10.1126/science.abg9853.

Mezzina, M. P., M. T. Manoli, M. A. Prieto, and P. I. Nikel (11/2020). "Engineering native and synthetic pathways in *Pseudomonas putida* for the production of tailored polyhydroxyalkanoates." In: *Biotechnology Journal*, p. 2000165. DOI: 10.1002/biot.202000165.

Mezzina, M. P., M. T. Manoli, M. A. Prieto, and P. I. Nikel (2021). "Engineering Native and Synthetic Pathways in *Pseudomonas putida* for the Production of Tailored Polyhydroxyalkanoates." In: *Biotechnology Journal* 16.3. DOI: 10.1002/biot.202000165.

Mi, J., A. Sydow, F. Schempp, D. Becher, H. Schewe, J. Schrader, and M. Buchhaupt (08/2016). "Investigation of plasmid-induced growth defect in *Pseudomonas putida*." In: *Journal of Biotechnology* 231, pp. 167–173. DOI: 10.1016/j.jbiotec.2016.06.001.

Mileva, D., D. Tranchida, and M. Gahleitner (2018). "Designing polymer crystallinity: An industrial perspective." In: *Polymer Crystallization* 1.2, pp. 1–16. DOI: 10.1002/pcr2.10009.

Millican, J. M. and S. Agarwal (05/2021). "Plastic Pollution: A Material Problem?" In: *Macromolecules* 54.10, pp. 4455–4469. DOI: 10.1021/acs.macromol.0c02814.

Mirdita, M., K. Schütze, Y. Moriwaki, L. Heo, S. Ovchinnikov, and M. Steinegger (06/2022). "ColabFold: making protein folding accessible to all." In: *Nature Methods* 19.6, pp. 679–682. DOI: 10.1038/s41592-022-01488-1.

Montazer, Z., M. B. Habibi Najafi, and D. B. Levin (01/2020). "Challenges with Verifying Microbial Degradation of Polyethylene." In: *Polymers* 12.1, p. 123. DOI: 10.3390/polym12010123.

Mozejko-Ciesielska, J., T. Pokoj, and S. Ciesielski (2018). "Transcriptome remodeling of *Pseudomonas putida* KT2440 during mcl-PHAs synthesis: effect of different carbon sources and response to nitrogen stress." In: *Journal of Industrial Microbiology and Biotechnology* 45.6, pp. 433–446. DOI: 10.1007/s10295-018-2042-4.

Mueller, W. F. (1962). "The Origins of the Basic Inventions Underlying Du Pont's Major Product and Process Innovations." In: *The Rate and Direction of Inventive Activity: Economic and Social Factors*. Princeton University Press, pp. 323–358.

Narancic, T., F. Cerrone, N. Beagan, and K. E. O'Connor (2020). "Recent Advances in Bioplastics: Application and Biodegradation." In: *Polymers* 12.4, p. 920. DOI: 10.3390/polym12040920.

Narancic, T., M. Salvador, G. M. Hughes, N. Beagan, U. Abdulmutalib, S. T. Kenny, H. Wu, M. Saccomanno, J. Um, K. E. O'Connor, and J. I. Jiménez (01/2021). "Genome analysis of the metabolically versatile *Pseudomonas umsongensis* GO16: the

genetic basis for PET monomer upcycling into polyhydroxyalkanoates." In: *Microbial Biotechnology*, pp. 1751–7915. DOI: 10.1111/1751-7915.13712.

Narancic, T., S. Verstichel, S. Reddy Chaganti, L. Morales-Gamez, S. T. Kenny, B. De Wilde, R. Babu Padamati, and K. E. O'Connor (09/2018). "Biodegradable Plastic Blends Create New Possibilities for End-of-Life Management of Plastics but They Are Not a Panacea for Plastic Pollution." In: *Environmental Science and Technology* 52.18, pp. 10441–10452. DOI: 10.1021/acs.est.8b02963.

Nayak, S. K. (11/2010). "Biodegradable PBAT/Starch Nanocomposites." In: *Polymer-Plastics Technology and Engineering* 49.14, pp. 1406–1418. DOI: 10.1080/03602559.2010.496397.

Neaţu, F., G. Culică, M. Florea, V. I. Parvulescu, and F. Cavani (11/2016). "Synthesis of Terephthalic Acid by p-Cymene Oxidation using Oxygen: Toward a More Sustainable Production of Bio-Polyethylene Terephthalate." In: *ChemSusChem* 9.21, pp. 3102–3112. DOI: 10.1002/cssc.201600718.

Nelson, K. E., C. Weinel, I. T. Paulsen, R. J. Dodson, H. Hilbert, V. A. P. Martins dos Santos, D. E. Fouts, S. R. Gill, M. Pop, M. Holmes, L. Brinkac, M. Beanan, R. T. DeBoy, S. Daugherty, J. Kolonay, R. Madupu, W. Nelson, O. White, J. Peterson, H. Khouri, I. Hance, P. C. Lee, E. Holtzapple, D. Scanlan, K. Tran, A. Moazzez, T. Utterback, M. Rizzo, K. Lee, D. Kosack, D. Moestl, H. Wedler, J. Lauber, D. Stjepandic, J. Hoheisel, M. Straetz, S. Heim, C. Kiewitz, J. Eisen, K. N. Timmis, A. Dusterhoft, B. Tummler, and C. M. Fraser (12/2002). "Complete genome sequence and comparative analysis of the metabolically versatile *Pseudomonas putida* KT2440." In: *Environmental Microbiology* 4.12, pp. 799–808. DOI: 10.1046/j.1462-2920.2002.00366.x.

Nelson, T. F., S. C. Remke, H.-P. E. Kohler, K. McNeill, and M. Sander (01/2020). "Quantification of Synthetic Polyesters from Biodegradable Mulch Films in Soils." In: *Environmental Science & Technology* 54.1, pp. 266–275. DOI: 10.1021/acs.est.9b05863.

Nghiem, N. P., S. Kleff, and S. Schwegmann (2017). "Succinic Acid : Technology Development and Commercialization." In: pp. 1–14. DOI: 10.3390/fermentation3020026.

Nguyen, D. M. C., D. J. Seo, K. Y. Kim, R. D. Park, D. H. Kim, Y. S. Han, T. H. Kim, and W. J. Jung (06/2013). "Nematicidal activity of 3,4-dihydroxybenzoic acid purified from Terminalia nigrovenulosa bark against Meloidogyne incognita." In: *Microbial Pathogenesis* 59-60, pp. 52–59. DOI: 10.1016/j.micpath.2013.04.005.

Nijkamp, K., R. G. M. Westerhof, H. Ballerstedt, J. A. M. de Bont, and J. Wery (03/2007). "Optimization of the solvent-tolerant *Pseudomonas putida* S12 as host for the production of p-coumarate from glucose." In: *Applied Microbiology and Biotechnology* 74.3, pp. 617–624. DOI: 10.1007/s00253-006-0703-0.

Nikel, P. I. and V. de Lorenzo (01/2013). "Implantation of unmarked regulatory and metabolic modules in Gram-negative bacteria with specialised mini-transposon delivery vectors." In: *Journal of Biotechnology* 163.2, pp. 143–154. DOI: 10.1016/j.jbiotec.2012.05.002.

Nikel, P. I. and V. de Lorenzo (11/2018). "*Pseudomonas putida* as a functional chassis for industrial biocatalysis: From native biochemistry to trans-metabolism." In: *Metabolic Engineering* 50, pp. 142–155. DOI: 10.1016/j.ymben.2018.05.005.

Nikel, P. I., E. Martínez-García, and V. de Lorenzo (05/2014). "Biotechnological domestication of *Pseudomonads* using synthetic biology." In: *Nature Reviews Microbiology* 12.5, pp. 368–379. DOI: 10.1038/nrmicro3253.

Nikodinovic, J., S. T. Kenny, R. P. Babu, T. Woods, W. J. Blau, and K. E. O'Connor (09/2008). "The conversion of BTEX compounds by single and defined mixed cultures to medium-chain-length polyhydroxyalkanoate." In: *Applied Microbiology and Biotechnology* 80.4, pp. 665–673. DOI: 10.1007/s00253-008-1593-0.

Nurk, A., A. Tamm, R. Hôrak, and M. Kivisaar (05/1993). "In-vivo-generated fusion promoters in *Pseudomonas putida*." In: *Gene* 127.1, pp. 23–29. DOI: 10.1016/0378-1119(93)90612-7.

Oehlmann, J., U. Schulte-Oehlmann, W. Kloas, O. Jagnytsch, I. Lutz, K. O. Kusk, L. Wollenberger, E. M. Santos, G. C. Paull, K. J. VanLook, and C. R. Tyler (2009). "A critical analysis of the biological impacts of plasticizers on wildlife." In: *Philosophical Transactions of the Royal Society B: Biological Sciences* 364.1526, pp. 2047–2062. DOI: 10.1098/rstb.2008.0242.

Okada, M. (02/2002). "Chemical syntheses of biodegradable polymers." In: *Progress in Polymer Science* 27.1, pp. 87–133. DOI: 10.1016/S0079-6700(01)00039-9.

Okino, S., R. Noburyu, and M. Suda (2008). "An efficient succinic acid production process in a metabolically engineered *Corynebacterium glutamicum* strain." In: pp. 459–464. DOI: 10.1007/s00253-008-1668-y.

Okoffo, E. D., S. O'Brien, J. W. O'Brien, B. J. Tscharke, and K. V. Thomas (2019). "Wastewater treatment plants as a source of plastics in the environment: a review of occurrence, methods for identification, quantification and fate." In: *Environmental Science: Water Research & Technology* 5.11, pp. 1908–1931. DOI: 10.1039/C9EW00428A.

Ornston, L. N. and D. Parke (1976). "Properties of an inducible uptake system for β-ketoadipate in *Pseudomonas putida*." In: *Journal of Biotechnology* 125.2, pp. 475–488.

Ostle, C., R. C. Thompson, D. Broughton, L. Gregory, M. Wootton, and D. G. Johns (04/2019). "The rise in ocean plastics evidenced from a 60-year time series." In: *Nature Communications* 10.1, p. 1622. DOI: 10.1038/s41467-019-09506-1.

Otto, M., B. Wynands, C. Lenzen, M. Filbig, L. M. Blank, and N. Wierckx (11/2019). "Rational engineering of phenylalanine accumulation in *Pseudomonas taiwanensis* to enable high-yield production of trans-cinnamate." In: *Frontiers in Bioengineering and Biotechnology* 7. DOI: 10.3389/fbioe.2019.00312.

Otto, M., B. Wynands, J. Marienhagen, L. M. Blank, and N. Wierckx (11/2020). "Benzoate synthesis from glucose or glycerol using engineered *Pseudomonas taiwanensis*." In: *Biotechnology Journal* 15.11, p. 2000211. DOI: 10.1002/biot.202000211.

Parales, R. E. and C. S. Harwood (1993). "Regulation of the *pcaIJ* genes for aromatic acid degradation in *Pseudomonas putida*." In: *Journal of Bacteriology* 175.18, pp. 5829–5838. DOI: 10.1128/JB.175.18.5829-5838.1993.

Pardo, I., R. K. Jha, R. E. Bermel, F. Bratti, M. Gaddis, E. McIntyre, W. Michener, E. L. Neidle, T. Dale, G. T. Beckham, and C. W. Johnson (11/2020). "Gene amplification, laboratory evolution, and biosensor screening reveal MucK as a terephthalic acid transporter in *Acinetobacter baylyi* ADP1." In: *Metabolic Engineering* 62, pp. 260–274. DOI: 10.1016/j.ymben.2020.09.009.

Parke, D., M. A. Garcia, and L. N. Ornston (10/2001). "cloning and genetic characterization of *dca* genes required for β-oxidation of straight-chain dicarboxylic acids in *Acinetobacter* sp. strain ADP1." In: *Applied and Environmental Microbiology* 67.10, pp. 4817–4827. DOI: 10.1128/AEM.67.10.4817-4827.2001.

Parvin, F. and S. M. Tareq (06/2021). "Impact of landfill leachate contamination on surface and groundwater of Bangladesh: a systematic review and possible public health risks assessment." In: *Applied Water Science* 11.6, p. 100. DOI: 10.1007/s13201-021-01431-3.

Pavlacky, D., C. Vetter, and V. J. Gelling (10/2013). "Thermosetting Polymers." In: *Environmental Degradation of Advanced and Traditional Engineering Materials*. CRC Press, pp. 397–397. DOI: 10.1201/b15568-32.

Peek, J., J. Roman, G. R. Moran, and D. Christendat (01/2017). "Structurally diverse dehydroshikimate dehydratase variants participate in microbial quinate catabolism." In: *Molecular Microbiology* 103.1, pp. 39–54. DOI: 10.1111/mmi.13542.

Pereira da Silva, J. S., J. M. Farias da Silva, B. G. Soares, and S. Livi (11/2017). "Fully biodegradable composites based on poly(butylene adipate-co-terephthalate)/peach palm trees fiber." In: *Composites Part B: Engineering* 129, pp. 117–123. DOI: 10.1016/j.compositesb.2017.07.088.

Pham, V. T. K., H. Rediers, M. G. K. Ghequire, H. H. Nguyen, R. De Mot, J. Vanderleyden, and S. Spaepen (04/2017). "The plant growth-promoting effect of the nitrogen-fixing endophyte Pseudomonas stutzeri A15." In: *Archives of Microbiology* 199.3, pp. 513–517. DOI: 10.1007/s00203-016-1332-3.

PlasticsEurope (2006). *The Compelling Facts About Plastics*. Tech. rep.

PlasticsEurope (2019). *Plastics - the Facts 2019*. Tech. rep. Brussels.

PlasticsEurope (2022). *Plastics – the Facts 2022*. Tech. rep. October. Brussels.

Polen, T., M. Spelberg, and M. Bott (08/2013). "Toward biotechnological production of adipic acid and precursors from biorenewables." In: *Journal of Biotechnology* 167.2, pp. 75–84. DOI: 10.1016/j.jbiotec.2012.07.008.

Preston, G. M. (06/2004). "Plant perceptions of plant growth-promoting Pseudomonas." In: *Philosophical Transactions of the Royal Society of London. Series B: Biological Sciences* 359.1446, pp. 907–918. DOI: 10.1098/rstb.2003.1384.

Prieto, A., I. F. Escapa, V. Martínez, N. Dinjaski, C. Herencias, F. de la Peña, N. Tarazona, and O. Revelles (02/2016). "A holistic view of polyhydroxyalkanoate metabolism in *Pseudomonas putida*." In: *Environmental Microbiology* 18.2, pp. 341–357. DOI: 10.1111/1462-2920.12760.

Qin, D. and J. Dong (03/2023). "Multi-Level Optimization and Strategies in Microbial Biotransformation of Nature Products." In: *Molecules* 28.6, p. 2619. DOI: 10.3390/molecules28062619.

RameshKumar, S., P. Shaiju, K. E. O'Connor, and R. B. P (02/2020). "Bio-based and biodegradable polymers - State-of-the-art, challenges and emerging trends." In: *Current Opinion in Green and Sustainable Chemistry* 21, pp. 75–81. DOI: 10.1016/j.cogsc.2019.12.005.

Reifsteck, R. A., S. Zhai, M. Gausmann, H. Ballerstedt, T. Tiso, L. M. Blank, and A. Jupke (08/2023). "Techno-Economic Comparison of Bio-Cycling Processes for Mixed Plastic Waste Valorization." In: *Chemie Ingenieur Technik* 95.8, pp. 1247–1258. DOI: 10.1002/cite.202300021.

Revelles, O., M. Espinosa-urgel, T. Fuhrer, U. Sauer, and J. L. Ramos (2005). "Multiple and Interconnected Pathways for L -Lysine Catabolism in *Pseudomonas putida* KT2440." In: 187.21, pp. 7500–7510. DOI: 10.1128/JB.187.21.7500.

Reynolds, D. and M. Kollef (12/2021). "The Epidemiology and Pathogenesis and Treatment of *Pseudomonas aeruginosa* Infections: An Update." In: *Drugs* 81.18, pp. 2117–2131. DOI: 10.1007/s40265-021-01635-6.

Rios, J., J. Lebeau, T. Yang, S. Li, and M. D. Lynch (2021). "A critical review on the progress and challenges to a more sustainable, cost competitive synthesis of adipic acid." In: *Green Chemistry* 23.9, pp. 3172–3190. DOI: 10.1039/D1GC00638J.

Rojas, A., E. Duque, G. Mosqueda, G. Golden, A. N. A. Hurtado, J. L. Ramos, and A. N. A. Segura (2001). "Three Efflux Pumps Are Required To Provide Efficient Tolerance to Toluene in *Pseudomonas putida* DOT-T1E." In: 183.13, pp. 3967–3973. DOI: https://doi.org/10.1128/jb.183.13.3967-3973.2001.

Rorrer, J. E., G. T. Beckham, and Y. Román-Leshkov (01/2021). "Conversion of Polyolefin Waste to Liquid Alkanes with Ru-Based Catalysts under Mild Conditions." In: *JACS Au* 1.1, pp. 8–12. DOI: 10.1021/jacsau.0c00041.

Rorrer, N. A., S. Nicholson, A. Carpenter, M. J. Biddy, N. J. Grundl, and G. T. Beckham (04/2019). "Combining reclaimed PET with bio-based monomers enables plastics upcycling." In: *Joule* 3.4, pp. 1006–1027. DOI: 10.1016/j.joule.2019.01.018.

Roy, R., G. Mukherjee, A. Das Gupta, P. Tribedi, and A. K. Sil (01/2021). "Isolation of a soil bacterium for remediation of polyurethane and low-density polyethylene: a promising tool towards sustainable cleanup of the environment." In: *3 Biotech* 11.1, p. 29. DOI: 10.1007/s13205-020-02592-9.

Ruiz, C., S. T. Kenny, T. Narancic, R. Babu, and K. O. Connor (12/2019). "Conversion of waste cooking oil into medium chain polyhydroxyalkanoates in a high cell density fermentation." In: *Journal of Biotechnology* 306, pp. 9–15. DOI: 10.1016/j.jbiotec.2019.08.020.

Salvachúa, D., C. W. Johnson, C. A. Singer, H. Rohrer, D. J. Peterson, B. A. Black, A. Knapp, and G. T. Beckham (10/2018). "Bioprocess development for muconic acid production from aromatic compounds and lignin." In: *Green Chemistry* 20.21, pp. 5007–5019. DOI: 10.1039/C8GC02519C.

Sanditov, D. S. and M. I. Ojovan (10/2017). "On relaxation nature of glass transition in amorphous materials." In: *Physica B: Condensed Matter* 523.August, pp. 96–113. DOI: 10.1016/j.physb.2017.08.025.

Sanluis-Verdes, A., P. Colomer-Vidal, F. Rodriguez-Ventura, M. Bello-Villarino, M. Spinola-Amilibia, E. Ruiz-Lopez, R. Illanes-Vicioso, P. Castroviejo, R. Aiese Cigliano,

M. Montoya, P. Falabella, C. Pesquera, L. Gonzalez-Legarreta, E. Arias-Palomo, M. Solà, T. Torroba, C. F. Arias, and F. Bertocchini (10/2022). "Wax worm saliva and the enzymes therein are the key to polyethylene degradation by Galleria mellonella." In: *Nature Communications* 13.1, p. 5568. DOI: 10.1038/s41467-022-33127-w.

Santana-Melo, G. F., B. V. Rodrigues, E. da Silva, R. Ricci, F. R. Marciano, T. J. Webster, L. M. Vasconcellos, and A. O. Lobo (07/2017). "Electrospun ultrathin PBAT/nHAp fibers influenced the in vitro and in vivo osteogenesis and improved the mechanical properties of neoformed bone." In: *Colloids and Surfaces B: Biointerfaces* 155, pp. 544–552. DOI: 10.1016/j.colsurfb.2017.04.053.

Sasoh, M., E. Masai, S. Ishibashi, H. Hara, N. Kamimura, K. Miyauchi, and M. Fukuda (03/2006). "Characterization of the Terephthalate Degradation Genes of Comamonas sp. Strain E6." In: *Applied and Environmental Microbiology* 72.3, pp. 1825–1832. DOI: 10.1128/AEM.72.3.1825-1832.2006.

Sato, K. (09/1998). "A "Green" route to adipic acid: direct oxidation of cyclohexenes with 30 percent hydrogen peroxide." In: *Science* 281.5383, pp. 1646–1647. DOI: 10.1126/science.281.5383.1646.

Sauter, D., M. Taoufik, and C. Boisson (05/2017). "Polyolefins, a Success Story." In: *Polymers* 9.6, p. 185. DOI: 10.3390/polym9060185.

Scheirs, J. and D. Priddy (2003). *Modern Styrenic Polymers: Polystyrenes and Styrenic Copolymers*. Wiley, p. 792.

Schläfli, H. R., M. A. Weiss, T. Leisinger, and A. M. Cook (11/1994). "Terephthalate 1,2-dioxygenase system from *Comamonas testosteroni* T-2: purification and some properties of the oxygenase component." In: *Journal of Bacteriology* 176.21, pp. 6644–6652. DOI: 10.1128/jb.176.21.6644-6652.1994.

Schlegel, H. G., H. Kaltwasser, and G. Gottschalk (1961). "A submersion method for culture of hydrogen-oxidizing bacteria: growth physiological studies." In: *Archiv fur Mikrobiologie* 38, pp. 209–22.

Schmidt, J., R. Wei, T. Oeser, L. Dedavid e Silva, D. Breite, A. Schulze, and W. Zimmermann (02/2017). "Degradation of Polyester Polyurethane by Bacterial Polyester Hydrolases." In: *Polymers* 9.12, p. 65. DOI: 10.3390/polym9020065.

Schubert, P., A. Steinbüchel, and H. G. Schlegel (1988). "Cloning of the Alcaligenes eutrophus genes for synthesis of poly-beta-hydroxybutyric acid (PHB) and synthesis of PHB in *Escherichia coli*." In: *Journal of bacteriology* 170.12, pp. 5837–5847. DOI: 10.1128/jb.170.12.5837-5847.1988.

Schwanemann, T., M. Otto, N. Wierckx, and B. Wynands (11/2020). "*Pseudomonas* as versatile aromatics cell factory." In: *Biotechnology Journal* 15.11, p. 1900569. DOI: 10.1002/biot.201900569.

Schyns, Z. O. G. and M. P. Shaver (02/2021). "Mechanical Recycling of Packaging Plastics: A Review." In: *Macromolecular Rapid Communications* 42.3, p. 2000415. DOI: 10.1002/marc.202000415.

Serranti, S. and G. Bonifazi (2019). "Techniques for separation of plastic wastes." In: *Use of Recycled Plastics in Eco-efficient Concrete*. January 2018. Elsevier, pp. 9–37. DOI: 10.1016/B978-0-08-102676-2.00002-5.

Shah, A. A., F. Hasan, A. Hameed, and S. Ahmed (2008). "Biological degradation of plastics: A comprehensive review." In: *Biotechnology Advances* 26.3, pp. 246–265. DOI: 10.1016/j.biotechadv.2007.12.005.

Shah, A. A., S. Kato, N. Shintani, N. R. Kamini, and T. Nakajima-Kambe (04/2014). "Microbial degradation of aliphatic and aliphatic-aromatic co-polyesters." In: *Applied Microbiology and Biotechnology* 98.8, pp. 3437–3447. DOI: 10.1007/s00253-014-5558-1.

Shen, L., E. Worrell, and M. K. Patel (11/2010). "Open-loop recycling: A LCA case study of PET bottle-to-fibre recycling." In: *Resources, Conservation and Recycling* 55.1, pp. 34–52. DOI: 10.1016/j.resconrec.2010.06.014.

Shen, X., Z. Wang, X. Huang, H. Hu, W. Wang, and X. Zhang (12/2017). "Developing genome-reduced *Pseudomonas chlororaphis* strains for the production of secondary metabolites." In: *BMC Genomics* 18.1, p. 715. DOI: 10.1186/s12864-017-4127-2.

Silva-Rocha, R., E. Martínez-García, B. Calles, M. Chavarría, A. Arce-Rodríguez, A. de las Heras, A. D. Páez-Espino, G. Durante-Rodríguez, J. Kim, P. I. Nikel, R. Platero, and V. de Lorenzo (01/2013). "The Standard European Vector Architecture (SEVA): a coherent platform for the analysis and deployment of complex prokaryotic phenotypes." In: *Nucleic Acids Res.* 41.D1, pp. D666–D675. DOI: 10.1093/nar/gks1119.

Simon, O., I. Klaiber, A. Huber, and J. Pfannstiel (2014). "Comprehensive proteome analysis of the response of *Pseudomonas putida* KT2440 to the flavor compound vanillin." In: *Journal of Proteomics* 109, pp. 212–227. DOI: 10.1016/j.jprot.2014.07.006.

Spalding, M. A. and A. Chatterjee (2017). *Handbook of Industrial Polyethylene and Technology*, p. 1410.

Stainer, R. and L. Ornston (1973). "The β-Ketoadipate Pathway." In: *Advances in Microbial Physiology*. Vol. 9. C, pp. 89–151. DOI: 10.1016/S0065-2911(08)60377-X.

Stegmann, P., V. Daioglou, M. Londo, D. P. van Vuuren, and M. Junginger (12/2022). "Plastic futures and their CO2 emissions." In: *Nature* 612.7939, pp. 272–276. DOI: 10.1038/s41586-022-05422-5.

Sulaiman, S., S. Yamato, E. Kanaya, J.-J. Kim, Y. Koga, K. Takano, and S. Kanaya (03/2012). "Isolation of a Novel Cutinase Homolog with Polyethylene Terephthalate-Degrading Activity from Leaf-Branch Compost by Using a Metagenomic Approach." In: *Applied and Environmental Microbiology* 78.5, pp. 1556–1562. DOI: 10.1128/AEM.06725-11.

Sullivan, K. P., A. Z. Werner, K. J. Ramirez, L. D. Ellis, J. R. Bussard, B. A. Black, D. G. Brandner, F. Bratti, B. L. Buss, X. Dong, S. J. Haugen, M. A. Ingraham, M. O. Konev, W. E. Michener, J. Miscall, I. Pardo, S. P. Woodworth, A. M. Guss, Y. Román-Leshkov, S. S. Stahl, and G. T. Beckham (10/2022). "Mixed plastics waste valorization through tandem chemical oxidation and biological funneling." In: *Science* 378.6616, pp. 207–211. DOI: 10.1126/science.abo4626.

Sun, Z., J. A. Ramsay, M. Guay, and B. Ramsay (11/2007a). "Increasing the yield of MCL-PHA from nonanoic acid by co-feeding glucose during the PHA accumulation stage in two-stage fed-batch fermentations of *Pseudomonas putida* KT2440." In: *Journal of Biotechnology* 132.3, pp. 280–282. DOI: 10.1016/j.jbiotec.2007.02.023.

Sun, Z., J. A. Ramsay, M. Guay, and B. A. Ramsay (02/2007b). "Carbon-limited fed-batch production of medium-chain-length polyhydroxyalkanoates from nonanoic acid by *Pseudomonas putida* KT2440." In: *Applied Microbiology and Biotechnology* 74.1, pp. 69–77. DOI: 10.1007/s00253-006-0655-4.

Takkellapati, S., T. Li, and M. A. Gonzalez (09/2018). "An overview of biorefinery-derived platform chemicals from a cellulose and hemicellulose biorefinery." In: *Clean Technologies and Environmental Policy* 20.7, pp. 1615–1630. DOI: 10.1007/s10098-018-1568-5.

Tao, Y., L. Fang, M. Dai, C. Wang, J. Sun, and Q. Fang (07/2020). "Sustainable alternative to bisphenol A epoxy resin: high-performance recyclable epoxy vitrimers derived from protocatechuic acid." In: *Polymer Chemistry* 11.27, pp. 4500–4506. DOI: 10.1039/D0PY00545B.

Teras, R., R. Hõrak, and M. Kivisaar (02/2000). "Transcription from fusion promoters generated during transposition of transposon Tn4652 is positively affected by integration host factor in *Pseudomonas putida*." In: *Journal of Bacteriology* 182.3, pp. 589–598. DOI: 10.1128/JB.182.3.589-598.2000.

Teufel, R., V. Mascaraque, W. Ismail, M. Voss, J. Perera, W. Eisenreich, W. Haehnel, and G. Fuchs (2010). "Bacterial phenylalanine and phenylacetate catabolic pathway revealed." In: *Proceedings of the National Academy of Sciences of the United States of America* 107.32, pp. 14390–14395. DOI: 10.1073/pnas.1005399107.

Teuten, E. L., J. M. Saquing, D. R. Knappe, M. A. Barlaz, S. Jonsson, A. Björn, S. J. Rowland, R. C. Thompson, T. S. Galloway, R. Yamashita, D. Ochi, Y. Watanuki, C. Moore, P. H. Viet, T. S. Tana, M. Prudente, R. Boonyatumanond, M. P. Zakaria, K. Akkhavong, Y. Ogata, H. Hirai, S. Iwasa, K. Mizukawa, Y. Hagino, A. Imamura, M. Saha, and H. Takada (2009). "Transport and release of chemicals from plastics to the environment and to wildlife." In: *Philosophical Transactions of the Royal Society B: Biological Sciences* 364.1526, pp. 2027–2045. DOI: 10.1098/rstb.2008.0284.

Thompson, M. G., Z. Costello, N. F. Hummel, P. Cruz-Morales, J. M. Blake-Hedges, R. N. Krishna, W. Skyrud, A. N. Pearson, M. R. Incha, P. M. Shih, H. Garcia-Martin, and J. D. Keasling (2019). "Robust Characterization of Two Distinct Glutarate Sensing Transcription Factors of *Pseudomonas putida* l -Lysine Metabolism." In: *ACS Synthetic Biology* 8.10, pp. 2385–2396. DOI: 10.1021/acssynbio.9b00255.

Thompson, M. G., M. R. Incha, A. N. Pearson, M. Schmidt, W. A. Sharpless, C. B. Eiben, P. Cruz-Morales, J. M. Blake-Hedges, Y. Liu, C. A. Adams, R. W. Haushalter, R. N. Krishna, P. Lichtner, L. M. Blank, A. Mukhopadhyay, A. M. Deutschbauer, P. M. Shih, and J. D. Keasling (08/2020). "Fatty acid and alcohol metabolism in *Pseudomonas putida*: functional analysis using random barcode transposon sequencing." In: *Applied and Environmental Microbiology* 86.21. Ed. by N.-Y. Zhou, pp. 1–23. DOI: 10.1128/AEM.01665-20.

Thompson, R. C., S. H. Swan, C. J. Moore, and F. S. Vom Saal (2009). "Our plastic age." In: *Philosophical Transactions of the Royal Society B: Biological Sciences* 364.1526, pp. 1973–1976. DOI: 10.1098/rstb.2009.0054.

Thomsen, T. B., C. J. Hunt, and A. S. Meyer (07/2022). "Influence of substrate crystallinity and glass transition temperature on enzymatic degradation of polyethy-

lene terephthalate (PET)." In: *New Biotechnology* 69.February, pp. 28–35. DOI: 10.1016/j.nbt.2022.02.006.

Thorvaldsdottir, H., J. T. Robinson, and J. P. Mesirov (03/2013). "Integrative Genomics Viewer (IGV): high-performance genomics data visualization and exploration." In: *Briefings in Bioinformatics* 14.2, pp. 178–192. DOI: 10.1093/bib/bbs017.

Thothong, S., A. Jarerat, K. R. Sriroth, and R. Tantatherdtam (01/2013). "Degradation of Porous Starch Granules and Poly(Butylene Adipate-co-Terephthalate)(PBAT) Blends: Soil Burial and Enzymatic Tests." In: *Advanced Materials Research* 651, pp. 12–17. DOI: 10.4028/www.scientific.net/AMR.651.12.

Tiso, T., N. Ihling, S. Kubicki, A. Biselli, A. Schonhoff, I. Bator, S. Thies, T. Karmainski, S. Kruth, A.-L. Willenbrink, A. Loeschcke, P. Zapp, A. Jupke, K.-E. Jaeger, J. Büchs, and L. M. Blank (08/2020a). "Integration of Genetic and Process Engineering for Optimized Rhamnolipid Production Using Pseudomonas putida." In: *Frontiers in Bioengineering and Biotechnology* 8, p. 976. DOI: 10.3389/fbioe.2020.00976.

Tiso, T., T. Narancic, R. Wei, E. Pollet, N. Beagan, K. Schröder, A. Honak, M. Jiang, S. Kenny, N. Wierckx, R. Perrin, L. Avérous, W. Zimmermann, K. O'Connor, and L. Blank (03/2020b). "Bio-upcycling of polyethylene terephthalate." In: *bioRxiv*, p. 2020.03.16.993592. DOI: 10.1101/2020.03.16.993592.

Tiso, T., T. Narancic, R. Wei, E. Pollet, N. Beagan, K. Schröder, A. Honak, M. Jiang, S. T. Kenny, N. Wierckx, R. Perrin, L. Avérous, W. Zimmermann, K. O'Connor, and L. M. Blank (03/2021). "Towards bio-upcycling of polyethylene terephthalate." In: *Metabolic Engineering* in press. DOI: 10.1101/2020.03.16.993592.

Tiso, T., B. Winter, R. Wei, J. Hee, J. de Witt, N. Wierckx, P. Quicker, U. T. Bornscheuer, A. Bardow, J. Nogales, and L. M. Blank (2022). "The metabolic potential of plastics as biotechnological carbon sources – Review and targets for the future." In: *Metabolic Engineering* 71.September, pp. 77–98. DOI: 10.1016/j.ymben.2021.12.006.

Tournier, V., C. M. Topham, A. Gilles, B. David, C. Folgoas, E. Moya-Leclair, E. Kamionka, M.-L. Desrousseaux, H. Texier, S. Gavalda, M. Cot, E. Guémard, M. Dalibey, J. Nomme, G. Cioci, S. Barbe, M. Chateau, I. André, S. Duquesne, and A. Marty (04/2020). "An engineered PET depolymerase to break down and recycle plastic bottles." In: *Nature* 580.7802, pp. 216–219. DOI: 10.1038/s41586-020-2149-4.

Tropin, T. V., J. W. Schmelzer, and V. L. Aksenov (01/2016). "Modern aspects of the kinetic theory of glass transition." In: *Physics-Uspekhi* 59.1, pp. 42–66. DOI: 10.3367/UFNe.0186.201601c.0047.

Tumen-Velasquez, M., C. W. Johnson, A. Ahmed, G. Dominick, E. M. Fulk, P. Khanna, S. A. Lee, A. L. Schmidt, J. G. Linger, M. A. Eiteman, G. T. Beckham, and E. L. Neidle (07/2018). "Accelerating pathway evolution by increasing the gene dosage of chromosomal segments." In: *Proceedings of the National Academy of Sciences* 115.27, pp. 7105–7110. DOI: 10.1073/pnas.1803745115.

Turner, A. (08/2018). "Black plastics: Linear and circular economies, hazardous additives and marine pollution." In: *Environment International* 117.February, pp. 308–318. DOI: 10.1016/j.envint.2018.04.036.

Utomo, R. N. C., W. J. Li, T. Tiso, C. Eberlein, M. Doeker, H. J. Heipieper, A. Jupke, N. Wierckx, and L. M. Blank (2020). "Defined Microbial Mixed Culture for Utilization of Polyurethane Monomers." In: *ACS Sustainable Chemistry and Engineering* 8.47, pp. 17466–17474. DOI: 10.1021/acssuschemeng.0c06019.

Vardon, D. R., M. A. Franden, C. W. Johnson, E. M. Karp, M. T. Guarnieri, J. G. Linger, M. J. Salm, T. J. Strathmann, and G. T. Beckham (2015). "Adipic acid production from lignin." In: DOI: 10.1039/c4ee03230f.

Venkatram, S., J. McCollum, N. Stingelin, and B. Brettmann (03/2023). "A close look at polymer degree of crystallinity versus polymer crystalline quality." In: *Polymer International* February. DOI: 10.1002/pi.6508.

Vert, M., Y. Doi, K.-H. Hellwich, M. Hess, P. Hodge, P. Kubisa, M. Rinaudo, and F. Schué (01/2012). "Terminology for biorelated polymers and applications (IUPAC Recommendations 2012)." In: *Pure and Applied Chemistry* 84.2, pp. 377–410. DOI: 10.1351/PAC-REC-10-12-04.

Vinuselvi, P., M.-K. Kim, S.-K. Lee, and C.-M. Ghim (02/2012). "Rewiring carbon catabolite repression for microbial cell factory." In: *BMB Reports* 45.2, pp. 59–70. DOI: 10.5483/BMBRep.2012.45.2.59.

Volke, D. C., P. Calero, and P. I. Nikel (06/2020). "*Pseudomonas putida*." In: *Trends in Microbiology* 28.6, pp. 512–513. DOI: 10.1016/j.tim.2020.02.015.

Vollmer, I., M. J. F. Jenks, M. C. P. Roelands, R. J. White, T. Harmelen, P. Wild, G. P. Laan, F. Meirer, J. T. F. Keurentjes, and B. M. Weckhuysen (09/2020). "Beyond mechanical recycling: giving new life to plastic waste." In: *Angewandte Chemie International Edition* 59.36, pp. 15402–15423. DOI: 10.1002/anie.201915651.

Volmer, J., C. Neumann, B. Bühler, and A. Schmid (10/2014). "Engineering of *Pseudomonas taiwanensis* VLB120 for constitutive solvent tolerance and increased specific styrene epoxidation activity." In: *Applied and Environmental Microbiology* 80.20, pp. 6539–6548. DOI: 10.1128/AEM.01940-14.

Walker, S., A. Ryan, and R. Rothman (2022). "Tipping points in polymer life cycle greenhouse gas emissions." In: pp. 1–17. DOI: doi.org/10.21203/rs.3.rs-1715591/v1.

Wang, H., J.-W. Ye, X. Chen, Y. Yuan, J. Shi, X. Liu, F. Yang, Y. Ma, J. Chen, F. Wu, Y. Lan, Q. Wu, Y. Tong, and G.-Q. Chen (06/2023). "Production of PHA copolymers consisting of 3-hydroxybutyrate and 3-hydroxyhexanoate (PHBHHx) by recombinant *Halomonas bluephagenesis*." In: *Chem. Eng. J.* 466.March, p. 143261. DOI: 10.1016/j.cej.2023.143261.

Wang, J., X. Shen, J. Rey, Q. Yuan, and Y. Yan (01/2018). "Recent advances in microbial production of aromatic natural products and their derivatives." In: *Applied Microbiology and Biotechnology* 102.1, pp. 47–61. DOI: 10.1007/s00253-017-8599-4.

Wang, Q. and C. T. Nomura (12/2010). "Monitoring differences in gene expression levels and polyhydroxyalkanoate (PHA) production in *Pseudomonas putida* KT2440 grown on different carbon sources." In: *Journal of Bioscience and Bioengineering* 110.6, pp. 653–659. DOI: 10.1016/j.jbiosc.2010.08.001.

Wang, Y. Z., Y. Zhou, and G. J. Zylstra (06/1995). "Molecular analysis of isophthalate and terephthalate degradation by *Comamonas testosteroni* YZW-D." In: *Environmental Health Perspectives* 103.suppl 5, pp. 9–12. DOI: 10.1289/ehp.95103s49.

Weaver, L. M. and K. M. Herrmann (11/1990). "Cloning of an aroF allele encoding a tyrosine-insensitive 3-deoxy-D-arabino-heptulosonate 7-phosphate synthase." In: *Journal of Bacteriology* 172.11, pp. 6581–6584. DOI: 10.1128/jb.172.11.6581-6584.1990.

Weber, C., C. Brückner, S. Weinreb, C. Lehr, C. Essl, and E. Boles (2012). "Biosynthesis of cis,cis-muconic acid and its aromatic precursors, catechol and protocatechuic acid, from renewable feedstocks by saccharomyces cerevisiae." In: *Applied and Environmental Microbiology* 78.23, pp. 8421–8430. DOI: 10.1128/AEM.01983-12.

Wei, R., T. Tiso, J. Bertling, K. O'Connor, L. M. Blank, and U. T. Bornscheuer (11/2020). "Possibilities and limitations of biotechnological plastic degradation and recycling." In: *Nature Catalysis* 3.11, pp. 867–871. DOI: 10.1038/s41929-020-00521-w.

Wei, R. and W. Zimmermann (2017). "Microbial enzymes for the recycling of recalcitrant petroleum-based plastics: how far are we?" In: *Microbial Biotechnology* 10.6, pp. 1308–1322. DOI: 10.1111/1751-7915.12710.

Wen, Q., Z. Chen, T. Tian, and W. Chen (10/2010). "Effects of phosphorus and nitrogen limitation on PHA production in activated sludge." In: *Journal of Environmental Sciences* 22.10, pp. 1602–1607. DOI: 10.1016/S1001-0742(09)60295-3.

Werner, A. Z., R. Clare, T. D. Mand, I. Pardo, K. J. Ramirez, S. J. Haugen, F. Bratti, G. N. Dexter, J. R. Elmore, J. D. Huenemann, G. L. Peabody, C. W. Johnson, N. A. Rorrer, D. Salvachúa, A. M. Guss, and G. T. Beckham (2021). "Tandem chemical deconstruction and biological upcycling of poly(ethylene terephthalate) to β-ketoadipic acid by *Pseudomonas putida* KT2440." In: *Metabolic Engineering* 67.June, pp. 250–261. DOI: 10.1016/j.ymben.2021.07.005.

Westhues, S., J. Idel, and J. Klankermayer (08/2018). "Molecular catalyst systems as key enablers for tailored polyesters and polycarbonate recycling concepts." In: *Science Advances* 4.8, eaat9669. DOI: 10.1126/sciadv.aat9669.

Whinfield, J. R. and J. T. Dickson (1946). *Improvements relating to the manufacture of highly polymeric substances.*

Wierckx, N., T. Narancic, C. Eberlein, R. Wei, O. Drzyzga, A. Magnin, H. Ballerstedt, S. T. Kenny, E. Pollet, L. Avérous, K. E. O'Connor, W. Zimmermann, H. J. Heipieper, A. Prieto, J. Jiménez, and L. M. Blank (2018). "Plastic biodegradation: challenges and opportunities." In: *Consequences of Microbial Interactions with Hydrocarbons, Oils, and Lipids: Biodegradation and Bioremediation.* Cham: Springer International Publishing, pp. 1–29. DOI: 10.1007/978-3-319-44535-9{_}23-1.

Wierckx, N., M. A. Prieto, P. Pomposiello, V. Lorenzo, K. O'Connor, and L. M. Blank (11/2015). "Plastic waste as a novel substrate for industrial biotechnology." In: *Microbial Biotechnology* 8.6, pp. 900–903. DOI: 10.1111/1751-7915.12312.

Wierckx, N. J. P., H. Ballerstedt, J. A. M. de Bont, J. H. de Winde, H. J. Ruijssenaars, and J. Wery (04/2008). "Transcriptome analysis of a phenol-producing *Pseudomonas*

putida S12 construct: genetic and physiological basis for improved production." In: *Journal of Bacteriology* 190.8, pp. 2822–2830. DOI: 10.1128/JB.01379-07.

Wierckx, N. J. P., H. Ballerstedt, J. A. M. de Bont, and J. Wery (12/2005). "Engineering of Solvent-Tolerant *Pseudomonas putida* S12 for Bioproduction of Phenol from Glucose." In: *Applied and Environmental Microbiology* 71.12, pp. 8221–8227. DOI: 10.1128/AEM.71.12.8221-8227.2005.

Wilkes, R. and L. Aristilde (09/2017). "Degradation and metabolism of synthetic plastics and associated products by *Pseudomonas* sp.: capabilities and challenges." In: *Journal of Applied Microbiology* 123.3, pp. 582–593. DOI: 10.1111/jam.13472.

World Economic Forum, Ellen MacArthur Foundation, and McKinsey & Company (2016). *The New Plastics Economy: rethinking the future of plastics.*

Worm, B., H. K. Lotze, I. Jubinville, C. Wilcox, and J. Jambeck (10/2017). "Plastic as a Persistent Marine Pollutant." In: *Annual Review of Environment and Resources* 42.1, pp. 1–26. DOI: 10.1146/annurev-environ-102016-060700.

Wu, P., Z. Li, J. Gao, Y. Zhao, H. Wang, H. Qin, Q. Gu, R. Wei, W. Liu, and X. Han (02/2023). "Characterization of a PBAT Degradation Carboxylesterase from Thermobacillus composti KWC4." In: *Catalysts* 13.2, p. 340. DOI: 10.3390/catal13020340.

Wynands, B. (2018). "Engineering of *Pseudomonas taiwanensis* VLB120 for the sustainable production of hydroxylated aromatics." PhD thesis. RWTH Aachen.

Wynands, B., F. Kofler, A. Sieberichs, N. da Silva, and N. Wierckx (07/2023). "Engineering a *Pseudomonas taiwanensis* 4-coumarate platform for production of para-hydroxy aromatics with high yield and specificity." In: *Metabolic Engineering* 78, pp. 115–127. DOI: 10.1016/j.ymben.2023.05.004.

Wynands, B., C. Lenzen, M. Otto, F. Koch, L. M. Blank, and N. Wierckx (05/2018). "Metabolic engineering of *Pseudomonas taiwanensis* VLB120 with minimal genomic modifications for high-yield phenol production." In: *Metabolic Engineering* 47, pp. 121–133. DOI: 10.1016/j.ymben.2018.03.011.

Wynands, B., M. Otto, N. Runge, S. Preckel, T. Polen, L. M. Blank, and N. Wierckx (09/2019). "Streamlined *Pseudomonas taiwanensis* VLB120 chassis strains with improved bioprocess features." In: *ACS Synthetic Biology* 8.9, pp. 2036–2050. DOI: 10.1021/acssynbio.9b00108.

Xin, X. F., B. Kvitko, and S. Y. He (2018). "*Pseudomonas syringae*: What it takes to be a pathogen." In: *Nature Reviews Microbiology* 16.5, pp. 316–328. DOI: 10.1038/nrmicro.2018.17.

Xu, Q., Z. Zheng, L. Zou, C. Zhang, F. Yang, K. Zhou, and J. Ouyang (2020). "A versatile *Pseudomonas putida* KT2440 with new ability : selective oxidation of 5 - hydroxymethylfurfural to 5 - hydroxymethyl - 2 - furancarboxylic acid." In: *Bioprocess and Biosystems Engineering* 43.1, pp. 67–73. DOI: 10.1007/s00449-019-02205-7.

Yim, H., R. Haselbeck, W. Niu, C. Pujol-Baxley, A. Burgard, J. Boldt, J. Khandurina, J. D. Trawick, R. E. Osterhout, R. Stephen, J. Estadilla, S. Teisan, H. B. Schreyer, S. Andrae, T. H. Yang, S. Y. Lee, M. J. Burk, and S. Van Dien (07/2011). "Metabolic engineering of *Escherichia coli* for direct production of 1,4-butanediol." In: *Nature Chemical Biology* 7.7, pp. 445–452. DOI: 10.1038/nchembio.580.

Yoon, M. G., H. J. Jeon, and M. N. Kim (2012). "Biodegradation of Polyethylene by a Soil Bacterium and AlkB Cloned Bioremediation & Biodegradation." In: 3.4. DOI: 10.4172/2155-6199.1000145.

Yoshida, S., K. Hiraga, T. Takehana, I. Taniguchi, H. Yamaji, Y. Maeda, K. Toyohara, K. Miyamoto, Y. Kimura, and K. Oda (03/2016). "A bacterium that degrades and assimilates poly(ethylene terephthalate)." In: *Science* 351.6278, pp. 1196–1199. DOI: 10.1126/science.aad6359.

Yu, J.-L., X.-X. Xia, J.-J. Zhong, and Z.-G. Qian (12/2014). "Direct biosynthesis of adipic acid from a synthetic pathway in recombinant *Escherichia coli*." In: *Biotechnology and Bioengineering* 111.12, pp. 2580–2586. DOI: 10.1002/bit.25293.

Zaaba, N. F. and M. Jaafar (09/2020). "A review on degradation mechanisms of polylactic acid: Hydrolytic, photodegradative, microbial, and enzymatic degradation." In: *Polymer Engineering & Science* 60.9, pp. 2061–2075. DOI: 10.1002/pen.25511.

Zhang, M., C. Gao, X. Guo, S. Guo, Z. Kang, D. Xiao, J. Yan, F. Tao, W. Zhang, W. Dong, P. Liu, C. Yang, C. Ma, and P. Xu (12/2018). "Increased glutarate production by blocking the glutaryl-CoA dehydrogenation pathway and a catabolic pathway involving l-2-hydroxyglutarate." In: *Nature Communications* 9.1, p. 2114. DOI: 10.1038/s41467-018-04513-0.

Zhang, M., Z. Kang, X. Guo, S. Guo, D. Xiao, Y. Liu, C. Ma, P. Xu, and C. Gao (08/2019). "Regulation of Glutarate Catabolism by GntR Family Regulator CsiR and LysR Family Regulator GcdR in *Pseudomonas putida* KT2440." In: *mBio* 10.4. Ed. by N. R. Salama. DOI: 10.1128/mBio.01570-19.

Zhao, M., D. Huang, X. Zhang, M. A. Koffas, J. Zhou, and Y. Deng (05/2018). "Metabolic engineering of *Escherichia coli* for producing adipic acid through the reverse adipate-degradation pathway." In: *Metabolic Engineering* 47, pp. 254–262. DOI: 10.1016/j.ymben.2018.04.002.

Zheng, J. and S. Suh (2019). "Strategies to reduce the global carbon footprint of plastics." In: *Nature Climate Change* 9.5, pp. 374–378. DOI: 10.1038/s41558-019-0459-z.

Zhu, Y., J. Yang, F. Mei, X. Li, and C. Zhao (2022). "Bio-based 1,4-butanediol and tetrahydrofuran synthesis: perspective." In: *Green Chemistry* 24.17, pp. 6450–6466. DOI: 10.1039/D2GC02271K.

Zobel, S., I. Benedetti, L. Eisenbach, V. de Lorenzo, N. Wierckx, and L. M. Blank (12/2015). "Tn7-Based Device for Calibrated Heterologous Gene Expression in *Pseudomonas putida*." In: *ACS Synthetic Biology* 4.12, pp. 1341–1351. DOI: 10.1021/acssynbio.5b00058.

Appendix

Supplemental data to:
Engineering adipic acid metabolism in Pseudomonas putida (Section 2.1)
Yannic S. Ackermann*, Wing-Jin Li*, Leonie Op de Hipt, Paul-Joachim Niehoff, William Casey, Tino Polen, Sebastian Köbbing, Hendrik Ballerstedt, Benedikt Wynands, Kevin O'Connor, Lars M. Blank and Nick Wierckx

Figure S1.: Promotor predictions for the intergentic region between *paaF* and *paaY*

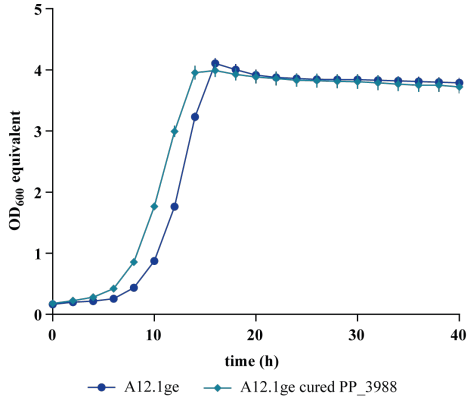

Figure S2.: Determination of the impact of the mutation in PP_3988 on the growth on adipate. Growth curves of *P. putida* A12.1ge and A12.1ge with cured mutation in PP_3988. Growth curves were measured with the Growth Profiler and the results were converted to an equivalent OD at 600 nm. Error bars indicate the standard error of the mean (n=3). (ge = genomically integrated P_{14e}-*dcaAKIJP*).

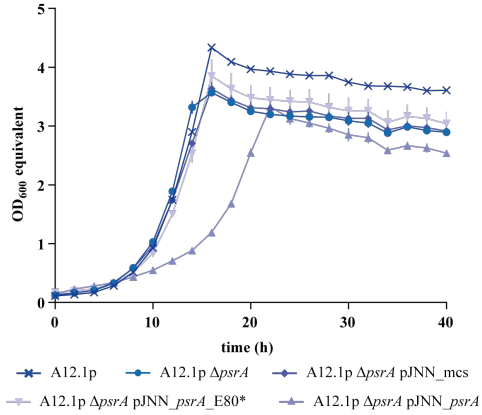

Figure S3.: Determination of the impact of the regulator PsrA on the growth on adipate. Growth curves of *P. putida* A12.1 Δ*psrA* with episomal expression of the *dcaAKIJP* genes and different overexpression constructs of *psrA* on compatible plasmid pJNN(mcs)t. Growth curves were measured in MSM with 30 mM adipate and 0.1 mM salicylate and antibiotics as appropriate. Growth Profiler data were converted to an equivalent OD at 600 nm. Error bars indicate the standard error of the mean (n=3). (p = pBNT-*dcaAKIJP*, * = stop codon).

Supplemental data to:

Bio-upcycling of even and uneven medium-chain-length diols and dicarboxylates to polyhydroxyalkanoates using engineered Pseudomonas putida (Section 2.2)

Yannic S. Ackermann*, Jan de Witt*, Mariella P. Mezzina, Christoph Schroth, Tino Polen, Pablo I. Nikel, Benedikt Wynands, Nick Wierckx

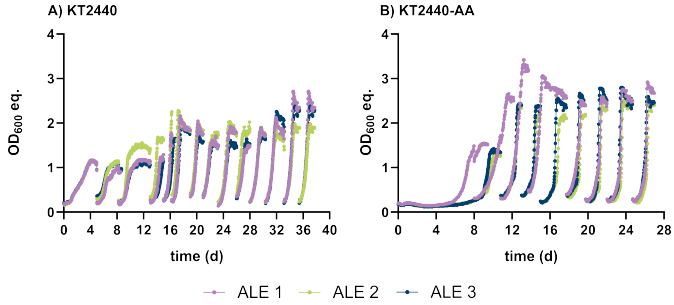

Figure S4.: Adaptive laboratory evolution of *P. putida* KT2440 wildtype (A) and KT2440-AA (B) on 1,6-hexanediol. ALE was performed by iterative inoculation after the stationary phase was reached. Since *P. putida* KT2440 did not grow with HDO as sole carbon source, 15 mM HDO and 15 mM BDO were used for the first two stages of ALE to enable growth. This concentration was shifted to 20 mM HDO and 10 mM BDO (stages 3-5) to 30 mM HDO (stages 6-14). *P. putida* KT2440-AA could grow with 30 mM HDO.

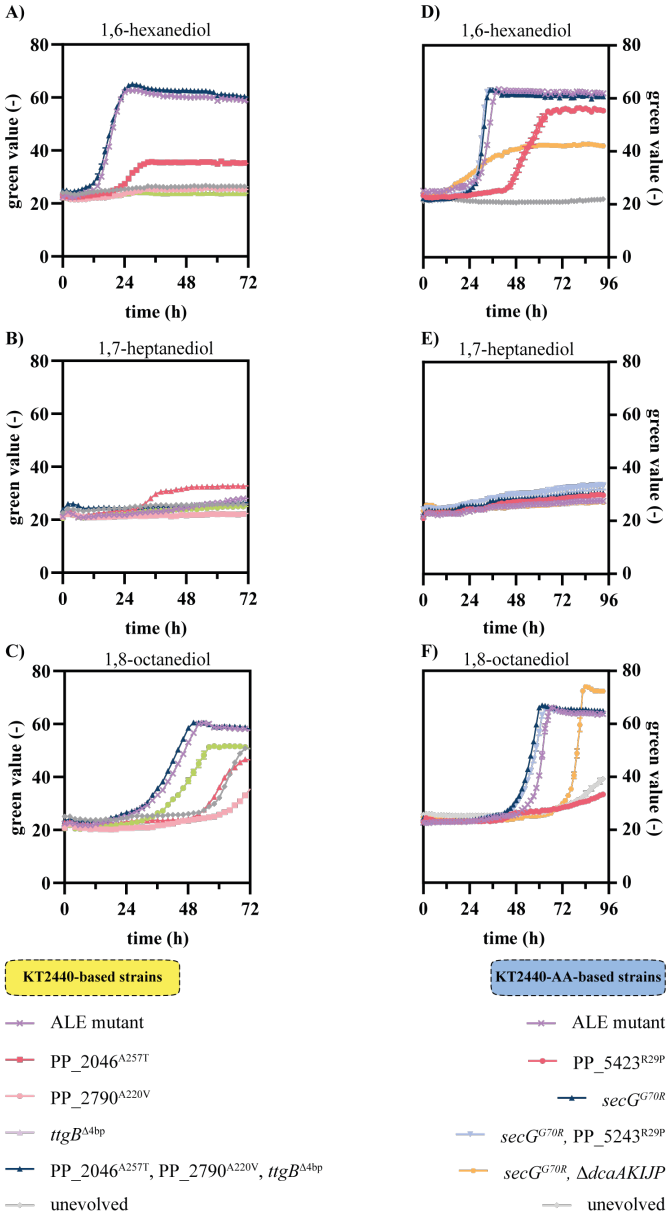

Figure S5.: Metabolic pathways of aliphatic diols in engineered *P. putida* KT2440. Extension of figure 2.2.1. *P. putida* KT2440 wild type-based strains (A-C) and *P. putida* KT2440-AA-based strains (D-F) were cultivated in mineral salts medium (MSM) supplemented with 1,6-hexanediol, 1,7-heptanediol, or 1,8-octanediol in concentrations that are C-mol equivalent to 30 mM 1,6-hexanediol. Growth was monitored using a Growth Profiler. Error bars indicate the standard error of the mean (n=3).

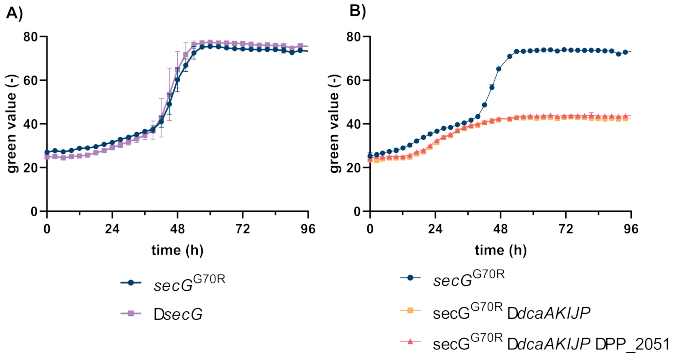

Figure S6.: Growth of *P. putida* KT2440-AA mutants on HDO. Strains were cultivated in MSM supplemented with 15 mM of HDO as sole carbon source. (A) Effect of $secG^{G70R}$ mutation on HDO metabolism. (B) Effect of Δ*dcaAKIJP* and ΔPP_2051.

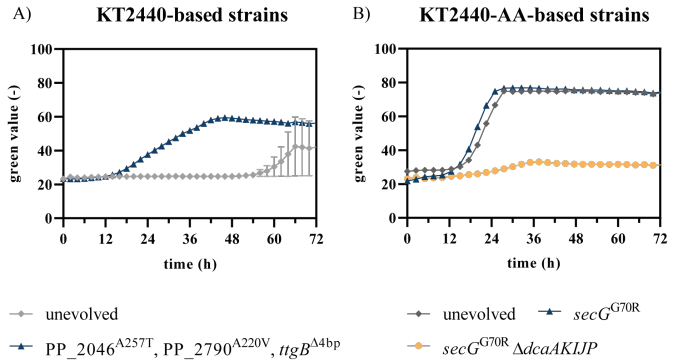

Figure S7.: Growth of *P. putida* strains on HDO Strains were cultivated in MSM supplemented with 15 mM of HDO as sole carbon source.

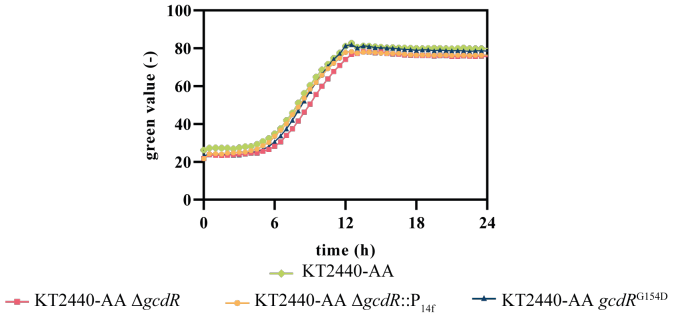

Figure S8.: Growth of *P. putida* KT2440-AA mutants on glutarate. Strains were cultivated in MSM supplemented with 36 mM glutarate as sole carbon source

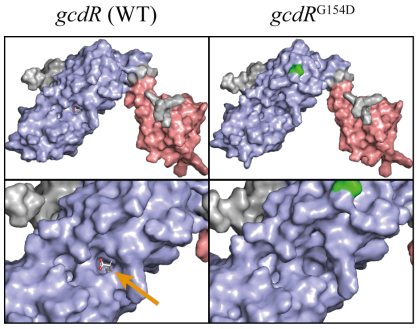

Figure S9.: Three-dimensional structures of GcdR predicted with ColabFold and visualized with PyMOL. Docking of glutaric acid was calculated using YASARA (orange arrow). Mutated amino acid (D154) is marked in green. The blue surface color indicates the effector binding domain and the red surface color indicates the DNA binding domain.

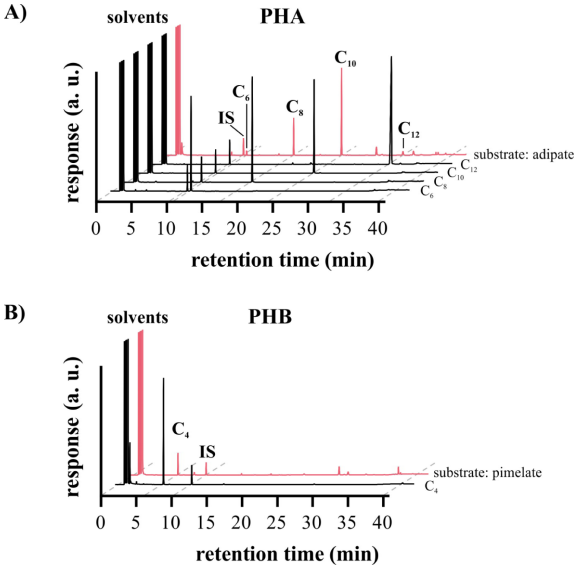

Figure S10.: Exemplary gas chromatography chromatograms of polyhydroxyalkanoates (A) and polyhydroxybutyrate (B). Methyl esters of 3-hydroxyacids (C_4-C_{12}) were quantified using analytical standards (black lines). As internal standard (IS) methyl benzoate was used. PHA production from adipate (A) and PHB production from pimelate (B) are shown in red. For better visibility, the y-axis was capped due to high responses of chloroform and methanol.

Supplemental data to:

Engineering of 1,4-butanediol and adipic acid metabolism in P. taiwanensis for upcycling to aromatic compounds. (Section 2.3)

Leonie Op de Hipt*, **Yannic S. Ackermann***, Hannah de Jong, Tino Polen, Benedikt Wynands, Nick Wierckx

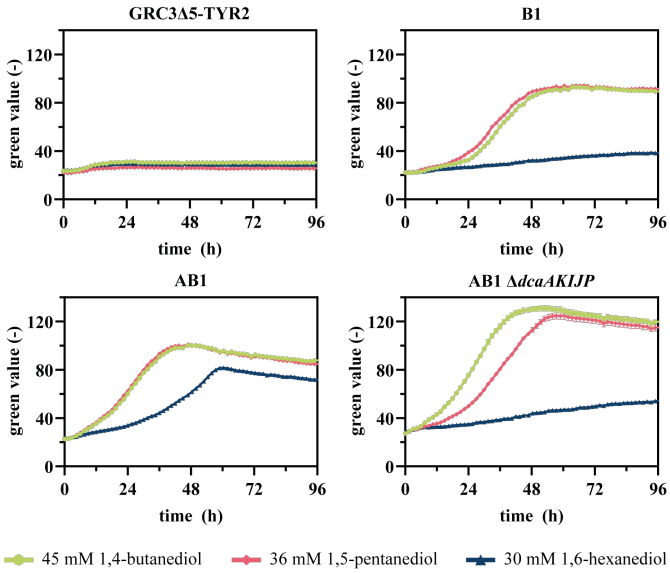

Figure S11.: Growth of *P. taiwanensis* strains evolved on BDO on diols with different chain lengths. All strains were cultivated in MSM with the indicated carbon sources at a C-molar equivalent to 45 mM BDO. Green values were measured via the Growth Profiler. Error bars derive from three technological replicates and indicate the SEM.

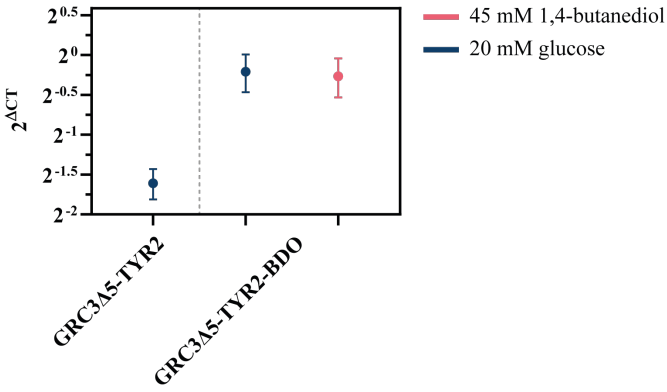

Figure S12.: RT-qPCR analysis of PVLB_10545 expression with and without the mutation PVLB_10540 ^{L480L}. *P. taiwanensis* GRC3 Δ5-TYR2 PVLB_10540^{L480L} PVLB_12690^{A247V} PVLB_13305^{S141P} was cultivated in MSM containing 20 mM glucose as well as MSM containing 45 mM BDO as sole carbon source and *P. taiwanensis* GRC3Δ5-TYR2 was cultivated in MSM containing 20 mM glucose as sole carbon source. Samples were taken at an optical density of 0.9 to 1.1. The measured Ct values were normalized to *rpoD*. Error bars derive from three biological replicates and indicate the SEM.

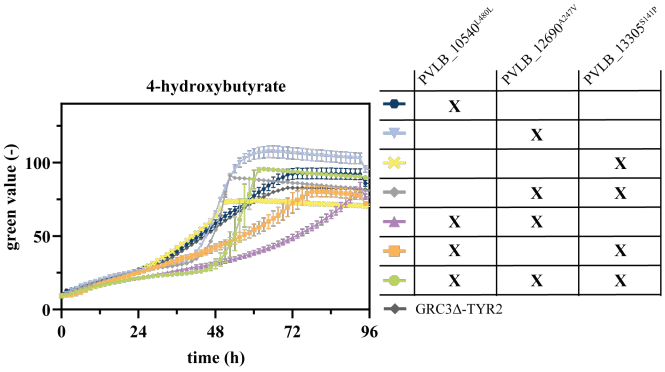

Figure S13.: Cultivation of reverse engineered *P. taiwanensis* GRC3Δ5-TYR2 strains for growth on 4-hydroxybutyrate. Growth curves of engineered strains carrying different mutations found during the whole genome sequencing of the ALE on BDO. All strains are cultivated in three-fold buffered MSM medium containing 45 mM of 4-hydroxyburate as sole carbon source. Error bars represent the standard error of the mean (n=3).

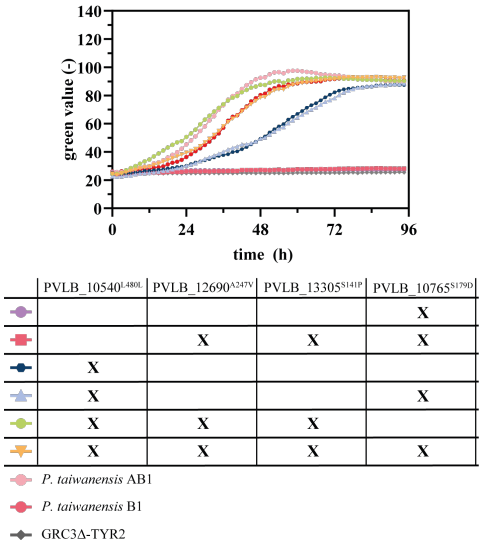

Figure S14.: Reverse engineering of PVLB_10765^{S141P} in *P. taiwanensis* GRC3Δ5-TYR2 strains. Growth curves of engineered strains carrying different mutations found during the whole genome sequencing of the ALE on BDO. All strains are cultivated in three-fold buffered MSM medium containing 45 mM of BDO as sole carbon source. Error bars represent the standard error of the mean (n=3).

Supplemental data to:
Bio-upcycling of PBAT mock hydrolysates by defined mixed cultures into protocatechuic acid (Section 2.4)
Yannic S. Ackermann, Benedikt Wynands, Nick Wierckx

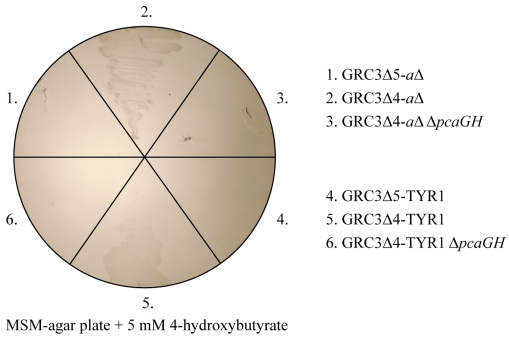

Figure S15.: Charackterizing growth on 4-hydroxybenzoate. All strains were spread out on MSM agar plate containing 5 mM 5-HB from a liquid overnight culture.

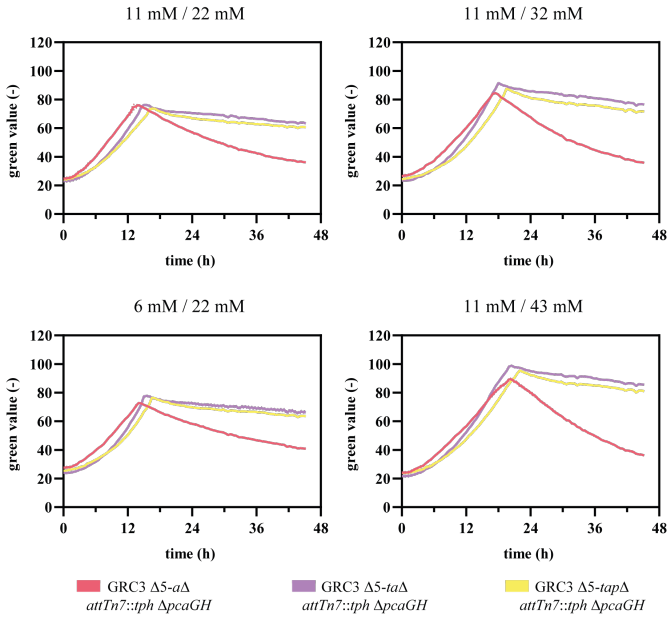

Figure S16.: Growth of different bio-transformation strains on mixture of TA and glucose. All strains were cultivated separately in MSM medium containing terephthalate and glucose as mentioned in the figure. Online growth curves were measured by the Growth Profiler. Error bars indicate the standard error of the mean (n=3).

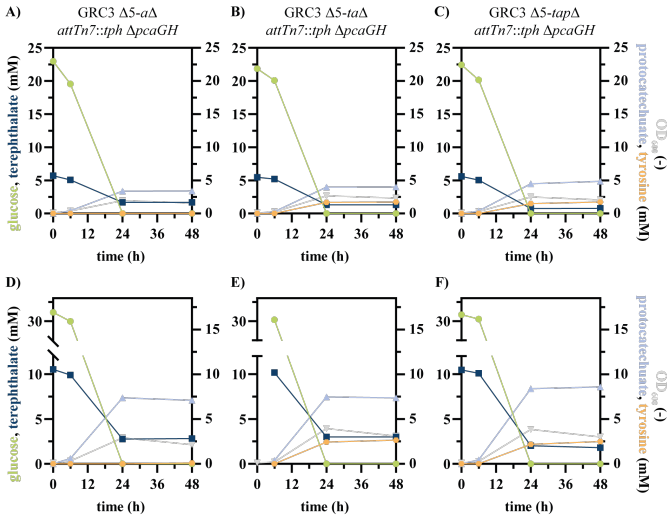

Figure S17.: Bio-transformation of TA into PCA with glucose as additional carbon source. All strains were cultivated separately in MSM medium containing terephthalate and glucose as mentioned in the figure. Samples were taken over time from separate System Duetz plates, which were all inoculated from the same master mix. (A-C) HPLC data from cultivations with 6 mM TA and 22 mM glucose. (D-F) HPLC data from cultivations with 11 mM TA and 32 mM glucose. Error bars indicate the standard error of the mean (n=2).

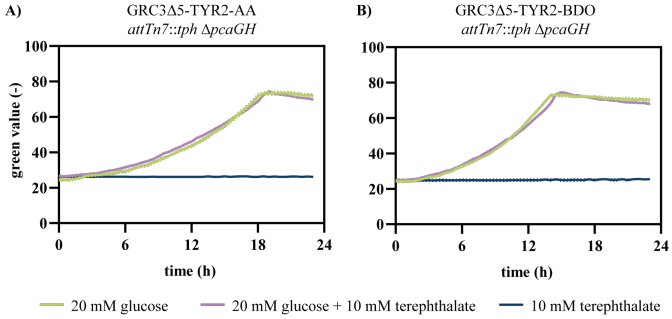

Figure S18.: Characterization of strains for bio-transformation of TA and glucose. All strains were cultivated separately in MSM medium containing terephthalate and/or glucose as mentioned in the figure. Online growth curves were measured using the Growth Profiler. Error bars indicate the standard error of the mean (n=3).

Table S1.: Strains used for molecular methods and for verifying the recycling of antibiotic resistance.

P. putida strain	Description	Reference	Chapter
E. coli			
HB101	F$^-$ mcrB mrr hsdS20(rB$^-$ mB$^-$) recA13 leuB6 ara-14 proA2 lacY1 galK2 xyl-5 mtl-1 rpsL20(SmR) gln V44λ^-	Boyer *et al.* 1969	all chapter
CC118λpir	Δ(ara-leu) araD ΔlacX74 galE galK phoA20 thi-1 rpsE rpoB argE(Am) recA1, lysogenized with λpir phage	Herrero *et al.* 1990	all chapter
PIR2	F$^-$ Δlac169 rpoS (Am) robA1 creC510 hsdR514 endA reacA1 uidA (ΔMlui)::pir	Life Technologies	all chapter
DH5α λpir	endA1 hsdR17 glnV44 (= supE44) thi-1 recA1 gyrA96 relA1 Φ 80dlacΔ (lacZ)M15 Δ(lacZYA-argF)U169 zdg-232::Tn10 uidA::pir$^+$	de Lorenzo lab all chapter	
P. putida			
BG14e	GmR, *P. putida* KT2440 with genomic insertion of pBG14e	Zobel *et al.* 2015	2.1
BG14f	GmR, *P. putida* KT2440 with genomic insertion of pBG14f	Zobel *et al.* 2015	2.1
BG14g	GmR, *P. putida* KT2440 with genomic insertion of pBG14g	Zobel *et al.* 2015	2.1
BG13_ KanRFRT	KmR with FRT flanking sequences, *P. putida* KT2440 with genomic insertion of pBG13_FRT_Kan	This work	2.1
BG14b_ FRT_Kan	KmR with FRT flanking sequences, *P. putida* KT2440 with genomic insertion of pBG14b_FRT_Kan	This work	2.1
BG14c_FRT_Kan	KmR with FRT flanking sequences, *P. putida* KT2440 with genomic insertion of pBG14c_FRT_Kan	This work	2.1
BG14d_FRT_Kan	KmR with FRT flanking sequences, *P. putida* KT2440 with genomic insertion of pBG14d_FRT_Kan	This work	2.1

Table S1.: Strains used for molecular methods and for verifying the recycling of antibiotic resistance.

***P. putida* strain**	**Description**	**Reference**	**Chapter**
BG14e_FRT_Kan	KmR with FRT flanking sequences, *P. putida* KT2440 with genomic insertion of pBG14e_FRT_Kan	This work	2.1
BG14f_FRT_Kan	KmR with FRT flanking sequences, *P. putida* KT2440 with genomic insertion of pBG14f_FRT_Kan	This work	2.1
BG14g_FRT_Kan	KmR with FRT flanking sequences, *P. putida* KT2440 with genomic insertion of pBG14g_FRT_Kan	This work	2.1
BG13_ ΔKan	*P. putida* KT2440 with genomic insertion of pBG13_FRT_Kan with kanamycin gene deletion caused by flippase activity	This work	2.1
BG14b_ ΔKan	*P. putida* KT2440 with genomic insertion of pBG14b_FRT_Kan with kanamycin gene deletion caused by flippase activity	This work	2.1
BG14c_ ΔKan	*P. putida* KT2440 with genomic insertion of pBG14c_FRT_Kan with kanamycin gene deletion caused by flippase activity	This work	2.1
BG14d_ ΔKan	*P. putida* KT2440 with genomic insertion of pBG14d_FRT_Kan with kanamycin gene deletion caused by flippase activity	This work	2.1
BG14e_ ΔKan	*P. putida* KT2440 with genomic insertion of pBG14e_FRT_Kan with kanamycin gene deletion caused by flippase activity	This work	2.1
BG14f_ ΔKan	*P. putida* KT2440 with genomic insertion of pBG14f_FRT_Kan with kanamycin gene deletion caused by flippase activity	This work	2.1
BG14g_ ΔKan	*P. putida* KT2440 with genomic insertion of pBG14g_FRT_Kan with kanamycin gene deletion caused by flippase activity	This work	2.1

Table S2.: Plasmids used in this work.

Plasmids	Description	Reference	Chapter
pRK600	Cm^R, oriV(ColE1), tra^+ mob^+ of RK2	Keen *et al.* 1988	2.1
pRK2013	Km^R, oriV(RK2/ColE1) -mob^+ tra^+	Figurski *et al.* 1979	2.1
pTNS1	Ap^R, oriV(R6K), TnSABC+D operon	Choi *et al.* 2005	2.1
pBBFLP	Helper plasmid used for antibiotic markers excision in *P. putida* strains; oriV(pBBR1) oriT(RK2) mob^+ λPR::FLP λ(cI857) sacB tet, Tc^R	de las Heras *et al.* 2008	2.1
pBNT_mcs(t)	Km^R, nagR/PnagAa promotor sytem without RBS, salicylate-inducible		2.1
pBNT_*dcaAKIJP*	pBNT_mcs(t) plasmid with *dcaAKIJP* from *A. baylyi*	This work	2.1
pBNT_*dcaAKIJP* from A12.1p	Evolved pBNT_*dcaAKIJP* isolated from strain A12.1p	This work	2.1
pBNT_*dcaAKIJP* from A6.1p	Evolved pBNT_*dcaAKIJP* isolated from strain A6.1p	This work	2.1
pEMG	KmR, oriV(R6K), lacZ α with two flanking I-SceI sites		2.1
pEMG_ΔPpaaF-paaYX::P14g	pEMG bearing the flanking regions of PpaaF and paaYX, the synthetic promotor P14g between these flanking regions	This work	2.1
pEMG_PP_2144	pEMG bearing flanking sequences of psrA (PP_2144)	This work	2.1
pEMG_paaF::14g	pEMG bearing flanking sequences of paaF and integration of the synthetic promotor 14g	This work	2.1

Table S2.: Plasmids used in this work.

Plasmids	Description	Reference	Chapter
pSNW2_ΔpaaYX	pSNW2 , pEMG with msfGFP, bearing flanking sequences of paaYX	This work	2.1
pSW-2	Gm^R, oriV(RK2), xylS, Pm I-SceI (transcriptional fusion of I-SceI to Pm)	Martínez-García *et al.* 2011	2.1
pJNN_mcs	Gm^R, PnagAa: nag promoter without RBS, salicylate-inducible	Wierckx *et al.* 2005	2.1
pJNN_PP_2144	pJNN plasmid with psrA from *P. putida* KT2440	This work	2.1
pJNN _PP_2144E80X	pJNN plasmid with evolved version of psrA from A12.1	This work	2.1
pBG14e_FRT _Kan_*dcaAKIJP*	pBG14e_FRT_Kan-derivate with *dcaAKIJP* from A. baylyi instead of msfGFP	This work	2.1
pBG13	Km^R, Gm^R, oriR6K, pBG-derived, promoter Pem7, msfGFP	Martínez-Garćía *et al.* 2015	2.1
pBG13_KanRFRT	Km^R flanked with FRT sites, oriV(R6K), pBG-derived, promoter Pem7, msfGFP	This work	2.1
pBG14b	Km^R, Gm^R, oriV(R6K), pBG-derived, promoter 14b, msfGFP	Zobel *et al.* 2015	2.1
pBG14c	Km^R, Gm^R, oriV(R6K), pBG-derived, promoter 14c, msfGFP	Zobel *et al.* 2015	2.1
pBG14d	Km^R, Gm^R, oriV(R6K), pBG-derived, promoter 14d, msfGFP	Zobel *et al.* 2015	2.1

Table S2.: Plasmids used in this work.

Plasmids	Description	Reference	Chapter
pBG14e	Km^R, Gm^R, oriV(R6K), pBG-derived, promoter 14e, msfGFP	Zobel *et al.* 2015	2.1
pBG14f	Km^R, Gm^R, oriV(R6K), pBG-derived, promoter 14f, msfGFP	Zobel *et al.* 2015	2.1
pBG14g	Km^R, Gm^R, oriV(R6K), pBG-derived, promoter 14g, msfGFP	Zobel *et al.* 2015	2.1
pBG14b _FRT_Kan	Km^R flanked with FRT sites, oriV(R6K), pBG-derived, promoter 14b, msfGFP	This work	2.1
pBG14c _FRT_Kan	Km^R flanked with FRT sites, oriV(R6K), pBG-derived, promoter 14c, msfGFP	This work	2.1
pBG14d _FRT_Kan	Km^R flanked with FRT sites, oriV(R6K), pBG-derived, promoter 14d, msfGFP	This work	2.1
pBG14e _FRT_Kan	Km^R flanked with FRT sites, oriV(R6K), pBG-derived, promoter 14e, msfGFP	This work	2.1
pBG14f _FRT_Kan	Km^R flanked with FRT sites, oriV(R6K), pBG-derived, promoter 14f, msfGFP	This work	2.1
pBG14g _FRT_Kan	Km^R flanked with FRT sites, oriV(R6K), pBG-derived, promoter 14g, msfGFP	This work	2.1
pEMG_PP_2051	pEMG harboring flanking sequences for ΔPP_2051	Li *et al.* 2020	2.2
pEMG_*dcaAKIJP*	pEMG harboring flanking sequences for Δ*dcaAKIJP*	This work	2.2
pEMG_*ttgB*Δ^{4bp}	pEMG harboring flanking sequences for *ttgB*Δ^{4bp}	This work	2.2

Table S2.: Plasmids used in this work.

Plasmids	Description	Reference	Chapter
pEMG_PP_2046^{A247T}	pEMG harboring flanking sequences for PP_2046^{A247T}	This work	2.2
pEMG_PP_2790^{A222V}	pEMG harboring flanking sequences for PP_2790^{A222V}	This work	2.2
pEMG_PP_5243^{R29P}	pEMG harboring flanking sequences for PP_5243^{R29P}	This work	2.2
pEMG_*secG*^{G70R}	pEMG harboring flanking sequences for *secG*^{G70R}	This work	2.2
pEMG_*secG*	pEMG harboring flanking sequences for Δ*secG*	This work	2.2
pEMG_PP_5003-6	pEMG harboring flanking sequences for ΔPP_5003-6	This work	2.2
pS6311·PHB	expression of *phaCAB*	This work	2.2
pSNW2_*gcdR*	pSNW2 harboring flanking sequences for Δ*gcdR*	This work	2.2
pSNW2_*gcdR*_*P*$_{14f}$	pSNW2 harboring flanking sequences for Δ*gcdR* and Integration of P_{14f}	This work	2.2
pSNW2_*gcdR*^{G148D}	pSNW2 harboring flanking sequences for *gcdR*^{G148D}	This work	2.2
pSNW2_*gcdR*^{G154D}	pSNW2 harboring flanking sequences for *gcdR*^{G154D}	This work	2.2
pBG14e_FRT_Kan_ *dcaAKIJP*	pBG14e_FRT_Kan-derivate with *dcaAKIJP* from *A. baylyi* instead of msfGFP	Ackermann et al. (2021)	2.3
pSNW2_PVLB_10540^{L480L}	pSNW2 bearing the flanking regions of SNV in PVLB_10540 identified in *P. taiwanensis* AB1	This work	2.3
pSNW2_PVLB_12690^{A247V}	pSNW2 bearing the flanking regions of SNV in PVLB_12690 identified in *P. taiwanensis* AB1	This work	2.3

Table S2.: Plasmids used in this work.

Plasmids	Description	Reference	Chapter
pSNW2_PVLB_13305^{S141P}	pSNW2 bearing the flanking regions of SNV in PVLB_13350 identified in *P. taiwanensis* AB1	This work	2.3
pSNW2_PVLB_10765^{G179D}	pSNW2 bearing the flanking regions of SNV in PVLB_10765 identified in *P. taiwanensis* AB1	This work	2.3
pSNW2_ΔpsrA	pSNW2 bearing the flanking regions of *psrA*	This work	2.3
pSNW2_attTn7_recycling	pSNW2 bearing the flanking regions of of any insert in *attTn7*-site for its recycling	Schwanemann et al. 2023	2.3
pSNW2_Δ*paaYX*	pSNW2 bearing the flanking regions of *paaYX*	This work	2.3
pSNW2_Δ*paaYX*::P_{14e}-*dcaAKIJP*	pSNW2 bearing the flanking regions of *paaYX* and the synthetic promoter 14e in combination with the *dcaAKIJP* from *A. baylyi* between these flanking regions	This work	2.3
pSNW2_curedrpmE	pSNW2 bearing the flanking regions of *rpmE*	This work	2.3
pEMGu_pcaGH	pEMG harboring flanking sequences for *pcaGH*	Wynands *et al.* 2018	2.4
psnw2_*pobA*	pEMG harboring flanking sequences for reintegration of *pobA*	this work	2.4
pBG14f_*quiC-aroG^{fbr}*	mini-Tn7 integration plasmid	this work	2.4
pBG14f_*ubiC^{fbr}-aroG^{fbr}*	mini-Tn7 integration plasmid	this work	2.4
pBG14f_*quiC-ubiC^{fbr}-aroG^{fbr}*	mini-Tn7 integration plasmid	this work	2.4

Table S2.: Plasmids used in this work.

Plasmids	Description	Reference	Chapter
pEMG_GFP_sensor_Landing_Pad_PVLB_02480_P_{14f}_RtPAL_*ech*_*vdh*_*fcs*	Integration of P_{14f}_RtPAL_*ech*_*vdh*_*fcs* at IGR of PVLB_02480_PVLB_02485	this work	2.4
pEMG_GFP_sensor_Landing_Pad_PVLB_02480_t0-P_{14f}_RpcTAL_*ech*_*vdh*_*fcs*	Integration of t0-P_{14f}_RpcTAL_*ech*_*vdh*_*fcs* at IGR of PVLB_02480_PVLB_02485	this work	2.4

Table S3.: Oligonucleotides used in this work.

Primer	Sequence 5'-3'	Template/purpose	Chapter
BW651	**CCATGCCAGCCCATGATAC**	mapping of Tn7-site integration in *P. putida*	2.1
BW652	**CATCCACGCCGAAGCATAC**		2.1
JaP03	**AGGGATAACAGGGTAATCTGCCAGCAGGGTGAAGGCATG**	KT2440 TS1 for ΔP_{paaF}-*paaYX*::P_{14g}	2.1
JaP04	**TAATTGCACGACCTAGGTATACTGACCACACCTGGTCG**		2.1
JaP05	**GGTCAGTATACCTAGGTCGTGCAATTATACCTGGCCGCG AGAGCCTGTCAATGGGCTTAATTAATGCTCTATGCGATA CAACAATGCAAGGCGCAAAATGTTTTCGCG**	KT2440 TS2 for ΔP_{paaF}-*paaYX*::P_{14g}	2.1
JaP06	**CCTGCAGGTCGACTCTAGAGCATGCGCGGGCGCCCCGG**		2.1
JuB10	**AGGGATAACAGGGTAATCTGCTTGCTCGGGTGCGTGAATG**	KT2440 TS1 for Δ*psrA*	2.1
JuB11	**GGCTCGGAACTGTCTTCGCCCGCGAAGG**		2.1

Table S3.: Oligonucleotides used in this work.

Primer	Sequence 5'-3'	Template/purpose	Chapter
JuB12	**TGACAGAAGCGGGCGCTTCCGCTAAGCT**	KT2440 TS2 for Δ*psrA*	2.1
JuB13	**GTAGATGGGCGTCCAACTGTTCAGCTGGACGTCCGTACGT**		2.1
YA01	**CAAGTTTTAAGAATTCGAGCTCGGTACC**	pBG14e_FRT_kan backbone	2.1
YA03	**ACGTCTTAATTCAGAATTGGTTAATTGGTTG**	pBNT_*dcaAKIJP*	2.1
YA04	**GCTCGAATTCTTAAAACTTGTACATTGACAC**		2.1
YA05	**CCGAGCGTTCTGAACAAATC**	pBG14e_FRT_Kan backbone	2.1
YA06	**GCTGCGTTCGGTCAAGGTTC**		2.1
YA07	**GCACGGTCGCGATGAGGTCG**	pBNT_*dcaAKIJP*	2.1
YA09	**GCTGGATAAAGGCCGTCTAC**	Sequencing of the *dcaAKIJP*-operon	2.1
YA10	**TGCGGGTCTTTGGTTCGATG**		2.1
YA11	**GGTTATGGCTGCTGCTTAC**		2.1
YA12	**TGGTCCGATTATGGCCAAAG**		2.1
YA13	**TGGCTGTGGCTTGTGCTACG**		2.1
YA14	**GGACGACTGGTACAATGG**		2.1
YA15	**TAGAAAACCTCCTTAGCATG**	pBG14e_FRT_Kan backbone	2.1
YA16	**CATGCTAAGGAGGTTTTCTAATGATTCGCGATGAAGGG**	pBNT_*dcaAKIJP*	2.1
YA17	**TCTAGAGTCGACCTGCAG**	Linearization of pEMG for Gibson	2.1
YA18	**GAATTCAGATTACCCTGTTATCC**		2.1

Table S3.: Oligonucleotides used in this work.

Primer	Sequence 5'-3'	Template/purpose	Chapter
YA19	**AATAGGGTTTCTCTAGAGTCGACCTGCAG**	pEMG_14g_paaF TS1 for ΔP_{paaF}-*paaYX*::P_{14g}	2.1
YA20	**AGCACTCCCCTTAATTAAGCCCATTGACAAGG**		2.1
YA21	**GCTTAATTAAGGGGAGTGCTCGCCTCAC**	KT244 TS2 for ΔP_{paaF}-*paaYX*::P_{14g}	2.1
YA22	**GACTCTAGAGAAACCCTATTCACCTGAAACCGC**		2.1
YA24	**AATACGCAAACCGCCTCTC**	MCS of pEMG	2.1
YA32	**CGTCAGTCGAGAGAATGAAGTTCAG**	Mapping of ΔP_{paaF}-*paaYX*::P_{14g}	2.1
YA33	**GGCCTCCGTAATGCGAAG**		2.1
YA34	**GGGCGAGGAATGCTTCGAAC**	Mapping of $\Delta psrA$	2.1
YA35	**ACGCAGGATGTCCTGCAACC**		2.1
YA36	**TAACAGGGTAATCTGAATTCACACAAGCTTTCGAACCG**	KT2440 TS1 & TS2 for curing of PP_3988 in A12	2.1
YA37	**TAACAGGGTAATCTGAATTCACACAAGCTTTCGCCTGCAGG TCGACTCTAGAGATGAGAAGTTTCGTGCCGAACCG**		2.1
YA38	**CCATGTCCCGGGCTTATATCTTG**	Mapping of PP_3988	2.1
YA39	**TGAGCGCCCAAGTTAAGCAAA**		2.1
YA42	**TAACAGGGTAATCTGAATTCTACCGACGGCACGTAACAG**	KT2440 TS1 for $\Delta paaYX$	2.1
YA43	**AGCACTCCCCGGCAACACTCTCGAAATGATTTG**		2.1
YA44	**GAGTGTTGCCGGGGAGTGCTCGCCTCAC**	KT2440 TS2 for $\Delta paaYX$	2.1
YA45	**GCCTGCAGGTCGACTCTAGAAAACCCTATTCACCTGAAAC CGC**		2.1
SK4	**AGTCAGAGTTACGGAATTGTAGG**	Mapping of ΔKmR	2.1

Table S3.: Oligonucleotides used in this work.

Primer	Sequence 5'-3'	Template/purpose	Chapter
SK5	**GTCGAGAAAATTGCCGAGCT**		2.1
SK264	**AATCTCTGATAATTGGACAAGGGTCCTTTTC**	pBG13 backbone for oriT and oriR6K	2.1
SK265	**TAAAAAACGCAATTGGACGTCGGCATCAAATAAAAC**		2.1
SK266	**ACGTCCAATTGCGTTTTTTATTGGTGAG**	pBELK for FRT flanked KmR	2.1
SK267	**GTTATGGAGCATTTTGGTCATGAGATTATCG**		2.1
SK268	**TGACCAAAATGCTCCATAACATCAAACATC**	pBG14b to pBG14g for Promoter, BCD2, msfGFP, terminator T0	2.1
SK269	**TTGTCCAATTATCAGAGATTTTGAGACAC**		2.1
JDW169	**ATTCGAGCTCGGTACCCGGGAATGGCTGCTCACAGAAC**	TS1 $\Delta dcaAKIJP$	2.2
JDW170	**TTTTAGAGAATTAAAACTGTCGCTAGAGAATTAAAG**		2.2
JDW171	**ACAGTTTTAATTCTCTAAAACCAGTTGATCAACACC**	TS2 $\Delta dcaAKIJP$	2.2
JDW172	**CAGGTCGACTCTAGAGGATCAAGCCGGTGTCGAAGCTG**		2.2
JDW208	**ATTCGAGCTCGGTACCCGGGACGCTGGGCCAGGGCGAA**	TS1 $ttgB\Delta^{4bp}$	2.2
JDW209	**GCGCCCTGGTATCGCCCTGGTGCTCTCGG**		2.2
JDW210	**CCAGGGCGATACCAGGGCGCCCTGGATC**	TS2 $ttgB\Delta^{4bp}$	2.2
JDW211	**CAGGTCGACTCTAGAGGATCGCCTGCAAACCGCCGAGC**		2.2
JDW215	**ATTCGAGCTCGGTACCCGGGATGGTCATGTTGGCCAGGTC CAG**	TS1 - PP_2046^{A247T} - TS2	2.2
JDW216	**CAGGTCGACTCTAGAGGATCCGCTGCTGGTCCGCGTGG**		2.2
JDW218	**ATTCGAGCTCGGTACCCGGGTGTGCTGCTTCGAACAGG**	TS1 - PP_2790^{A222V} - TS2	2.2

Table S3.: Oligonucleotides used in this work.

Primer	Sequence 5'-3'	Template/purpose	Chapter
JDW219	**CAGGTCGACTCTAGAGGATCGCTGATCAGCCACTTGCAG**		2.2
JDW223	**ATTCGAGCTCGGTACCCGGGAGCTGTACTGTCACGTCAATATTC**	TS1 - PP_5243^{R29P} - TS2	2.2
JDW224	**CAGGTCGACTCTAGAGGATCGCGGTTTGGTGAGTTTTTC**		2.2
JDW228	**ATTCGAGCTCGGTACCCGGGAAGGCCTGCAACTGTTCTAGCTTGC**	TS1 - *secG*^{G70R} - TS2	2.2
JDW229	**CAGGTCGACTCTAGAGGATCGCGGCCCAGGCCAAAGGC**		2.2
JDW297	**ATTCGAGCTCGGTACCCGGGAAGCCTCCAAGACCCTCAG**	TS1 ΔPP_5003-6	2.2
JDW298	**TCCAGCAGGCCTACGACGCTCCGTTGTC**		2.2
JDW299	**AGCGTCGTAGGCCTGCTGGAGATGTAGTG**	TS2 ΔPP_5003-6	2.2
JDW300	**CAGGTCGACTCTAGAGGATCGCGAACTTGAAGAAGCCTTC**		2.2
JDW305	**ATTCGAGCTCGGTACCCGGGACATCGAGGATTGCGCTG**	TS1 ΔsecG	2.2
JDW306	**AACTGAACAACGGGTTTCAAGTAGTAGTATTGC**		2.2
JDW307	**TTGAAACCCGTTGTTCAGTTTCCTGCGG**	TS2 ΔsecG	2.2
JDW308	**CAGGTCGACTCTAGAGGATCATTGATGGCCTGGCAGGTAAAG**		2.2
YA89	**TAACAGGGTAATCTGAATTCGTCCAGGCTCTGCGCCCG**	TS1 Δ*gcdR*, also used for SNV	2.2
YA90	**GTTGACGTACCCCTGTAGTCAATTATTTTAAACACCTACAGATGTATGTATATGTCGC**		2.2
YA91	**GACTACAGGGGTACGTCAACCTCACTTGTAAG**	TS2 Δ*gcdR*, also used for SNV	2.2
YA92	**GCCTGCAGGTCGACTCTAGAGAACACATTGTCCATGAC**		2.2

Table S3.: Oligonucleotides used in this work.

Primer	Sequence 5'-3'	Template/purpose	Chapter
YA95	**CCCTGTAGTCAATTATTTTAAACACCTACAGATGTATGTA TATGTCGC**	TS1 $\Delta gcdR$ and P_{14f} integration	2.2
YA96	**TAAAATAATTGACTACAGGGTTAATTAAGCCCGTTGAC ATGACATGGTTTTGAGGGTATAATGTGGCGACCTAGGG TACGTCAACCTCACTTGTAAG**	TS2 $\Delta gcdR$ and P_{14f} integration	2.2
YA145	**GCAACCATCCCCGAGCAATACG**	qPCR amplicon *gcdH*	2.2
YA146	**ATCACCAGCGACGACTGCACAC**		
LO01	**TCTAGAGTCGACCTGCAG**	pSNW2 backbone	2.3
LO02	**GAATTCAGATTACCCTGTTATCC**		
LO32	**TAACAGGGTAATCTGAATTCGCGGCCCAGAACCTGCTG**	Genomic region around SNV in PVLB_10540^{L480L}	2.3
LO33	**GCCTGCAGGTCGACTCTAGACCTGGATGATCTTCGCGGC**		
LO24	**TAACAGGGTAATCTGAATTCGTACGGGTTGGCCGACGA**	Genomic region around SNV in PVLB_12690^{A247V}	2.3
LO27	**GCCTGCAGGTCGACTCTAGACTTGACGTCGGCCTCGTCG**		
LO28	**TAACAGGGTAATCTGAATTCGCATATCCTGCCCAACGC**	Genomic region around SNV in PVLB_13350^{S141P}	2.3
LO31	**GCCTGCAGGTCGACTCTAGACTCGAACTGTTCACAGGCC**		
LO36	**TAACAGGGTAATCTGAATTCCTCGCCACCGGTTCGGCATAG**	Genomic region around SNV in PVLB_10765^{G179D}	2.3
LO37	**GCCTGCAGGTCGACTCTAGACGCGACCCGGCCAAGGCC**		
LO61	**TTCCGACAGTTCGTGATCGCC**	Mapping of the deletion in PVLB_02465 and intergenic region between PVLB_02465 and *putA*	2.3
LO63	**AACAGCTACACCATCCTGC**		
YA54	**TAACAGGGTAATCTGAATTCCGGCACGCAGCAAGCGCT**	TS1 $\Delta paaYX$	2.3

Table S3.: Oligonucleotides used in this work.

Primer	Sequence 5'-3'	Template/purpose	Chapter
YA55	**AGCGCATCATCTCGCACCTCCAGAAATGATTTGAAGCG**		
YA56	**GAGGTGCGAGATGATGCGCTTTCGTTAC**	TS2 $\Delta paaYX$	2.3
YA57	**GCCTGCAGGTCGACTCTAGATTCAGGCAAACAAAAGGAATG**		
YA60	**TAACAGGGTAATCTGAATTCTTCAGGTCGACTTCGATG**	TS1 $\Delta psrA$	2.3
YA61	**CGCCCAGTGTGACTACTCCGCCAGACAAAC**		
YA62	**CGGAGTAGTCACACTGGGCGGGGCAGGG**	TS2 $\Delta psrA$	2.3
YA63	**GCCTGCAGGTCGACTCTAGACAGGCGTTGAACGCGACCG**		
YA79	**AGGGATAACAGGGTAATCTGAATTCGGCCTGCAAGGCATGGCG**	TS1 $\Delta paaYX$ together with integration of $dcaAKIJP$	2.3
YA80	**CTGTTCGGTTCGTTCATCCATGTATCGCTTTTTTCAGCGTG**		
YA81	**ATACATGGATGAACGAACCGAACAGGCTTATG**	amplify $P_{14e}\_dcaAKIJP\_T1$ for integration at $paaYX$	2.3
YA82	**AAAGCGCATCATCTGGATTCTCACCAATAAAAAACG**		
YA83	**GGTGAGAATCCAGATGATGCGCTTTCGTTAC**	TS2 $\Delta paaYX$ together with integration of $dcaAKIJP$	2.3
YA84	**TGCATGCCTGCAGGTCGACTCTAGATTCAGGCAAACAAAAGGAATG**		
YA141	**TAACAGGGTAATCTGAATTCTACTGGGCGGTCCACAGGC**	TS1 - $rpmE$(WT) - TS2	2.3
YA142	**GCCTGCAGGTCGACTCTAGACACCCAGCGTCGCTGCCC**		
YA158	**ACAAATTCGAAACCCGTTCGACC**	qPCR amplicon $rpmE$	2.3
YA159	**TGTCCAGGACTTTCTGCTTACCAG**		
YA160	**GCTCGTCTGCAACGCAACTTCC**	qPCR amplicon nuclease (PVLB_01640)	2.3

Table S3.: **Oligonucleotides used in this work.**

Primer	Sequence 5'-3'	Template/purpose	Chapter
YA161	**GTCAATGGCAACACCCAGCGTC**		
YA162	**AGCTCTCCAAGCCAACTGCCAC**	qPCR amplicon *maeB*	2.3
YA163	**TGCCATCGGAGATCACCGCAAC**		
YA174	**TCTCTTGATGCGCCCGTACCAG**	qPCR amplicon *priA*	2.3
YA175	**CATCATCATCGGAACGCGCTCG**		
YA67	**GAATTCGAGCTCGGTACC**	linaerization of pBG14f	2.4
YA68	**TAGAAAACCTCCTTAGCATG**		
YA69	**TTAATCATGCTAAGGAGGTTTTCTAATGCGTTTGATGCCC CTC**	amplify *quiC* from VLB genome	2.4
YA70	**TCAGCGACTCAGTGGCCG**		
YA71	**GTTGAGCCGGCCACTGAGTCGCTGATAATTAGAGAAGGAG GTCTAACAAATGTCACACCCCGCGTTAAC**	amplify $ubiC^{fbr}$ with RBS	2.4
YA72	**TTAGTACAACGGTGACGCC**		
YA73	**TTTACCGGCGTCACCGTTGTACTAAACTAGGCATAAGGAG GTATTAGTTATGAACTACCAAAACGATGATCTGCGCATCA AGG**	amplify $aroG^{fbr}$ with RBS	2.4
YA74	**ATCCCCGGGTACCGAGCTCGAATTCTTAGCCGCGCCGGGCC TT**		
YA75	**TTAATCATGCTAAGGAGGTTTTCTAATGTCACACCCCGCGT TAAC**	amplify $ubiC^{fbr}$ w/o RBS	2.4
YA76	**GTTGAGCCGGCCACTGAGTCGCTGAACTAGGCATAAGGAGG TATTAGTTATGAACTACCAAAACGATGATCTGCGCAT-CAAGG**	amplify $aroG^{fbr}$ with RBS for combination with *quiC*	2.4
YA97	**GAATTCGAGCTCGGTACC**	amplify pEMG_GFP_sensor_Landing_Pad _PVLB_02480_PVLB_02485 without promoter	2.4

Table S3.: Oligonucleotides used in this work.

Primer	Sequence 5'-3'	Template/purpose	Chapter
YA98	**TTAATTAAAGAGCCTTTCGCG**		
YA99	**GCGAAAGGCTCTTTAATTAAGCCCGTTGACATGACATGGTTTTG**	amplify P_{14f}_RtPAL_*ech_vdh_fcs*	2.4
YA100	**CGGGTACCGAGCTCGAATTCTCAAGGCCGCACCTTGGC**		
YA153	**GCGAAAGGCTCTTTAATTAATTAATTAAGCCCGTTGAC**	amplify RpcTAL	2.4
YA156	**GCTCGAATTCTTAGTTATTCACGCTCTTC**		
YA157	**GAATAACTAAGAATTCGAGCTCGGTACCCG**	amplify *ech_vdh_fcs*	2.4
YA100	**CGGGTACCGAGCTCGAATTCTCAAGGCCGCACCTTGGC**		

Danksagung

Mein besonderer Dank gilt Prof. Dr. Nick Wierckx, der es mir ermöglicht hat, in diesem internationalen Konsortium an diesem hochaktuellen Thema zu arbeiten. Ich bin dankbar für die hervorragende Betreuung, die stetige Unterstützung meiner Arbeit und Ideen sowie für unzählige anregende Diskussionen und schönen Dienstreisen. Es war mir eine große Freude, auf dem Campus des Forschungszentrums zu arbeiten, Teil deiner Arbeitsgruppe zu sein und das Wachstum der "Mikats" mitzuerleben. Ich hatte eine Wunderbare Zeit und hätte es mir nicht viel besser vorstellen können. Danke Nick!
Außerdem möchte ich Prof. Dr. Ilka Axmann dafür danken, dass sie sich bereit erklärt hat, meine Co-Betreuerin zu sein.
Danken möchte ich auch dem einzig wahren Postdoc Benedikt Wynands. Deine unglaubliche Geduld und deine tägliche gute Laune haben mir das Leben im Labor sehr erleichtert. Egal worum es ging, du hattest immer ein offenes Ohr und gute Tipps zur Lösung des Problems.
Darüber hinaus möchte ich mich bei meinen Mix-Up Projektpartnern aus ganz Europa sowie bei den Studenten Leonie Op de Hipt und Hannah de Jong bedanken, deren Master- bzw. Bachelorarbeiten ich betreuen durfte. Es hat Spaß gemacht mit euch zu arbeiten.
Ich möchte mich bei allen Kolleginnen und Kollegen des IBG-1 für die freundliche und angenehme Arbeitsatmosphäre am Forschungszentrum Jülich und für die technische, administrative und wissenschaftliche Unterstützung bedanken.
Ein großes Dankeschön geht auch an die schnell wachsende, aber stets familiäre Arbeitsgruppe "Microbial Catalysis". Vielen Dank, Tobias Schwanemann, Jakob Rönitz, Felicia Zlati, Franziska Kofler, Nadine da Silva, Ronja Weskott, Felix Herrmann, Thomas Konjetzko, Tobias Probanowski, Pascal Künzel, Alina Grankin für die Unterstützung, spannenden Diskussionen und netten Gesprächen. Und ein besonderes Dankeschön an die Quatschköppe der AG Philipp Ernst, Thorsten Lechtenberg, Leonie Op de Hipt und meinen Lieblingsbürokollegen Jan de Witt. Ihr habt mir jeden Tag versüßt!
An dieser Stelle möchte ich mich ganz besonders bei all meinen Freunden bedanken, auf die ich mich immer verlassen kann und die mich immer unterstützt haben. Danke an meine ganze Familie, vor allem Ute und Klaus, die mir diesen Weg ermöglicht hat.
Zuletzt Danke ich meiner Freundin Johanna Senska für die Unterstützung, ihr Verständnis, ihre Geduld und unseren Zusammenhalt in schwierigen und stressigen Phasen. Danke!

Eidesstattliche Erklärung

Ich versichere an Eides Statt, dass die Dissertation von mir selbständig und ohne unzulässige fremde Hilfe unter Beachtung der „Grundsätze zur Sicherung guter wissenschaftlicher Praxis an der Heinrich-Heine-Universität Düsseldorf“ erstellt worden ist. Die Dissertation wurde in der vorgelegten oder in ähnlicher Form noch bei keiner anderen Institution eingereicht. Ich habe bisher keine erfolglosen Promotionsversuche unternommen.

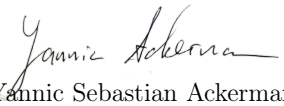

Yannic Sebastian Ackermann

Band / Volume 269
The complex inositol metabolism of *Corynebacterium glutamicum* and its application for the production of rare inositols
P. Ramp (2023), VI, 161 pp
ISBN: 978-3-95806-699-1

Band / Volume 270
Spin- and orbital-dependent band structure of unconventional topological semimetals
K. Hagiwara (2023), v, 115 pp
ISBN: 978-3-95806-701-1

Band / Volume 271
Neutron scattering
Experimental Manuals of the JCNS Laboratory Course held at Forschungszentrum Jülich and at the Heinz-Maier-Leibnitz Zentrum Garching edited by T. Brückel, S. Förster, K. Friese, M. Kruteva, M. Zobel and R. Zorn (2023), ca 150 pp
ISBN: 978-3-95806-705-9

Band / Volume 272
Ab-initio investigation of the interplay between the hyperfine interaction and complex magnetism at the nanoscale
S. R. S. Shehada (2023), ix, xi, 119 pp
ISBN: 978-3-95806-718-9

Band / Volume 273
Analysis of the signal transduction cascade tuning the 2-oxoglutarate dehydrogenase activity in *Corynebacterium glutamicum*
L. Sundermeyer (2023), VI, 119 pp
ISBN: 978-3-95806-722-6

Band / Volume 274
Multicellular defense against phage infection in *Streptomyces* – impact of secondary metabolites and mycelial development
L. Kever (2023), iv, 246 pp
ISBN: 978-3-95806-724-0

Band / Volume 275
Investigation of the electronic band structure of 2D transition metal dichalcogenides via angle-resolved photoemission spectroscopy
B. Parashar (2023), xvii, 156 pp
ISBN: 978-3-95806-725-7

Band / Volume 276
Strain- and process engineering for polyketides production with *Pseudomonas taiwanensis* VLB120 in two-phase cultivations
T. P. Schwanemann (2023), 230 pp
ISBN: 978-3-95806-726-4

Band / Volume 277
Quantitative atomic-level investigation of solid materials through multidimensional electron diffraction measurements
H. L. Lalandec-Robert (2024), xxi, 152 pp
ISBN: 978-3-95806-735-6

Band / Volume 278
Studies on the cAMP-responsive regulatory network of *Corynebacterium glutamicum*
N. Wolf (2024), iii, 122 pp
ISBN: 978-3-95806-736-3

Band / Volume 279
Rare-earth atoms on two-dimensional materials: ab initio investigation of magnetic properties
J. P. Carbone (2024), 235 pp
ISBN: 978-3-95806-740-0

Band / Volume 280
Communities of Niche-optimized Strains (CoNoS) – a novel concept for improving biotechnological production
R. Zuchowski (2024), VIII, 168 pp
ISBN: 978-3-95806-743-1

Band / Volume 281
Enabling mixed microbial upcycling of plastic monomers
Y. S. Ackermann (2024), XVI, 203 pp
ISBN: 978-3-95806-749-3

Weitere ***Schriften des Verlags im Forschungszentrum Jülich*** unter
http://wwwzb1.fz-juelich.de/verlagextern1/index.asp

Schlüsseltechnologien / Key Technologies
Band / Volume 281
ISBN 978-3-95806-749-3

Mitglied der Helmholtz-Gemeinschaft

JÜLICH
Forschungszentrum